IL
NUOVO CIMENTO
ORGANO DELLA SOCIETÀ ITALIANA DI FISICA
SOTTO GLI AUSPICI DEL CONSIGLIO NAZIONALE DELLE RICERCHE

VOL. IV, N. 4 *Serie decima* 1° Ottobre 1956

Experimental Decay Law of the Diffracted Light Remaining in the Liquids at the Stopping of the Ultrasonic Waves.

F. PORRECA

Istituto di Fisica Sperimentale dell'Università - Napoli

(ricevuto il 2 Maggio 1956)

Summary. — In this paper an experimental device is described in order to measure the decay law of the diffracted light intensity remaining in the colloidal solutions, which show the lines permanence effect at the stopping of the supersonic waves. It has been possible to state that such an intensity decreases in time exponentially and the decay constant k of different substances is inversely proportional to the concentration c of the suspended particles. Moreover, the value $K \cdot c$ depends only upon the substances under examination and it represents a parameter giving roughly the measure of the electric interaction between the suspended particles and the liquid dipoles, to which the light permanence effect is due.

---

1. – It has been shown previously that the permanence of the ultrasonic grating in the liquid suspensions is due essentially to the possibility of the suspended particles of binding with some liquid particles so that the medium has a small variation $\Delta\mu$ (about 10^{-6}) of the refractive index. Till now [1,8]

(1) A. CARRELLI and F. PORRECA: *Nuovo Cimento*, **9**, 90 (1952).
(2) A. CARRELLI and F. PORRECA: *Nuovo Cimento*, **10**, 98 (1953).
(3) A. CARRELLI and F. PORRECA: *Nuovo Cimento*, **10**, 883 (1953).
(4) A. CARRELLI and F. PORRECA: *Nuovo Cimento*, **10**, 1406 (1953).
(5) F. FANTI and F. PORRECA: *Nuovo Cimento*, **1**, 532 (1955).
(6) A. CARRELLI and F. PORRECA: *Nuovo Cimento*, **1**, 527 (1955).
(7) F. PORRECA: *Nuovo Cimento*, **2**, 904 (1955).
(8) F. PORRECA: *Nuovo Cimento*, **3**, 371 (1956).

experimental facts referred only to the duration t_p of the permanence of the diffracted lines, measured from the final instant of the ultrasonic emission. But it is clear that another important point is the measurement of the intensity I_p of the diffracted lines and the statement of its variation against time.

In fact, in a previous paper ([8]) it was established that the effect appears only in the polar liquids; probably in this case the building of the phase grating is due to the electric interaction between the suspended particles and the dipoles of the dispersing liquid medium.

Therefore one may foresee that measurements of the diffracted light intensity must be useful in the knowledge of the electric interactions which take place around the suspended particles, changing the optical properties (refractive index) of the liquid.

In this paper we describe the experimental device adopted and we give the results obtained in the determination of the decay law of the diffracted light I_p against time

$$I_p = I_p(t) \,. \tag{1}$$

The measurement method is the following: a previously ([3]) described optical device allows to observe the lines diffracted by the ultrasonic grating and the diffracted light is detected by a photocell. The corresponding photocurrent is amplified, recorded by an oscillograph, and the light pattern on its screen measures the intensity I_p.

It is to remember, however, that such a light energy flux is very small. In fact, the intensity of the diffracted light producing the spectrum remaining at the stopping of the ultrasounds, is about 1‰ of the central line (zero order) intensity. In order to increase the sensitivity of the measurement method, the photocell is screened from this light, blocking up with a wire (0.4 mm diameter) the luminous rays proceeding from the zero order.

Without ultrasounds, no radiation falls on the photocathodic surface of the cell; with ultrasounds it receives the light energy flux of the spectrum produced by the ultrasonic grating; at the stopping of the ultrasonic waves only the weak light due to the permanence effect of the lines remains during its duration t_p. It is nevertheless to observe that when no diffraction rays fall on the cell, after this time t_p, the common background is weakly increased from the very small photocurrent intensity due to the light diffused by the suspension.

Owing to the very small light intensity to record, the employement of a single photocell (initially the Philips 90CV vacuum cell (*) was employed)

(*) We found the employement of a semiconductor selenium cell to be impossible as we noted experimentally that, differently from the vacuum cell, it rectifies the sur-

caused some experimental complications due to the amplification of very low intensity corresponding signals, hardly distinguishable from the background (*).

To partially simplify these difficulties we employed the RCA 931A photomultiplier, whose amplification gain of the photoelectric current is about 10^6 times that of the Philips 90CV, for the same luminous signal flux. In such a way, notwithstanding the small intensity of the light to be recorded, the output photocurrent increases to some microamperes.

To establish the decay law (1) during the duration t_p of the diffracted light which one observes from the instant the supersonic waves are stopped, the output photocurrent is amplified and recorded by an oscillograph whose response on the screen is practically instantaneous with regard to the long t_p duration values and gives faithfully the luminous intensity effect against time.

2. – The Fig. 1 shows in details the block diagram of the experimental device employed in the measurements.

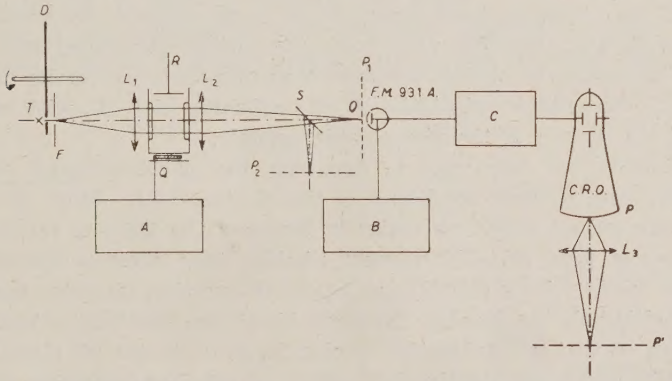

Fig. 1. – *A*) V. S. Oscillator; *B*) Photocell power supply; *C*) L. F. Amplifier.

The light source T is fed by d. c. and the luminous beam, falling on the slit F of the collimator L_1, is modulated in low frequency (870 Hz) by a plexiglass disk D, revolving around an axis which is parallel to the optical axys of the system. The disk annulus, facing the slit F, is divided in trans-

---

rounding radio-frequency field, produced by the oscillator feeding the piezoelectric quartz. Such a signal produces a photocurrent much larger than that corresponding to the light radiation to be measured.

(*) In fact, the luminous intensity of the image of the collimator slit in the optical device produces a current of about 10^{-10} A (directly measured by the microgalvanometer Lange) and therefore the luminous flux due to the measuring effect produces a photocurrent certainly not bigger than about 10^{-13} A.

parent and opaque surfaces, with such a shape that the revolution of the disk produces approximately sinusoidal light pulses.

At this point it is to note that the employement of this luminous source modulated in low frequency does not deform the photomultiplier response.

The output current is therefore modulated faithfully with the falling luminous flux and, consequently, its amplification and recording on the oscillograph screen is easier.

Coming out from the collimator, the parallel light beam crosses the trough containing the medium subjected to the ultrasounds and the image of the F_1 slit appears on the P_1 focal plane of the converging lens L_2. In this plane the blocking wire is situated, parallel to the slit F and to the ultrasonic wavefront, and its trace in the Fig. 1 plane is indicated with O. In this way, only the diffracted light producing the spectrum higher orders, except the zero order line, falls on the photomultiplier cathodic surface.

The employement of a small plane mirror S at 45° with the principal optical axis of the system and situated a little before the plane P_1, allows the observation of the diffraction spectrum produced on the plane P_2 by a simple magnifying glass and simplifies very much the preliminary experimental arrangements necessary to obtain the stationary ultrasonic waves, by the translation and the suitable orientation of the reflecting plate R, with respect to the emitting surface of the piezoelectric crystal .

Particularly we took care in designing the photomultiplier supply to obtain the best stability conditions of the photocurrent. After the step-up transformer output which conveniently increases the 150 a.c. main voltage, the full-wave type 5R4-GY vacuum rectifier tube supplies the maximum requested anode voltage (900 V) and a potential partitor gives the due voltage to the multiplier's ten dinodes. Two suitable chokes establish the best filtering conditions, so that no modulation coming from the mains (50 Hz) affects the photomultiplier output signal; after that it goes in the measuring apparatus.

Evidently to measure the photocurrent one can use a microammeter, but only to know its order of magnitude. In fact, it is clear, owing to the large inertia of the common galvanometer and microammeter, whose oscillation periods are compared with the duration time of the effect, the proceeding in time of the output photocurrent readings on these apparatus does not give us faithfully the decay law of the corresponding light flux fallen on the photocell.

To be successfull in our aim we thought to employ an oscillograph (Philips GM 5659). First, the photocurrent is suitably amplified, with a proper ([9]) amplifier in order to detect the modulated photocurrent and afterwards it is put in the oscillograph's vertical deflecting plates.

The height h of the luminous pattern appearing on the scope screen, if the

([9]) J. STRONG: *Proceeding of Experimental Physics* (1948).

diffracted light during the emission of the ultrasounds falls on the photocell, is directly proportional to the corresponding luminous flux and the decay pattern of h, after the stopping of the ultrasounds, gives us the decay law of the diffracted light remaining in the medium against time.

It was very advantageous to magnify the pattern appearing on the scope screen, by the L_3 converging optical system magnifying this pattern on the P' plane about three times.

3. – First of all, we show the different pattern in time of the diffracted light produced in water and in an aqueous suspension giving the effect.

Fig. 2 refers to the water and shows the pattern of the diffracted light flux from the $t = 0$ initial emission of the ultrasounds, during its duration (7 s) and immediately afterwards. We record on the ordinates the relative values of the height h of the luminous pattern observed on the P' plane, which, as we said before, we can consider to be proportional to the diffracted light flux (except the zero order) detected from the photomultiplier. The abscissae give the time instant at which h readings take place.

We see in Fig. 2 the graph of the diffracted light flux in water: from the initial instant of the ultrasonic emission ($t = 0$) the diffracted light quantity

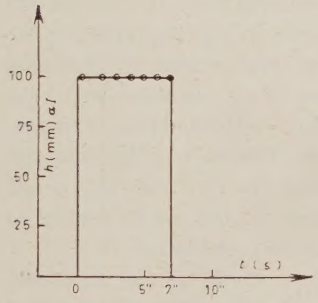

Fig. 2.

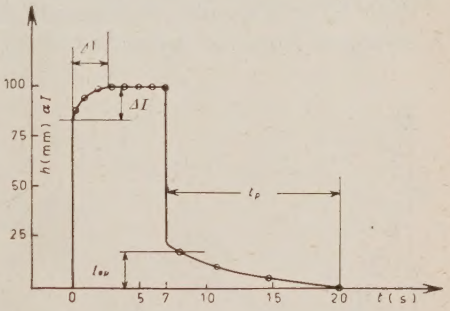

Fig. 3.

reaches instantaneously the maximal value, remaining steady till the ultrasonics stop ($t = 7$ s). At this instant the diffracted lines instantaneously disappear and h decreases to zero. Obviously, we conclude that in water the diffracted light appears only if the diffracting ultrasonic grating is in the liquid and during the emission the diffracted light quantity remains steady.

Fig. 3 shows the graph of the diffracted light flux in a suspension of starch in water, during and after a 7 s ultrasonic emission (*).

(*) This ultrasonic duration is so chosen that it is long enough to produce a remarkable permanence effect, but not too long to cause heat convection currents in the liquid, destroying the standing wave condition.

One observes that the light flux diffracted during the ultrasounds does not reach its maximal value immediately after the $t = 0$ starting instant of the ultrasonic waves, but after a Δt delay of some seconds (in the case under examination $\Delta t = (2.5 \pm 1)$ s). Moreover, the diffracted light flux does not decrease to zero instantaneously as soon as the ultrasonics stop ($t = 7$ s), but it persists during a certain time t_p corresponding to the duration of the diffracted lines permanence (in the case under examination $t_p = (13 \pm 1.5)$ s).

The ΔI intensity increase (see Fig. 3), at the starting of the ultrasonic waves, is due to the light flux increase, as some new diffracted lines appear during the ultrasonics, as we noted [4] before (inverted permanence effect).

Evidently, during the Δt interval, necessary in order to reach a practically steady value of the light intensity distribution, the suspended particles are gathered by the ultrasonic standing waves in uniformly spaced parallel planes at the distance from each other of $\lambda/2$, producing the phase grating which remains after the stopping of the ultrasounds. In the range of the experimental error, this ΔI increase, due to the diffracted light from this second phase grating, which is to be added to the supersonic one, equalizes the I_{0p} value measuring the maximal light flux of the even order diffracted lines remaining immediately after the stopping of the supersonic waves.

This I_{0p} light quantity decreases in time and becomes zero after a duration t_p measured from the instant at which the supersonics stop. According to the slowness with which it decreases in time, it is possible with the described experimental arrangement to establish experimentally the decay law (1), from the direct h readings on the scope screen as the time is progressing.

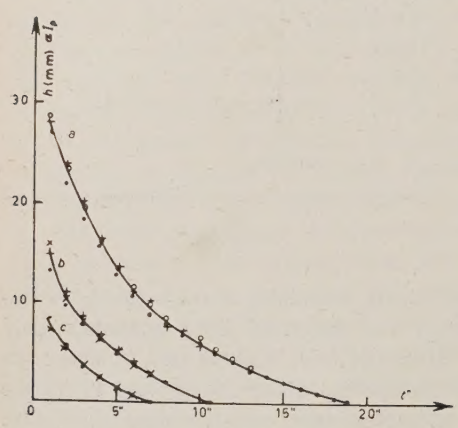

Fig. 4.

Fig. 4 shows a few measurement sets of the $h \propto I_p(t)$ readings in the case of a starch in water suspension of $c = 0.100$ g/l (a curve); $c = 0.075$ g/l (b curve) and $c = 0.050$ g/l (c curve) concentration.

Respectively the duration t_p of the permanence effect is (18.5 ± 1.5) s; (10 ± 1) s and (6.5 ± 1) s.

Fig. 5 shows the graphs of $h \propto I_p(t)$ in the suspensions of $BaSO_4$ in H_2O (d curve) and Fe_2O_3 in H_2O (e curve) with the same $c = 0.50$ g/l concentration: the duration t_p of the whose permanence effect is (14 ± 1) s and (9.5 ± 1) s respectively.

In order to state the analytic equation (1) following which I_p decays in time, the graphs of Fig. 6 facilitate the solution. They show the log h values against time, relatively to all the curves of Fig. 4 and 5. Taking into account the experimental error, the patterns of these logarithmical curves are straight lines and therefore we can deduce that the diffracted light intensity, remaining at the stopping of the ultrasounds, decays against time with an exponential law

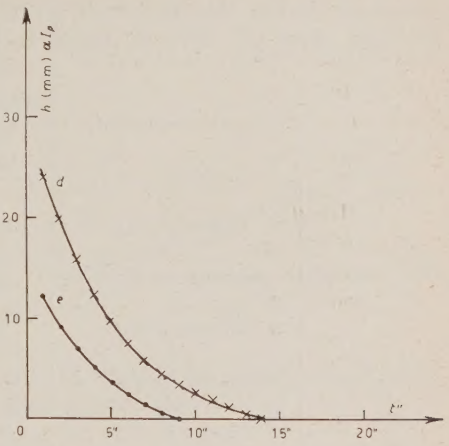

Fig. 5.

$$I_p = I_{0p} \exp[-kt] . \tag{2}$$

The slope rate of the straight lines Fig. 6 is the value of the k decay coefficient.

In the Table I the precent k values of the different substances under exami-

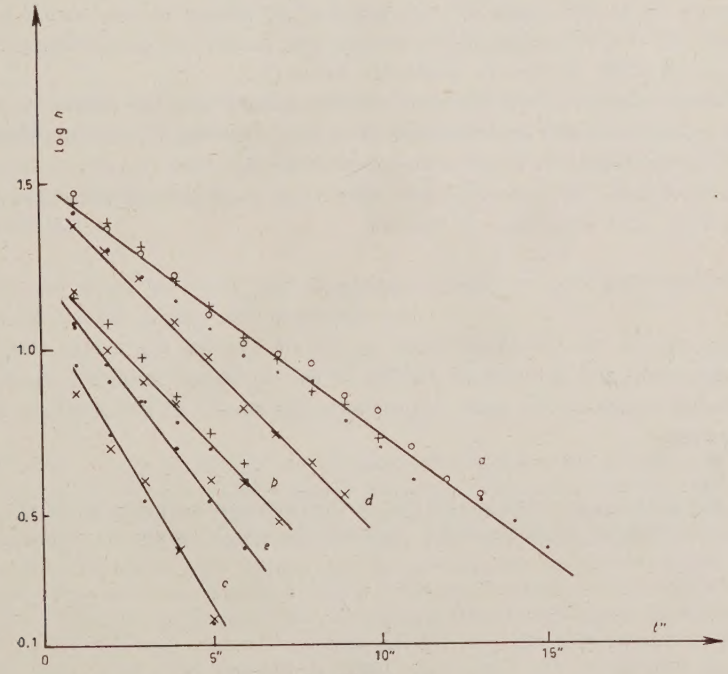

Fig. 6.

nation are shown, compared with the maximal one of the substance producing the least effect ($c = 0.050$ g/l starch in water).

TABLE I.

	c g/l	K %
Starch in H_2O	0.050	100
Starch in H_2O	0.075	58.5 ± 6
Starch in H_2O	0.100	44.0 ± 7
$BaSO_4$ in H_2O	0.50	61.0 ± 5
Fe_2O_3 in H_2O	0.50	79.5 ± 4

At this point it is suitable to note that, at the stopping of the supersonic waves, we experimentally observe, in the conditions described before, to remain a few diffracted lines only (the 3th or 4th order ones) and therefore we can suppose to be in the range of very small ν parameter values, which is characteristic of the diffracting phase grating and is directly proportional to the maximal variation of the $\Delta\mu$ refractive index (*).

In these conditions ν is certainly smaller than 2 and the diffracted orders intensity (and of course the diffracted total light quantity I_ν) can be considered directly proportional to ν and consequently to $\Delta\mu$ ([10]).

That assumed, we can moreover state that the maximal refractive index decays with time according to the law

$$\Delta\mu = \Delta\mu_0 \exp[-kt], \tag{3}$$

referring $\Delta\mu_0$ to the maximal value of $\Delta\mu$ at the instant $t = 0$, when the ultrasonics stop and a maximal density of the particles' number is reached in the parallel planes at the same $\lambda/2$ distance, by means of the standing supersonic waves.

(*) For instance, it is well known that in the phase grating produced by the ultrasounds, assuming the refractive index changing sinusoidally across the grating, is

$$\nu = \frac{2\pi \cdot \Delta\mu \cdot L}{\lambda},$$

being L the size of the grating and λ the light wavelength.

([10]) L. BERGMANN: *Der Ultraschall*, (1949), p. 194 and 199.

Finally, we still note that the $\tau = 1/k$ values of the starch in water suspensions are directly proportional to the c concentration of the dispersed substance, as the curve a of Fig. 7 shows. In the same figure the curve b refers to $BaSO_4$ in H_2O and the curve c to Fe_2O_3 in H_2O.

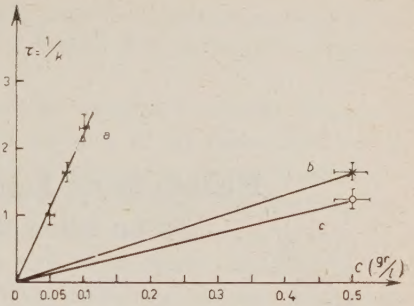

Fig. 7.

The most important point is that the corresponding straight lines are differently inclined and their rate, expressed by τ/c, does not depend upon the concentration but is a parameter depending only upon the material constituents of the medium under examination. Table II shows the τ/c values computed in this way.

TABLE II.

	τ/c
Starch in H_2O	20 ± 2
$BaSO_4$ in H_2O	3.3 ± 1
Fe_2O_3 in H_2O	2.5 ± 1

These values can represent a measurable variable of the electric interaction supposed existing [8] between the colloidal particles and the dipoles of the dispersing liquid, to which is due the variation $\Delta\mu$ of the refractive index producing the phase grating which remains at the stopping of the supersonic standing waves.

* * *

We are much indebted to Prof. CARRELLI for his able guidance and precious discussions during the present work.

RIASSUNTO

In questo lavoro viene descritto un dispositivo sperimentale realizzato per misurare la legge di diminuzione dell'intensità della luce diffratta che rimane al cessare degli ultrasuoni nelle soluzioni colloidali che presentano l'effetto. Viene sperimentalmente stabilito che tale intensità diminuisce nel tempo con legge esponenziale e la costante K di decadimento per le varie sostanze risulta inversamente proporzionale alla concentrazione c della sostanza dispersa. Il valore del prodotto Kc dipende solo dalle sostanze in esame e rappresenta un parametro che dà una misura dell'interazione elettrostatica tra le particelle in sospensione ed i dipoli del liquido, a cui è dovuto l'effetto di persistenza della luce.

IL NUOVO CIMENTO Vol. IV, N. 4 1° Ottobre 1956

Multiple Small Angle Scattering of Waves by an Inhomogeneous Medium.

P. Gosar

Institut za Elektrozveze - Ljubljana, Yugoslavia

(ricevuto il 21 Maggio 1956)

Summary. — Proceeding from the scalar wave equation the problem of the multiple small angle scattering by an inhomogeneous medium with very small fluctuations of the refractive index is solved. The theory involves an extension of the work of Debye and Bueche on the scattering of light by an amorphous solid for the case, where the Rayleigh-Gans-Born approximation is no more valid. A generalized autocorrelation function $\gamma(\boldsymbol{r}, \boldsymbol{s})$ considers the phase shift of the plane light wave passing through the particular fluctuation of the refractive index. It is a function of the correlation distance vector $\boldsymbol{r}$ and of the unit wave normal $\boldsymbol{s}$. The theory is applicable to dense systems, where « corpuscular » theories fail to be admissible.

1. – Introduction.

In this paper we shall treat the multiple scattering of light waves in passing a parallel beam of light through a thick sheet of inhomogeneous medium. We assume that the medium is non-absorbing and that the differences of the refractive indices between differents parts of the medium are very small. Further the extensions of single domains of the fluctuations of the refractive index are great in comparison with the wave length.

The example for such an inhomogeneous medium are the Christansen filter, chromatic emulsions, a turbulent atmosphere, inhomogeneous solids, etc.

If we know the dielectric constant for each point of the medium, the problem of the multiple scattering reduces to solve the wave equation with appropriate boundary conditions. Actually the solution is too difficult. In

practice we also don't know the exact values of the dielectric constant for all points of the medium. We can have only statistical data for the fluctuations of the dielectric constant.

The multiple scattering by inhomogeneous medium is usually treated in another way. The medium is divided in domains of the fluctuations of the refractive index. Single domains represent scattering centres or scatterers of light. The division of the medium is not always possible. This depends from the nature of the inhomogeneous medium. Construction is actually only then possible, if the fluctuations of the refractive index from average value are concentrated about certain one from another separated points. If the distances between particular scattering centers are great enough, the interference effects between the light waves scattered by the different centers can be neglected. In this case the multiple scattering problem is solved by the multiple convolution of the angular distribution of the intensity of light scattered by single isolated centers. To evaluate the angular distribution of the light scattered by the inhomogeneous medium we must first solve the scattering problem for single centers surrounded with the infinite homogeneous medium.

On this base are founded the theories of Wentzel [1], Bothe [2], Williams [3], Rossi-Greisen [4], Molière [5-7], Dexter-Beeman [8], Snyder-Scott [9], etc. These theories of the multiple scattering are called « corpuscular » because they are derived from the idea of the geometrical paths of the particles and neglect their wave nature. The above theories deal with the multiple scattering of electrons passing through a thin metal sheet, further with the multiple small angle scattering of X-rays, with the scattering of cosmic rays, etc.

If a system of scattering centers is dense, i.e. the distances between the neighbouring scatterers are very small, the mutual influence of scatterers cannot be neglected.

We shall treat the problem of a dense system in the case of very small fluctuations of the refractive index and, if the dimensions of the scattering centers are great in comparison with the wave length. A similar case of the propagation of scalar waves through an inhomogeneous medium, consisting of randomly distributed isotropically scattering point scatterers, was discussed

[1] G. Wentzel: *Ann. Phys.* (4), *Lpz.*, **69**, 335 (1922).
[2] W. W. Bothe: *Zeits. f. Phys.*, **54**, 161 (1929).
[3] E. J. Williams: *Proc. Roy. Soc.*, A **169**, 531 (1939).
[4] B. Rossi and K. Greisen: *Rev. Mod. Phys.*, **13**, 240 (1941).
[5] G. Molière: *Zeits. f. Naturf.*, **2***a*, 133 (1947).
[6] G. Molière: *Zeits. f. Naturf.* **3***a*, 78 (1948).
[7] G. Molière: *Zeits. f. Naturf.*, **10***a*, 177 (1955).
[8] D. L. Dexter and W. W. Beeman: *Phys. Rev.*, **76**, 1783 (1949).
[9] S. Snyder and W. T. Scott: *Phys. Rev.*, **76**, 220 (1949).

by FOLDY [10]. Recently LAX [11,12] extended and completed the Foldy's theory for the case of different types of scattering centers and theirs distribution in space. EKSTEIN's work [13] on the solution of the Schrödinger wave equation for the system of scattering centers is also relative to our problem. In our attack of the multiple scattering problem we used some ideas of FOLDY, LAX and EKSTEIN, as it will be seen.

2. – Theory.

A plane light wave, which propagates in an optically homogeneous infinite medium in the direction of the axis z of the space co-ordinate system, falls upon a planparallel sheet of the inhomogeneous medium. The boundary planes of this medium are parallel to the co-ordinate plane (x, y) and cut the axis z at $z = 0$ and $z = d$. The area of the sheet is S_0.

We can assume due to the small fluctuations of the refractive index in the inhomogeneous medium that the light wave in the sheet satisfies the scalar wave equation instead of the vector wave equation

$$\Delta\psi(\boldsymbol{r}) + k^2(\boldsymbol{r})\psi(\boldsymbol{r}) = 0 \,. \tag{1}$$

Function $\psi(\boldsymbol{r})$ represents the light wave. Wave number $k(\boldsymbol{r}) = 2\pi n(\boldsymbol{r})/\lambda$ [$n(\boldsymbol{r})$ = refractive index, λ = wave length] is a function of the position vector $\boldsymbol{r}$.

The boundary condition for the solution of this differential equation is as follows: At great distances from the sheet, that is from the center of the co-ordinate system, the function $\psi(\boldsymbol{r})$ must represent the plane incident wave and the divergent scattered wave, the amplitude of which varies with the angle of scattering θ. For such a point $\boldsymbol{R} = (X, Y, Z)$ this boundary condition can be written in a mathematical form

$$\psi(\boldsymbol{R}) \approx \exp[ik_0 Z] + f(\theta)\frac{\exp[ik_0 R]}{R} \,. \tag{2}$$

$f(\theta)$ is the amplitude function of the scattered wave, where the scattering angle θ is the angle between the directions of the position vector $\boldsymbol{R}$ and the axis z. The constant $k_0 = 2\pi n_0/\lambda$ is a wave number of the homogeneous medium surrounding the sheet. The value of the refractive index $n_0 = \sqrt{\varepsilon_0}$

(10) L. FOLDY: *Phys. Rev.*, **67**, 107 (1945).
(11) M. LAX: *Phys. Rev.*, **85**, 621 (1952).
(12) M. LAX: *Rev. Mod. Phys.*, **23**, 287 (1951).
(13) H. EKSTEIN: *Phys. Rev.*, **83**, 721 (1951).

will be later chosen in such a manner to facilitate our calculations. The choice of the refractive index n_0 of the homogeneous medium is not essential for the solution of the problem. We shall see that it is advisable to take the dielectric constant ε_0 to be complex. Thus we put

$$\varepsilon_0 = \langle\varepsilon\rangle + i\varkappa\,, \tag{3}$$

where $\langle\varepsilon\rangle$ is the average value of the dielectric constant $\varepsilon(\boldsymbol{r})$ of the inhomogeneous medium and $\varkappa$ is some small positive real constant. Further we write

$$k_0 = k' + i\frac{\mu}{2}\,, \tag{4}$$

where $k' = 2\pi\sqrt{\langle\varepsilon\rangle}/\lambda$ and $\mu = 2\pi\varkappa/\lambda\sqrt{\langle\varepsilon\rangle}$. The homogeneous medium surrounding the sheet absorbs the light waves. The absorption coefficient is μ.

Postulating that $\psi(\boldsymbol{r})$ and its first derivatives are continuous in all points of the space, the integral form of the equation (1) is

$$\psi(\boldsymbol{r}_1) = \exp[ik_0 z_1] - \frac{1}{4\pi}\int_V \frac{\exp[ik_0 r_{12}]}{r_{12}}[k_0^2 - k^2(\boldsymbol{r}_2)]\psi(\boldsymbol{r}_2)\,\mathrm{d}\tau_2 \tag{5}$$

[MOTT (14)]. r_{12} is the distance between the points $\boldsymbol{r}_1$ and $\boldsymbol{r}_2$ and $\mathrm{d}\tau_2$ is a volume element around the point $\boldsymbol{r}_2$. The integral extends only throughout the volume of the inhomogeneous medium V, because the integrand is in the outer space equal to zero.

Only the values of $\psi(\boldsymbol{r})$ at great distances R from the inhomogeneous medium are of the interest to us. In this case the equation (5) can be simplified. If $\boldsymbol{s}$ is the unit vector of the direction of the observation point $\boldsymbol{R}$, we have in the first approximation

$$\psi(\boldsymbol{R}) \approx \exp[ik_0 Z] - \frac{\exp[ik_0 R]}{4\pi R}\int_V \exp[-ik_0\boldsymbol{s}\cdot\boldsymbol{r}_2][k_0^2 - k^2(\boldsymbol{r}_2)]\psi(\boldsymbol{r}_2)\,\mathrm{d}\tau_2\,. \tag{6}$$

Hence,

$$f(\theta) = -\frac{1}{4\pi}\int_V \exp[-ik_0\boldsymbol{s}\cdot\boldsymbol{r}_2][k_0^2 - k^2(\boldsymbol{r}_2)]\psi(\boldsymbol{r}_2)\,\mathrm{d}\tau_2\,. \tag{7}$$

The expression in the square bracket of the integral (7) can be written as

$$k_0^2 - k^2(\boldsymbol{r}_2) = \left(\frac{2\pi}{\lambda}\right)^2[\varepsilon_0 - \varepsilon(\boldsymbol{r}_2)] = -\left(\frac{2\pi}{\lambda}\right)^2 \Delta\varepsilon(\boldsymbol{r}_2)\,, \tag{8}$$

(14) N. F. MOTT and H. S. W. MASSEY: *The Theory of Atomic Collisions* (London, 1949), p. 116.

where $\Delta\varepsilon(\boldsymbol{r}_2)$ means the difference between the dielectric constant in the point $\boldsymbol{r}_2$ and the dielectric constant ε_0 of the surrounding medium. The differential cross-section of the inhomogeneous medium of thickness d for the scattering of light into the direction $\boldsymbol{s}$ is thus

$$(9) \quad \sigma(\boldsymbol{s}, d) = \sigma(\theta, d) = f(\theta) f^*(0) =$$

$$= \frac{\pi^2}{\lambda^4} \int_{\dot{V}} \int_{\dot{V}} \exp\left[\frac{\mu}{2} \boldsymbol{s} \cdot (\boldsymbol{r}_1 + \boldsymbol{r}_2)\right] \exp[-ik' \boldsymbol{s} \cdot (\boldsymbol{r}_1 - \boldsymbol{r}_2)] \Delta\varepsilon(\boldsymbol{r}_1) \Delta\varepsilon^*(\boldsymbol{r}_2) \psi(\boldsymbol{r}_1) \psi^*(\boldsymbol{r}_2) \, \mathrm{d}\tau_1 \, \mathrm{d}\tau_2 \, .$$

To this point the derivation is exact and the differential cross-section can be accurately evaluated, if we know the internal field $\psi(\boldsymbol{r})$ in the sheet. This is unknown. We make use of the idea of the average field introduced by FOLDY and LAX. We distinguish a macrostructure and microstructure of the internal field $\psi(\boldsymbol{r})$. In the macrostructural description of $\psi(\boldsymbol{r})$ we don't take into account the small local variations of $\psi(\boldsymbol{r})$ due to the single fluctuations of the refractive index. Thus from the macrostructural point of view we can consider the field in the vicinity of some chosen point $\boldsymbol{r}_0$ to be composed of plane waves, i.e.

$$(10) \qquad [\psi(\boldsymbol{r})]_{\text{macro.}} = \int_{\dot{\Omega}} a(\boldsymbol{s}, z_0) \exp[ik' \boldsymbol{s} \cdot \boldsymbol{r}] \, \mathrm{d}\Omega \, .$$

The integration extends over the whole space angle $\Omega = 4\pi$. The amplitude and the phase of the plane waves are given by $a(\boldsymbol{s}, z_0)$. This is a function of the unit wave normal $\boldsymbol{s}$ and of the position vector $\boldsymbol{r}$. It follows from the symmetry considerations that $a(\boldsymbol{s}, z_0)$ is a function only of the co-ordinate z_0 of the vector $\boldsymbol{r}_0$. The wave number of the macrostructural plane waves is chosen to be equal to the average value of $k(\boldsymbol{r})$ in the inhomogeneous medium, i.e. to k'. The above expression for $[\psi(\boldsymbol{r})]_{\text{macro.}}$ is reasonable only, if the function $a(\boldsymbol{s}, z_0)$ changes very slowly with the position vector $\boldsymbol{r}_0$. This is in our case true and we can assume $a(\boldsymbol{s}, z_0)$ to be nearly constant in a space, the dimensions of which are great in comparison with the dimensions of the scattering centres and their distances from neighboring centers.

The microstructural description of the field $\psi(\boldsymbol{r})$ considers the small deviations of $\psi(\boldsymbol{r})$ from the plane waves due to the fluctuations of the refractive index. We take into account the microstructural changes of $\psi(\boldsymbol{r})$ with a factor $g(\boldsymbol{r}, \boldsymbol{s})$, which is a function of the position vector $\boldsymbol{r}$ and of the unit wave normal $\boldsymbol{s}$ of the single macrostructural wave. The factor $g(\boldsymbol{r}, \boldsymbol{s})$ is determined so, that the real internal field can be described as

$$(11) \qquad \psi(\boldsymbol{r}) = \int_{\dot{\Omega}} a(\boldsymbol{s}, z_0) \, g(\boldsymbol{r}, \boldsymbol{s}) \exp[ik' \boldsymbol{s} \cdot \boldsymbol{r}] \, \mathrm{d}\Omega \, .$$

It is very difficult to determine the exact values of $g(\boldsymbol{r}, \boldsymbol{s})$. The essential part of our calculation is to obtain an appropriate approximation for $g(\boldsymbol{r}, \boldsymbol{s})$. We assume that the inhomogeneous medium can be divided in isolated scattering centers and that the average value of the refractive index for single scatterers is equal to the average value of the refractive index for the whole medium. Factor $g(\boldsymbol{r}, \boldsymbol{s})$ measures the modification of the plane wave passing through the single scatterer in the direction $\boldsymbol{s}$. It is evident, that $g(\boldsymbol{r}, \boldsymbol{s})$ is a function only of the relative position of the point $\boldsymbol{r}$ to the scattering center, to which the point $\boldsymbol{r}$ belongs. $g(\boldsymbol{r}, \boldsymbol{s})$ does not depend from the absolute position of the scattering center. As the fluctuations of the refractive index are small and the dimensions of the scattering centers great, the amplitude of the wave passing through the scattering center varies very little. But the changes of the phase are important and can be determined in the first approximation by the optical path of the ray passing through the scattering center, along the line of the direction $\boldsymbol{s}$, to the point $\boldsymbol{r}$. Thus, the phase shift $\varphi(\boldsymbol{r}, \boldsymbol{s})$ for the point $\boldsymbol{r}$ and the direction $\boldsymbol{s}$ of the incident wave is given by

$$\varphi(\boldsymbol{r}, \boldsymbol{s}) = \frac{2\pi}{\lambda} \int [n(s) - \langle n \rangle] \, \mathrm{d}s \, . \tag{12}$$

This integral extends over the parameter s, which measures the distance along the line passing through the point $\boldsymbol{r}$ in the direction $\boldsymbol{s}$, from the point, where this line enters the scattering center, to the point $\boldsymbol{r}$. In the integrand $n(s)$ means the refractive index of a given point s of the line and $\langle n \rangle = \sqrt{\langle \varepsilon \rangle}$.

Neglecting the changes of the amplitude in the scattering center the correction factor $g(\boldsymbol{r}, \boldsymbol{s})$ is equal to

$$g(\boldsymbol{r}, \boldsymbol{s}) = \exp [i\varphi(\boldsymbol{r}, \boldsymbol{s})] \, . \tag{13}$$

Considering the expression (11) for the internal field $\psi(\boldsymbol{r})$ we obtain from (9) the following expression for the differential cross-section $\sigma(\boldsymbol{s}, d)$

$$\begin{aligned} \sigma(\boldsymbol{s}, d) = \frac{\pi^2}{\lambda^4} \int_{\Omega} \mathrm{d}\Omega_1 \int_{\Omega} \mathrm{d}\Omega_2 \int_{V} \int_{V} \exp \left[\frac{\mu}{2} \boldsymbol{s} \cdot (\boldsymbol{r}_1 - \boldsymbol{r}_2) \right] \exp [ik \boldsymbol{s} \cdot (\boldsymbol{r}_1 - \boldsymbol{r}_2)] \cdot \\ \cdot \exp [ik' \boldsymbol{s}_1 \cdot \boldsymbol{r}_1] \exp [-ik' \boldsymbol{s}_2 \cdot \boldsymbol{r}_2] \Delta\varepsilon(\boldsymbol{r}_1) g(\boldsymbol{r}_1, \boldsymbol{s}_1) \cdot \\ \cdot \Delta\varepsilon^*(\boldsymbol{r}_2) g^*(\boldsymbol{r}_2, \boldsymbol{s}_2) a(\boldsymbol{s}_1, z_1) a^*(\boldsymbol{s}_2, z_2) \, \mathrm{d}\tau_1 \, \mathrm{d}\tau_2 \, . \end{aligned} \tag{14}$$

Here we put $a(\boldsymbol{s}, z_0)$ from the equation (11) equal to $a(\boldsymbol{s}, z)$, what is admissible, as $a(\boldsymbol{s}, z_0)$ changes slowly with the position vector.

To an easier evaluation of this integral we choose the dielectric constant of the medium surrounding the planparallel sheet so, that the average value

of the $\Delta\varepsilon(\boldsymbol{r})g(\boldsymbol{r}, \boldsymbol{s})$, taken over the whole inhomogeneous medium, is equal to zero. This is possible only if ε_0 is complex. Taking for ε_0 the expression (3) the constant $\varkappa$ is now determined from the equation

$$\langle \Delta\varepsilon(\boldsymbol{r})g(\boldsymbol{r}, \boldsymbol{s})\rangle = \langle[\varepsilon(\boldsymbol{r}) - \langle\varepsilon\rangle]\exp[i\varphi(\boldsymbol{r}, \boldsymbol{s})]\rangle - i\varkappa\langle\exp[i\varphi(\boldsymbol{r}, \boldsymbol{s})]\rangle = 0\,. \tag{15}$$

Hence,

$$\varkappa = \frac{\langle[\varepsilon(\boldsymbol{r}) - \langle\varepsilon\rangle]\exp[i\varphi(\boldsymbol{r}, \boldsymbol{s})]\rangle}{i\langle\exp[i\varphi(\boldsymbol{r}, \boldsymbol{s})]\rangle}\,. \tag{16}$$

Now we shall show, that $[\varepsilon(\boldsymbol{r}) - \varepsilon_0]\exp[i\varphi(\boldsymbol{r}, \boldsymbol{s})]$ is imaginary and $\exp[i\varphi(\boldsymbol{r}, \boldsymbol{s})]\rangle$ is real. This is necessary since $\varkappa$ must be real.

It follows from the definition of the average value, that

$$\langle[\varepsilon(\boldsymbol{r}) - \langle\varepsilon\rangle]\exp[i\varphi(\boldsymbol{r}, \boldsymbol{s})]\rangle = \frac{1}{V}\int_V [\varepsilon(\boldsymbol{r}) - \langle\varepsilon\rangle]\exp[i\varphi(\boldsymbol{r}, \boldsymbol{s})]\,\mathrm{d}\tau\,, \tag{17}$$

where the integral extends only throughout the volume occupied by the scattering centers. Taking into account, that $\varepsilon(\boldsymbol{r})$ $\varepsilon\rangle$ is nearly equal to $2\langle n\rangle\cdot[n(\boldsymbol{r}) - \langle n\rangle]$, and considering the equation (12), we see, that the integration can be performed over one space coordinate of the direction $\boldsymbol{s}$. The above integral for a single scattering center gives

$$\int[\varepsilon(\boldsymbol{r}) - \langle\varepsilon\rangle]\exp[i\varphi(\boldsymbol{r}, \boldsymbol{s})]\,\mathrm{d}\tau = \frac{\lambda\langle n\rangle}{i\pi}\int_S \{\exp[i\varphi(\boldsymbol{\rho})] - 1\}\,\mathrm{d}S\,. \tag{18}$$

Here the integration extends over the co-ordinate plane S, perpendicular to the direction $\boldsymbol{s}$. The function $\varphi(\boldsymbol{\rho})$ in the integrand represents the total phase shift of the ray emerging from the scattering center and passing through the point of the plane S given by the position vector $\boldsymbol{\rho}$.

The integral (17) has a real value, as positive and negative values of $\varphi(\boldsymbol{\rho})$ are equally probable. Thus we proved, that $[\varepsilon(\boldsymbol{r})$ $\varepsilon_0]\exp[i\varphi(\boldsymbol{r}, \boldsymbol{s})]$ is imaginary. Similarly $\exp[i\varphi(\boldsymbol{r}, \boldsymbol{s})]\rangle$ is real, as positive and negative values of $\varphi(\boldsymbol{r}, \boldsymbol{s})$ are equally probable.

The integrand of the integral expression (14) for $\sigma(\boldsymbol{s}, d)$ contains rapidly oscillating terms. At great distances $\boldsymbol{r}_1 - \boldsymbol{r}_2$ no correlation exists between the value $\Delta\varepsilon(\boldsymbol{r}_1)g(\boldsymbol{r}_1, \boldsymbol{s}_1)$ and $\Delta\varepsilon(\boldsymbol{r}_2)g(\boldsymbol{r}_2, \boldsymbol{s}_2)$. Thus for the evaluation of the integral only the average value of the product $\Delta\varepsilon(\boldsymbol{r})g(\boldsymbol{r}, \boldsymbol{s})$ is important, if $|\boldsymbol{r}_1 - \boldsymbol{r}_2|$ is great. As this average value is zero, we may, for the calculation of $\sigma(\boldsymbol{s}, d)$, consider only the distances $|\boldsymbol{r}_1 - \boldsymbol{r}_2|$, which are of the order of magnitude of the dimensions of the scattering centers.

Similarly only those values of the integrand, which belong to the small

values of s_1 s_2 , contribute mostly to the result of the integration. Thus we may exchange in all non-oscillating and slowly variable terms of the integrand s_2 with s_1.

Taking into account the above considerations and introducing new variables $r_2 = r_2$ and $r = r_1 - r_2$ in (14) we obtain

$$(19)\quad \sigma(s, d) =$$

$$= \frac{\pi^2}{\lambda^4}\int_{\Omega} \mathrm{d}\Omega_1 \int_{\Omega} \mathrm{d}\Omega_2 \int_{V} \mathrm{d}\tau_2\, a(s_1, z_2)\, a^*(s_1, z_2) \exp[\mu s \cdot r_2] \exp[\quad ik\,(s_2 \quad s_1)\cdot r_2] \cdot$$

$$\cdot \int \Delta\varepsilon(r_2 + r)\, g(r_2 - r, s_1)\, \Delta\varepsilon^*(r_2)\, g^*(r_2, s_1) \exp[-ik'(s - s_1)\cdot r]\, \mathrm{d}\tau\ .$$

The first volume integral extends throughout the volume V of the inhomogeneous medium and the second throughout the volume, defined by all possible differences $r_1 - r_2$.

If we restrict only to small angle scatterings, which largely predominate in an inhomogeneous medium of our type, we can put $s \cdot r_2$ to be equal to z_2. Further we see, that the vector $s_2 \quad s_1$ is nearly exactly perpendicular to the axis z. As in an inhomogeneous medium with great scattering centers in comparison with the wave length no correlation exists between the value of the highly oscillating term $\exp[-ik'(s_2 - s_1)\cdot r_2]$ and the value of $\Delta\varepsilon(r_2 + r)\cdot g(r_2 - r, s_1)\, \Delta\varepsilon^*(r_2) g^*(r_2, s_1)$ for different r_2, we can substitute in the second volume integral of (19) $\Delta\varepsilon(r_2 - r) g(r_2 - r, s_1)\, \Delta\varepsilon^*(r_2) g^*(r_2, s_1)$ with the average value $\overline{\Delta\varepsilon(r_2 - r) g(r_2 - r, s_1)\, \Delta\varepsilon^*(r_2) g^*(r_2, s_1)}$ taken over the whole inhomogeneous medium.

Thus, introducing cylindrical co-ordinates $x_2 = \eta \cos\varphi$, $y_2 = \eta \sin\varphi$, $z_2 = z$ in (19), we obtain

$$(20)\quad \sigma(s, d) =$$

$$= \frac{\pi^2}{\lambda^4}\int_{\Omega} \mathrm{d}\Omega_1 \int \overline{\Delta\varepsilon(r_2 - r) g(r_2 - r, s_1)\, \Delta\varepsilon^*(r_2) g^*(r_2, s_1)} \exp[\quad ik\,(s \quad s_1)\cdot r]\, \mathrm{d}\tau \cdot$$

$$\cdot \int_{\Omega} \mathrm{d}\Omega_2 \int_{V} a(s_1, z)\, a^*(s_1, z) \exp[\mu z] \exp[-ik'\vartheta\eta \cos(\varphi - \varphi_0)]\, \eta\, \mathrm{d}\eta\, \mathrm{d}\varphi\, \mathrm{d}z\ .$$

The angle φ_0 is the azimuth of the vector $s_2 \quad s_1$ and ϑ is the angle between the directions s_1 and s_2 or $|s_2 - s_1| \approx \vartheta$. The cross-section of the inhomogeneous medium being a circle of radius b, i.e. $b^2\pi = S_0$, the last integral after the integration over φ and η gives

$$(21)\qquad \frac{2\pi b J_1(k'\vartheta b)}{k'\vartheta} \int_0^d a(s_1, z)\, a^*(s_1, z) \exp[\mu z]\, \mathrm{d}z\ .$$

We now substitute the integration over the whole space angle $\Omega = 4\pi$ with the integration over the tangential plane, as the term $J_1(k'\vartheta b)/\vartheta$ rapidly diminishes with the angle ϑ. So we have

$$\int_{\Omega} \frac{J_1(k'\vartheta b)}{\vartheta}\,\mathrm{d}\Omega_2 = 2\pi\int_0^{\infty} J_1(k'\vartheta b)\,\mathrm{d}\vartheta = \frac{2\pi}{k'b}\,. \tag{22}$$

Hence,

$$\sigma(\boldsymbol{s}, d) = \frac{\pi^2}{\lambda^2\langle\varepsilon\rangle}\int_{\Omega}\mathrm{d}\Omega_1\int\langle\Delta\varepsilon(\boldsymbol{r}_2+\boldsymbol{r})g(\boldsymbol{r}_2+\boldsymbol{r}, \boldsymbol{s}_1)\Delta\varepsilon^*(\boldsymbol{r}_2)g^*(\boldsymbol{r}_2, \boldsymbol{s}_1)\rangle\cdot \tag{23}$$

$$\cdot\exp\left[-ik'(\boldsymbol{s}-\boldsymbol{s}_1)\cdot\boldsymbol{r}\right]\mathrm{d}\tau\int_0^{d} a(\boldsymbol{s}_1, z)a^*(\boldsymbol{s}_1, z)\exp\left[\mu z\right]\mathrm{d}z\,.$$

The final result is independent from the choice of the shape of the cross-section of the inhomogeneous medium.

For the further calculation of $\sigma(\boldsymbol{s}, d)$ it is reasonable to introduce the autocorrelation function $\gamma(\boldsymbol{r}, \boldsymbol{s})$ for the quantity $\Delta\varepsilon(\boldsymbol{r})g(\boldsymbol{r}, \boldsymbol{s})$ defined by

$$\gamma(\boldsymbol{r}, \boldsymbol{s}) = \frac{\langle\Delta\varepsilon(\boldsymbol{r}_1)g(\boldsymbol{r}_1, \boldsymbol{s})\Delta\varepsilon^*(\boldsymbol{r}_1+\boldsymbol{r})g^*(\boldsymbol{r}_1+\boldsymbol{r}, \boldsymbol{s})\rangle}{\Delta\varepsilon(\boldsymbol{r}_1)\Delta\varepsilon^*(\boldsymbol{r}_1)\rangle} = \tag{24}$$

$$= \frac{\int\Delta\varepsilon(\boldsymbol{r}_1)g(\boldsymbol{r}_1, \boldsymbol{s})\Delta\varepsilon^*(\boldsymbol{r}_1+\boldsymbol{r})g^*(\boldsymbol{r}_1+\boldsymbol{r}, \boldsymbol{s})\mathrm{d}\tau_1}{\int_{\tau}\Delta\varepsilon(\boldsymbol{r}_1)\Delta\varepsilon^*(\boldsymbol{r}_1)\mathrm{d}\tau_1}\,.$$

The integration extends throughout the whole volume of the inhomogeneous medium.

This autocorrelation function is an extension of the autocorrelation function $\gamma(r)$ for $\varepsilon(\boldsymbol{r}) = \varepsilon$, which DEBYE and BUECHE [15] used in the calculation of the scattering of light by amorphous solids. The Debye and Bueche autocorrelation function is applicable only in the limits of the validity of the Rayleigh-Gans-Born approximation.

From the expression (24) it follows, that $\gamma(\boldsymbol{r}, \boldsymbol{s})$ is a function only of the absolute value $r = |\boldsymbol{r}|$ and of the angle β between $\boldsymbol{r}$ and $\boldsymbol{s}$. We can write $\gamma(\boldsymbol{r}, \boldsymbol{s}) = \gamma(r, \cos\beta)$. Further $\gamma^*(r, \cos\beta) = \gamma(r, -\cos\beta)$ and $\gamma(0, 0) = 1$. If r increases beyond the average dimension of the scattering centers, the autocorrelation function $\gamma(\boldsymbol{r}, \boldsymbol{s})$ falls rapidly to zero.

In the evaluation of $\sigma(\boldsymbol{s}, d)$ we shall use the following transformation of $\gamma(\boldsymbol{r}, \boldsymbol{s})$

$$E(\boldsymbol{s}, \boldsymbol{s}_1) = \int\exp\left[-ik'(\boldsymbol{s}-\boldsymbol{s}_1)\cdot\boldsymbol{r}\right]\gamma(\boldsymbol{r}, \boldsymbol{s}_1)\,\mathrm{d}\tau\,. \tag{25}$$

[15] P. DEBYE and A. M. BUECHE: *Journ. Appl. Phys.*, **20**, 518 (1949).

The integration extends over all space. As we deal only with small angle scatterings, we put $\boldsymbol{s} - \boldsymbol{s}_1 = \vartheta$, where ϑ is as above the angle between $\boldsymbol{s}$ and $\boldsymbol{s}_1$. Then we introduce the polar coordinate system with the axis z' in the direction $\boldsymbol{s}_1$. Taking into account, that the vector $\boldsymbol{s} - \boldsymbol{s}_1$ lies nearly in the plane (x', y') of the new coordinate system, we obtain

$$(26)\quad E(\boldsymbol{s}, \boldsymbol{s}_1) = E(\vartheta) = \int_0^\infty \int_0^\pi \int_0^{2\pi} \exp[-ik'\vartheta r \sin\beta \cos q]\,\gamma(r, \cos\beta)\, r^2 \sin\beta \,\mathrm{d}r\,\mathrm{d}\beta\,\mathrm{d}q = 2\pi \int_0^\infty \int_0^\pi J_0(k'\vartheta r \sin\beta)\,\gamma(r, \cos\beta)\, r^2 \sin\beta \,\mathrm{d}r\,\mathrm{d}\beta\,.$$

$E(\vartheta)$ is real. This follows from the relation $\gamma(r, -\cos\beta) = \gamma^*(r, \cos\beta)$.

Using the autocorrelation function $\gamma(\boldsymbol{r}, \boldsymbol{s})$ the equation (23) now reads.

$$(27)\quad \sigma(\boldsymbol{s}, d) = \frac{\pi^2 \langle \Delta\varepsilon(\boldsymbol{r})\, \Delta\varepsilon^*(\boldsymbol{r})\rangle}{\lambda^2\, \varepsilon} \int_\Omega \mathrm{d}\Omega_1 E(\boldsymbol{s}, \boldsymbol{s}_1) \int_0^d a(\boldsymbol{s}_1, z)\, a^*(\boldsymbol{s}_1, z) \exp[\mu z]\,\mathrm{d}z\,.$$

This equation for the scattering cross-section postulates the knowledge of the properties of the inhomogeneous medium given by ε, $\Delta\varepsilon(\boldsymbol{r})\,\Delta\varepsilon^*(\boldsymbol{r})$ and by the autocorrelation function $\gamma(\boldsymbol{r}, \boldsymbol{s})$: besides we must know the amplitudes of the macrostructural plane waves in the medium.

Taking some new approximations we proceed in the following way: We assume, that the amplitudes of the macrostructural plane waves are independent of the thickness d of the inhomogeneous medium. This assumption is admissible, as we deal with small angle scatterings. The light waves scattered at points with $z > z_0$ have very little influence on the field $\psi(\boldsymbol{r})$ at points with $z = z_0$. With this assumption we obtain, by differentiation of the equation (27) with respect to d, the result

$$(28)\quad \frac{\partial\sigma(\boldsymbol{s}, d)}{\partial d} = \frac{\pi^2 \langle \Delta\varepsilon(\boldsymbol{r})\, \Delta\varepsilon^*(\boldsymbol{r})\rangle}{\lambda^2 \langle\varepsilon\rangle} \exp[\mu d] \int_\Omega a(\boldsymbol{s}_1, d)\, a^*(\boldsymbol{s}_1, d)\, E(\boldsymbol{s}, \boldsymbol{s}_1)\,\mathrm{d}\Omega_1\,.$$

Now we can get by use of the Kirchhoff-Huygens principle the correlation between the amplitude of the waves emerging from the inhomogeneous medium $a(\boldsymbol{s}, d)\, a^*(\boldsymbol{s}, d)$ and the scattering cross-section. The field at the point of observation $\boldsymbol{R}$ can be derived from the field in the plane $z = d$ by the equation

$$(29)\quad \psi(\boldsymbol{R}) = \frac{k_0}{2\pi i} \int_S \frac{\exp[ik_0 r_{12}]}{r_{12}} \cos(n, r_{12})\, \psi(\boldsymbol{r}_2)\,\mathrm{d}S$$

[SOMMERFELD [16]].

[16] A. SOMMERFELD: *Optik* (Wiesbaden, 1948), p. 204.

The integration extends over the whole plane $z = d$. Here r_{12} denotes the distance between the point $\boldsymbol{R}$ and some point $\boldsymbol{r}$ in the integration plane. (n, r_{12}) is the angle between the normal on the plane S and the direction of the distance vector $\boldsymbol{r}_{12}$. As the observation point is very distant, we put $r_{12} = R - \boldsymbol{s}_1 \cdot \boldsymbol{r}_2$. Further we take, due to small angle scattering, $\cos(n, r_{12}) = 1$. Considering only the scattered waves and neglecting the diffraction of the incident plane wave on the edge of the inhomogeneous medium we have

$$\psi(\boldsymbol{R}) = \frac{k_0}{2\pi i} \frac{\exp[ik_0 R]}{R} \int_S \exp[-ik_0 \boldsymbol{s} \cdot \boldsymbol{r}_2] \psi(\boldsymbol{r}_2) \, \mathrm{d}S \,. \tag{30}$$

Now the integration extends only over the area S_0 of the surface of the inhomogeneous medium. We assume for $\psi(\boldsymbol{r})$ the field of plane waves emerging from the inhomogeneous medium in the point $\boldsymbol{r}$ of the surface S. Thus,

$$\psi(\boldsymbol{r}_2) = \int_\Omega a(\boldsymbol{s}, d) \exp[ik' \boldsymbol{s} \cdot \boldsymbol{r}_2] \, \mathrm{d}\Omega \,. \tag{31}$$

Hence,

$$\psi(\boldsymbol{R}) = \frac{k_0}{2\pi i} \frac{\exp[ik_0 R]}{R} \int_\Omega \mathrm{d}\Omega_1 a(\boldsymbol{s}_1, d) \int_S \exp\left[\frac{\mu}{2} \boldsymbol{s} \cdot \boldsymbol{r}_2\right] \exp[-ik'(\boldsymbol{s} - \boldsymbol{s}_1) \cdot \boldsymbol{r}_2] \, \mathrm{d}S \,. \tag{32}$$

The exponential term $\exp[(\mu/2)\boldsymbol{s} \cdot \boldsymbol{r}_2]$ in (32) is nearly equal to $\exp[(\mu/2)d]$. Considering this and the fact, that the vector $\boldsymbol{s} - \boldsymbol{s}_1$ lies approximately in the plane (x, y), we obtain by the integration over S the following expression for $\psi(R)$

$$\psi(\boldsymbol{R}) = \frac{\exp[ik_0 R]}{R} \frac{k_0 b}{ik'} \exp\left[\frac{\mu}{2} d\right] \int_\Omega a(\boldsymbol{s}_1, d) \frac{J_1(k' \vartheta b)}{\vartheta} \, \mathrm{d}\Omega_1 \,, \tag{33}$$

where ϑ is the angle between $\boldsymbol{s}$ and $\boldsymbol{s}_1$. We see, that only values of $a(\boldsymbol{s}_1, d)$ with $\boldsymbol{s}_1$ near to $\boldsymbol{s}$ contribute mostly to the integral in (33). As $a(\boldsymbol{s}, d)$ varies little with $\boldsymbol{s}$, this integral can be performed so, that we put $a(\boldsymbol{s}_1, d)$ before the integral sign. Thus we get

$$\psi(\boldsymbol{R}) = \frac{\lambda}{i\langle n \rangle} a(\boldsymbol{s}, d) \exp\left[\frac{\mu}{2} d\right] \frac{\exp[ik_0 R]}{R} \,. \tag{34}$$

Here we approximate k_0 with k'.

Hence,

$$\sigma(\boldsymbol{s}, d) = \frac{\lambda^2}{\langle \varepsilon \rangle} a(\boldsymbol{s}, d) a^*(\boldsymbol{s}, d) \exp[\mu d] \,. \tag{35}$$

Combining (28) with (35) we obtain the following equation for $\sigma(\boldsymbol{s}, d)$

$$\frac{\partial\sigma(\boldsymbol{s}, d)}{\partial d} = \frac{\pi^2\langle\Delta\varepsilon(\boldsymbol{r})\,\Delta\varepsilon^*(\boldsymbol{r})\rangle}{\lambda^4}\int_{\Omega}\sigma(\boldsymbol{s}_1, d)\,E(\boldsymbol{s}, \boldsymbol{s}_1)\,\mathrm{d}\Omega_1\,. \tag{36}$$

This is a sort of transport equation and can be solved by the use of the Bessel-Fourier transformation. The solution of this equation is

$$\sigma(\vartheta, d) = \frac{1}{2\pi}\int_0^{\infty}\exp\left[dH(\alpha)\right]J_0(\vartheta\alpha)\alpha\,\mathrm{d}\alpha\,, \tag{37}$$

where $H(\alpha)$ is the Bessel-Fourier transformation of the function

$$h(\vartheta) = \frac{\pi^2\langle\Delta\varepsilon(\boldsymbol{r})\,\Delta\varepsilon^*(\boldsymbol{r})\rangle}{\lambda^4}\,E(\vartheta)\,, \tag{38}$$

i.e.

$$H(\alpha) = 2\pi\int_0^{\infty}h(\vartheta)J_0(\alpha\vartheta)\vartheta\,\mathrm{d}\vartheta\,. \tag{39}$$

The integration constant $1/2\pi$ in the expression (37) is chosen so, that

$$\int_0^{\infty}\sigma(\vartheta, 0)2\pi\vartheta\,\mathrm{d}\vartheta = 1\,. \tag{40}$$

At the distance R from the sheet of the inhomogeneous medium the light flux per unit of space angle in the direction $\boldsymbol{s}$ is equal to

$$I(\vartheta, d) = \frac{I_0}{2\pi}\exp\left[-\mu R\right]\int_0^{\infty}\exp\left[dH(\alpha)\right]J_0(\vartheta\alpha)\alpha\,\mathrm{d}\alpha\,, \tag{41}$$

where I_0 is the flux of the incident light. The term $\exp[-\mu R]$ measures the extinction of light waves in the inhomogeneous medium and the absorption in the surrounding medium and must here be taken into account, as the differential cross-section (37) is calculated for the reference point $R = 0$.

We surrounded the inhomogeneous medium with the special light absorbing medium only to facilitate our calculations. If we now put $\varkappa = 0$, we obtain with nearly the same approximation

$$I(\vartheta, d) = \frac{I_0}{2\pi}\exp\left[-\mu d\right]\int_0^{\infty}\exp\left[dH(\alpha)\right]J_0(\vartheta\alpha)\alpha\,\mathrm{d}\alpha\,. \tag{42}$$

In this case the light is nowhere absorbed. Because of this $H(0)$ must be equal to μ. This can be shown to be true. Thus the final formula for the angular distribution of the scattered light reads

$$I(\theta, d) = \frac{I_0}{2\pi}\int_0^\infty \exp[d(H(\alpha) - H(0))] J_0(\theta\alpha)\alpha\,\mathrm{d}\alpha\,. \tag{43}$$

3. – Comparison with « Corpuscular » Theories.

In the case of great distances between scattering centers our theory is in agreement with the « corpuscular » theories.

To prove this, we put in (25) for $\gamma(\boldsymbol{r}, \boldsymbol{s})$ the integral expression (23) and then we change the order of the integration. Thus we obtain for the function $h(\vartheta)$ the following expression

$$h(\vartheta) = \frac{\pi^2}{\lambda^4}\frac{1}{V}\int_V \mathrm{d}\tau_1\, \Delta\varepsilon(\boldsymbol{r}_1)\, g(\boldsymbol{r}_1, \boldsymbol{s}_1)\int \Delta\varepsilon^*(\boldsymbol{r}_1+\boldsymbol{r})\, g^*(\boldsymbol{r}_1+\boldsymbol{r}, \boldsymbol{s}_1)\cdot \tag{44}$$

$$\cdot \exp[-ik'(\boldsymbol{s}-\boldsymbol{s}_1)\cdot\boldsymbol{r}]\,\mathrm{d}\tau\,.$$

The extinction coefficient is here very small. We may in the equation (44) neglect the coefficient $\varkappa$. Hence, the first integration in (44), taken over the whole volume V of the inhomogeneous medium, may be taken only over the volume of the scattering centres. But the second volume integral is performed in the first approximation only over the distances of the order of the dimensions of single scattering centers. Putting the new variable $\boldsymbol{r}_2 = \boldsymbol{r}_1 - \boldsymbol{r}$ in (44) we obtain

$$h(\vartheta) = \frac{1}{V}\sum_{m=1}^{N}\left\{\frac{\pi}{\lambda^2}\int \Delta\varepsilon(\boldsymbol{r}_1)\, g(\boldsymbol{r}_1, \boldsymbol{s}_1)\exp[ik'(\boldsymbol{s}-\boldsymbol{s}_1)\cdot\boldsymbol{r}_1]\,\mathrm{d}\tau_2\right\}_m \cdot \tag{45}$$

$$\cdot\left\{\frac{\pi}{\lambda^2}\int \Delta\varepsilon^*(\boldsymbol{r}_2)\, g^*(\boldsymbol{r}_2, \boldsymbol{s}_1)\exp[-ik'(\boldsymbol{s}-\boldsymbol{s}_1)\cdot\boldsymbol{r}_2]\,\mathrm{d}\tau_2\right\}_m = \frac{1}{V}\sum_{m=1}^{N} v(\boldsymbol{s}, \boldsymbol{s}_1)\, v^*(\boldsymbol{s}, \boldsymbol{s}_1)\,.$$

The index m at the brackets signalizes, that the integration is taken over the volume of the m-th scatterer in the inhomogeneous medium. The summation runs over all N scatterers. Here we introduced a new function

$$v_m(\boldsymbol{s}, \boldsymbol{s}_1) = \frac{\pi}{\lambda^2}\int \Delta\varepsilon(\boldsymbol{r})\, g(\boldsymbol{r}, \boldsymbol{s}_1)\exp[ik'(\boldsymbol{s}-\boldsymbol{s}_1)\cdot\boldsymbol{r}]\,\mathrm{d}\tau\,. \tag{46}$$

The vector $\boldsymbol{s} - \boldsymbol{s}_1$ is nearly perpendicular to $\boldsymbol{s}_1$. Thus we may perform the

integration first over one space co-ordinate in the direction s_1 similiarly, as we made this in the equation (18). We obtain

$$v_m(\boldsymbol{s}, \boldsymbol{s}_1) = \frac{\langle n \rangle}{i\lambda} \int_S \{\exp[i\varphi(\boldsymbol{\rho})] - 1\} \exp[ik'(\boldsymbol{s} - \boldsymbol{s}_1)\cdot\boldsymbol{\rho}]\, \mathrm{d}S\,, \tag{47}$$

where S, $\boldsymbol{\rho}$, $\varphi(\boldsymbol{\rho})$ have already known meaning.

The formula (47) is nothing else but the expression for the Fraunhofer diffraction on the plane phase screen with the phase shift given by $\varphi(\boldsymbol{\rho})$. See MOLIÈRE [5]! Thus the expression (47) is a solution of the scattering problem for a single isolated scattering center. This solution is based on the idea, that the light wave is shifted in the phase by $\varphi(\boldsymbol{\rho})$ in passing through the scattering center. So, the differential scattering cross section $\sigma_m(\boldsymbol{s}, \boldsymbol{s}_1)$ for the m-th scattering center is $\sigma_m(\boldsymbol{s}, \boldsymbol{s}_1) = v_m(\boldsymbol{s}, \boldsymbol{s}_1) v_m^*(\boldsymbol{s}, \boldsymbol{s}_1)$. Hence

$$h(\vartheta) = \frac{1}{V} \sum_{m=1}^{N} \sigma_m(\boldsymbol{s}, \boldsymbol{s}_1)\,. \tag{48}$$

Using this expression in (43) the resultant formula is identical with the formula given by the « corpuscular » theories.

4. – Conclusions.

Proceeding from the scalar wave equation the problem of the multiple small angle scattering in an inhomogeneous medium is solved. The solution postulates the knowledge of some properties of the inhomogeneous medium given by statistical data, i.e. $\langle \varepsilon \rangle$, $\langle \Delta\varepsilon(\boldsymbol{r})\, \Delta\varepsilon^*(\boldsymbol{r}) \rangle$ and $\gamma(\boldsymbol{r}, \boldsymbol{s})$. The autocorrelation function $\gamma(\boldsymbol{r}, \boldsymbol{s})$ is an extension of the Debye and Bueche autocorrelation function $\gamma(r)$ for the case, where the Rayleigh-Gans-Born approximation is no more admissible. The principal assumptions of the theory are as follows:

1) The inhomogeneous medium is non-absorbing and the differences of the refractive indices between different parts of the medium are very small.

2) The medium can be divided in domains of the fluctuations of the refractive index. The dimensions of domains are great in comparison with the wave length.

3) The average value of the refractive index in single domains is equal to the average value of the whole inhomogeneous medium.

4) The amplitudes of the macrostructural waves are independent from the thickness of the sheet of the inhomogeneous medium.

5) Only small angle scatterings are considered.

The assumptions 2) and 3) can be partially dropped. But then the difficulty arises in the appropriate determination of the lower limit of the integral (12) defining the phase $\varphi(\boldsymbol{r}, \boldsymbol{s})$.

The advantage of the theory is its applicability to dense systems. The theory can be used for the propagation of light through the Christiansen filter or cromatic emulsions, for the propagation of radio waves through the turbulent atmosphere, for the multiple scattering of electrons passing through a thin metal sheet, etc.

RIASSUNTO (*)

Partendo dall'equazione scalare delle onde si risolve il problema dello scattering multiplo sotto piccolo angolo da parte di un mezzo non omogeneo con piccolissime fluttuazioni dell'indice di rifrazione. La teoria comprende un'estensione del lavoro di Debye e Bueche sullo scattering della luce da parte di un solido amorfo per il caso in cui l'approssimazione di Rayleigh-Gans-Born non è più valida. L'na funzione di autocorrelazione $\gamma(\boldsymbol{r}, \boldsymbol{s})$ tien conto dello spostamento di fase dell'onda luminosa piana passante per una data fluttuazione dell'indice di rifrazione. Si tratta di una funzione del vettore della distanza di correlazione $\boldsymbol{r}$ e della normale unitaria $\boldsymbol{s}$ all'onda. La teoria è applicabile a sistemi densi in cui le teorie « corpuscolari » cessano di essere ammissibili.

IL NUOVO CIMENTO Vol. IV, N. 4 1° Ottobre 1956

Analysis of an Electron Shower Associated with a Very Energetic He Nucleus.

N. SEEMAN and R. G. GLASSER

Nucleonics Division Naval Research Laboratory - Washington D.C.

(ricevuto il 26 Maggio 1956)

Summary. — An event has been observed which is interpreted as the direct production of an electron pair by a helium nucleus of the cosmic radiation. The primary helium nucleus has a measured energy of $(1.7 \pm 0.5) \cdot 10^5$ GeV. The pair has an energy of 20 ± 4 GeV and initiates an electron shower.

1. – Introduction.

An unusual event has been observed in an emulsion stack exposed in a ballon flight (~ 95000 feet) near the geomagnetic equator (10° N) which can be interpreted as the direct production of an electron pair by a heavy charged particle. An extremely energetic particle whose grain density (four times the minimum) and delta ray density imply a charge of two enters the stack at a zenith angle of 56°. After 62 mm, two «shower» tracks (lightly ionizing tracks) are seen to diverge slowly from the primary track. The opening angle of approximately 0.001 radian can be attributed mainly to multiple Coulomb scattering. The point of origin of the pair cannot be spatially resolved from the parent track. It can be approximately located by the observed increase in ionization from four to six times minimum. The pair subsequently (after several millimeters) gives rise to an electron shower which develops and proceeds through the stack together with the primary heavy particle. 75 mm after the formation of the original pair (total path length in emulsion of 13.7 cm), the He nucleus collides with an emulsion nucleus forming a star ($6-43\alpha$) [1] con-

[1] Bristol notation. See article by CAMERINI, LOCK, and PERKINS in J. G. WILSON: *Progress in Cosmic Ray Physics*, **1** (New York, 1952).

taining a very highly collimated « jet » of shower particles. The energy of the primary particle, estimated from the angular distribution of the shower, as described below, is $1.7 \cdot 10^5$ GeV.

Fig. 1 is a schematic projection drawing of the first nine events (pairs and tridents) of the cascade shower. The secondary electrons have not been continued in the drawing so as to avoid the confusion of the many crossing and scattering tracks. As can be seen from the figure, the multiplicative processes are not observed until the initial pair of electrons has traveled more than seven millimeters and diverged appreciably from the primary particle. The next eight events then occur on or very close to the electron tracks rather than that of the He-particle. Event « *H* » is the last apparent trident (trident or pseudo-trident) [2] found. The rapid spread and degradation of the shower after this has not been shown in the diagram.

The geometry (lateral distance of point of origin of secondary events from the tracks of the initial pair, e_1 and e_2) and the energy measurements both are consistent with the conclusion that the electron shower was initiated by the first pair, and there is no firm evidence for any further electromagnetic processes related to the primary track.

It is of interest to note that three successive events, *E*, *G*, and *H* occurring along the track of the higher energy electron e_1, are all apparent tridents. This may not be anomalous in view of the pseudo-trident correction [2] (of at least 30 per cent) to be applied, and the poor statistics involved.

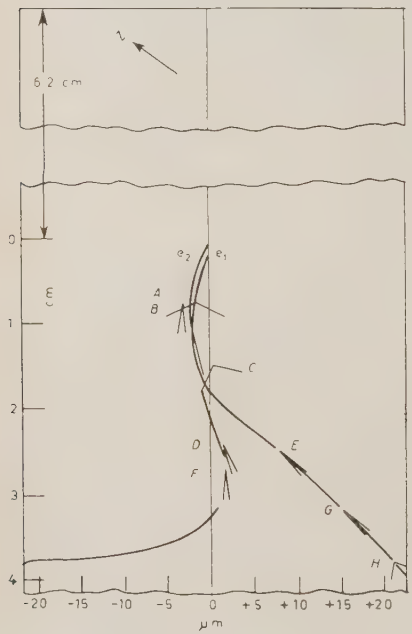

Fig. 1. – Projection drawing showing only the first nine events of the electron shower. The lateral scale has been greatly magnified (1000×) in an effort to show the position of the origin of the secondary electron events relative to the initial pair e_1 and e_2 and the incoming He particle (the center line). The degradation of the shower after event *H* (last apparent trident) is not shown.

[2] M. M. Block and D. T. King: *Phys. Rev.*, **95**, 171 (1954).

2. – Energy Measurements on the Electron Tracks.

Since the emulsion in which these measurements were carried out has a distortion of the order of 300 covans, direct scattering measurements on all but the very slowest electrons gave no information. However, the tracks are quite parallel to one another and to the primary particle so that it was possible to carry out relative scattering measurements which eliminate the effects of distortion.

As described in the appendix, when relative scattering measurements are carried out on two tracks one of which is appreciably more energetic than the other, the result is a measurement of the multiple scattering of the less energetic track. Since the particles in this event all have energies large compared to their rest masses, the measurement of the multiple scattering gives directly an estimate of the energy of the particle. If three tracks of nearly the same energy are measured, the method permits one to obtain the energies of all three. Since the He nucleus is much more energetic than the other tracks in this event, it was measured as a reference track whenever this was convenient. Some intermediate energy tracks were inconveniently far from the path of the primary and closer to one of the tracks of the first electron pair. The latter was then employed as a reference track provided that the track being measured belonged to an electron of appreciably lower energy.

The « noise » value used was determined by a relative scattering measurement using 50 μm cells, between the He-particle and the first two electron tracks. The value obtained was

$$D_{\text{noise}} = (0.10 \pm 0.02)\ \mu\text{m} .$$

This value was checked by eliminating noise between basic cells and higher cells (the Bristol method) on several tracks, and found to be in agreement within statistical error. It is noteworthy that this value of the noise is lower than that obtained by the same observer for ordinary multiple scattering measurements on tracks of similar grain density in undistorted emulsion. One would expect that the noise value for relative scattering measurements would be $\sqrt{2}$ times as large as for ordinary scattering if the noise were due to independent displacements of the measured track from the trajectory of the particle. The fact that the noise is lower in relative scattering has been noted previously ([3]) although the reasons for it are not understood. It may be due to the elimination of small scale distortions such as those which cause the correlated deflections observed by Biswas *et al.* ([4]).

([3]) M. Schein, Haskin and Lord: private communication.

([4]) N. N. Biswas, B. Peters and Rama: *Proc. Ind. Acad. Sci.*, **41**, 159 (1953).

Table I gives the energy measurements on the first nine events of the shower. The value resulting from direct measurement of track e_1 (one of the members of the initial pair) is shown in parentheses since this value is lower than the measured energy in events which appear to be secondaries originating from this track. The apparent trident E is formed along this track (see Fig. 1). Another apparent trident, event G, is formed along the highest energy track of E. The total energy of G plus the energy of the two lower energy members of event E add up to (30 $\pm$ 7) GeV. This discrepancy could possibly be due to a bremsstrahlung loss of energy by particle e_1 in the length of track used for the measurement or before, that is, e_1 could have radiated a γ-ray which subsequently converts to a pair as event E or G. (This would imply that E or G is actually a pseudo-trident). However, track e_1 scatters appreciably between this section and the formation of event E (see Fig. 1). Since E and G

Table I.

Event	Longitudinal distance (mm)	Radial distance (μm)	Energy (GeV)			Total Energy (GeV)
			1	2	3	
e_1, e_2	0	0	(11 $\pm$4)	3.8 $\pm$0.9	—	(15 $\pm$4)
A	7.7	0.3	0.011 $\pm$ .004	0.0008 $\pm$ .0003	—	0.012 $\pm$ .004
B	8.1	0.8	0.33 $\pm$ .10	0.064 $\pm$ .032	—	.39 $\pm$ .11
C	15.3	2.2	0.11 $\pm$ .03	0.008 $\pm$ .002	—	.12 $\pm$ .03
D*	24.8	0.2	0.11 $\pm$0.03	0.11 $\pm$ .03	—	.22 $\pm$ .04
E*	25.2	0	35^{+130}_{-20}	$2.8^{+1.0}_{-0.8}$	0.7 $\pm$0.2	39^{+130}_{-20}
F	27.8	> 2	2.1 $\pm$0.6	0.14 $\pm$ .06	—	2.2 $\pm$0.6
G*	31.9	0	18 $\pm$7	6.3 $\pm$1.8	2.0 $\pm$0.4	26 $\pm$7
H*	37.9	0	—	0.006 $\pm$ .001	—	—

Pair e_1; e_2 is the initial pair, the other events are pairs or tridents in the order of their formation. Track 1 in each event is the highest energy member of the event, track 2 the next highest and track 3 the lowest. The radial distance is the distance of the point of origin of the pair to the nearest track. Events with an asterisk are apparent tridents, others are pairs. See text for explanation of parenteses around some of the energy values above.

occur (to within about 0.3 μm) on track e_1, it is unlikely that either could have been due to a γ-ray radiated as far back as the section of track used for the measurement of track e_1. The most likely explanation is that we are dealing with a statistical fluctuation. The probability of getting a discrepancy as large as this by chance is about 2 per cent. In this case the true energy of e_1 can be best estimated from a combination of the direct measurement with that of the measurements on the secondary events. This gives (16 $\pm$ 4) GeV as the estimate of the energy of e_1. The energy estimate for the initial pair is then (20 $\pm$ 4) GeV.

3. – Energy of He-Particle.

The collision of the He-particle with a nucleus of the emulsion occurs only about 2.7 mm from the point at which the He-particle would have left the edge of the stack. It is difficult therefore to be sure that all the tracks in the dense central core have been resolved. From the apparent grain density of the tracks it appeared that they were all near minimum ionization, and hence that the 43 lightly ionizing tracks represent all of the fast charged particles produced in the event. It is possible, however, that one or two have been missed. The median angle of these shower tracks is .009 radians.

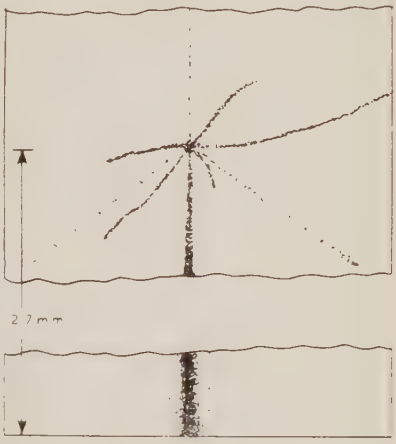

Fig. 2. – Projection drawing of the star containing a jet produced by the He nucleus interacting with an emulsion nucleus.

The apparent velocity of the center of mass system has been deduced by the method of the Rome group ([5]), in what they call the spectrum independent approximation, which is based on measurements of the angles of emission of the charged particles. The method consists in averaging the logarithm of the cotangent of the angles in the laboratory system. This is used as an estimate of the logarithm of γ, where $\gamma = (1 - \beta^2)^{-\frac{1}{2}}$ and β is the velocity of the center of mass. The energy was also estimated by the method of DILWORTH *et al.* ([6]) which uses the angle θ_f of the cone containing a fraction, f, of the particles and one measures γ by

$$\gamma^2 = \cot \theta_f \cot \theta_{1-f} .$$

These two methods are not independent.

Applying the method of the Rome group, one gets $\gamma = 152$ with an error of approximately 14 per cent. Using the method of DILWORTH *et al.* for various

([5]) C. CASTAGNOLI, G. CORTINI, C. FRANZINETTI, A. MANFREDINI and D. MORENO: *Nuovo Cimento*, **10**, 1539 (1953).

([6]) C. C. DILWORTH, S. J. GOLDSACK, T. F. HOANG and L. SCARSI: *Nuovo Cimento*, **11**, 424 (1954).

values of f we have:

f	γ
$\frac{1}{2}$	109
$\frac{1}{3}$	114
$\frac{1}{4}$	156
all	154

where the last value is an r.m.s. average of γ for all values of f in steps of one particle. One might expect that the last value given is the best of those by the Dilworth method. The value of γ will be taken to be 150 ± 20.

If the event were a nucleon-nucleon collision then the energy of the incident particle could be calculated as

$$\frac{E}{Mc^2} = 2\gamma^2 - 1. \tag{1}$$

However, the collision is more complex, as the incident particle is a He nucleus, and since gray tracks are present, the target nucleus must have had an atomic weight of at least 12 and possibly as high as 135. The part of the collision in which the shower is produced may be in fact essentially a superposition of primary nucleon-nucleon collisions with no significant secondary interactions in which case Eq. (1) again applies. If, on the other hand, an intra-nuclear cascade develops the use of (1) will tend to underestimate the true energy, and the same is true if there is appreciable scattering of the shower tracks inside the nucleus. Thus the estimated energy of the He nucleus obtained from (1) is $\geqslant (1.7 \pm 0.5) \cdot 10^5$ GeV.

4. – Discussion.

This event could be due to the direct production of an electron pair by the He nucleus in the field of an emulsion nucleus. (This is analogous to the trident process for electrons). To compute the probability for the event on this hypothesis we have used the formulas given by Rossi [7] which are based on the theory of Bhabha [8]. We find that the mean free path for an α-particle of the observed energy $(1.7 \cdot 10^5)$ GeV to produce a pair of electrons with energy from 20 GeV to the maximum possible is ~ 290 cm.

Consider now the latest data in regard to the primary alpha flux and energy

(7) B. Rossi: *High Energy Particles* (New York, 1952), p. 86.
(8) H. J. Bhabha: *Proc. Roy. Soc.*, A **152**, 559 (1935).

spectrum near the geomagnetic equator (SINGER [9]) quotes a primary alpha flux of 20 particles/m²/ster/s and spectrum $I = I_0 E^{-1.16}$. From this we conclude that approximately one α-particle of energy $\geqslant 10^5$ GeV would be expected to penetrate our emulsion stack (46 pellicles, 600 μm thick, 6″ · 5″ each) during our flight. Therefore, considering the observed path length and the computed mean free path, we estimate a probability of 0.02 that we should observed direct pair production due to an α-particle of energy greater than or equal to that of this event.

If we had considered the production of a pair at any energy, the mean free path would have been five centimeters. This is due to the fact that production of low energy pairs contributes the greatest part to the integral cross-section.

Another possible explanation of this event is that of bremsstrahlung emitted by the primary α-particle (and subsequent conversion to the initial pair). However, present electromagnetic theory, which gives essentially correct results for electrons up to fairly high energies, indicates an inverse square dependence of the cross-section for bremsstrahlung with mass. This is a very severe restriction of the process for α-particles since $(m_e/m_\alpha)^2 \approx 2 \cdot 10^{-8}$. The energy dependence is slow and does not help much even at the very high energy of this α-particle. A calculation for the cross-section has been carried out, based upon CHRISTY and KUSAKA's computation [10,11] and utilizing the measured energy of the primary. Integration of the photon energy distribution (over all energies from that estimated for the photon producing the observed shower to the maximum possible) gives a cross section

$$\Phi_{\text{rad}} = 4.1 \cdot 10^{29} \text{ cm}^2 \text{ in emulsion} .$$

This corresponds to a mean free path in emulsion of approximately 3000 m. Using the same assumptions concerning α-particle flux as above we compute the probability on the bremsstrahlung hypothesis to be $\sim 4 \cdot 10^{-5}$.

We have considered in addition, the following possible explanations:

a) The creation of a ^{6}He nucleus in an isomeric state, or Coulomb excitation to this state and the subsequent decay by γ-emission. (^{3}He and ^{4}He have no known isomeric states). The probability on the basis of this hypothesis is less than 10^{-5}.

---

[9] Information presented at the *IUPAP International Cosmic Ray Conference*, Guanajuato, Mexico, August, 1955.

[10] R. F. CHRISTY and S. KUSAKA: *Phys. Rev.*, **59**, 405, 414 (1941). They compute the differential radiation probabilities for particles of arbitrary mass and spin 0, $\frac{1}{2}$ and 1 (normal magnetic moment).

[11] B. ROSSI: *High Energy Particles* (New York), p. 61.

b) The collision of a primary nucleus above the stack producing a π^0 whose decay γ-ray converts in almost exact coincidence with the α-particle (the α-particle being a result of the fragmentation of the heavy primary). The probability, under this assumption is less than 10^{-7}.

c) A helium hyperfragment produced in the fragmentation of a heavier primary somewhere above and outside the stack. The decay of the Λ^0 hyperon into a neutron and π^0 has been postulated. Corresponding to this decay mode, a hyperfragment might, for example, disintegrate according to the scheme,

$$^4\mathrm{He}^* \to {}^4\mathrm{He} + \pi^0 + Q\,. \tag{2}$$

The subsequent decay of the π^0 ($\pi^0 \to 2\gamma$) could then be the origin of the γ-ray which initiates the observed electron shower. The probability here is less than 10^{-9}.

d) A chance coincidence of the paths of a γ-ray and an α-particle of these energies. This probability is less than 10^{-15}.

5. – Conclusions.

The explanation of this event by the mechanism of direct pair production has been shown to be reasonable. Several other hypotheses have been considered and have been found to be unlikely. It is interesting to note that in the theory as developed by BHABHA the cross-section for direct pair production by heavy charged particles is essentially independent of the mass of the heavy particle. This is to be contrasted with the bremsstrahlung process which contains an inverse square dependence on the mass and therefore, for α-particles, leads to a smaller cross-section than for direct pair production. (For electrons, the cross-section of bremsstrahlung is larger than for trident production.)

* * *

We should like to express our thanks to Dr. MAURICE M. SHAPIRO for his advice and encouragement and Messrs. BERTRAM STILLER and F. W. O'DELL for their aid. We would like to thank Dr. C. GOEBEL for calling our attention to the high probability for direct pair production as an explanation for this event, and also Drs. G. SNOW and J. EHRMAN for informative discussions.

APPENDIX

The theory of ordinary multiple Coulomb scattering has been worked out by many authors. We have used the Gaussian approximation to derive relationships between quantities treated in these theories and the second differences of relative scattering measurements. The principal advantage of the relative scattering measurement is that it cancels out most of the contribution of distortion to the measurements, and also any stage noise which might be present.

Denote by $\overline{D_{ij}}$ the expected value of the average of the absolute values of the second differences in a series of measurements of the relative projected distance of tracks i and j. Denote by $\overline{D_i}$ the same function of the measurements of the position of track i. $\overline{N}$ is the expected value of the random noise in the measurement of second differences along a single track. $\overline{C}$ is the correlated noise which occurs in both tracks being measured and hence cancels out in the difference ($\overline{C}$ can include the effect of distortion and stage noise). $\overline{S_i}$ is the expected value of the true second difference of points on the trajectory of track i.

Then we have:

$$\overline{D_i}^2 = \overline{N}^2 + \overline{C}^2 + \overline{S_i}^2 \tag{A.1}$$

$$\overline{D_{ij}}^2 = 2\overline{N}^2 + \overline{S_i}^2 + \overline{S_j}^2 \tag{A.2}$$

We would expect that $\overline{S_i}$ would have the ordinary $\frac{3}{2}$ power dependence on cell length, that $\overline{N}$ would be independent of cell length and that $\overline{C}$ would be very irregular in its cell length dependence. If measurements are made on three nearly parallel tracks, then from equation (A.2) we obtain:

$$\overline{S_1}^2 = \tfrac{1}{2}[\overline{D_{12}}^2 + \overline{D_{13}}^2 - \overline{D_{23}}^2] - N^2 \tag{A.3}$$

and similar expressions for S_2 and S_3. So in principle we can get information on the energies of all three tracks from such a measurement. However, if track 1, say, is much stiffer than tracks 2 and 3, then $\overline{D_{12}}$ and $\overline{D_{13}}$ will contain a negligible contribution from $\overline{S_1}$ and when $\overline{S_1}^2$ is computed from (A.3), it will be small compared with its error. However, the measurements of $\overline{S_2}$ and $\overline{S_3}$ will be quite good and will amount to measuring tracks 2 and 3 with respect to track 1 as a baseline. In this case $\overline{D_{12}}$ (or $\overline{D_{13}}$) is already a measure of $\overline{S_2}$ (or $\overline{S_3}$), with noise to be subtracted.

The standard deviation of measurement by this procedure can be computed by the standard methods for combination of errors.

RIASSUNTO (*)

Si è osservato un evento che si interpreta come la produzione diretta di una coppia di elettroni da parte di un nucleo di elio della radiazione cosmica. Il nucleo d'elio primario ha un'energia misurata di $(1.7 \pm 0.5) \cdot 10^5$ GeV. La coppia ha un'energia di 20 ± 4 GeV e dà inizio a uno sciame elettronico.

(*) *Traduzione a cura della Redazione.*

IL NUOVO CIMENTO Vol. IV, N. 4 1° Ottobre 1956

On the Collective Description of Nuclear Surface Oscillation.

T. Tamura (*)

Institute for Theoretical Physics - University of Copenhagen, Copenhagen, Denmark

(ricevuto il 29 Maggio 1956)

Summary. – A general method for a collective description of a many particle system, which was introduced by Miyazima and the present author and applied to the case of weak coupling surface oscillation of the atomic nuclei, is extended here to the case of strong coupling, and our results are compared with those of other authors.

1. – Introduction.

In recent years, a number of papers have been published [1-11] with a view to unifying the individual particle and the collective particle aspects of atomic nuclei: the authors succeeded in deriving a Hamiltonian, parts of which de-

(*) On leave of absence from the Tokyo University of Education, Tokyo, Japan.

[1] D. L. Hill and J. A. Wheeler: *Phys. Rev.*, **89**, 1102 (1953).

[2] A. Bohr: *Rotational States of Atomic Nuclei* (Copenhagen, 1954); Especially Appendix.

[3] G. Süssmann: *Zeits. f. Phys.*, **139**, 543 (1954).

[4] D. R. Inglis: *Phys. Rev.*, **96**, 1059 (1954); **97**, 701 (1955).

[5] T. Marumori, J. Yukawa and R. Tanaka: *Prog. Theor. Phys.*, **13**, 442 (1955); T. Marumori and E. Yamada: *Prog. Theor. Phys.*, **13**, 557 (1955); T. Marumori: *Prog. Theor. Phys.*, **14**, 608 (1955).

[6] H. A. Tolhoek: *Physica*, **21**, 1 (1955).

[7] F. Coester: *Phys. Rev.*, **99**, 170 (1955).

[8] S. Tomonaga: *Prog. Theor. Phys.*, **13**, 467, 482 (1955).

[9] R. Nataf: *Compt. Rend.*, **240**, 2510 (1955); **241**, 31 (1955).

[10] H. J. Lipkin, A. de Shalit and I. Talmi: *Nuovo Cimento*, **11**, 773 (1955).

[11] F. Villars: Mimeographed note sent to Dr. A. Bohr.

scribe individual particle motions while other parts describe the surface oscillation ([12]) together with the coupling term between these two.

The work of MIYAZIMA and the present author ([13]) was carried out along similar lines, however, a new technique was introduced, using some new redundant co-ordinates, together with an appropriate number of subsidiary conditions, in order to cancel the added degrees of freedom. After performing several canonical transformations a Hamiltonian is obtained, part of which just reproduces Bohr's Hamiltonian ([12]) in the weak coupling approximation. Among the above mentioned papers, those by NATAF ([9]), LIPKIN *et al.* ([10]), and Villars ([11]), which came to our attention after our former paper had been submitted for publication, were based on ideas essentially similar to ours, and were applied to the strong coupling case.

Since our method, however, seems to be quite general in its scope and, in some cases, much simpler than others, it might be worthwhile to exemplify its application to the case of strong coupling. The present paper is devoted to this purpose.

Our results are compared, in Sect. 2 and Sect. 3, with those of the above mentioned authors. NATAF ([9]) and LIPKIN *et al.* ([10]) have confined their development to rotational motions, while VILLARS ([11]) included also vibrational and dilatational motions; in his theory these motions have been considered only in two dimensions, and therefore we have extended our application also to the three-dimensional case including all these types of collective motions. The results are summarized in Sect. 4, while Sect. 5 contains a discussion of the problem.

The basic idea of our method is explained in detail in our former paper ([13]). However, as the center of mass motion is the simplest example of collective motions, it might be instructive here to illustrate the application of our method to the separation of the center of mass motion from individual particle motions.

For the sake of simplicity, we take the one-dimensional motion and start with the Schrödinger equation for a many particle system

$$H_0\psi_0 = E\psi_0 \,, \tag{1}$$

$$H_0 = -\hbar^2/2\mu \sum_n \nabla_x^{(n)2} + V(x) \quad (*) \,, \tag{2}$$

([12]) A. BOHR: *Dan. Mat. Fys. Medd.*, **26**, no. 14 (1952); A. BOHR and B. MOTTELSON: *Dan. Mat. Fys. Medd.*, **27**, no. 16 (1953).

([13]) T. MIYAZIMA and T. TAMURA: *Prog. Theor. Phys.*, **15**, 255 (1956).

(*) Here and in the following, potential energy of a particle system is abbreviated as $V(x)$, or $V(x, y)$ or $V(x, y, z)$ in one, two and three dimensional cases, respectively, but we consider it to be a symmetric function of particle coordinates and to depend only on relative distances of the latter.

introducing a new redundant co-ordinate X, together with a momentum P which is canonically conjugate to X. As the Hamiltonian (2) is a function only of the particle co-ordinates and momenta, while the operators X and P are assumed to be independent of particle variables, the introduction of the latter causes no change of our original system.

This fact, however, means at the same time that our system is highly degenerate in so far as the motions described by X and P are concerned. In order to remove this degeneracy we introduce the subsidiary condition

$$X\psi_0 = 0\,, \tag{3}$$

which will soon be proved to be most appropriate for our present purpose. It is also clear that the introduction of this subsidiary condition causes no change in our original system, because the operator in (3) is independent of particle variables.

Next, defining the symmetrical function of particle co-ordinates

$$x = \sum_n x_n/N\,,$$

we perform a canonical transformation

$$\psi_0 \to \psi_1 = U_1^{-1}\psi_0\,; \qquad U_1 = \exp\left[(i/\hbar)Px\right]. \tag{4}$$

Then, (3) changes into

$$(X - x)\psi_1 = 0 \tag{5}$$

and H_0 changes into

$$H_1 = U_1^{-1}H_0U_1 = -\hbar^2/2\mu \sum_n (\nabla_x^n + (i/\hbar)\,P/N)^2 + V(x)\,. \tag{6}$$

If we introduce a new operator

$$\pi = (\hbar/i) \sum_n \nabla_x^{(n)}$$

which satisfies

$$[\pi, x] = \hbar/i\,,$$

and perform the second canonical transformation

$$\psi_1 \to \psi_2 = U_2^{-1}\psi_1\,; \qquad U_2 = \exp\left[-(i/\hbar)\,\pi X\right], \tag{7}$$

then (5) changes into

$$x\psi_2 = 0\,, \tag{8}$$

and H_1 changes into

$$H_2 = U_2^{-1} H_1 U_2 = \left(H_0 - \frac{1}{2\mu N} \pi^2 \right) + \frac{1}{2\mu N} P^2 . \tag{9}$$

The first term in (9), together with the subsidiary condition (8), describes the internal motion in the center of mass co-ordinate system, while the second term describes the center of mass motion, and thus separation of these two kinds of motion is completely performed.

It should be noted that this simple discussion is sufficient to replace the somewhat lengthy arguments given in Sect. 2 and Sect. 3 of the paper by LIPKIN *et al.* [10] and Sect. 2 of VILLAR's paper [11].

2. – Strong Coupling Surface Motion in a Two-Dimensional Nucleus.

We first define three quantities as in VILLAR's paper, given by

$$\text{(10) (*)} \qquad \begin{cases} \tau = \sum (x_n^2 + y_n^2) , \\ \beta = 2\sqrt{\xi_1^2 + \xi_2^2} \qquad (\xi_1 = \tfrac{1}{2} \sum (x_n^2 - y_n^2),\ \xi_2 = \sum x_n y_n) \\ \varphi = \tfrac{1}{2} \operatorname{tg}^{-1} \xi_2 / \xi_1 . \end{cases}$$

Then, if we introduce the three operators

$$\text{(11)} \qquad \begin{cases} \pi_\tau = \dfrac{\hbar}{4\tau i} \sum \{ (\nabla_x^{(n)} \tau) \nabla_x^{(n)} + (\nabla_y^{(n)} \tau) \nabla_y^{(n)} \} , \\ \pi_\beta = \dfrac{\hbar}{i} \dfrac{\tau}{4(1 - \beta^2)} \sum \{ (\nabla_x^{(n)} \beta) \nabla_x^{(n)} + (\nabla_y^{(n)} \beta) \nabla_y^{(n)} \} , \\ \pi_\varphi = \dfrac{\hbar}{i} \sum \{ x_n \nabla_y^{(n)} - y_n \nabla_x^{(n)} \} , \end{cases}$$

we can easily show that they satisfy the canonical commutation relations

$$[\pi_\tau, \tau] = [\pi_\beta, \beta] = [\pi_\varphi, \varphi] = \hbar / i , \tag{12}$$

while all other commutators vanish.

Now we write the original Hamiltonian, its eigenfunction, and eigenvalue

(*) Throughout this paper, indices occurring doubly should be interpreted to mean summation indices.

as H_0, ψ_0, and E, respectively; then

$$H_0\psi_0 = E\psi_0 , \tag{13}$$

where

$$H_0 = -(\hbar^2/2)\mu \sum_n (\nabla_x^{(n)2} + \nabla_y^{(n)2}) + V(x, y) . \tag{14}$$

Following the procedure described in the preceding section we impose on ψ_0 the subsidiary conditions

$$t\psi_0 = b\psi_0 = \theta\psi_0 = 0 , \tag{15}$$

and perform a canonical transformation

$$\psi_0 \to \psi_1 = U_1^{-1}\psi_0 ; \qquad U_1 = \exp[(i/\hbar)(P_\theta\varphi + P_b\beta + P_t\tau)] , \tag{16}$$

where P_θ, P_b and P_t are momentum operators, canonically conjugate respectively, with θ, b and t, and assumed to commute. Then (13) becomes

$$H_1\psi_1 = E\psi_1 , \tag{17}$$

where

$$\begin{aligned}
H_1 = U_1^{-1}H_0H_1 = {} & H_0 + (i/\hbar)\{[H_0, \varphi]P_\theta + [H_0, \beta]P_b + [H_0, \tau]P_t\} + \\
& + (i^2/\hbar^2)\{[[H_0, \varphi], \varphi]P_\theta^2 + [[H_0, \beta], \beta]P_b^2 + [[H_0, \tau], \tau]P_t^2 + \\
& + 2[[H_0, \varphi], \beta]P_\theta P_b + 2[[H_0, \beta], \tau]P_bP_t + 2[[H_0, \tau], \varphi]P_tP_\varphi\} = \\
= {} & H_0 + (1/2\mu)\{\sum[\nabla_\nu^{(n)}, \varphi]^2P_\theta^2 + \sum[\nabla_\nu^{(n)}, \beta]^2P_b^2 + \sum[\nabla_\nu^{(n)}, \tau]^2P_t^2\} + \\
& + (1/\mu)\{\sum[\nabla_\nu^{(n)}, \varphi][\nabla_\nu^{(n)}, \beta]P_\theta P_b + \sum[\nabla_\nu^{(n)}, \beta][\nabla_\nu^{(n)}, \tau]P_bP_t - \sum[\nabla_\nu^{(n)}, \tau][\nabla_\nu^{(n)}, \varphi]P_tP_\theta\} - \\
& - (i\hbar/2\mu)\{\sum\Delta^{(n)}\varphi P_\theta + \sum_n \Delta^{(n)}\beta P_b + \sum\Delta^{(n)}\tau P_t\} - \\
& - (i\hbar/\mu)\{\sum[\nabla_\nu^{(n)}, \varphi]\nabla_\nu^{(n)}P_\theta + \sum[\nabla_\nu^{(n)}, \beta]\nabla_\nu^{(n)}P_b - \sum[\nabla_\nu^{(n)}, \tau]\nabla_\nu^{(n)}P_t\} .
\end{aligned} \tag{18}$$

and in this representation the subsidiary condition is

$$(\theta - \varphi)\psi_1 = (b - \beta)\psi_1 = (t - \tau)\psi_1 = 0 . \tag{19}$$

If we now perform the second canonical transformation

$$\psi_1 \to \psi_2 = U_2^{-1}\psi_1 ; \qquad U_2 = \exp[-(i/\hbar)\pi_\varphi\theta] ,$$

H_1 changes into $H_2 = U_2^{-1}H_1U_2$, and the subsidiary condition changes into

$$(b-\beta)\psi_2 = (t-\tau)\psi_2 = \varphi\psi_2 = 0\,. \tag{20}$$

Here, H_2 has the same form as H_1, except that P_θ which appeared in the latter should be replaced by $(P_\theta - \pi_\varphi)$ in the former. Thus, using the following relation which can easily be derived (*)

$$\begin{cases} \sum[\nabla_2^{(n)}, \tau]^2 = 4\tau\,, \quad \sum[\nabla_\nu^{(n)}, \beta]^2 = 4(1-\beta^2)/\tau\,, \quad \sum[\nabla_\nu^{(n)}, \varphi]^2 = 1/\beta^2\tau\,, \\ \sum_n \Delta_n\tau = 4N\,, \quad \sum_n \Delta_n\beta = 4(1-N\beta^2)/\tau\beta\,, \quad \sum_n \Delta_n\varphi = 0\,, \\ \sum[\nabla_\nu^{(n)}, \tau][\nabla_\nu^{(n)}, \beta] = \sum[\nabla_\nu^{(n)}, \beta][\nabla_\nu^{(n)}, \varphi] = \sum[\nabla_\varkappa^{(n)}, \varphi][\nabla_\nu^{(n)}, \tau] = 0\,, \end{cases} \tag{21}$$

we finally obtain the explicit form of H_2:

$$H_2 = H_0 + H_{\text{rot}} + H_{\text{vib}} + H_{\text{dil}} + H_{\text{coupl}}\,, \tag{22}$$

where

$$H_{\text{rot}} = \frac{1}{2\mu\beta^2\tau}(P_\theta - \pi_\varphi)^2\,, \tag{22a}$$

$$H_{\text{vib}} = \frac{4(1-\beta^2)}{2\mu\tau}P_b^2 - \frac{4i\hbar}{2\mu}\frac{1}{\beta}(1-N\beta^2)P_b\,, \tag{22b}$$

$$H_{\text{dil}} = \frac{4\tau}{2\mu}P_t^2 - \frac{4i\hbar N}{2\mu}P_t\,, \tag{22c}$$

$$H_{\text{coupl}} = -\frac{i\hbar}{\mu}\sum[\nabla_\nu^{(n)}, \varphi]\nabla_\nu^{(n)}(P_\theta - \pi_\varphi) - \\ -\frac{i\hbar}{\mu}\sum[\nabla_\nu^{(n)}, \beta]\nabla_\nu^{(n)}P_b - \frac{i\hbar}{\mu}\sum[\nabla_\nu^{(n)}, \tau]\nabla_\nu^{(n)}P_t\,. \tag{22d}$$

If, in equations (22*a*), (22*b*), and (22*c*), we replace P_b and P_t by $(i/\hbar)(\partial/\partial b)$ and $(i/\hbar)(\partial/\partial t)$, and also β and τ by b and t, by virtue of (20), then these equations can be rewritten as

$$H_{\text{rot}} = \frac{1}{2\mu b^2 t}(P_\theta - \pi_\varphi)^2\,, \tag{22a'}$$

(*) This relation has also been obtained by VILLARS.

$$H_{\rm vib} = -\frac{4\hbar^2}{2\mu t}\left[(1-b^2)\frac{\partial^2}{\partial b^2} + \frac{1}{b}(1-Nb^2)\frac{\partial}{\partial b}\right], \tag{22b'}$$

$$H_{\rm coll} = -\frac{4\hbar^2 t}{2\mu}\left[\frac{\partial^2}{\partial t^2} - \frac{N}{t}\frac{\partial}{\partial t}\right]. \tag{22c'}$$

The Hamiltonians (22a'), (22b'), and (22c') are the same as those obtained by VILLARS [11]. Our derivation, however, appears to be simpler and our subsidiary conditions (20) are also easier to manage. To explain this fact we consider, for the sake of simplicity, only the vibrational motion and use the adiabatic assumption that the frequency of internal motions is much higher than that of the vibrational motion. Then we can consider temporarily b in (20) to be constant, in taking the average of, e.g., H_0 over internal motions. If we write the eigenfunction of H_0, when the subsidiary condition is not taken into account, as Φ, this average value has the form

$$\langle H_0 \rangle = \int \Phi^* H_0 \delta(\beta - b)\Phi \, {\rm d}x \,, \tag{23}$$

the insertion of the δ-function embodying the subsidiary condition (20) (*). Equation (23) can, however, be rewritten by using the general relation

$$f(\beta)\delta(\beta - b) = \left(f(\beta) - (b - \beta_0)\frac{\partial f(\beta)}{\partial \beta} + \tfrac{1}{2}(b-\beta_0)^2 \frac{\partial^2 f(\beta)}{\partial \beta^2} - \ldots\right)\delta(\beta - \beta_0);$$

(β_0 is a constant)

and also the fact that

$$\partial f(\beta) = (i/\hbar)[\pi_\beta, f(\beta)] \,, \quad \text{etc.} \,,$$

π_β being defined in (11), as follows,

$$\begin{aligned}\langle H_0 \rangle = {} & \int \Phi^* H_0 \delta(\beta - \beta_0)\Phi \, {\rm d}x + \\ & + (i/\hbar)\int \Phi^*[\pi_\beta, H_0]\delta(\beta - \beta_0)\Phi \, {\rm d}x(b - \beta_0) + \\ & + (i^2/2\hbar^2)\int \Phi^*\{\pi_\beta, [\pi_\beta, H_0]\}\delta(b - \beta_0)\Phi \, {\rm d}x(b - \beta_0)^2 + \ldots \,,\end{aligned} \tag{24}$$

This expression means that, after performance of the integrations which

(*) This technique was suggested in the lecture of Professor TOMONAGA at the Institute for Fundamental Physics, Kyoto, in May, 1955.

appear in (24), $'H_0$ can be interpreted to have a form of a power series expansion in powers of $(b-\beta_0)$ with constant coefficients, and thus can be used as a potential energy term for the collective vibrational motion.

We finally note that the last condition $\varphi\psi_2 = 0$ in (20) has the same meaning as $(\sum x_n y_n)\psi_2 = 0$, as is easily seen from the definition of φ in (10). This fact indicates that we are considering a co-ordinate system relative to the principal axis of an ellipse.

3. – Three-Dimensional Case with Rotational Motion.

In this section we consider only rotational motions; the inclusion of vibrational motions will be treated in the following section.

A simple extension of the method outlined in the preceding section suggests the introduction of

$$(25)\qquad \begin{cases} \xi_1 = \frac{1}{2}\sum (y_n^2 - z_n^2)\,, \quad \xi_2 = \frac{1}{2}\sum (z_n^2 - x_n^2)\,, \quad \xi_3 = \frac{1}{2}\sum (x_n^2 - y_n^2)\,, \\ \eta_1 = \sum y_n z_n\,, \quad \eta_2 = \sum z_n x_n\,, \quad \eta_3 = \sum x_n y_n\,, \end{cases}$$

and the definition

$$(26)\qquad \varphi_1 = \tfrac{1}{2}\,\mathrm{tg}^{-1}(\eta_1/\xi_1)\,, \quad \varphi_2 = \tfrac{1}{2}\,\mathrm{tg}^{-1}(\eta_2/\xi_2)\,, \quad \varphi_3 = \tfrac{1}{2}\,\mathrm{tg}^{-1}(\eta_3/\xi_3)\,,$$

together with

$$(27)\qquad \begin{cases} L_1 = (\hbar/i)\sum (y_n\nabla_z^{(n)} - z_n\nabla_y^{(n)}), \qquad L_2 = (\hbar/i)\sum (z_n\nabla_x^{(n)} - x_n\nabla_z^{(n)}), \\ L_3 = (\hbar/i)\sum (x_n\nabla_y^{(n)} - y_n\nabla_x^{(n)})\,. \end{cases}$$

However, the angles φ_i defined in (26) can never be integrals of the equations of motion for a rotor, and some deeper insight into the geometrical meaning of our canonical transformation is necessary.

The geometrical meaning of the calculation performed in the preceding section may be interpreted as follows. Consider a system of particles which are distributed with a constant density over an ellipse, the principal axis of which makes an angle φ with the space fixed X coordinate (Fig. 1*a*). Now we consider at the same time an imaginary rotor with the same moment of inertia as the above defined ellipse, and the angle between the principal axis of the rotor and the space fixed X co-ordinate will be denoted by θ. Then the subsidiary condition (15) means that, in the representation ψ_0, the principal axis of the rotor coincides with the X co-ordinate (Fig. 1*a*; dotted line). Next, in the representation ψ_1, where $\theta = \varphi$, this imaginary rotor changes its orientation so that it is just superposed on the ellipse (Fig. 1*b*), and finally in the repre-

sentation ψ_2, the co-ordinate system itself is rotated so as to confine the internal motion to the principal co-ordinate system, and the rotational motion is represented by the motion of the imaginary rotor (Fig. 1*c*).

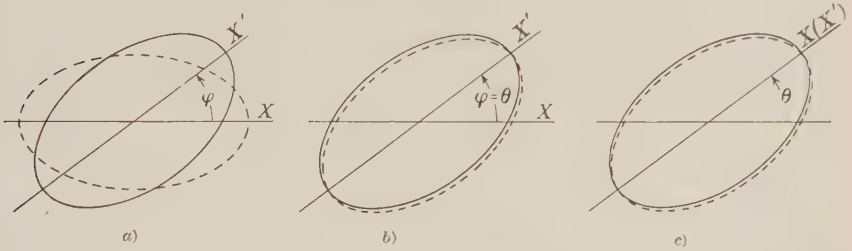

Fig. 1 *a*, *b*, *c*. – Explanation of the geometrical meaning of the various representations.

The angle φ of (10) was indeed found from this geometrical picture. We consider an orthogonal coordinate transformation given by

$$x'_n = x_n \cos\varphi + y_n \sin\varphi\,, \qquad y'_n = -\,x_n \sin\varphi + y_n \cos\varphi\,.$$

Then, the condition that

$$\sum x'_n y'_n = 0 \tag{28}$$

just gives the solution (10) for φ.

From these considerations it is now clear that, in three-dimensional case, some Eulerian angles ϑ_λ should be introduced instead of φ, in (26). These ϑ_λ's should be defined as solutions of the equations

$$\sum x'_n y'_n = \sum y'_n z'_n = \sum z'_n x'_n = 0\,, \tag{29}$$

or equivalently of the equations (*)

$$\begin{cases} Y'_{21} = \sum D^{(2)}_{\mu 1} Y_{2\mu} = 0\,, \quad Y'_{2-1} = \sum D^{(2)}_{\mu-1} Y_{2\mu} = 0\,, \\ Y'_{22} - Y'_{2-2} = \sum (D^{(2)}_{\mu 2} - D^{(2)}_{\mu-2}) Y_{2\mu} = 0\,, \end{cases} \tag{30}$$

where $D^{(2)}_{\mu\mu'}$ is Wigner's D-function ([14]), viz. the representation of the three-dimensional rotation group of order two, and is a function of the ϑ_λ's. This

(*) Here and in the following, the notation Y_{lm} means $\sum_u r_n^l Y_{lm}(\theta_n; \varphi_n)$, while Y'_{lm} means the corresponding quantity in the primed co-ordinate system.

([14]) E. P. WIGNER: *Gruppentheorie* (Braunschweig, 1931).

fact explains that the ϑ_λ's should be obtained as functions of the particle co-ordinates, but (30) is much too complicated and it would be difficult to solve it for the ϑ_λ's. It is very gratifying, however, to note that in our calculation we do not actually need the explicit form of ϑ_λ, but their differentiation coefficients with respect to particle coordinates, namely $\partial\vartheta_\lambda/\partial x_\nu^{(n)}$.

To obtain the explicit form for these quantities, we first differentiate both sides of (30) with respect to $x_\nu^{(n)}$. Then, for example, the first equation of (30) gives

$$\sum \frac{\partial D_{\mu 1}^{(2)}}{\partial \vartheta_\lambda} \frac{\partial \vartheta_\lambda}{\partial x_\nu^{(n)}} Y_{2\mu} = - D_{\mu 1}^{(2)} \frac{\partial Y_{2\mu}}{\partial x_\nu^{(n)}} .$$

and similarly for the other two equations. Then, this system of equations is a set of coupled linear equations for three unknowns $\partial\vartheta_\lambda/\partial x_\nu^{(n)}$, and indeed it is possible to solve it by using the convenient formula [12]

$$\partial D_{\mu\mu'}^{(2)}/\partial x_\nu^{(n)} = - i \sum q_{k\lambda} D_{\mu m}^{(2)} (M_i)_{m\mu'} , \tag{31}$$

where $q_{i\lambda}$ is defined by CASIMIR [15], and the result is given in the fairly simple form

$$\partial\vartheta_\lambda/\partial x_\nu^{(n)} = \sum q_i^\lambda A^{-1} a_{ij} D_{\mu j}^{(2)} \partial Y_{2\mu}/\partial x_\nu^{(n)} \equiv \sum q_i^\lambda G_{i\nu}^{(n)} , \tag{32}$$

which is the defining equation for $G_{i\nu}^{(n)}$ and where i takes the values 1, 2 and 3 (which means x, y and z), while j takes the values 1, -1, 2, and -2, and A is given by

$$A = 4 Y'_{22} (3 Y'^2_{20} - 2 Y'^2_{22}) , \tag{32a}$$

while the a_{ij}'s are given by

$$\left\{ \begin{array}{ll} a_{11} = a_{1-1} = 4i Y'_{22} (Y'_{22} - \sqrt{\tfrac{3}{2}}\, Y'_{20}) , & a_{12} = a_{1-2} = 0 , \\ -a_{21} = a_{2-1} = 4 Y'_{22} (Y'_{22} + \sqrt{\tfrac{3}{2}}\, Y'_{20}) , & a_{22} = a_{2-2} = 0 , \\ a_{31} = a_{3-1} = 0 , & -a_{32} = a_{32} = i(3 Y'^2_{20} - 2 Y'^2_{22}) . \end{array} \right. \tag{32b}$$

Finally, q_i^λ is defined by CASIMIR [15].

Next, we introduce the three angular momenta defined by

$$\varkappa_\lambda = \sum p_{i\lambda} L_i , \tag{33}$$

where the coefficients $p_{i\lambda}$ are again defined by CASIMIR and the L_i's are given in (27). As we have already obtained the explicit form of $\partial\vartheta_\lambda/\partial x_\nu^{(n)}$ in (32), it is now possible to calculate the commutation relation between $\varkappa_\lambda$ and ϑ_λ, and

---

[15] H. B. G. CASIMIR: *Rotation of a Rigid Body in Quantum Mechanics*, Diss. (Groningen, 1931). The definition of the Eulerian angles used in our paper is the same as that used in this book.

by means of some calculation we can actually show that the result is given by

$$[\pi_\lambda, \vartheta_{\lambda'}] = (\hbar/i)\,\delta_{\lambda\lambda'}\,, \tag{34}$$

i.e. the π_λ's are just the operators which are canonically conjugate to the ϑ_λ's. If we note that the $p_{\nu\lambda}$'s are functions of the ϑ_λ's, then it is possible to calculate commutation relations between the π_λ's, using (34) and the well-known commutation relations among the L_i's, and in fact we find that they commute:

$$[\pi_\lambda, \pi_{\lambda'}] = 0\,. \tag{35}$$

After these preparations, we now proceed to extend the procedure developed in the preceding section to the three dimensional case. As before we start with the equation of motion

$$H_0\psi_0 = E\psi_0\,; \qquad H_0 = -(\hbar^2/2\mu)\sum \nabla_\nu^{(n)*}\nabla_\nu^{(n)} + V(x, y, z)\,, \tag{36}$$

together with the subsidiary conditions

$$\theta_\lambda\psi_0 = 0\,. \tag{37}$$

Next we introduce operators P_λ's, which are canonically conjugate to θ_λ's, namely which satisfy

$$[P_\lambda, \theta_{\lambda'}] = (\hbar/i)\delta_{\lambda\lambda'}\,. \tag{38}$$

The P_λ's can be interpreted to be equal to $(\hbar/i)\,\partial/\partial\theta_\lambda$, and so they clearly commute:

$$[P_\lambda, P_{\lambda'}] = 0\,; \tag{39}$$

because of this relation, the canonical transformation defined by

$$\psi_0 \to \psi_1 = U_1^{-1}\psi_0\,; \qquad U_1 = \exp[(i/\hbar)\sum P_\lambda\vartheta_\lambda] \tag{40}$$

can have a well defined meaning. By this canonical transformation the subsidiary condition (37) changes into

$$(\theta_\lambda - \vartheta_\lambda)\psi_1 = 0\,, \tag{41}$$

while the equation of motion (36) changes into

$$\begin{cases} H_1\psi_1 = E\psi_1\,, \\ H_1 = U_1^{-1}H_0U_1 = H_0 + (i/\hbar)\sum[H_0, \vartheta_\lambda]P_\lambda + (i^2/2\hbar^2)\sum[[H_0, \vartheta_\lambda], \vartheta_{\lambda'}]P_\lambda P_{\lambda'}\,. \end{cases} \tag{42}$$

Next, we perform the second canonical transformation

$$\psi_1 \to \psi_2 = U_1^{-1}\psi_1 \; ; \qquad U_2 = \exp\left[-(i/\hbar)\sum \pi_\lambda \theta_\lambda\right] \tag{43}$$

and note that this canonical transformation can again have a well defined meaning by virtue of the commutativity of π_λ's among themselves, as shown in (35). Then using (34), we immediately see that the subsidiary condition becomes

$$\vartheta_\lambda \psi_2 = 0 \, . \tag{44}$$

On the other hand, the transformation of the Hamiltonian is not so easy to perform, because in this case the operators π_λ do not commute with the kinetic energy part of H_0, due to the fact that their expansion coefficients $p_{i\lambda}$ are functions of the Eulerian angles and, in turn, functions of the particle coordinates. Therefore we discuss the calculation of the transformation for each term of H_1 separately.

Firstly, the third term of H_1 changes into

$$(i^2/2\hbar^2)\sum U_2^{-1}[[H_0, \vartheta_\lambda], \vartheta_{\lambda'}]U_2 \cdot U_2^{-1}P_\lambda P_{\lambda'}U_2 \, . \tag{45}$$

It is easily seen, by using (35) and (38), that the second factor in equation (45) is simply equal to $(P_\lambda - \pi_\lambda)(P_{\lambda'} - \pi_{\lambda'})$, while for the evaluation of the first factor we note that the following relation holds:

$$[[H_0, \vartheta_\lambda], \vartheta_{\lambda'}] = -\frac{\hbar^2}{\mu}\sum \frac{\partial \vartheta_\lambda}{\partial x_\nu^{(n)*}} \frac{\partial \vartheta_\lambda}{\partial x_\nu^{(n)}} \, . \tag{46}$$

Then, we can evaluate the right-hand side of this formula by using the explicit form of $\partial\vartheta_\lambda/\partial x_\nu^{(n)}$ given in (32), and the result is simply given by

$$[[H_0, \vartheta_\lambda], \vartheta_{\lambda'}] = -(\hbar^2/\mu)\sum G_{ii'}q_i^\lambda q_{i'}^{\lambda'} \, , \tag{47}$$

where

$$G_{ii'} = \sum (-)^\nu G_{i\nu}^{(n)} G_{i'-\nu}^{(n)} \, ,$$

and explicitly they are

$$G_{11} = \sum (y_n'^2 + z_n'^2)/(\sum (y_u'^2 - z_n'^2))^2 \, ,$$

(G_{22} and G_{33} are obtained by cyclically changing x_n', y_n', and z_n'),

$$G_{ii'} = 0 \quad \text{for} \quad i \neq i' . \tag{48}$$

It is important to note that this $G_{ii'}$ commutes with the π_λ's because it is a function of particle co-ordinates in the primed co-ordinate system, which should be and indeed is, invariant against any rotation of the unprimed co-ordinate system. On the other hand, q_i^λ do not, of course, commute with π_λ, but as they are explicit functions of ϑ_λ, the result of the canonical transformation performed is that they change into $\bar{q}_i^\lambda$, where the bar means that $\bar{q}_i^\lambda$ has the same functional form as q_i^λ, but its arguments are now $\vartheta_\lambda+\theta_\lambda$, instead of being ϑ_λ. Summarizing these steps we obtain for the expression (45)

$$U_2^{-1}(i^2/2\hbar^2)[[H_0, \vartheta_\lambda], \vartheta_{\lambda'}]P_\lambda P_{\lambda'} U_2^{-1} = \tag{49}$$

$$= (1/2\mu) \sum G_{ii'}\bar{q}_i^\lambda \bar{q}_i^{\lambda'}(P_\lambda - \pi_\lambda)(P_{\lambda'} - \pi_{\lambda'}) .$$

We now proceed to the calculation of the contribution of the second term of H_1 and first mention that

$$[H_0, \vartheta_\lambda] = -\hbar(^2/2\mu)\left|2 \sum_\nu \frac{\partial \vartheta_\lambda}{\partial x_\nu^{(n)}} \nabla_\nu^{(n)*} + \sum_n \Delta^{(n)}\vartheta_\lambda\right| . \tag{50}$$

Noting the relation

$$\sum_n \Delta^{(n)}\vartheta_\lambda = \sum G_{ii}q_i^{\lambda'}\partial q_i^\lambda/\partial\vartheta_{\lambda'} = (i/\hbar) \sum G_{ii}q_i^{\lambda'}[\pi_{\lambda'}, q_i^\lambda] ,$$

we first obtain

$$U_2^{-1} \sum_n \Delta^{(n)}\vartheta_\lambda U_2 = (i/\hbar) \sum G_{ii'}\bar{q}_i^{\lambda'}[\pi_{\lambda'}, \bar{q}_i^\lambda] . \tag{51}$$

For the calculation of the transformation of the first term in the bracket of (50), we rewrite (32) in the following form:

$$\partial\vartheta_\lambda/\partial x_\nu^{(n)} = \sqrt{50/3} \sum (-)^{1+N+\nu} A^{-1} a_{ij} q_i^\lambda (2j1 - N\,|\,211n) D^{(1)}_{-\nu n} Y^{(n)'}_{1N} .$$

Then we get

$$U_2^{-1}(\partial\vartheta_\lambda/\partial x_\nu^{(n)})U_2 = \sqrt{50/3} \sum (-)^{1+N+\nu} A^{-1} a_{ij}\bar{q}_j^\lambda (2j1 - N\,|\,211n)\bar{D}^{(1)}_{-n\nu} Y^{(n)'}_{1N} . \tag{52}$$

Regrettably the calculation of $U_2^{-1}\nabla_\nu^{(n)}U_2$ is not so simple; it will be shown in the Appendix. The result, however, is very simple and is given by

$$U_2^{-1}\nabla_\nu^{(n)}U_2 = \sum \bar{D}^*_{\nu m} D_{m'm}\nabla_{m'}^{(n)} + (i/\hbar) \sum G_{i\nu}^{(n)}(\bar{q}_i^\lambda - q_i^\lambda)\pi_\lambda . \tag{53}$$

Using (51), (52), and (53), we can summarize the result of the transfor-

mation of the second term of H_1 as follows:

$$(54)\qquad U_2^{-1}(i/\hbar)[H_0, \vartheta_\lambda]P_\lambda U_2 =$$
$$= (1/\mu)\sum G_{ii}\bar{q}_i^{\lambda}(\bar{q}_i^{\lambda'} - q_i^{\lambda'})\pi_{\lambda'}(P_\lambda - \pi_\lambda) + (1/2\mu)\sum G_{ii}\bar{q}_i^{\lambda'}[\pi_{\lambda'}, q_i^{\lambda}](P_\lambda - \pi_\lambda) -$$
$$- (1/\mu)\sum G_{ii}q_i^{\lambda'}[\pi_{\lambda'}, \bar{q}_i^{\lambda}](P_\lambda - \pi_\lambda) - (i\hbar/\mu)\sum G_{i\nu}^{(n)}\nabla_\nu^{(n)*}\bar{q}_{i\lambda}(P_\lambda - \pi_\lambda)\,.$$

Finally, the calculation of $U_2^{-1}H_0U_2$ is not difficult, because

$$U_2^{-1}H_0U_2 = -(\hbar^2/2\mu)\sum U_2^{-1}\nabla_\nu^{(n)*}U_2\cdot U^{-1}\nabla_\nu^{(n)}U_2\,,$$

and we can use (53) for the evaluation of the right-hand side. We will show only the result which is given by

$$(55)\qquad U_2^{-1}H_0U_2 = H_0 + (1/2\mu)\sum G_{ii}\{(\bar{q}_i^{\lambda} - q_i^{\lambda})\pi_\lambda(\bar{q}_i^{\lambda'} - q_i^{\lambda'})\pi_\lambda +$$
$$+ (\bar{q}_i^{\lambda} - q_i^{\lambda})[\pi_\lambda, q_i^{\lambda'}]\pi_{\lambda'} - q_i^{\lambda}[\pi_\lambda, (\bar{q}_i^{\lambda'} - q_i^{\lambda'})]\pi_{\lambda'}\}\,.$$

Addition of (49), (54), and (55) just gives $H_2 = U_2^{-1}H_1U_2$, which after rearrangement of several terms has the very simple form

$$(56)\qquad H_2 = H_0 - (i\hbar/\mu)\sum G_{i\nu}^{(n)}\nabla_\nu^{(n)*}(\bar{q}_i^{\lambda}P_\lambda - q_i^{\lambda}\pi_\lambda) +$$
$$+ (1/2\mu)\sum G_{ii}(\bar{q}_i^{\lambda}P_\lambda - q_i^{\lambda}\pi_\lambda)(\bar{q}_i^{\lambda'}P_{\lambda'} - q_i^{\lambda'}\pi_{\lambda'})\,.$$

In (56), $\bar{q}_i^{\lambda}$ means the same function as q_i^{λ}, but now its arguments are θ_λ instead of being $\theta_\lambda + \vartheta_\lambda$. This replacement of $\bar{q}_i^{\lambda}$ by $\bar{q}_i^{\lambda}$ is effected because of the subsidiary condition (44), but such a replacement is allowed, of course, only when $\bar{q}_i^{\lambda}$ operates directly on ψ_2. In (56), this fact is already taken into account.

The fact that q_i^{λ} is a function only of θ_λ, and contains no ϑ_λ, allows us to rewrite (56) in a more understandable form. Namely, if we write

$$\sum q_i^{\lambda}P_\lambda = P_i\,,$$

then these P_i's satisfy the commutation relation

$$(57)\qquad [P_i, P_{i'}] = -i\hbar P_{i\times i'}\,,$$

and consequently they can be interpreted as the angular momentum operators referred to the axis of the rotor.

Similar terms, in (56), which contain $q_i^{\lambda}\pi_\lambda$ cannot be treated in the same way, because π_λ is expanded with coefficients $p_{i\lambda}$, instead of with $q_{i\lambda}$. How-

ever, it is very helpful to note that (i) the term $\sum G_{i\nu}q_i^\lambda\pi_\lambda$ originally had the form $\sum(-)^\nu G_{i\,-\nu}^{(n)}G_{i\nu}^{(n)}q_i^\lambda\pi_\lambda$, that (ii) $\sum G_{i\nu}^{(n)}q_i^\lambda$ was the solution for $\partial\vartheta_\lambda/\partial x_\nu^{(n)}$, and that (iii) it is also possible to obtain the solution for $\partial\vartheta_\lambda/\partial x_\nu^{(n)}$ in the form

$$\partial\vartheta_\lambda/\partial x_\nu^{(n)} = \sum G_{i\nu}^{\prime(n)}p_i^\lambda\,, \tag{58}$$

where $G_{i\lambda}^{\prime(n)}$ is a much more complicated function than $G_{i\nu}^{(n)}$, but coincides with the latter under the condition $\vartheta_\lambda = 0$ (*). Using these fates we can now rewrite $\sum G_{ii}q_i^\lambda\pi_\lambda$ as

$$\sum G_{ii}q_i^\lambda\pi_\lambda = \sum(-)^\nu G_{i\,-\nu}^{(n)}G_{i\nu}^{\prime(n)}p_i^\lambda\pi_\lambda\,, \tag{59}$$

and here clearly

$$p_i^\lambda\pi_\lambda = L_i\,. \tag{60}$$

As these L_i's are those defined in (27), they satisfy the usual commutation relation of angular momenta, and can be interpreted as describing the internal angular momenta, under the subsidiary condition (44), or equivalently under the condition

$$(\sum x_n y_n)\psi_2 = (\sum y_n z_n)\psi_2 = (\sum z_n x_n)\psi_2 = 0\,. \tag{61}$$

Using (60), (59) now becomes

$$\sum G_{ii}q_i^\lambda\pi_\lambda = \sum(-)^\nu G_{i\,-\nu}^{(n)}G_{i\nu}^{\prime(n)}L_i\,, \tag{62}$$

but there $G_{i\,-\nu}^{(n)}$ and $G_{i\nu}^{\prime(n)}$ are functions of particle co-ordinates in the primed as well as the unprimed co-ordinate system, and in order to rewrite them as functions only of the unprimed co-ordinate system, it is necessary to make them first operate directly on ψ_2, and afterwards return to their original position. This rearrangement has to be performed very carefully, because these functions do not commute with L_i. It is possible, however, to show that their commutators with L_i are equal to zero, when operated directly on ψ_2, using (61); thus (62) finally becomes

$$\sum G_{ii}q_i^\lambda\pi_\lambda = \sum\tilde{G}_{ii}L_i\,, \tag{63}$$

(*) This coincidence is very natural, because $G_{i\nu}^{(n)}$ can be interpreted to have, so to say, the meaning of $\partial\varphi_i/\partial x_\nu^{(n)}$, where φ_i is the angle defined in (26), the particle co-ordinates used in the definition of ξ_i and η_i, in (25), being considered to be referred to the primed co-ordinate system, while $G_{i\nu}^{\prime(n)}$ is the corresponding expression in the unprimed co-ordinate system, and so they must coincide in the limit of $\vartheta_\lambda = 0$, because in this limit both co-ordinate systems coincide.

where the tilde means that $\tilde{G}_{ii}$ is the same function as G_{ii}, but its arguments are now the particle coordinates in the unprimed coordinate system.

By applying similar reasonings to other terms of (56), we now obtain

$$H_2 = H_0 - (i\hbar/\mu)\sum \tilde{G}^{(n)}_{iy}\nabla^{*(n)}_{y}(P_i - L_i) + (1/2\mu)\sum \tilde{G}_{ii}(P_i - L_i)^2 , \tag{64}$$

or using the explicit form of $G^{(n)}_{iy}$ in (32) and of G_{ii} in (48), we finally arrive at the following form of H_2:

$$H_2 = H_0 + (1/2\mu)\left\{\frac{2i}{\sum (y_n^2 - z_n^2)}\mu_x(P_y - L_y) - \right. \\ \left. - \frac{\sum (y_n^2 + z_n^2)}{(\sum (y_n^2 - z_n^2))^2}(P_x - L_x)^2 + \text{cycl. perm. of } x, y, z\right\} , \tag{65}$$

where $\mu_x = \hbar(y_n\nabla^{(n)}_z + z_n\nabla^{(n)}_y)$, as used by LIPKIN *et al.* [10], and we see that our result (64) just coincides with theirs, if the subsidiary condition (61) is taken into account.

It is regrettable that, in deriving these results, somewhat lengthy calculations are needed, but, nevertheless, it is gratifying that we can employ the same principle as used in Sects. 1 and 2 as well as in our former paper [13].

4. – Three-Dimensional Case with Rotation and Vibration.

Introduction of the vibrational motion is now only a matter of straightforward extension of the content of Sects. 2 and 3, and to that purpose we first introduce two new quantities defined by

$$\begin{cases} \beta = (4\pi/3NR_0^2)[2Y'^2_{22} + Y'^2_{20}]^{\frac{1}{2}} , \\ \gamma = \operatorname{tg}^{-1}[\sqrt{2}\,Y'_{22}/Y'_{20}] . \end{cases} \tag{66}$$

Then the starting equation of motion is

$$H_0\psi_0 = E\psi_0 ; \qquad H_0 = -\hbar^2/2\mu\sum_n \Delta^{(n)} + V(x, y, z) , \tag{67}$$

together with the subsidiary condition

$$\theta_\nu\psi_0 = b\psi_0 = c\psi_0 = 0 . \tag{68}$$

To this system we perform the first canonical transformation

$$\psi_0 \to \psi_1 = U_1^{-1}\psi_0 ; \qquad U_1 = \exp[(i/\hbar)(P_\lambda\vartheta_\lambda + P_b\beta + P_c\gamma)] ,$$

where P_b and P_c are assumed to satisfy the following commutation relations

$$[P_b, b] = [P_c, c] = \hbar/i\,, \qquad [P_b, c] = [P_c, b] = [P_b, P_c] = 0\,.$$

Then (69) changes into

$$H_1\psi_1 = E\psi_1\,; \qquad H_1 = U_1^{-1}H_0U_1 = H_0 + H_1^{\mathrm{rot}} + H_1^{\mathrm{vib}}\,,$$

where H_1^{rot} is equal to H_1 in (42) minus H_0, while H_1^{vib} is

$$\begin{aligned}(70)\qquad H_1^{\mathrm{vib}} &= (i/\hbar)\{[H_0, \beta]P_b + [H_0, \gamma]P_c\} + \\ &+ (i^2/2\hbar^2)\{[[H_0, \beta], \beta]P_b^2 + [[H_0, \gamma], \gamma]P_c^2 + 2[[H_0, \beta], \gamma]P_bP_c\},\end{aligned}$$

and the subsidiary conditions now become

$$(\theta_\lambda - \vartheta_\lambda)\psi_1 = (b - \beta)\psi_1 = (c - \gamma)\psi_1 = 0\,.$$

Next we perform the second canonical transformation

$$\psi_1 \to \psi_2 = U_2^{-1}\psi_1\,; \qquad U_2 = \exp[-(i/\hbar)\pi_\lambda\theta_\lambda]\,,$$

namely just the same transformation as performed in (43) in the preceding section. Then, the result of this transformation applied to the first two terms of H_1 is given by the expression shown in (65), and we denote this as $H_0 + H_2^{\mathrm{rot}}$. On the other hand, it may seem on first sight that some complication again occurs concerning the calculation of the transformation of H_1^{vib} because, although β and γ commute with π_λ, H_0 does not. However, we can prove that, nevertheless, $[H_0, \beta]$, $[[H_0, \beta], \beta]$ and others commute with π_λ, and this fact further means that no change occurs to H_1^{vib} by this canonical transformation. Therefore, we obtain the final form of our equation of motion as

$$(71)\qquad H_2\psi_2 = E\psi_2\,; \qquad H_2 = H_0 + H_2^{\mathrm{rot}} + H_1^{\mathrm{vib}}\,,$$

and the subsidiary condition is now

$$(72)\qquad \vartheta_\lambda\psi_2 = (b - \beta)\psi_2 = (c - \gamma)\psi_2 = 0\,.$$

Our only remaining task is to express H_1^{vib} in a more explicit form, and to this purpose we first show the following formulae which are not so difficult

to obtain:

$$(73a)\qquad \frac{-\hbar^2}{2\mu}\sum\frac{\partial\beta}{\partial x_\nu^{(n)*}}\frac{\partial\beta}{\partial x_\nu^{(n)}}=\frac{-\hbar^2}{2B}\left(1+\left(\frac{4\pi}{3NR_0^2}\right)^3\left(\frac{5}{2\pi}\right)^2\frac{1}{\beta^2}(\xi_1-\xi_2)(\xi_2-\xi_3)(\xi_3-\xi_1)\right),$$

$$(73b)\qquad \frac{-\hbar^2}{2\mu}\sum_n\Delta^{(n)}(\beta)=\frac{-\hbar^2}{2B}\cdot\frac{4}{\beta}\left(1+\left(\frac{4\pi}{3NR_0^2}\right)^3\left(\frac{5}{4\pi}\right)^2\frac{1}{\beta^2}(\xi_1-\xi_2)(\xi_2-\xi_3)(\xi_3-\xi_1)\right),$$

$$(73c)\qquad \frac{-\hbar^2}{2\mu}\sum\frac{\partial\gamma}{\partial x_\nu^{(n)*}}\frac{\partial\gamma}{\partial x_\nu^{(n)}}=\frac{\hbar^2}{2B}\frac{1}{\beta^2}\left(1+\left(\frac{4\pi}{3NR_0^2}\right)^3\left(\frac{5}{2\pi}\right)^2\cdot\frac{1}{\beta^2}(\xi_1-\xi_2)(\xi_2-\xi_3)(\xi_3-\xi_1)\right),$$

$$(73d)\qquad \frac{-\hbar^2}{2\mu}\sum_n\Delta^{(n)}\gamma=\frac{-\hbar^2}{2B}\frac{1}{\beta^2}\left(3\cot 3\gamma+\frac{5}{3\sqrt{3}NR_0^2}\frac{1}{\xi_1\xi_2\xi_3}\right.$$

$$\left.\cdot\{\xi_1\xi_2(\xi_1-\xi_2)^2+\xi_2\xi_3(\xi_2-\xi_3)^2+\xi_3\xi_1(\xi_3-\xi_1)^2\}-\frac{\sqrt{5}\beta\sin 3\gamma}{4\sqrt{2}\pi}\right),$$

$$(73e)\qquad \frac{-\hbar^2}{2\mu}\sum\frac{\partial\beta}{\partial x_\nu^{(n)*}}\frac{\partial\gamma}{\partial x_\nu^{(n)}}=\frac{-\hbar^2}{2B}\cdot\frac{-3\sin 3\gamma}{40}\sqrt{\frac{2}{5\pi}},$$

where

$$B=3NR_0^2\mu/8\pi$$

is the mass operator used by Bohr [12].

These expressions are rather long, but if we note that the second (and the third) terms in the brackets in (73*a*) through (73*d*) are all one order of β smaller than their respective first terms and, further, that (73*e*) has the same order of magnitude as the second term of (73*b*), we can neglect these terms in the first order approximation. Then, if we replace β and γ, respectively, by b and c, by virtue of the subsidiary condition (72), we can summarize the result as

$$(74)\qquad H_1^{\text{vib}}=\frac{1}{2B}\left(P_b^2+\frac{\hbar}{i}\frac{4}{b}P_b+\frac{1}{b^2}P_c^2+\frac{\hbar}{i}\frac{3\operatorname{ctg}3c}{b^2}P_c\right)+H_{\text{coupl}}^{\text{vib}},$$

where

$$(75)\qquad H_{\text{coupl}}^{\text{vib}}=(\hbar/2\mu i)\sum\left\{[\nabla_\nu^{*(n)},\beta]\nabla_\nu^{(n)}P_b+[\nabla_\nu^{(n)*},\gamma]\nabla_\nu^{(n)}P_c\right\}.$$

is the coupling term between the internal and the vibrational motions. If we further rewrite the first term of (74) by using the fact that we can replace

P_b and P_c by $(\hbar/i)(\partial/\partial b)$ and $(\hbar/i)(\partial/\partial c)$, respectively, the H_1^{vib} changes into

$$(76)\qquad \begin{cases} H_1^{\text{vib}} = \dfrac{-\hbar^2}{2B}\left(\dfrac{\partial^2}{\partial b^2}+\dfrac{4}{b}\dfrac{\partial}{\partial b}+\dfrac{1}{b^2}\dfrac{\partial^2}{\partial c^2}+\dfrac{3\operatorname{ctg} c}{b^2}\dfrac{\partial}{\partial c}\right)+H_{\text{coupl}}^{\text{vib}}, \\ \quad = \dfrac{-\hbar^2}{2B}\left(\dfrac{1}{b^4}\dfrac{\partial}{\partial b}b^4\dfrac{\partial}{\partial b}+\dfrac{1}{b^2}\dfrac{1}{\sin 3c}\dfrac{\partial}{\partial c}\sin 3c\dfrac{\partial}{\partial c}\right)+H_{\text{coupl}}^{\text{vib}}, \end{cases}$$

and we see that the first term just has reproduced Bohr's operator for vibrational motion [12], which was denoted there as T_{vib}.

5. – Discussion.

In the preceding section, it was shown that our general technique can be applied in many cases, giving the required results fairly easily; we thus succeeded in obtaining the Hamiltonian for collective motions from the one for individual particle motions.

Nevertheless, the separation between the collective and the individual motions is not complete because of the appearance of the second term in (76) and terms in (65) which are linear in P_λ's. These terms are by no means small compared with the terms which describe collective motions, as, e.g., was noticed by NATAF [9] and by BOHR and MOTTELSON [16].

This difficulty is also related to the fact that the moment of inertia which appeared in Sect. 3 does not agree with the experimental value [17].

It is easily seen that these difficulties are caused by the fact that the collective motion described by our Hamiltonian corresponds to that of the irrotational motion, and that this is a consequence of the special choice of ϑ_λ in Sect. 3. It is hoped, therefore, to find some other new functions, at the beginning, instead of this ϑ_λ, so that both these difficulties can be removed at the same time. Such a treatment will be discussed elsewhere.

* * *

The author expresses his sincere thanks to Professor AAGE BOHR for his continued interest in this work and many helpful discussions. His thanks are due Professor NIELS BOHR for his kind hospitality and the Rask-Ørsted Foundation for financial support. He is indebted to Professor F. VILLARS for permission to refer to his unpublished work.

[16] A. BOHR and B. MOTTELSON: *Dan. Mat. Fys. Medd.*, **30**, no. 1 (1955).
[17] See, e.g., K. W. FORD: *Phys. Rev.*, **95**, 1250 (1954).

Appendix

In this appendix we show the details of the calculation of

$$\exp\left[(i/\hbar)\pi_\lambda\theta_\lambda\right]\nabla_\nu^{(n)}\exp\left[-(i/\hbar)\pi_\lambda\theta_\lambda\right],$$

which appeared in (53) in the text, and we do this, as an illustration, for the case of $\nu = 1$. By virtue of the commutativity of π_i's among themselves, the result of the canonical transformation is independent of the λ with which we begin and, for the sake of simplicity, we begin with $\lambda = 3$.

Now

$$\text{(A.1)}\qquad \exp\left[(i/\hbar)\pi_3\theta_3\right]\nabla_1^{(n)}\exp\left[-(i/\hbar)\pi_3\theta_3\right] = \nabla_\nu^{(n)} + (i/\hbar)[\pi_3, \nabla_1^{(n)}]\theta_3 + (i^2/2\hbar^2)[\pi_3, [\pi_3, \nabla_1^{(n)}]]\theta_3^2 + \cdots .$$

Then, using the explicit form of π_3 given in (33), we calculate the commutators $[\pi_3, \nabla_\nu^{(n)}]$ and obtain

$$\text{(A.2)}\qquad \begin{cases} [\pi_3, \nabla_1^{(n)}] = B_{ni}^{(n)}F_{1ni} - (i\hbar/\sqrt{2})\sin\vartheta_2\exp\left[i\vartheta_1\right]\nabla_0^{(n)} + \hbar\cos\vartheta_2\nabla_1^{(n)}, \\ [\pi_3, \nabla_{-1}^{(n)}] = B_{ni}^{(n)}F_{-1ni} + (i\hbar/\sqrt{2})\sin\vartheta_2\exp\left[-i\vartheta_1\right]\nabla_0^{(n)} - \hbar\cos\vartheta_2\nabla_{-1}^{(n)}, \\ [\pi_3, \nabla_0^{(n)}] = B_{ni}^{(n)}F_{0ni} - (i\hbar/\sqrt{2})\sin\vartheta_2\exp\left[i\vartheta_1\right]\nabla_{-1}^{(n)} \quad \exp\left[-i\vartheta_1\right]\nabla_1^{(n)}, \end{cases}$$

where

$$\text{(A.3)}\qquad B_{ni}^{(n)} = \sqrt{50/3}(2j1 - N\,|\,211n)A^{-1}a_{ij}(-)^N\Upsilon_{1N}^{(n')},$$

and

$$\text{(A.4)}\qquad F_{mni} = (-)^m D_{-mn}^{(1)}\{q_i^2(\operatorname{ctg}\vartheta_2\pi_3 - \operatorname{cosec}\vartheta_2\pi_1) + q_i^1\sin\vartheta_2\pi_2\}.$$

In performing the calculation of $[\pi_3, [\pi_3, \nabla_1^{(n)}]]$, we note that the factor B_{ni} in the first term of $[\pi_3, \nabla_1^{(n)}]$ commutes with π_3, while in the factor F_{mni} the quantities which do not commute with π_3 are q_i^2, q_i^1 and $D_{-mn}^{(1)}$. However, these quantities are explicit functions of ϑ_3, and thus we can write the commutator $[\pi_3, F_{mni}]$ as

$$\text{(A.5)}\qquad [\pi_3, F_{mni}] = (-)^m\frac{\hbar}{i}\left\{\left(\frac{\partial}{\partial\vartheta_3}D_{-mn}^{(1)}q_i^2\right)\cdot(\cos\vartheta_2\pi_3 - \operatorname{cosec}\vartheta_2\pi_1) + \left(\frac{\partial}{\partial\vartheta_3}D_{-mn}^{(1)}q_i^1\right)\sin\vartheta_2\pi_2\right\}.$$

We further note that, in the second and the third terms of the right-hand side of $[\pi_3, \nabla_1^{(n)}]$, the only quantities which do not commute with π_3 are $\nabla_1^{(n)}$'s, but all commutation relations $[\pi_3, \nabla_\nu^{(n)}]$ are already given in (A.2).

Having these facts in mind, it is now possible to calculate $[\pi_3, [\pi_3, \nabla_1^{(n)}]]$ and other higher commutators and we obtain the following explicit form for the expression of (A.1):

$$
\begin{aligned}
&\text{(A.6)}\quad \exp[(i/\hbar)\pi_3\vartheta_3]\nabla_1^{(n)}\exp[-(i/\hbar)\pi_3\vartheta_3] = \\
&= \left\{\left(1 + i\cos\vartheta_2\vartheta_3 - \frac{1+\cos^2\vartheta_2}{2}\cdot\frac{\vartheta_3^2}{2!} - i\frac{\cos^2\vartheta_2}{3!}\vartheta_3^3 + \frac{1+\cos^2\vartheta_2}{2}\cdot\frac{\vartheta_3^4}{4!} - \cdots\right)\nabla_1^{(n)} - \right. \\
&+ \frac{1}{\sqrt{2}i}\exp[i\vartheta_1]\left(i\sin\vartheta_2\vartheta_3 - \frac{1}{2!}\sin\vartheta_2\cos\vartheta_2\vartheta_3^2 - i\frac{1}{3!}\sin\vartheta_2\vartheta_3^3 + \right. \\
&\left.\left. + \frac{1}{4!}\sin\vartheta_2\cos\vartheta_2\vartheta_3^4 + \cdots\right)\nabla_0^{(n)} + \exp[2i\vartheta_1]\frac{\sin\vartheta_2}{2}\left(\frac{1}{2!}\vartheta_3^2 - \frac{1}{4!}\vartheta_3^4 + \cdots\right)\nabla_{-1}^{(n)}\right\} + \\
&+ (i/\hbar)B_{ni}^{(n)}\left\{a_{(1)}F_{1ni} + a_{(2)}\left((1/\sqrt{2})\sin\vartheta_2 F_{0ni} + i\cos\vartheta_2 F_{1ni}\right) + \right. \\
&\left. - a_{(3)}\left(\frac{\sin\vartheta_2}{2}F_{-1ni} - \frac{1+\cos^2\vartheta_2}{2}F_{1ni} + \frac{i}{\sqrt{2}}\sin\vartheta_2\cos\vartheta_2 F_{0ni}\right)\right\},
\end{aligned}
$$

where, in the second term, the $a_{(i)}$'s are the following operators:

$$
\text{(A.7)}\quad \begin{cases} a_{(1)} = \vartheta_3 - \dfrac{\vartheta_3^2}{2!}\dfrac{\hat{c}}{\hat{c}\vartheta_3} + \dfrac{\vartheta_3^3}{3!}\dfrac{\hat{c}^2}{\hat{c}\vartheta_3^2} - \cdots, \\ a_{(2)} = \left(\dfrac{\vartheta_3^2}{2!} + \dfrac{\vartheta_3^3}{3!}\dfrac{\hat{c}}{\partial\vartheta_3} + \dfrac{\vartheta_3^4}{4!}\dfrac{\hat{c}^2}{\hat{c}\vartheta_3^2} + \cdots\right) - \left(\dfrac{\vartheta_3^4}{4!} + \dfrac{\vartheta_3^5}{5!}\dfrac{\hat{c}}{\hat{c}\vartheta_3} + \cdots\right) + \left(\dfrac{\vartheta_3^6}{6!} + \cdots\right)\cdots, \\ a_{(3)} = \left(\dfrac{\vartheta_3^3}{3!} + \dfrac{\vartheta_3^4}{4!}\dfrac{\hat{c}}{\hat{c}\vartheta_3} + \cdots\right) - \left(\dfrac{\vartheta_3^5}{5!} + \dfrac{\vartheta_3^6}{6!}\dfrac{\hat{c}}{\hat{c}\vartheta_3} + \cdots\right) + \left(\dfrac{\vartheta_3^7}{7!} + \cdots\right)\cdots. \end{cases}
$$

(A.6) is very long indeed but, as for the first term, we see that it can be summarized in the compact form

$$
\begin{aligned}
&\text{(A.8)}\quad [(\sin^2\vartheta_2/2) + i\cos\vartheta_2\sin\vartheta_3 + ((1+\cos^2\vartheta_2)/2)\cos\vartheta_3]\nabla_1^{(n)} - \\
&- (i/\sqrt{2})\exp[i\vartheta_1](-\sin\vartheta_2\cos\vartheta_2 + i\sin\vartheta_2\sin\vartheta_3 + \sin\vartheta_2\cos\vartheta_2\cos\vartheta_3)\nabla_0^{(n)} + \\
&+ \exp[2i\vartheta_1](\sin^2\vartheta_2/2)(1-\cos\vartheta_3)\nabla_{-1}^{(n)} = \\
&= \sum D_{1m}^{(1)*}(\vartheta_1, \vartheta_2, \vartheta_3 + \vartheta_3)D_{m'm}^{(1)}(\vartheta_1, \vartheta_2, \vartheta_3)\nabla_{m'}^{(n)}.
\end{aligned}
$$

For the evaluation of the second term in (A.6), it is necessary, from now on, to perform the calculation separately for different suffixes i which appear as a summation index, and we here illustrate the case of $i = 1$. Before starting

this calculation, however, we perform on (A.6) the further canonical transformation induced by $\exp[-(i/\hbar)(\pi_1\theta_1+\pi_2\theta_2)]$ and obtain

$$\begin{aligned}(A.9)\quad &\exp[(i/\hbar)\pi_\lambda\theta_\lambda]\nabla_1^{(n)}\exp[-(i/\hbar)\pi_\lambda\theta_\lambda]=\\ &=\sum D^{(1)*}_{1m}(\vartheta_1+\theta_1,\vartheta_2+\theta_2,\vartheta_3+\theta_3)D^{(1)}_{m'm}(\vartheta_1+\theta_1,\vartheta_2+\theta_2,\vartheta_3)\cdot\\ &\cdot\exp[(i/\hbar)(\pi_1\theta_1+\pi_2\theta_2)]\nabla_{m'}^{(n)}\exp[-(i/\hbar)(\pi_1\theta_1+\pi_2\theta_2)]+\\ &+(i/\hbar)B^{(n)}_{ni}\{a_{(1)}\overline{\overline{F}}_{1ni}+a_{(2)}[(1/\sqrt{2})\sin(\vartheta_2+\theta_2)\overline{\overline{F}}_{0ni}+i\cos(\vartheta_2+\theta_2)\overline{\overline{F}}_{1ni}]+\\ &+a_{(3)}[(\sin^2(\vartheta_2+\theta_2)/2)\overline{\overline{F}}_{-1ni}-([1+\cos^2(\vartheta_2+\theta_2)]/2)\overline{\overline{F}}_{1ni}+\\ &+(i/\sqrt{2})\sin(\vartheta_2+\theta_2)\cos(\vartheta_2+\theta_2)\overline{\overline{F}}_{0ni}]\}\,,\end{aligned}$$

where the double bar on F_{mni} means that here the arguments ϑ_1 and ϑ_2 are changed into $\vartheta_1+\theta_1$ and $\vartheta_2+\theta_2$, respectively, while ϑ_3 remains unchanged. The evaluation of the last factor in the first term of (A.9) is again as tedious as the case illustrated in (A.6), but it is gratifying to note that no terms which contain π_2 as a factor appear from this term, but solely from the second term in (A.9). Therefore, if we limit our illustration to such terms, the task is much simplified.

Now, in (A.9), the term which contains π_2 as a factor and corresponds to $i=1$ is given in the form

$$\begin{aligned}(A.10)\quad &-(1/\hbar)\exp[i(\vartheta_1+\theta_1)]\{B_{11}([1-\cos(\vartheta_2+\theta_2)]/4)\cdot(a_{(1)}-ia_{(2)}-a_{(3)})\cdot\\ &\cdot(\exp[-2i\vartheta_3]+1)+B_{-11}([1+\cos(\vartheta_2+\theta_2)]/4)\cdot(a_{(1)}+ia_{(2)}-a_{(3)})\cdot\\ &\cdot(\exp[2i\vartheta_3]-1)+B_{01}(\sin(\vartheta_2+\theta_2)/\sqrt{2})a_{(1)}\sin\vartheta_3\}\pi_2\,.\end{aligned}$$

Then, using the result

$$\begin{aligned}&(a_{(1)}\mp ia_{(2)}-a_{(3)})\{\exp[\mp 2i\vartheta_3]-1\}=\\ &\qquad=\pm i\{\exp[\mp(2i\vartheta_3+i\theta_3)]-1\}\{\exp[-i\theta_3]-1\}\,,\end{aligned}$$

and

$$a_{(1)}\sin\vartheta_3=\cos\vartheta_3-\cos(\vartheta_3+\theta_3)\,,$$

together with the fact that $B_{11}=B_{-11}$, which plays an essential part here, we can show that (A.10) may be summarized in the following very simple form:

$$(A.11)\qquad -(i/\hbar)\sum B^{(n)}_{n1}\overline{D}_{-1n}(\overline{q}_1^2-q_1^2)\pi_2\,.$$

The case where $i=2$ and 3 can also be calculated similarly, and if we use the explicit form of $B^{(n)}_{ni}$ given in (A.3), the whole term in (A.9) which contains a factor π_2 is given by

$$(A.12)\qquad (i/\hbar)\sqrt{50/3}\sum A^{-1}a_{ij}(2j1-N\,|\,211n)(-)^N Y'^{(n)}_{1N}\overline{D}_{-1n}(\overline{q}_i^2-q_i^2)\pi_2\,.$$

Terms in (A.9) which are proportional to π_1 or π_3 can be calculated similarly, although it is much more cumbersome. The whole expression for (A.9) is now summarized in the simple form

$$\text{(A.13)}\quad \exp\left[(i/\hbar)\pi_\lambda\theta_\lambda\right]\nabla_1^{(n)}\exp\left[-(i/\hbar)\pi_\lambda\theta_\lambda\right] =$$

$$= \sum \overline{D}^{(1)*}_{1m} D^{(1)}_{m'm}\nabla^{(n)}_{m'} - (i\hbar)\sqrt{50\,3}\sum A^{-1}a_{\lambda j}(2j1\ \ N\ 211n)(\ \ )^N Y^{*}_{1N}\overline{D}_{1n}(\overline{q}^{\lambda}_{i}\quad q^{\lambda}_{i})\pi_\lambda -$$

$$= \sum \overline{D}^{(1)*}_{1m} D^{(1)}_{m'm}\nabla^{(n)}_{m'} + (i/\hbar)\sum G^{(n)}_{i1}(\overline{q}^{\lambda}_{i} - q^{\lambda}_{i})\pi_\lambda\,.$$

The calculations for ∇_0 and ∇_{-1} are similar, and we finally obtain the result given in (53) in the text.

RIASSUNTO (*)

Si estende al caso dell'accoppiamento forte un metodo generale per la descrizione collettiva di un sistema di più particelle introdotto da MIYAZIMA e dallo scrivente e applicato al caso delle oscillazioni superficiali dei nuclei atomici con accoppiamento debole, e si confrontano i risultati con quelli di altri autori.

(*) *Traduzione a cura della Redazione.*

On the Anomalous Magnetic Moment of μ-Mesons.

S. Hirokawa, H. Komori and S. Ogawa (*)

Institute for Theoretical Physics, Nagoya University - Nagoya
Department of Physics, Hiroshima University (*) - Hiroshima, Japan

(ricevuto il 4 Giugno 1956)

Summary. — From the analysis of the cosmic ray bursts produced by μ-mesons, the upper limit of the magnitude of the anomalous magnetic moment of μ-mesons is estimated. As a result, the anomalous magnetic moment of μ-mesons is found to be smaller than 80 percent of the normal Dirac moment.

1. – Introduction.

In 1941, Christy and Kusaka [1] tried to determine the spin of the μ-meson by analyzing cosmic ray bursts. Since then, its spin has been generally accepted to be zero or one-half.

Recently, various unstable particles have been found and some attempts [2] to classify these complicated phenomena have been made. The introduction of the concept of « family » (e.g., nucleon family, lepton family, etc.) may be useful for such a purpose. Now, on the ground of the similarity in the coupling constants among those processes, namely β-decay, μ-e decay and μ-capture, the view-point of « Universal Fermi Interaction » has been proposed [3]. According to this theory, we assume the spin of the μ-meson to be one-half, and treat electrons, neutrinos and μ-mesons as a whole, i.e., as belonging to the lepton family. In contrast with the nucleon family which has both strong and weak interactions with other fields, the lepton family is generally considered not to interact strongly with other fields (*). Although this interpretation has

(1) R. F. Christy and S. Kusaka: *Phys. Rev.*, **59**, 414 (1941).
(2) For example, R. G. Sachs: *Phys. Rev.*, **99**, 1573 (1955).
(3) O. Klein: *Nature*, **161**, 897 (1948).
(*) A possible model for understanding all weak interactions has been proposed by one of us (S.O.). S. Ogawa: *Progr. Theor. Phys.*, **15**, 487 (1956).

been widely confirmed in the process in which electrons participate, it has not been definitely established in the reaction containing μ-mesons. It is of interest to investigate if there exist other interactions than the universal Fermi interaction in the reaction concerning μ-mesons, or not [4]. Even if there exists a boson field which strongly interacts only with μ-mesons, and not with other particles (electrons, nucleons and π-mesons, etc.), we may be unable to observe a strong interaction between μ-mesons and other particles in the present stage of the experimental technique. This situation will, however, be clarified by analyzing the interaction of μ-mesons with their self fields, e.g., analyzing the anomalous magnetic moment (a.m.m.) of the μ-meson. It is the first object of this paper.

In the second place, we shall consider the type of electromagnetic interaction. An essential expression of the electromagnetic interaction is assumed to have a form

$$eA_\mu \sum_a j_\mu(a) ,$$

where e, A_μ and $j_\mu(a)$ are the charge constant, the electromagnetic potential and the current of particle a. However, the electromagnetic interaction is not necessarily restricted to this type so far as the gauge invariance is assured. For the investigation on the family of particles and on the interaction among them, it will be important to make clear whether the essential type of the electromagnetic interaction is restricted to the above type. If it is confirmed that there are no strong interactions among the lepton-family, the estimation of the a.m.m. of μ-mesons will give a clue to the above problem.

The magnitude of the a.m.m. of μ-mesons will be estimated from the analysis of the electromagnetic transition of μ-mesons, for example, the scattering of μ-mesons by nuclei [5], the level-shift in a μ-mesonic atom [6] and the π-μ decay associated with a photon [7]. However, at the present stage of the experimental technique, the study of these phenomena determines the amount of a.m.m. of μ-mesons only in the order of magnitude. The analysis of cosmic ray bursts does not give precise information on the a.m.m. due to the limitation of theory and experiment. However, if a μ-meson has an a.m.m. other than the normal Dirac moment, this anomaly will affect the energy spectrum of μ-mesons at sea level. The spectrum is obtained from the intensity-depth

---

[4] K. Iwata, S. Ogawa, H. Okonogi and S. Oneda: *Progr. Theor. Phys.*, **13**, 19 (1955).

[5] E.g., I. B. Mc Diarmid: *Phil. Mag.*, **45**, 933 (1954); G. D. Rochester and A. W. Wolfendale: *Phil. Mag.*, **45**, 980 (1954).

[6] V. L. Fitch and J. Rainwater: *Phys. Rev.*, **92**, 789 (1953).

[7] N. F. Fry: *Phys. Rev.*, **86**, 418 (1952).

curve of the μ-mesons underground taking account of the energy losses. Further, the a.m.m. will also affect the burst size. These effects will make our estimate a little more precise. Our practical calculation is the same as that of CHRISTY and KUSAKA.

In addition to the above discussions, some information will be given on the energy spectrum of μ-mesons at sea level.

2. – The Energy Spectrum of μ-Mesons at Sea Level.

As already mentioned in the preceding section, we shall take the spin of μ-mesons to be one-half. To obtain the energy spectrum of μ-mesons at sea level from the intensity-depth curve, we follow the method of HAYAKAWA and TOMONAGA [8]. Let E eV be the energy of a μ-meson, then the energy loss $-(\mathrm{d}E/\mathrm{d}x)$ per g cm^{-2} is given as follows:

$$
\begin{aligned}
(-\mathrm{d}E/\mathrm{d}x)_{\mathrm{ion}} &= (2.20 + 0.191\delta^2)\cdot 10^6 \text{ eV per g cm}^{-2} \\
(-\mathrm{d}E/\mathrm{d}x)_{\mathrm{brem}} &= (1.02 + 0.352\delta^2 + 1.87\delta^4)\cdot 10^{-6}\, E \text{ eV per g cm}^{-2} \quad (*) \\
(-\mathrm{d}E/\mathrm{d}x)_{\mathrm{pair}} &= 1.60\cdot 10^{-6}\, E \text{ eV per g cm}^{-2} \\
(-\mathrm{d}E/\mathrm{d}x)_{\text{n-int}} &= 2.50\cdot 10^{-7}\, E \text{ eV per g cm}^{-2} \\
(-\mathrm{d}E/\mathrm{d}x)_{C} &= 0.100 \ln (E/100^9)\cdot 10^6 \text{ eV per g cm}^{-2} \text{ (but only for } E > 10^9 \text{ eV)},
\end{aligned}
$$

where ion represents the ionization, brem the bremsstrahlung, pair the electron pair creation, n-int the nuclear interaction, C the Čerenkov radiation and δ the amount of a.m.m. to the normal Dirac moment. As we intend to estimate the upper limit of a.m.m., we must under-estimate the intensity of μ-mesons at sea level as far as possible. Accordingly, we neglect a term proportional to E^2 in the case of $\delta > 0$. For the cross-section of nuclear interaction of μ-mesons, we use the value of BRADDICK and LEONTIC [9], $3.2\cdot 10^{-30}$ cm^2/nucleon [+], for energies greater than about 12 GeV. According to TOMONAGA [10],

---

[8] S. HAYAKAWA and S. TOMONAGA: *Progr. Theor. Phys.*, **4**, 287 (1949).

(*) In the work of Pauli, there is a careless mistake. We have recalculated this equation by the use of Batdorf-Thomas' (B-T) result. As to the lower limit for the integration over the impact parameter, we followed the procedure taken by B-T. Some remarks on this point are given by POWELL.

W. PAULI: *Rev. Mod. Phys.*, **13**, 203 (1941); S. B. BATDORF and R. THOMAS: *Phys. Rev.*, **59**, 621 (1941); J. L. POWELL: *Phys. Rev.*, **75**, 32 (1949).

[9] H. J. J. BRADDICK and B. LEONTIC: *Phil. Mag.*, **45**, 1287 (1954).

[+] Previously, BRADDICK derived from his experiment a value larger by one order than this. Therefore, the value of George who calculated the energy loss of nuclear interaction basing on the earlier value of Braddick is also large. E. P. GEORGE: *Progress in Cosmic Ray Phys.*, Vol. I (Amsterdam, 1952).

[10] S. TOMONAGA: *Sci. Pap. Inst. Phys. Chem. Res. (Japan)*, **37**, 399 (1940).

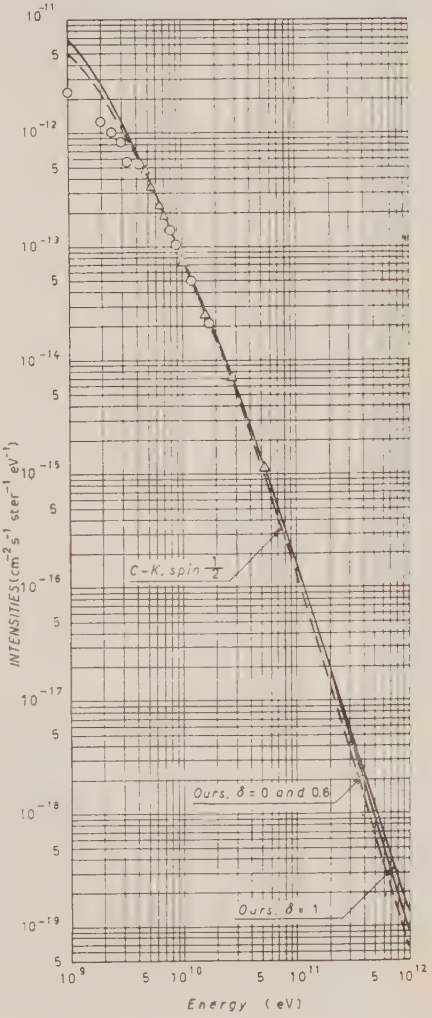

Fig. 1. – The differential energy spectrum of μ-mesons at sea level. The circles represent experimental determinations by WILSON. The triangles represent experimental data of CARO *et al.*. The theoretical curve is normalized at 53 GeV. The spectrum for $\delta = 0.8$ is not illustrated in order to avoid confusion in the graph. δ is the magnitude of the a.m.m.. C-K represents the result of CRHISTY and KUSAKA for spin $\frac{1}{2}$.

the a.m.m. does not affect the cross-section of electron pair creation. As for the process of the nuclear interaction of μ-mesons, its cross-section is represented by the product of the momentum spectrum of photons and the cross-section of the π-meson creation by a photon. The cross-section of bremsstrahlung in the extreme relativistic case, assuming the atomic number of earth is 10, is $1.3 \cdot 10^{-27}$ cm². If we accept the value of $3.2 \cdot 10^{-30}$ cm²/nucleon for the cross-section of nuclear interaction, the contribution of the process of nuclear interaction to that of bremsstrahlung is estimated to be about 5 percent for the earth, assuming the atomic number Z to be 10 and the mass number 20. We suppose that the same situation will also hold in the process occurring in the a.m.m.. Adding together the above expressions, we obtain for the total rate of energy loss at high energies

$$(-\mathrm{d}E/\mathrm{d}x)_{\mathrm{tot}} = a + bE + c \ln (E/10^9)$$

$$a = (2.20 + 0.191\delta^2) \cdot 10^6 \text{ eV per g cm}^{-2}$$

$$b = (2.87 + 0.35\delta^2 + 1.87\delta^4) \cdot 10^{-6} \text{ per g cm}^{-2}$$

$$c = 1.00 \cdot 10^5 \text{ eV per g cm}^{-2}.$$

Using the above equations and taking account of the nuclear interaction participating in the a.m.m., the energy spectra at sea level are calculated. They are shown in Fig. 1, in which the experimental data [11] directly measured are also plotted. The point of normalization of the theory to the experiment is taken at 53 GeV. As previously mentioned, we should under-estimate the intensity of μ-mesons at sea level as far as possible. Accordingly, we normalize the theoretical value to the experimental one at the largest value of energy which is measured at sea level. As is easily seen from Fig. 1, the a.m.m. does not affect appreciably the energy spectrum below 70 GeV. In the energy region between 8 GeV and 53 GeV the theoretical intensity agrees with the experimental one very well. In the energy region lower than 8 GeV, however, the theoretical value somewhat exceeds the experimental one. This feature indicates that the μ-mesons are associated with the other component (mainly air showers with small sizes) in the measurements not too deep underground. Thus, for the differential energy spectrum of μ-mesons at sea level, we shall use the experimental spectrum in the energy region lower than 53 GeV and the theoretical one at energies above this.

Now, denoting the μ-meson energy in eV, zenith angle and solid angle by E_0, θ and $\mathrm{d}\Omega$, respectively, we can express the differential energy spectrum by

$$N(E_0)\,\mathrm{d}E_0\,\mathrm{d}\Omega = 1.45\cdot10^{-3}\cdot\frac{(9.7\cdot10^9)^{1.8}}{(E_0+1.8\cdot10^9\sec\theta)^{2.8}}\,\mathrm{d}E_0\,\mathrm{d}\Omega$$

for $1.5\cdot10^{10}\ \mathrm{eV}\leqslant E_0\leqslant 5.3\cdot10^{10}\ \mathrm{eV}$ (*), independently of δ and by

$$N(E_0)\,\mathrm{d}E_0\,\mathrm{d}\Omega = 6.57\cdot10^{-5}\cdot\frac{(5.48\cdot10^{10})^{\gamma-1}}{(E_0+1.8\cdot10^9\sec\theta)^{\gamma}}\,\mathrm{d}E_0\,\mathrm{d}\Omega \qquad \text{for } 5.3\cdot10^{10}\ \mathrm{eV}\leqslant E_0\,,$$

where the relation of δ to γ is given in Table I.

TABLE I. – *Relation of δ to γ.*

δ	0	0.6	0.8	1.0
γ	3.3	3.2	3.2	3.1

We take account of all the processes and appropriate values for the energy losses, and obtain the theoretical energy spectrum which agrees very fairly

[11] J. G. WILSON: *Nature*, **158**, 415 (1946); D. E. CARO, J. K. PARRY and H. D. RATHGEBER: *Nature*, **165**, 689 (1950).

(*) In our analysis of bursts, μ-mesons with energy less than $1.5\cdot10^{10}$ eV are not necessary to be taken into account.

with the experimental one in the energy region between 8 GeV and ~ 53 GeV. Then, the vertical intensity in the region $5.3 \cdot 10^{10}$ eV $< E_0 < 10^{12}$ eV may be represented as

$$N(E_0)\,\mathrm{d}E_0\,\mathrm{d}\Omega \propto (E_0 + 1.8 \cdot 10^9)^{-\gamma}$$

where $\gamma = 3.2 \div 3.3$ (*).

For several values of μ-meson energy E_0, the vertical intensities result from Table II.

TABLE II. – *Vertical intensities of μ-mesons at sea level.*

E_0 (eV)	$5.3 \cdot 10^{10}$	$5.3 \cdot 10^{11}$	$5 \cdot 10^{11}$	$5 \cdot 10^{12}$
$N(E_0)\,\mathrm{d}E_0\,\mathrm{d}\Omega$ (particles/cm² s sterad eV)	$(1.2 \pm 0.15) \cdot 10^{-51}$	$(1.6 \pm 0.2) \cdot 10^{-16}$	$(7.8 \pm 1.2) \cdot 10^{-19}$	$(7.6 \pm 1.5) \cdot 10^{-20}$

3. – The Burst Frequencies Produced by μ-Mesons.

In this section, we shall present a brief account of the burst frequencies $N(S)$ whose size is larger than S. The expressions of $N(S)$ are the following:

$$N(S) = \frac{11.3\ (\ )}{4 \ln (183/Z^{\frac{1}{3}})} \left(\frac{mc^2}{\mu c^2}\right)^2 \cdot 1.45 \cdot 10^{-3} \cdot \left(\frac{9.7 \cdot 10^{9}}{15\beta S}\right)^{1.8} \int_0^\infty \frac{\exp[-1/E]}{E^{2.3}}\,\mathrm{d}E \cdot$$

$$\cdot \int_0^{\varepsilon_{\max}(15\beta S)} \varepsilon^{1.8}\,\mathrm{d}\varepsilon \int \frac{\mathrm{d}\Omega \sigma(15\beta S(E/\varepsilon), \varepsilon)}{(1 + 1.8 \cdot 10^9\ \varepsilon \sec\theta / 15\beta S)^{2.8}}, \quad \text{for } 1.5 \cdot 10^{10}\ \text{eV} \leqslant E_0 \leqslant 5.3 \cdot 10^{10}\ \text{eV},$$

independently of δ, and

$$N(S) = \frac{11.3\ (^+)}{4 \ln (183/Z^{\frac{1}{3}})} \left(\frac{mc^2}{\mu c^2}\right)^2 \cdot 6.57 \cdot 10^{-5} \cdot \left(\frac{5.48 \cdot 10^{10}}{15\beta S}\right)^{\gamma-1} \int_0^\infty \frac{\exp[-1/E]}{E^{\gamma-0.5}}\,\mathrm{d}E \cdot$$

$$\cdot \int_0^{\varepsilon_{\max}(15\beta S)} \varepsilon^{\gamma-1}\,\mathrm{d}\varepsilon \int \frac{\mathrm{d}\Omega \sigma(15\beta S(E/\varepsilon), \varepsilon)}{(1 + 1.8 \cdot 10^9\ \varepsilon \sec\theta / 15\beta S)^{\gamma}}, \quad \text{for } E_0 \geqslant 5.3 \cdot 10^{10}\ \text{eV},$$

(*) Since it is shown later that the anomaly δ is not larger than 1, it is not necessary to take for γ the value 3.1.

(+) From the correction of the cascade function, the factor of Christy and Kusaka 13.5 is reduced to 11.3.

where $\sigma(15\beta S(E/\varepsilon), \varepsilon)$ is the sum of the cross-sections of ionization, bremsstrahlung and pair creation. Each term is expressed by

$$\sigma(15\beta SE, \varepsilon)_{\text{ion}}\,\mathrm{d}\varepsilon = \pi r_0^2 \left\{2\,\frac{\mu c^2}{mc^2}\,\frac{\mu c^2}{15\beta SE}\,\frac{1}{\varepsilon}\left(1-\varepsilon+\frac{\varepsilon^2}{2}\right)+\frac{1-\varepsilon}{\varepsilon}\,\delta^2\right\}\mathrm{d}\varepsilon\,,$$

$$\sigma(15\beta SE, \varepsilon)_{\text{brem}}\,\mathrm{d}\varepsilon = r_0^2\alpha Z^2\left\{\left(\frac{16}{3}\,\frac{1-\varepsilon}{\varepsilon}+4\varepsilon\right)\ln 2A\,\frac{1-\varepsilon}{\varepsilon^2}+\right.$$

$$\left.+\left(\frac{\varepsilon}{2}\ln^2 2A\,\frac{1-\varepsilon}{\varepsilon^2}-3\varepsilon\ln 2A\,\frac{1-\varepsilon}{\varepsilon^2}\right)\delta^2+\left(A\,\frac{1-\varepsilon}{\varepsilon}-\frac{\varepsilon}{2}\ln 2A\,\frac{1-\varepsilon}{\varepsilon}\right)\delta^4\right\}\mathrm{d}\varepsilon \quad (*)\,,$$

and

$$\sigma(15\beta SE, \varepsilon)_{\text{pair}}\,\mathrm{d}\varepsilon = \frac{8}{\pi}\,(\alpha Z)^2 r_0^2\xi^2\ln(2\xi)\,\mathrm{d}\varepsilon/\varepsilon\,,$$

respectively. Here,

$r_0 = e^2/\mu c^2$,

Z : atomic number. We put $Z = 76.1$, which is derived from the apparatus of SCHEIN and GILL ([12]).

mc^2: electron mass.

μc^2 : μ-meson mass ($\mu c^2 = 207\, mc^2$).

β : critical energy in shower theory. We put $\beta = 17$ MeV, which is derived from the apparatus of same authors.

E : Transfered energy, in units of $15\beta S$, into secondaries ($E = \varepsilon E_0$).

α : fine structure constant.

$A = 18\beta SE/(\mu c^2 Z^{\frac{1}{3}})$.

ξ : Lorentz factor.

The relation of δ and γ is given in Table I. We neglected the process of the Čerenkov radiation, since we could suppose that it does not give an appreciable effect to the bursts.

(*) In the first term, for $(12E_0/(5\mu c^2 Z^{\frac{1}{3}}))\cdot((1-\varepsilon)/\varepsilon)$, $\frac{1}{2}$ is neglected.

([12]) M. SCHEIN and P. S. GILL: *Rev. Mod. Phys.*, **11**, 267 (1939). In their experiment, the bursts with more than $1.9\cdot 10^7$ ion pairs are measured. Their results satisfy our requirements. On this point, see ref. ([17]).

In the calculation of $N(S)$, we have replaced ε by $\langle\varepsilon\rangle_{\text{AV}} = \frac{3}{4}$ in the integration over the angles and calculated numerically other integrals. The burst rate produced by the nuclear interaction of μ-mesons is estimated to be 10 percent of that produced by the bremsstrahlung, since the cross-section of bremsstrahlung for $Z = 76.1$ is $4.2 \cdot 10^{-27}$ cm^2, and the cross-section of nuclear interaction for the nucleus of this mass number being 2 times the atomic number is $4.8 \cdot 10^{-28}$ cm^2. The burst frequencies produced by the ionization, bremsstrahlung and pair production are shown in Table III. The result of adding the process of nuclear interaction to these three processes is represented in Fig. 2.

The error in our calculation is estimated to be 60 percent, most of which (~ 50 percent) is due to the uncertainty of the cascade function.

As is clear from Table III, the bursts are mainly produced by the bremsstrahlung. In comparison with the experiment, we can conclude that the a.m.m. is not larger than 0.8 times the normal Dirac moment. The result indicates that no modification is needed to our previous note ([13]).

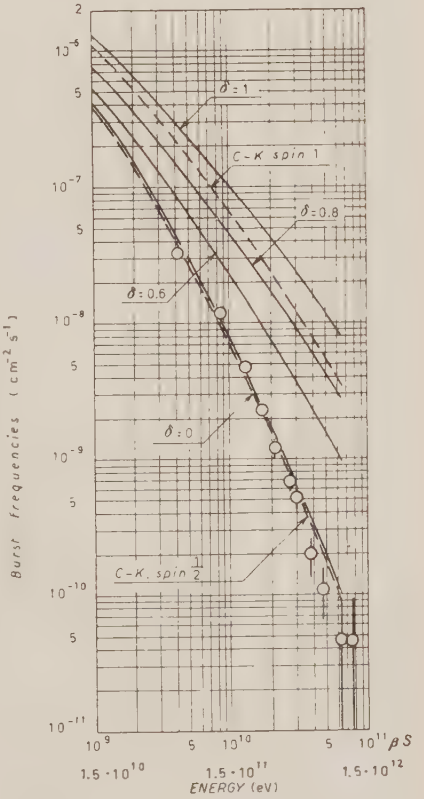

Fig. 2. – The burst frequencies as functions of the number of particles, S, and of the energy. Theoretical values represent the frequencies of burst produced by the ionization, bremsstrahlung, electron pair creation and nuclear interaction due to μ-mesons with and without a.m.m.. β is the critical energy of matter. δ is the magnitude of the a.m.m. C-K represents the results of CRHISTY and KUSAKA for spin $\frac{1}{2}$ and spin 1 respectively. The experimental values of SCHEIN and GILL are expressed by circles.

([13]) S. HIROKAWA, H. KOMORI and S. OGAWA: *Progr. Theor. Phys.*, **14**, 494 (1955).

TABLE III. – *Burst frequencies per* $cm^2\,s$ *produced by three processes. For any value of* βS, *the frequencies produced by ionization, bremsstrahlung and pair creation are given in order. In the work of Christy and Kusaka (C-K), the process of pair creation is not treated.*

βS	$\delta = 0$	$\delta = 0.6$	$\delta = 0.8$	$\delta = 1.0$	C-K spin $\frac{1}{2}$	C-K spin 1
	$1.1 \cdot 10^{-7}$	$1.2 \cdot 10^{-7}$	$1.3 \cdot 10^{-7}$	$1.4 \cdot 10^{-7}$	$8.7 \cdot 10^{-8}$	$1.2 \cdot 10^{-7}$
10^9	$3.0 \cdot 10^{-7}$	$4.2 \cdot 10^{-7}$	$6.4 \cdot 10^{-7}$	$1.2 \cdot 10^{-6}$	$3.2 \cdot 10^{-7}$	$1.0 \cdot 10^{-6}$
	$2.2 \cdot 10^{-9}$	$2.2 \cdot 10^{-9}$	$2.2 \cdot 10^{-9}$	$2.2 \cdot 10^{-9}$	—	—
	$2.9 \cdot 10^{-8}$	$3.3 \cdot 10^{-8}$	$3.7 \cdot 10^{-8}$	$4.1 \cdot 10^{-8}$	$1.8 \cdot 10^{-8}$	$3.2 \cdot 10^{-8}$
$2 \cdot 10^9$	$1.2 \cdot 10^{-7}$	$2.0 \cdot 10^{-7}$	$3.3 \cdot 10^{-7}$	$6.3 \cdot 10^{-7}$	$1.2 \cdot 10^{-7}$	$4.8 \cdot 10^{-7}$
	$7.0 \cdot 10^{-10}$	$7.0 \cdot 10^{-10}$	$7.0 \cdot 10^{-10}$	$7.0 \cdot 10^{-10}$	—	—
	$6.0 \cdot 10^{-9}$	$7.0 \cdot 10^{-9}$	$7.9 \cdot 10^{-9}$	$9.7 \cdot 10^{-9}$	$3.3 \cdot 10^{-9}$	$8.1 \cdot 10^{-9}$
$4 \cdot 10^9$	$3.8 \cdot 10^{-8}$	$8.1 \cdot 10^{-8}$	$1.4 \cdot 10^{-7}$	$2.9 \cdot 10^{-7}$	$3.8 \cdot 10^{-8}$	$2.1 \cdot 10^{-7}$
	$1.9 \cdot 10^{-10}$	$1.9 \cdot 10^{-10}$	$1.0 \cdot 10^{-10}$	$1.9 \cdot 10^{-10}$	—	—
	$6.7 \cdot 10^{-10}$	$9.1 \cdot 10^{-10}$	$1.1 \cdot 10^{-9}$	$1.5 \cdot 10^{-9}$	$5.4 \cdot 10^{-10}$	$2.1 \cdot 10^{-9}$
$8 \cdot 10^9$	$1.1 \cdot 10^{-8}$	$3.1 \cdot 10^{-8}$	$5.9 \cdot 10^{-8}$	$1.3 \cdot 10^{-7}$	$1.0 \cdot 10^{-8}$	$8.7 \cdot 10^{-8}$
	$4.8 \cdot 10^{-11}$	$4.8 \cdot 10^{-11}$	$4.8 \cdot 10^{-11}$	$4.8 \cdot 10^{-11}$	—	—
	$7.3 \cdot 10^{-11}$	$1.2 \cdot 10^{-10}$	$1.7 \cdot 10^{-10}$	$2.8 \cdot 10^{-10}$	$8.1 \cdot 10^{-11}$	$5.5 \cdot 10^{-10}$
$16 \cdot 10^9$	$2.5 \cdot 10^{-9}$	$1.0 \cdot 10^{-8}$	$2.1 \cdot 10^{-8}$	$5.1 \cdot 10^{-8}$	$2.5 \cdot 10^{-9}$	$3.3 \cdot 10^{-8}$
	$1.2 \cdot 10^{-11}$	$1.2 \cdot 10^{-11}$	$1.2 \cdot 10^{-11}$	$1.2 \cdot 10^{-11}$	—	—
	$7.8 \cdot 10^{-12}$	$1.9 \cdot 10^{-11}$	$2.9 \cdot 10^{-11}$	$5.3 \cdot 10^{-11}$	$1.2 \cdot 10^{-11}$	$1.5 \cdot 10^{-10}$
$32 \cdot 10^9$	$5.6 \cdot 10^{-10}$	$3.1 \cdot 10^{-9}$	$7.6 \cdot 10^{-9}$	$2.0 \cdot 10^{-8}$	$5.1 \cdot 10^{-10}$	$1.2 \cdot 10^{-8}$
	$2.7 \cdot 10^{-12}$	$2.7 \cdot 10^{-12}$	$2.7 \cdot 10^{-12}$	$2.7 \cdot 10^{-12}$	—	—
	$8.3 \cdot 10^{-13}$	$3.1 \cdot 10^{-12}$	$5.2 \cdot 10^{-12}$	$1.1 \cdot 10^{-11}$	$1.6 \cdot 10^{-12}$	$3.9 \cdot 10^{-11}$
$64 \cdot 10^9$	$1.0 \cdot 10^{-10}$	$9.0 \cdot 10^{-10}$	$2.5 \cdot 10^{-9}$	$7.1 \cdot 10^{-9}$	$9.0 \cdot 10^{-11}$	$3.7 \cdot 10^{-9}$
	$6.2 \cdot 10^{-13}$	$6.2 \cdot 10^{-13}$	$6.2 \cdot 10^{-13}$	$6.2 \cdot 10^{-13}$	—	

5. – Discussion.

Although our result is not inconsistent with the result of μ-mesons with no a.m.m., there remain some ambiguities. These ambiguities seem inevitable in the analysis of a.m.m. from cosmic ray bursts. Many attempts have been performed to restrict the magnitude of the a.m.m. of μ-mesons, while their limitations are looser than ours.

PEASLEE [14] has concluded that δ should be less than the order of one from studying the μ-meson intensities at 3 000 m.w.e..

[14] D. C. PEASLEE: *Nuovo Cimento*, **9**, 56 (1952).

After the present work was completed, we could see a paper by FOWLER ([15]). He analyzes various phenomena involving μ-mesons, taking into account meson finite size effects in a relativistic way. His result is consistent with ours.

WALKER ([16]) has obtained a reasonable result that δ is less than nine times the normal moment from the analysis of the spectrum of knock-on electrons by the μ-meson component.

The same author stated that δ does not exceed 0.4 times the normal Dirac moment in accordance with the data of DRIGGERS ([17]), in whose burst experiment a large low pressure cloud chamber is used. But his reduction may not be a well-grounded argument. For, the number of ion pairs in the experiment of Driggers is small, $3.0 \cdot 10^5 \div 1.2 \cdot 10^6$ ion pairs. According to CARMICHAEL ([18]), it is pointed out that in this range the main contribution to the burst is due to the α-particles and protons and that the μ-mesons, if any, are of low energies.

There is an attempt([19]) to interpret the anomalous large angle scattering of μ-mesons underground by taking account of the a.m.m.. However, it is difficult to restrict the magnitude of a.m.m. from these experiments, because of an uncertainty in the charge distribution of nuclei.

The experiments with an accelerator seem favourable for our purpose. Indeed, there are two attempts to investigate the a.m.m. of μ-mesons, namely, the study of the X-ray spectra from the μ-mesonic atoms and of the spectra of μ-mesons in the radiative π-μ decay. As to the former, as has already been pointed out by several authors ([20]), we can not derive a definite result from this method, because there are two uncertain factors, the spin of μ-mesons and the charge distribution of nuclei. To avoid the second uncertainty, the idea to use hydrogen as a target nucleus has occurred to us. However, there may be some difficulties on the experimental technique at present. As to the radiative π-μ decay ([21]), the task is only to increase the number of events. In this connection, the frequency of radiative π-μ decays is of the order of 10^{-4} of that of ordinary decay.

([15]) G. N. FOWLER: *Nuclear Phys.*, **1**, 125 (1956).

([16]) W. D. WALKER: *Phys. Rev.*, **90**, 234 (1953).

([17]) F. E. DRIGGERS: *Phys. Rev.*, **87**, 1080 (1952).

([18]) H. CARMICHAEL: *Phys. Rev.*, **74**, 1667 (1948). We are indebted to Mr. H. HASEGAWA for calling our attention to Carmichael's work.

([19]) R. GATTO: *Nuovo Cimento*, **12**, 613 (1954).

([20]) L. N. COOPER and E. M. HENLY: *Phys. Rev.*, **92**, 801 (1953); J. A. WHEELER: *Phys. Rev.*, **92**, 812 (1953).

([21]) G. E. A. FIALHO: *Report on the New Research Technique in Physics* (Rio de Janeiro, 1954), p. 275.

We are indebted to Prof. S. SAKATA for calling our attention to this work.

* * *

The authors wish to thank Prof. S. HAYAKAWA for his valuable discussions and to express their gratitude to Prof. S. SAKATA for the interest shown to this work. Two of us (S.H. and H.K.) are also indebted to the « Yukawa-Yomiuri Fellowship » for financial aid.

RIASSUNTO (*)

Dall'analisi dei burst di raggi atomici prodotti da mesoni μ si stima il limite superiore della grandezza del momento magnetico anomalo dei mesoni μ. Si trova che il momento magnetico anomalo dei mesoni μ è dell'80 % inferiore al momento normale di Dirac.

(*) *Traduzione a cura della Redazione.*

IL NUOVO CIMENTO Vol. IV, N. 4 1° Ottobre 1956

Inelasticity in Collisions Between Pions and Lead Nuclei.

M. Cresti, W. D. B. Greening, L. Guerriero, A. Loria and G. Zago

Istituto di Fisica dell'Università - Padova
Istituto Nazionale di Fisica Nucleare - Sezione di Padova

M. Deutschmann

Max-Planck-Institut für Physik - Göttingen

(ricevuto il 21 Giugno 1956)

Summary. — From direct measurements of the energy of charged pions (from 0.5 to 5 GeV) interacting with Pb nuclei, and of the energy of the neutral pions produced in these interactions, the fraction of the primary energy radiated as π^0-mesons is shown to be 0.17 ± 0.04; from this follows a mean inelasticity $\overline{\gamma} \approx 0.5$. The data show that low and high values of γ are preferred, with a minimum at intermediate values.

1. – Introduction.

In high energy nuclear interactions a certain proportion of the available energy of the primary particle is absorbed inelastically in the production of mesons. Our present knowledge about the coefficient of inelasticity γ, defined as the ratio between the energy of all the secondary mesons and the primary energy, is still rather incomplete. In his theory of the multiple production of mesons in nucleon-nucleon collisions, Heisenberg [1] assumes that γ depends on the collision parameter of the two colliding particles, and he finds that the mean value $\overline{\gamma}$ varies rather slowly with the primary energy. Values of $\overline{\gamma}$ in carbon and lead have been derived by Budini and Poiani [2] from experimental data on the absorption in these materials of the N-com-

[1] W. Heisenberg: *Kosmische Strahlung* (Berlin, 1953), p. 148.
[2] P. Budini and G. Poiani: *Nuovo Cimento*, **10**. 1288 (1953).

ponent of cosmic rays. Several other authors ([3-6]) have studied jets in photoemulsions and have obtained the mean value $\bar{\gamma}$ for the inelasticity as well as information about the distribution of the individual values of γ. In this paper we present the results of a direct determination of the inelasticity in collisions between pions and lead nuclei, based on the simultaneous measurement of the momentum of a cosmic ray particle in a magnetic chamber, and of the mesons produced by it in a multiplate chamber, derived from the electron cascade due to the neutral pions.

2. – Experimental Procedure.

Fig. 1 shows the layout of the two cloud chambers as installed at the Laboratorio della Marmolada at 2000 m above sea-level. The upper chamber, having a cylindrical volume of 25 cm diameter and 8 cm illuminated depth, is immersed in a magnetic field of 6000 ± 100 gauss, corresponding to a maximum detectable momentum of 5 GeV at its centre and 3 GeV at the sides. The lower chamber has a volume of $(70 \times 70 \times 20)$ cm^3 and contains lead plates 1 cm thick, originally 21 in number but later reduced to 15 for the greater part of the photographs. A thickness of 1 cm was the best compromise between the need for mechanical rigidity of the plates and the desire to study the showers in as great detail as possible.

Suitable events were those in which a primary was produced in the lead block Σ, passed through the magnetic chamber, and then interacted in the plate chamber below it. Care was taken not to introduce a selection bias through the counter system, and therefore no counters were installed below the multiplate chamber as this would have discriminated against low-energy events. Instead, two trays, A and B, each of 10 counters, were placed in the positions seen in Fig. 1. Coincidences were required from two or more counters in each of the two trays.

To trace a particle from one chamber into the other the following procedures were used. For a track seen in the magnetic chamber a reprojection method gave its point of entry into the plate chamber; tracks appearing in the lower chamber were extrapolated into the magnetic chamber by means of a specially constructed stereoscope. Tracks were considered as being due

---

([3]) C. C. Dilworth, S. J. Goldsack, T. F. Hoang and L. Scarsi: *Nuovo Cimento*, **10**, 1261 (1953).

([4]) C. Castagnoli, G. Cortini, C. Franzinetti, A. Manfredini and D. Moreno: *Nuovo Cimento*, **10**, 1539 (1953).

([5]) T. F. Hoang: *Journ. de Phys.*, **15**, 337 (1954).

([6]) G. Bertolino: *Nuovo Cimento*, **3**, 141 (1956).

to the same particle when the derived and actual positions agreed laterally to within $\pm$ 1 cm in both chambers, and when the reprojection method gave the position in the plate chamber to within $\pm$ 3 cm in depth. For the majority of events a decision was not difficult since the material between the

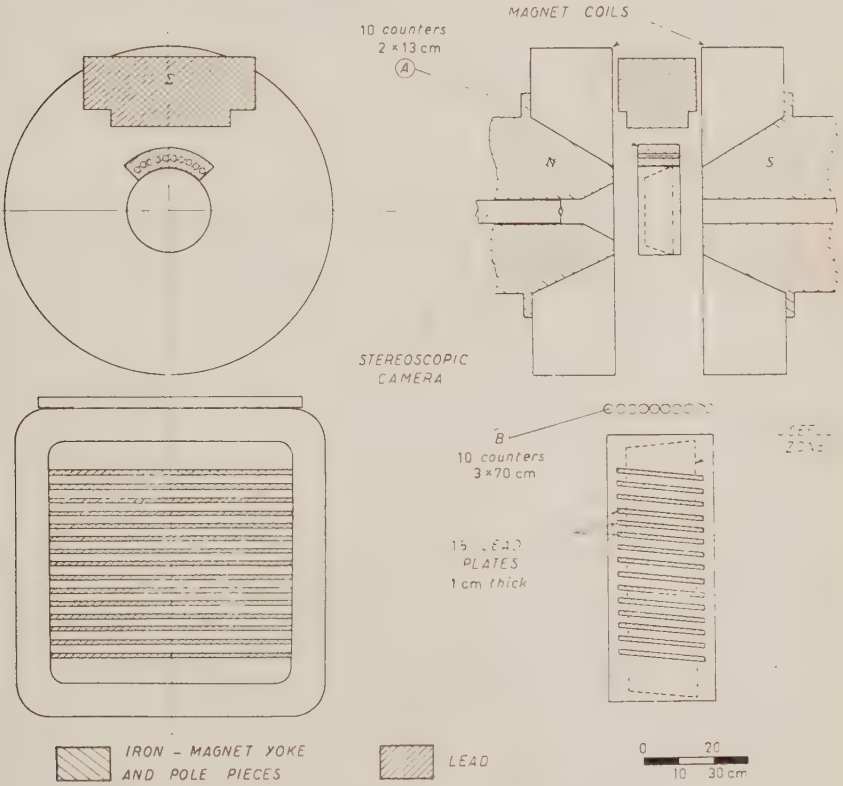

Fig. 1. – Layout of the two cloud chambers.

chambers had been kept to a minimum (5 mm of glass and approximately 3 mm of copper which form part of the upper chamber, and 20 mm of aluminium in the roof of the lower chamber, a total of about 10 g/cm^2).

The curvature of the tracks in the magnetic field has been obtained by a full-size reprojection of the photographs through the original lenses onto a screen representing a plane parallel to that of the chamber and free to move in depth. Horizontal co-ordinates have been measured at regular vertical intervals, the depth being continuously adjusted to maintain the two images

superimposed. Thus the track was reconstructed in space and the need to take into account the variation of magnification with depth was eliminated. The radius of curvature has then been calculated by the method of least squares.

Interactions produced in the lower chamber were studied as completely as possible. The energy E_{π^0} of the electron showers due to the decay of the neutral pions has been obtained from the electron track lengths by using the criteria and the energy-track length relation given by BENDER (7).

3. – Results.

To obtain the energy of the primary from its momentum as measured in the upper chamber, the nature of the particle must be known. For momenta below 1 GeV/c, pions and protons can be distinguished by their ionization, and in this range only one proton giving a visible interaction has been found whereas there are 36 interacting pions. For higher momenta the proportion of proton primaries may be estimated by assuming that the numbers of proton- and neutron-induced showers in the lower chamber are equal. In a representative sample of showers which were sufficiently well collimated to show that their primaries (whether ionizing or not) must have come from the lead block Σ, we have observed 7 neutron-induced showers having $n_s \geqslant 3$ penetrating particles, or with $E_{\pi^0} \sim 1$ GeV, against 34 showers having the same characteristics but which were produced by charged primaries. Thus the proportion of protons amongst the charged primaries is not more than 16%, a value which is in good agreement with the results of other workers (8,9). We have therefore concluded that the fraction of protons is sufficiently small to allow us to consider our results as being directly applicable to interactions between pions and lead nuclei.

For the primary energy E_p we have taken the total energy, since a pion interacting with a complex nucleus can also make available its own rest energy.

In 102 cases the primary particles could be followed from one chamber into the other: 63 were judged to be positive and 36 negative, while for 3 the sign was not recognizable. We have found 42 particles with $E_p \leqslant 1$ GeV: in addition to the proton there were 29 π^+ and 12 π^-. The resulting positive excess of 2.5 ± 1.2 is rather high but is not inconsistent with present information on meson production. Of the 57 particles with $E_p > 1$ GeV, 33 were

(7) P. A. BENDER: *Nuovo Cimento*, **2**, 980 (1955).

(8) U. CAMERINI, P. H. FOWLER, W. O. LOCK and H. MUIRHEAD: *Phil. Mag.*, **41**, 413 (1950).

(9) P. H. FOWLER: *Phil. Mag.*, **41**, 169 (1950).

positive and 24 negative: the difference between these last two figures may be accounted for by the presence of protons.

TABLE I.

E_p (in GeV)	No. of events	$\bar{E}_p$ (in GeV)	N_0	$\bar{E}_{\pi^0}$ (in GeV)	$\bar{n}_s$	$\bar{N}_g$	$\bar{N}_h$
0.15 to 0.9	30	0.56	6	0.08	0.6	0.5	0.9
0.9 to 1.4	29	1.08	14	0.15	1.0	0.6	1.0
1.4 to 5.0	28	2.70	16	0.64	1.2	0.8	1.2
> 5	15	—	6	1.2	1.9	1.1	1.1

E_p – total energy of the primary particles.
N_0 – number of events with $E_{\pi^0} > 0$.
$\bar{E}_{\pi^0}$ – mean energy of the photoelectronic component.
$\bar{n}_s$ – mean number of penetrating particles with $I/I_{\min} < 1.5$.
$\bar{N}_g$ – mean number of particles with $1.5 > I/I_{\min} > 3$.
$\bar{N}_h$ – mean number of particles with $I/I_{\min} > 3$.

In Table I the primaries have been divided according to their energy E_p into three approximately equal groups, and a fourth group which consists of those particles with energy greater than 5 GeV. For the 87 cases having $E_p \leqslant 5$ GeV, the distribution of the number of events with different values of n_s is given in Table II. Below the observed frequencies are the calcuated frequencies which would result from a Poisson law distribution with a mean value $\bar{n}_s = 0.9$, i.e. equal to that which actually results from our observed frequencies. The agreement is very good (see also DEUTSCHMANN [10]), from which we conclude that, as was to be expected, there is no appreciable contribution from elastic collisions, which would have increased the frequencies at $n_s = 1$ and $n_s = 0$ (charge exchange). The low frequency of charge exchange allows us to consider the observed π^0 as being new particles produced in the interactions: this wil give us the possibility of tentatively treating pion-nucleus collisions whith the same methods used for nucleon-nucleus collisions. Supposing that the frequency distribution for the π^0-mesons is also given by a Poisson law, it follows that the total number of π^0-mesons is not much higher than 36, which is the number of events in which they are produced. Thus our data are consistent with the figure of 0.5 for the ratio of neutral to charged pions which has been found by several authors [11-13].

[10] M. DEUTSCHMANN: *Zeits. f. Naturf.*, **9***a*, 477 (1954).
[11] R. R. DANIEL, J. H. DAVIES, J. H. MULVEY and D. H. PERKINS: *Phil. Mag.*, **43**, 753 (1952).
[12] G. SALVINI and Y. B. KIM: *Phys, Rev.*, **88**, 40 (1952).
[13] M. F. KAPLON, W. D. WALKER and M. KOSHIBA: *Phys. Rev.*, **93**, 1424 (1954).

TABLE II. – *Distribution of the number n_s of penetrating particles (minimum ionization) for the 87 showers produced by primaries with $E_p < 5$ GeV.*

n_s	0	1	2	3	4
Observed distribution	36	32	13	5	1
Poisson distribution	35.3	32	14.4	4.3	1

3·1. *The mean inelasticity.* – We define γ' as the ratio of the energy of the π^0 to that of the primary:

$$\gamma' = \frac{E_{\pi^0}}{E_p} . \tag{1}$$

As the mean value $\overline{\gamma}'$ for all the 87 events with $E_p \leqslant 5$ GeV we obtain:

$$\overline{\gamma}' = 0.17 \pm 0.04 , \tag{2}$$

where the error is the statistical error.

Instead of the above mean value $\overline{\gamma}'$ which is valid in the laboratory system, it would be preferable to have the corresponding figure $\overline{\gamma}'^*$ for the centre of mass system. It is possible to calculate a minimum value for this by supposing that the π^0-mesons are emitted forwards in the direction of the incoming primary, and that this interacts with only one nucleon. One finds that $\overline{\gamma}^*_{\min} = 0.15$, i.e. the difference between the two systems is negligible.

To calculate the inelasticity $\overline{\gamma}$ (the ratio between the energy of all the secondary mesons and the primary energy), we must know the average ratio of the energy of the charged pions to that of the neutral pions. It is reasonable to assume that the spectra of the two types of meson are the same, in which case this ratio will be the same as that for the corresponding frequencies: in other words, we assume that $\overline{\gamma} = 3 \cdot \overline{\gamma}'$. This assumption is justified by the following independent evaluation of $\overline{\gamma}$, (see also [14]). For the 87 interactions, we have measured the total kinetic energy of all the visible proton tracks; this sum is 15 GeV. The mean number of tracks with a ionization > 1.5 times minimum is 1.7 per interaction, which agrees fairly well with the mean number of 2 for grey tracks per star observed by the Bristol group [15] for the same average primary energy. However, the corresponding number of 8 for black tracks (having an average energy of 10 MeV per track) found by the same group, cannot be observed by us (*) since, in general, tracks

[14] G. PUPPI and N. DALLAPORTA: *Prog. Cosmic Ray Physics* (Amsterdam, 1952), p. 381.

[15] U. CAMERINI, J .H. DAVIES, P. H. FOWLER, C. FRANZINETTI, H. MUIRHEAD, W. O. LOCK, D. H. PERKINS and G. YEKUTIELI: *Phil. Mag.*, **42**, 1241 (1951).

(*) The definition of grey and black tracks used by us differs from that of the Bristol group (see Table I).

with more than 6.8 times minimum will not escape from the lead plates. Assuming that practically no such tracks are seen, we have added to the 15 GeV for the visible proton, a further 7 GeV, representing 80 MeV per interaction for the non-visible protons. For the neutrons we add another 33 GeV (125 neutrons to 82 protons in the Pb nucleus). Thus of a total primary energy of 124 GeV, 55 GeV are carried away by the nucleons, leaving 69 GeV for all the pion secondaries. Since the total π^0-energy is 25 GeV, we find the ratio

$$\frac{E_{\text{mesons}}}{E_{\pi^0}} = 2.8 \,. \tag{3}$$

As a result of the above considerations, we use a ratio of the order of 3, which leads to the result

$$\bar{\gamma} \approx 0.5 \,. \tag{4}$$

Fig. 2. – Distribution of the γ' values.

3·2. *Distribution of the inelasticity.* – In Fig. 2 the frequency distribution $\varphi(\gamma')$ has been plotted for the 36 interactions in which π^0 are produced. Events with $\gamma' = 0$ have not been included in the diagram. The mean minimum value $\bar{\gamma}'_{\min} = 0.09$ is equal to the ratio between the rest energy of the π^0-meson and the mean primary energy $\bar{E}_p = 1.46$ GeV. Since we know only the part $E_{\pi^0} = \eta \cdot E_\pi$ of the total secondary meson energy E_π, we may put

$$\gamma' = \eta \cdot \gamma \,. \tag{5}$$

It is possible to calculate the relation between the observed distribution $\varphi(\gamma')$ and the corresponding function $f(\gamma)$ in the following way. Consider a certain value γ': then the frequency $\varphi(\gamma')$ will be made up of contributions from interactions having γ between γ' and 1. Since $\gamma = \gamma'/\eta$, we obtain:

$$\varphi(\gamma') = \int_{\gamma'}^{1} \frac{P(\eta)}{\eta} \cdot f(\gamma'/\eta) \cdot \mathrm{d}\eta \,, \tag{6}$$

where $P(\eta)$ is the probability that a certain fraction η of the energy radiated as mesons appears as π^0-mesons. This function cannot be calculated analytically, though for events where a large number of mesons are produced we would expect $P(\eta)$ to have a maximum at $\eta = \frac{1}{3}$. In our case, however the mean number of mesons (both neutral and charged) per interaction in which at least one pion is produced is only 1.8 and the curve for $P(\eta)$ is so flat that we can approximate it to a constant. By means of (6) we can compare our measured distribution with an expectation function $f(\gamma)$.

For the mesons produced in nucleon-nucleon interactions, HEISENBERG [1] makes the simple assumption that γ depends on the collision parameter, b, of the two nucleons:

$$\gamma = \exp\left[-\frac{b}{\text{const}}\right], \tag{7}$$

and from this he finds

$$f(\gamma) = \text{const}\,\frac{1}{\gamma}\cdot\log\frac{1}{\gamma}\,. \tag{8}$$

Introducing (8) in (6) we obtain:

$$\varphi(\gamma') = \text{const}\left(\frac{1}{\gamma'}\cdot\log\frac{1}{\gamma'} - \frac{1}{\gamma'} + 1\right). \tag{9}$$

This function is plotted in Fig. 2 as broken curve 1. It appears that the curve and the histogram agree in their general form for low γ' values, which are strongly preferred. At high values the histogram is richer than the curve, a fact which is to be expected owing to the complexity of the interactions in the lead nucleus. We have therefore tried to describe the collisions with a heavy nucleus by means of the following simple model. We assume that for an incoming pion which hits the central part of the lead nucleus, say inside a radius $R - R_0$ (where $R = R_0\cdot A^{\frac{1}{3}}$ = nuclear radius), the interaction is completely inelastic, i.e. $\gamma = 1$, or

$$f_1(\gamma)\,\mathrm{d}\gamma = \text{const}\,\delta(1-\gamma)\,\mathrm{d}\gamma\,, \tag{10}$$

where δ is the Dirac δ-function. If on the other hand we are dealing with a peripheral collision (in the range from $(R - R_0)$ to $(R + R_0)$, taking R_0 as being the radius of the pion as well as of the nucleon), then we assume that γ depends on the collision parameter b, $(0 \leqslant b \leqslant 2\cdot R_0)$, given by (7). So we get

$$f_2(\gamma)\cdot\mathrm{d}\gamma = 2\pi R\cdot\mathrm{d}b = \text{const}\,\frac{\mathrm{d}\gamma}{\gamma}\,. \tag{11}$$

For a Pb nucleus, we may take the relative contributions from the central and peripheral zones as being equal to the corresponding geometrical cross-sections, in which case we have

$$\frac{\sigma_{\text{cent}}}{\sigma_{\text{periph}}} = \frac{\pi(R - R_0)^2}{4\pi R \cdot R_0} \approx 1 \,. \tag{12}$$

Thus we can sum (10) and (11) (*) to give

$$f(\gamma)\cdot \mathrm{d}\gamma = \text{const}\left[\frac{K}{\gamma} + \delta(1-\gamma)\right]\cdot \mathrm{d}\gamma \,. \tag{13}$$

where $1/K = \log(1/\bar{\gamma}'_{\text{min}})$; and taking into account (6),

$$\varphi(\gamma') = \text{const}\left[K\left(\frac{1}{\gamma'} - 1\right) + 1\right]. \tag{14}$$

The full curve 2 represents equation (14): the agreement with the histogram is quite satisfactory in view of the very simple model we have used. In any case one should note that only a peak in $f(\gamma)$ for $\gamma \sim 1$ can produce a finite frequency $\varphi(\gamma')$ for $\gamma' \sim 1$, as is found experimentally. Thus we conclude that our data provide evidence for the frequent occurrence in lead nuclei of interactions having $\gamma \sim 1$.

Another representation of the function $f(\gamma)$ has been given by BUDINI and MOLIÈRE ([16]). They choose the general expression

$$f(\gamma) = \text{const}\,\frac{1}{\gamma}\cdot \log^{\alpha-1}\frac{1}{\gamma}\,, \tag{15}$$

in which the exponent α has to be adjusted to agree with experiment. For $\alpha = 2$ this equation is identical with the Heisenberg formula (8), and for $\alpha = 1$ it coincides with (11). Only for $\alpha < 1$ we get the pole at $\gamma = 1$ which is necessary to explain our histogram. On the other hand it can be shown that $\alpha = 0$ would be too small since then the function could no longer account for the observed increase of the frequency with decreasing γ'. We have therefore tried $\alpha = 0.5$; the corresponding curve 3 in Fig. 2 shows reasonable agreement with the histogram.

(*) Observing that the integrals of both are equal when taken between the limits from $\bar{\gamma}_{\text{min}} = 0.09$ to $\gamma = 1$.

([16]) P. BUDINI and G. MOLIÈRE: *Kosmische Strahlung* (Berlin, 1953), p. 367.

4. – Discussion.

We can compare our $\bar{\gamma}$ value with the results of other workers. For Pb and C there exists a calculation by BUDINI and POIANI [2] which is based on experimental data relating to the absorption of the N-component of cosmic rays in Pb, C and air. They obtain $\bar{\gamma}_C = 0.25 \pm 0.1$ for carbon, and various values between $\bar{\gamma}_{Pb} = 0.45 \pm 0.37$ and $\bar{\gamma}_{Pb} = 0.86 \pm 0.52$ for lead, which are comparable with our value $\bar{\gamma} \approx 0.5$. More significant is the ratio of our $\bar{\gamma}$ to their $\bar{\gamma}_C$: this is equal to 2, and compares very well with the ratio of the inelasticities in lead and carbon as measured by DEUTSCHMANN [10], who obtained $\bar{\gamma}_{Pb}/\bar{\gamma}_C = 1.9 \pm 0.3$. Thus we have a further confirmation for the figure of $\bar{\gamma} = 0.2$ for air which was adopted by BUDINI and MOLIÈRE [16] in their theory of the nuclear cascade in the atmosphere, and by BERETTA *et al.* [17] in their study of the positive excess.

It is not possible to compare quantitatively our $\bar{\gamma}$ value with those obtained from studies of jets in photoemulsions [1-6], since there are differences in the selection criteria for the events. We have considered all interactions, including those which result in the production of black prongs only, or in which there are no visible secondary particles at all, i.e. we have included interactions with $\gamma = 0$. In photoemulsions, however, for obvious reasons, only those interactions are counted which produce a conspicuous star with several shower particles, so allowing an energy determination from the opening angle of the jet. Therefore in this latter case there is a bias against low inelasticities.

One result is common to both of these two different types of experiment; in fact, the phenomenon of two distinct classes of events, one with high and one with low γ values, which we have found necessary to postulate in order to explain our measured distribution of γ', has already been found from studies of jets. Thus from our analysis, we think that these two classes of events in jets may be explained by the occurrence of central and peripheral collisions in heavy nuclei.

* * *

We wish to thank Professor A. ROSTAGNI for his support, and one of us (M.D.) has to thank Professor W. HEISENBERG for discussions and for permission to work in Italy. We are grateful to the Società Adriatica di Elettricità (S.A.D.E) for their continuous help, and in particular to the Direttore Centrale Ing. M. MAINARDIS, to Ing. B. CARUSO, Ing. A. SABBADINI and to

[17] E. BERETTA, I. FILOSOFO, B. SOMMACAL and G. PUPPI: *Nuovo Cimento*, **10**, 1354 (1953).

Sig. A. Carestiato. Thanks are also due to the officials of the Società Torno e C. Valuable assistance during the course of the experiments was rendered by F. Dovico.

RIASSUNTO

Da misure dirette dell'energia di mesoni π carichi compresi nell'intervallo fra 0.5 e 5 GeV, interagenti con nuclei di piombo, e dell'energia dei π^0 prodotti in queste reazioni, si ricava che la frazione dell'energia primaria che dà origine a π^0 è 0.17 ± 0.04: da questo deriva un'anelasticità media $\bar{\gamma} \approx 0.5$. I dati mostrano che i valori di γ vicini a 0 e ad 1 sono più frequenti dei valori intermedi.

An Investigation of the First Rotational Level of ^{169}Tm.

A. Bisi, S. Terrani and L. Zappa

Istituto di Fisica Sperimentale del Politecnico - Milano

(ricevuto il 25 Giugno 1956)

Summary. — The possibility of the β decay of ^{169}Er to the known rotational levels of ^{169}Tm has been investigated. No evidence of a complex decay was found. The transition energy results: $E_0 = (340 \pm 2)$ keV and the half-life: $T_{\frac{1}{2}} = (9.0 \pm 0.2)$ d. The low energy transitions of ^{169}Tm from the decay of ^{169}Yb were investigated with a proportional counter spectrometer and by using a coincidence technique. The 23.4 keV γ-ray arising in the transition between the third and the second rotational level was observed; its relative intensity was obtained. No clear evidence was found of a γ-ray which should have arisen from the de-excitation of the first rotational level.

1. – Introduction.

The radiations from the excited states of ^{169}Tm, following the electron capture decay of ^{169}Yb, have been extensively investigated by Johansson (see Fig. 1) [1] and by Cork *et al.* [2]. Good evidence was found of an anomalous rotational band with $K = \frac{1}{2}$, in strict agreement with the theoretical predictions of the Bohr-Mottelson unified model. A further discussion of the rotational spectrum of ^{169}Tm has been made by Mottelson and Nilsson [3].

As regards the decay $^{169}\text{Er} \rightarrow {}^{169}\text{Tm}$, no γ-rays were reported up to date. By the present work it was intended to investigate the possibility of excitation

(1) S. A. E. Johansson: *Phys. Rev.*, **100**. 835 (1955).

(2) J. M. Cork, M. K. Brice, D. W. Martin, L. C. Schmid and R. G. Helmer: *Phys. Rev.*, **101**, 1042 (1956).

(3) B. R. Mottelson and S. G. Nilsson: *Zeits. f. Phys.*, **141**. 217 (1955).

of the rotational levels of ^{169}Tm in the β decay of ^{169}Er. Moreover it was attempted to investigate the very low energy transitions (10 and 23 keV) present in the decay of ^{169}Yb.

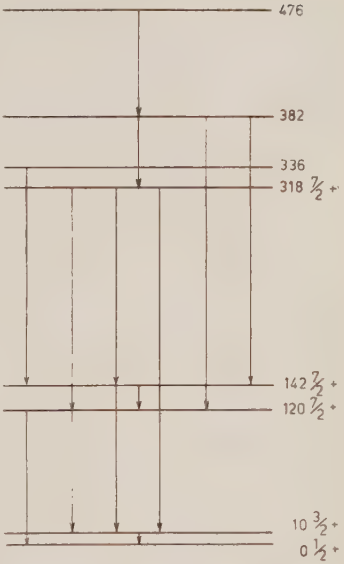

Fig. 1. Level scheme of ^{169}Tm proposed by JOHANSSON.

2. – Radiations from ^{169}Er.

The sample of ^{169}Er was obtained by slow neutron irradiation of spectroscopically pure erbium oxide in the Harwell reactor. The specific activity was about 30 mC/g.

a) γ *spectrum.* – The γ spectrum was investigated by means of a scintillation spectrometer and of a proportional counter spectrometer. The pulse heights were analyzed by means of a twenty channel electronic pulse analyzer ([4]). At energies greater than 100 keV very faint γ lines (110 and 206 keV) were observed. The relative intensity of these γ-rays and of the β-rays of ^{169}Er was: $\gamma_{206}:\gamma_{110}:\beta = 9\cdot10^{-4}:10^{-4}:1$. The half-life of the two γ radiations was found to be (6.8 ± 0.3) d. From that it can be inferred that: 1) traces of ^{177}Lu ($T\,\frac{1}{2} = 6.8$ d ([5])) were present as impurity in the active sample; 2) the γ-ray transition of 110 keV energy, reported by JOHANSSON and by CORK *et al.* in the de-excitation of the second rotational level of ^{169}Tm, if excited in the decay of ^{169}Er, would have an intensity lower than 10^{-4} per β-ray.

At lower energies a search was made in the proportional counter, of the γ-rays arising from the de-excitation of the first rotational level. This level, as postulated by JOHANSSON, must occur at 10 keV energy; CORK *et al.*, on the basis of their measurements, suggest a value of 8.4 keV. The possibility of the *L*-shell conversion is then questionable by considering that the critical X-ray absorption energy relative to the L_{III}-shell ($Z = 69$) is 8.66 keV according to HILL, CHURCH and MIHELICH ([6]). We have ascertained that γ radiations of such energy or *L* X-rays from their *L*-shell internal conversion, if present in the decay of ^{169}Er, would have an intensity lower than $2\cdot10^{-2}$

([4]) E. GATTI: *Nuovo Cimento*, **11**, 153 (1954).

([5]) J. M. HOLLANDER, I. PERLMAN and G. T. SEABORG: *Rev. Mod. Phys.*, **25**, 469 (1953).

([6]) R. D. HILL, E. L. CHURCH and J. W. MIHELICH: *Rev. Sci. Instr.*, **23**, 523 (1952).

per β-ray. The rather high value of this upper limit is due to the presence of a spurious peak at about 7.5 keV. This peak corresponds to the L X-radiation characteristic of Yb arising from the decay of ^{170}Tm present as impurity in the sample.

b) β spectrum. – The β spectrum was investigated in a high transmission intermediate image β-ray spectrometer using a β source (0.04 mg/cm² thick) electro-plated on a thin Cu foil ~ 0.5 mg/cm²). The Fermi plot of the obtained spectrum is shown in Fig. 2. The end-point occurs at

$$E_0 = (340 \pm 2) \text{ keV} .$$

The plot appears to be a straight line down to about 50 keV.

The intensity of the β-rays was followed over 30 days. The half-life was found to be

$$T_{\frac{1}{2}} = (9.0 \pm 0.2) \text{ d} .$$

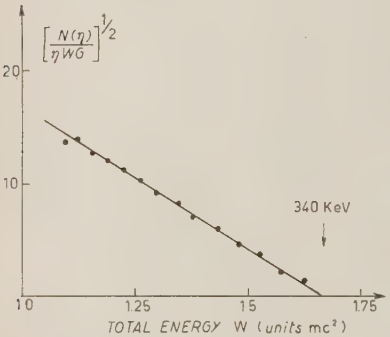

Fig. 2. – Fermi plot of the β spectrum of ^{169}Er.

3. – Low Energy Radiations from the Decay of ^{169}Yb.

^{169}Yb was obtained by slow neutron irradiation of spectroscopically pure ytterbium oxide in the Harwell reactor. The active sample was studied when the short-lived activities had practically disappeared.

The γ spectrum obtained in the proportional counter spectrometer is shown in Fig. 3. The high energy peak (50.1 keV) was identified as due to K X-rays characteristic of Tm (50.41 keV). A faint γ-ray at (23.4 ± 0.2) keV energy was distinctly revealed.

By means of a coincidence arrangement between the scintillation and the proportional counter spectrometer the 23.4 keV γ-rays were ascertained to be time coincident with the K X-rays characteristic of Tm. The identification of this γ-rays transition with that shown in the decay scheme of Fig. 1 is straightforward.

The intensity of the 23.4 keV γ-rays was measured relatively to the K X-rays intensity. After correction for the detection efficiencies we obtained

$$\frac{I_{\gamma_{23}}}{I_K} = (4.7 \pm 0.5) \cdot 10^{-3} . \tag{1}$$

As concerns the intense peak at lower energy our results are:

a) The energy calibration was made by using as standards the K_α X-radiations arising from the decay of ^{55}Fe, ^{75}Se, ^{109}Cd (for K_α X-rays energy we intend the weighed mean of the K_{α_1} and K_{α_2} X-rays energy). We have ob-

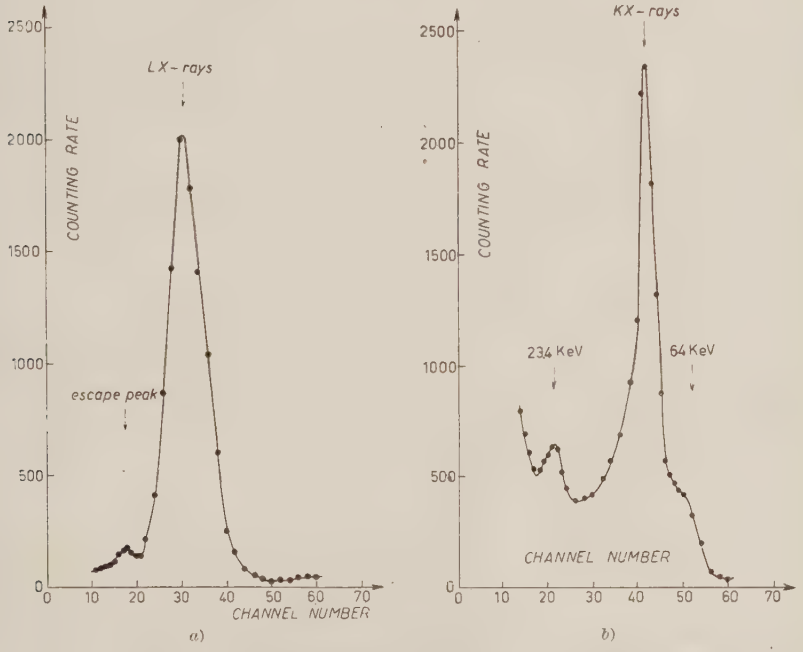

Fig. 3. – Low energy γ radiations from ^{169}Yb observed in the proportional counter spectrometer: *a*) *L* X-rays; *b*) 23.4 keV γ-rays and *K* X-rays.

tained: $E_0 = (7.6 \pm 0.2)$ keV, in very close agreement with the energy of the *L* X-rays characteristic of Tm (L_{α_1} X-ray energy = 7.18 keV, L_{β_1} X-ray energy = 8.10 keV).

b) The peak appears to be substantially simmetric. A comparison of its shape with that shown by the *L* X-ray peaks arising from the decay of ^{153}Gd, ^{170}Tm, ^{181}W, ^{195}Au does not give evidence of any appreciable anomalies in the general trend. It can be inferred that a contribution of a γ-ray to the high (or low) energy side of the peak, should be very low.

(7) B. L. Robinson and R. W. Fink: *Rev. Mod. Phys.*, **27**, 424 (1955).
(8) A. Bisi and L. Zappa: *Nuovo Cimento*, **12**, 211 (1954).

c) A coincidence measurement was carried out between the K X-rays and the L X-rays. Only the pulses belonging to the K X-ray peak obtained in the scintillation spectrometer were used to trigger the coincidence circuit. If the L X-rays emission arised from the reorganisation of the atom ionized in the K-shell, the following equation could be written:

$$\frac{I_{KL}}{I_K} = n_{LK}\omega_{LK}\varepsilon_L \,, \tag{2}$$

where I_{KL} is the counting rate due to L X-K X coincidences and I_K the counting rate due to K X-rays;

n_{LK} is the number of L-shell vacancies produced in the filling of a K-shell vacancy;

ω_{LK} is the L-fluorescence yield for transitions to the L level following the K X-rays emission;

ε_L is the detection efficiency of the proportional counter for L X-rays.

With the n_{LK} value obtained from the discussion of ROBINSON and FINK [7] and with the calculated ε_L [8] we have from eq. (1)

$$\omega_{LK} = 0.31 \,.$$

This value is about two times greater than the right ω_{LK} (for $Z = 69$) which, on the basis of the data available up to date, probably lies between 0.18 and 0.28 [7]. The disagreement however does not appear so serious as to give a clear evidence of the existence of a transition whose energy is lower than 11 keV but higher than the L X-ray absorption energy of Tm. In effect the disagreement can be easily understood by considering that the numerous γ cascades of the decay scheme strongly increase the rate of L X-K X coincidences.

This conclusion is supported by the relative intensities of the L X-rays and of the K X-rays emitted from the sample. We have obtained in fact

$$\frac{I_L}{I_K} = 0.30 \pm 0.03 \,.$$

With the same extreme assumption on which eq. (2) was based, it can be deduced from this result that:

$$\omega_{LK} = 0.34 \,.$$

4. – Discussion.

As regards the β decay of ^{169}Er, our values for the transition energy and for the half-life are in very good agreement with previous measurements. The decay was found to be a simple one; in particular no evidence of a branching to the first rotational level of ^{169}Tm, was found from the investigation of the γ spectrum. The log ft value (log $ft = 6.1$) and the shape of the β spectrum are consistent with a first forbidden transition ($\Delta I = 0, 1$; yes) $\frac{1}{2}- \rightarrow \frac{1}{2}+$. The ground state spin and parity of ^{169}Tm were known ([3]). The assignment of spin and parity to the ground state of ^{169}Er agrees both with the predictions of the nuclear shell model and with the recent classification of strongly deformed nuclei made by MOTTELSON and NILSSON ([9]).

The results obtained in the investigation of the low energy radiations from ^{169}Yb can be summarized as follows:

a) The measured intensity ratio, eq. (1), between the 23.4 keV γ radiation and the K X-radiation is in satisfactory agreement with that deduced by JOHANSSON for interpreting his coincidence measurements ($I_{23}/I_K = 5.8 \cdot 10^{-3}$).

b) As pointed out in the preceding section no clear evidence was found of the existence of a strong γ radiation between 7 and 11 keV nor of the existence of an intense L conversion of this radiation. However our results could agree with the results of CORK *et al.* if it were assumed that the 8.4 keV γ transition is strongly converted in the M- and N-shells.

* * *

We are indebted to Prof. G. BOLLA for his constant interest.

([9]) B. R. MOTTELSON and S. G. NILSSON: *Phys. Rev.*, **99**, 1615 (1955).

RIASSUNTO

Viene studiata la transizione $^{169}\text{Er} \rightarrow {}^{169}\text{Tm}$. Si trova che il decadimento è semplice; non si osserva l'emissione delle radiazioni γ provenienti dalla diseccitazione dei livelli della famiglia rotazionale del ^{169}Tm. L'energia massima dello spettro β risulta $E_0 = (340 \pm 2)$ keV e il periodo di dimezzamento: $T_{\frac{1}{2}} = (9.0 \pm 0.2)$ d. Le transizioni di bassa energia nel ^{169}Tm presenti nel decadimento dell'^{169}Yb vengono studiate utilizzando uno spettrometro a contatore proporzionale ed una tecnica di coincidenza. La radiazione γ (23.4 keV) proveniente dalla transizione tra il terzo ed il secondo livello rotazionale è stata osservata e se ne è misurata l'intensità relativa a quella della radiazione KX. Non si è ottenuta una chiara dimostrazione dell'esistenza delle radiazioni γ che dovrebbero provenire dalla diseccitazione del primo livello.

A Coincidence Arrangement for the Detection of Low Energy Quanta.

A. Bisi and L. Zappa

Istituto di Fisica Sperimentale del Politecnico - Milano

E. Germagnoli

Laboratori CISE - Milano

(ricevuto il 25 Giugno 1956)

Summary. — An experimental arrangement, in which a proportional counter and a scintillation γ-ray spectrometer are used in coincidence, is found to be useful in investigations concerning the decay of low energy γ- or X-rays emitters. Some results which have been obtained with the described method are given.

1. – Introduction.

Proportional counters have been extensively used for low energy quanta spectrometry. In order to get information about the decay features of soft γ and X emitters, a coincidence apparatus employing a proportional counter and a single crystal γ spectrometer has been found to be useful. Owing to the fact that the collection time of the electrons in a proportional counter is less than 1 μs, reasonably fast coincidence circuits can easily be operated in connection with γ and X crystal detectors and proportional counters.

The extremely low efficiency of proportional counters for hard γ-rays and their high efficiency for radiations as soft as L X-rays and K X-rays from light elements, which are emitted in atomic rearrangements following the decay of nuclei by electron capture and internal conversion processes, made it possible to measure L-shell fluorescence yields and other data which are connected with the features of radioactive decays.

A few results will be described below. For such measurements an A—CH_4 (90% A) filled proportional counter, which was provided with a 23 mg cm^{-2} polyethylene window, has been used. The diameter of the counter was 7 cm, its effective length 30 cm and the wire diameter 0.1 mm. With a total pressure of 120 cm_{Hg} and an applied voltage of 3200 V it operated at a multiplication factor of about 10^3. The geometry of the experimental apparatus is schematically given in Fig. 1.

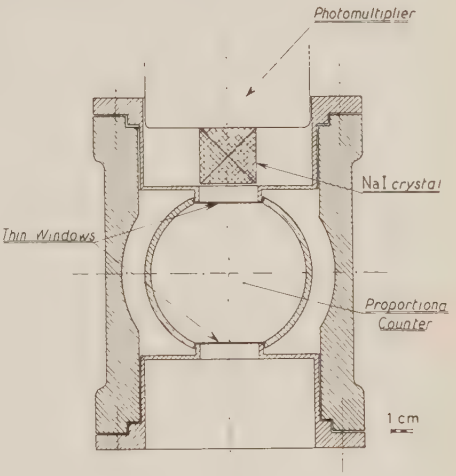

Fig. 1. – Experimental arrangement. When convenient, the source can be located within the proportional counter.

2. – Probability of K-Capture in ^{85}Sr.

The decay scheme of ^{85}Sr is well known and is reported in Fig. 2 [1]. The photopeak of the 513 keV γ line, detected with the single crystal γ spectrometer, was used to trigger the coincidence circuit; K X-rays of Rb (13.37 keV), produced by the electron capture process, were found to be time-coincident with the γ-rays and were revealed with the proportional counter. The resolving time of the coincidence circuit was fixed at about 10 μs, considering that the 513 keV level of ^{85}Rb has a half-life of 0.9 μs.

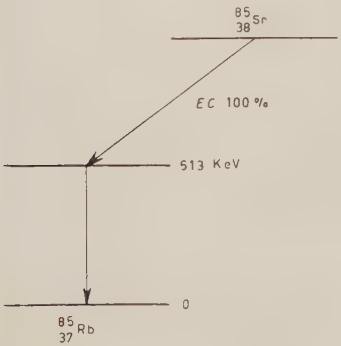

Fig. 2 – Decay scheme of ^{85}Sr.

The following equation holds

$$P_K = \frac{I_{K\gamma}}{I_\gamma} \frac{1}{\omega_K \varepsilon_K} \qquad (1)$$

(1) J. M. Hollander, I. Perlmann and G. T. Seaborg: *Rev. Mod. Phys.*, **25**, 469 (1953).

where P_K is the probability of K-capture;

$I_{K\gamma}$ and I_γ are the counting rates due to coincidences and to γ-rays contributing to the photopeak of the 513 keV line;

ω_K is the K fluorescence yeld of Rb;

ε_K is the efficiency of the proportional counter for 13.37 keV quanta ([2]).

When experimental values are inserted into (1) a P_K value of 0.88 ± 0.04 is found, which is quite consistent with the value 0.91 that is expected for an electron capture process whose transition energy is much larger than the binding energy of K-shell. This is actually true for ^{85}Sr ([3]).

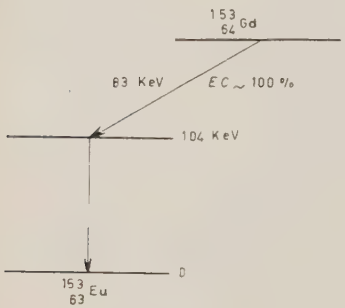

Fig. 3. – Decay scheme of ^{153}Gd.

3. – $\overline{\omega}_L$ of Eu from the Decay of ^{153}Gd.

The decay scheme of ^{153}Gd is given in Fig. 3 ([4]). A mean L-fluorescence yield $\overline{\omega}_L$ ([5]) of Eu can be defined according to the following formula

$$\frac{I_{L\gamma}}{I_\gamma} = \varepsilon_L (n_{LK} + P_L/P_K)\overline{\omega}_L(1 + P_L/P_K)^{-1},$$

where $I_{L\gamma}$ is the intensity of L X-γ coincidences, I_γ is the intensity of the 104 keV line, ε_L is the efficiency of L X-rays detector and n_{LK} is the number of L-shell vacancies produced in filling a K-shell vacancy. The L/K-capture ratio P_L/P_K can be assumed to be $0.68 \pm 0{,}02$ ([4]). With the experimental value $I_{L\gamma}/I_\gamma = 4.37 \cdot 10^{-2}$ and considering that $n_{LK} = 0.85$ and $\varepsilon_L = 0.28$ we get $\overline{\omega}_L = 0.17 \pm 0.02$.

The obtained value of $\overline{\omega}_L$ is in satisfactory agreement with the data recently discussed by ROBINSON and FINK ([5]).

([2]) A. BISI an L. ZAPPA: *Nuovo Cimento*, **12**, 211 (1954).
([3]) R. W. KING: *Rev. Mod. Phys.*, **26**, 327 (1954).
([4]) A. BISI, E. GERMAGNOLI and L. ZAPPA: to be published.
([5]) B. L. ROBINSON and R. W. FINK: *Rev. Mod. Phys.*, **27**, 424 (1955).

4. – ω_{LK} of Ir from the Decay of ^{191}Os.

According to the decay scheme of ^{191}Os [1] (see Fig. 4) the L-shell fluorescence yield of Ir for transitions to the L-level following a K vacancy is given by the equation

$$\omega_{LK} = \frac{1}{\varepsilon_L}\left[\frac{I_{LK}}{I_K} - \frac{I_{L\gamma}}{I_\gamma}\right],$$

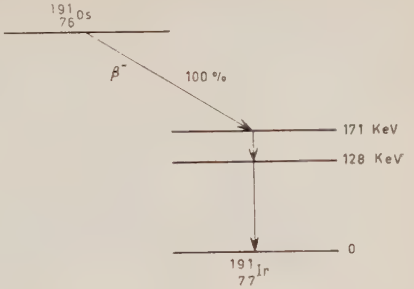

Fig. 4. – Decay scheme of ^{191}Os.

where I_{LK} and $I_{L\gamma}$ are the intensities of L X-K X and L X-γ coincidences, I_K is the counting rate due to K X quanta and I_γ is the intensity of γ-rays belonging to the 128 keV line.

A typical spectrum of L X-rays, obtained in coincidence measurements, is given in Figure 5. With the geometry indicated in Fig. 1, corresponding to $\varepsilon_L = 7.7 \cdot 10^{-2}$, an ω_{LK} value equal to 0.17 ± 0.02 was found.

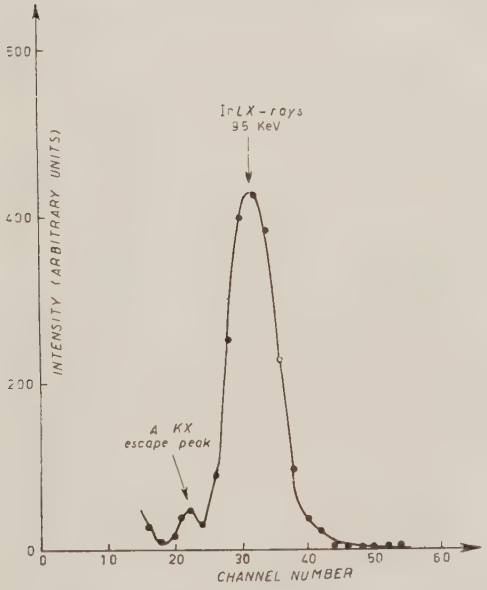

Fig. 5. – Line due to LX-radiations of Ir (9.5 keV) obtained with the proportionl counter. Coincidence circuit triggered bu the KX line of Ir.

* * *

Thanks are due to Prof. G. Bolla for his continuous interest in these investigations.

RIASSUNTO

Si descrive una tecnica di coincidenza tra un contatore proporzionale e uno spettrometro a scintillazione che è risultata utile in ricerche di spettrometria X e γ di bassa energia. Alcuni risultati ottenuti con questo metodo sono brevemente riassunti.

IL NUOVO CIMENTO Vol. IV, N. 4 1° Ottobre 1956

Conservation Laws and other Identities in Bonnor's Unified Field Theory.

S. I. Husain

Department of Mathematics, University of Delhi - Delhi (India)

(ricevuto il 25 Giugno 1956)

Summary. — The field equations of the unified field theory, given by W. B. Bonnor (1) are considered and the conservation laws in the field have been studied. The paper has been divided into two parts, in the first of which the invariant and non-invariant forms of conservation laws have been studied, and in the second part an alternative procedure analogous to that adopted by Schrödinger (4) in his purely affine fields has been sketched. It has been shown that the conservation laws which hold in Schrödinger's and Einstein's (2) field also hold in the present case. The momentum-energy tensors in this case have been shown to satisfy sixteen identities which are seen to be akin to those obtained by Schrödinger (4).

Introduction.

Bonnor (1) has modified the field equations of the unified field theory as developed by Einstein (2), so as to yield Lorentz's equations of motion which include Coulomb's force between charged particles. This, as it has been shown by Callaway (3), is not true in the case of Einstein's (2) field equations. To deduce the modified field equations, he has taken the Hamiltonian

$$\mathfrak{H} = \mathfrak{g}^{ik}R_{ik} + p^2\mathfrak{g}^{ik}g_{ik}, \tag{0.1}$$

(1) W. B. Bonnor: *Proc. Roy. Soc.*, A **226**, 336 (1954).
(2) A. Einstein: *The Meaning of Relativity*, 4th Ed. (Princeton, 1953), Appendix II.
(3) J. Callaway: *Phys. Rev.*, **92**, 1567 (1953).

where

$$\mathfrak{g}^{ik} = \omega g^{ik}, \qquad \omega = \sqrt{-\det \cdot g_{ik}} = \sqrt{-g},$$

R_{ik} is the contracted curvature tensor and p is a real or imaginary constant (which need not be given a definite value at the present stage). A bar or a hook denotes the symmetric or the skew-symmetric part. Proceeding on the lines of EINSTEIN ([2]) he obtained his field equations in the form

$$\underline{g_{ik;l}}(= g_{ik,l} - g_{\alpha k}\Gamma^{\alpha}_{il} - g_{i\alpha}\Gamma^{\alpha}_{lk}) = 0 \tag{0.2}$$

$$\Gamma^{\varrho}_{i\underset{\vee}{\varrho}} = 0 \tag{0.3}$$

$$\underline{R_{ik}} + p^2 \underline{g_{ik}} U = 0 \tag{0.4}$$

and

$$R_{\underset{\vee}{[ik,l]}} + p^2 U_{\underset{\vee}{[ik,l]}} = 0, \tag{0.5}$$

where

$$U_{ik}\,\delta\mathfrak{g}^{ik} = \delta(\mathfrak{g}^{ik} g_{\underset{\vee}{kl}})$$

giving

$$u_{ik} = g_{\underset{\vee}{ki}} - g^{mn}_{\vee} g_{im} g_{nk} + \tfrac{1}{2} g^{mn}_{\vee} g_{nm} g_{ik}\,. \tag{0.6}$$

In the Part I of the present paper, conservation laws in their invariant and non-invariant forms have been obtained in the case of Bonnor's field equations. The method adopted is similar to that in the case of general relativity (symmetric case). In Part II it has been pointed out that these conservation laws can also be obtained by proceeding as SCHRÖDINGER ([1]) has done in the case of purely affine theory; and their identity with the conservation laws of the purely affine theory has been shown. Further the sixteen identities which Schrödinger obtained for the «Momentum-energy tensors» are also found to hold in the present case.

Part I.

1. – Consider the integral

$$I = \int \mathfrak{H}\, d\tau \tag{1.1}$$

and contemplate its variation under the conditions (0.2) and

$$\mathfrak{g}^{ik}_{\vee,k} = 0 \tag{1.2}$$

([1]) E. SCHRÖDINGER: *Proc. Roy. Irish Acad.*, A **52** (1948-50).

(which is equivalent to the condition (0.3)). We obtain

$$\delta I = \int W_{ik}\,\delta \mathfrak{g}^{ik}\,\mathrm{d}\tau\,, \tag{1.3}$$

where

$$W_{ik} = R_{ik} + p^2 u_{ik}\,, \tag{1.4}$$

since

$$\delta\sqrt{-g} = \tfrac{1}{2}\sqrt{-g}\,g^{\mu\nu}\,\delta g_{\mu\nu} = -\tfrac{1}{2}\sqrt{-g}\,g_{\mu\nu}\,\delta g^{\mu\nu},$$

we get

$$\delta \mathfrak{g}^{ik} = \sqrt{-g}(\delta g^{ik} - \tfrac{1}{2} g^{ik} g_{\mu\nu}\,\delta g^{\mu\nu})\,.$$

Hence

$$W_{ik}\,\delta \mathfrak{g}^{ik} = -\,{}^{*}\mathfrak{T}_{ik}\,\delta g^{ik} \tag{1.5}$$

where

$${}^{*}\mathfrak{T}_{ik} = -\sqrt{-g}\,(W_{ik} - \tfrac{1}{2} g_{ik} g^{\mu\nu} W_{\mu\nu})\,.$$

An equivalent form of (1.3) under the same restriction (1.2) is therefore

$$\delta I = -\int {}^{*}\mathfrak{T}_{ik}\,\delta g^{ik}\,\mathrm{d}\tau\,. \tag{1.6}$$

We then consider a variation of g^{ik} merely by a change of frame, which cannot alter the value of the invariant integral I, and hence $\delta I = 0$.

Let the infinitesimal transformation be

$$\overline{x}^k = x^k + \lambda \eta^k + \lambda^2 \zeta^k + \ldots\,, \tag{1.7}$$

where η^k etc., and their first differentials are arbitrary infinitesimal functions of x^k, and as $\lambda \to 0$, this approaches to identity.

Our invariant integral then takes the form

$$I = \int \mathfrak{H}(\overline{g}^{ik}(\overline{x}), \ldots)\,\mathrm{d}\tau'\,,$$

where $\mathfrak{H}$ is of course the same function of the

$$\overline{g}^{ik}(\overline{x}) = g^{lm}(x)\,\frac{\partial \overline{x}^i}{\partial x^l}\,\frac{\partial \overline{x}^k}{\partial x^m}$$

and of their derivative with respect to $\bar{x}$, as it was before of the $g'^{ik}(x)$ and their derivative w.r.t. x. If we now suppose that at the boundary the transformation shall approach to identity for any λ, the limits of integration in $\bar{x}$ will be the same as they were in x. Since the notation for the integration variable does not matter, the only change is that the argument is now not $g^{ik}(\bar{x})$ but $\bar{g}^{ik}(\bar{x})$. Now

$$\bar{g}^{ik}(\bar{x}) - g^{ik}(\bar{x}) = g^{lm}(x)\frac{\partial \bar{x}^i}{\partial x^l}\frac{\partial \bar{x}^k}{\partial x^m} - g^{ik}(\bar{x}) =$$

$$= \left(g^{lm}(\bar{x}) - \frac{\partial g^{lm}(\bar{x})}{\partial \bar{x}^r}\lambda\eta^r\right)\left(\delta_l^i + \lambda\frac{\partial \eta^i}{\partial x^l}\right)\left(\delta_m^k + \lambda\frac{\partial \eta^k}{\partial x^m}\right) - g^{ik}(\bar{x}) .$$

To the order of approximation we are taking here, we can replace η_l and $\partial\eta^k/\partial x^m$ etc., by $\eta_l'(\bar{x})$ and $\partial\eta^k(\bar{x})/\partial\bar{x}^m$ etc. Hence the above expression reduces to

$$\bar{g}^{ik}(\bar{x}) - g'^{ik}(\bar{x}) = \lambda\left\{g'^{rk}(\bar{x})\frac{\partial\eta^k(\bar{x})}{\partial\bar{x}^r} - g'^{ik}(\bar{x})\frac{\partial\eta^s(\bar{x})}{\partial\bar{x}^s} - \frac{\partial g'^{ik}(\bar{x})}{\partial\bar{x}^r}\eta^r(\bar{x})\right\} . \tag{1.8}$$

Since this must vanish at the border for any λ, we may use (1.6) with the first order terms in λ for δg^{ik}. Dropping the unnecessary dashes, we get

$$\delta I = -\int {}^*\mathfrak{T}_{ik}\left(g^{ir}\frac{\partial\eta^k}{\partial x^r} + g^{rk}\frac{\partial\eta^i}{\partial x^r} - \frac{\partial g^{ik}}{\partial x^r}\eta^r\right)\mathrm{d}\tau = 0 ,$$

i. e.

$$0 = \int\left[{}^*\mathfrak{T}_{ik}\frac{\partial g^{ik}}{\partial x^s} + \frac{\partial(g^{ir}{}^*\mathfrak{T}_{is})}{\partial x^r} + \frac{\partial(g^{ri}{}^*\mathfrak{T}_{si})}{\partial x^r}\right]\eta^s\,\mathrm{d}\tau .$$

Now η^s is quite arbitrary, hence we get the identities

$${}^*\mathfrak{T}_{ik}g^{ik}_{,s} + (g^{ir}{}^*\mathfrak{T}_{is} + g^{ri}{}^*\mathfrak{T}_{si})_{,r} = 0 . \tag{1.9}$$

If we put

$${}^*\mathfrak{T}_s^r = \tfrac{1}{2}(g^{ir}{}^*\mathfrak{T}_{is} + g^{ri}{}^*\mathfrak{T}_{si}) ,$$

the above identity takes the form

$$\boxed{{}^*\mathfrak{T}^r_{r,s} + \tfrac{1}{2}{}^*\mathfrak{T}_{ik}g^{ik}{}_{,s} = 0} . \tag{1.10}$$

I

This is the conservation law in the Bonnor's unified field. In this case

$${}^*\mathfrak{T}_{ik} = -\sqrt{-g}(R_{ik} - \tfrac{1}{2}g_{ik}g^{\mu\nu}R_{\mu\nu}) - \sqrt{-g}(U_{ik} - \tfrac{1}{2}g_{ik}g^{\mu\nu}u_{\mu\nu})p^2 ,$$

putting

$$\mathfrak{T}_{ik} = -\sqrt{-g}\,(R_{ik} - \tfrac{1}{2} g_{ik} g^{\mu\nu} R_{\mu\nu}) \tag{1.11}$$

and simplifying the second bracket by substituting for the U_{ik} from (0.6) and using the results

$$g^{mn} g_{ml} = \delta^n_l = g^{nm} g_{lm}$$

$$g^{mn} g_{mn} = 4 \qquad \text{and} \qquad g^{mn} g_{\underset{\vee}{mn}} = g^{\underset{\vee}{mn}} g_{mn}$$

we obtain that

$$^*\mathfrak{T}_{ik} = \mathfrak{T}_{ik} - p^2 \{ \mathfrak{g}_{\underset{\vee}{ki}} - \mathfrak{g}^{\underset{\vee}{mn}} (g_{im} g_{nk} + \tfrac{1}{2} g_{ik} g_{nm}) \}. \tag{1.12}$$

Then

$$\begin{aligned} ^*\mathfrak{T}^r_s &= \mathfrak{T}^r_s - \tfrac{1}{2} p^2 \{ g^{ir} \mathfrak{g}_{\underset{\vee}{\cdot i}} - g^{ir} \mathfrak{g}^{\underset{\vee}{mn}} (g_{im} g_{ns} + \tfrac{1}{2} g_{is} g_{nm}) + \\ &\qquad + g^{ri} \mathfrak{g}_{\underset{\vee}{i\cdot}} - g^{ri} \mathfrak{g}^{\underset{\vee}{mn}} (\delta g_{sm} g_{ni} + \tfrac{1}{2} g_{si} g_{nm}) \} \\ &= \mathfrak{T}^r_s + \tfrac{1}{2} p^2 \delta^r_s \mathfrak{g}^{\underset{\vee}{mn}} g_{nm}. \end{aligned}$$

Hence we obtain

$$^*\mathfrak{T}^r_s = \mathfrak{T}^r_s + \tfrac{1}{2}\, \delta^r_s p^2 \mathfrak{g}^{mn} g_{\underset{\vee}{nm}}. \tag{1.13}$$

Now

$$\begin{aligned} &^*\mathfrak{T}^r_{s,r} + \tfrac{1}{2}\, ^*\mathfrak{T}_{ik} g^{ik}{}_{,s} = \\ &\qquad = \mathfrak{T}^r_{s,r} + \tfrac{1}{2} \mathfrak{T}_{ik} g^{ik}{}_{,s} + p^2 [\tfrac{1}{2} (\mathfrak{g}_{\underset{\vee}{ki}} g^{ik})_{,s} - \tfrac{1}{2} g^{ik}{}_{,s} \{ \mathfrak{g}_{\underset{\vee}{ki}} - \mathfrak{g}^{\underset{\vee}{mn}} (g_{im} g_{nk} + \tfrac{1}{2} g_{ik} g_{nm}) \}]. \end{aligned}$$

The expression inside the square bracket is

$$\tfrac{1}{2} \mathfrak{g}_{\underset{\vee}{ki}} g^{ik}{}_{,s} + \tfrac{1}{2} \mathfrak{g}^{\underset{\vee}{mn}} g_{im} g_{nk} g^{ik}{}_{,s} + \tfrac{1}{4} g_{ik} g^{ik}{}_{,s} \mathfrak{g}^{\underset{\vee}{mn}} g_{nm}.$$

Now

$$g_{im} g_{nk} g^{ik}{}_{,s} = -\, g_{nm,s}$$

$$g_{ik} g^{ik}{}_{,s} = -\, 2 \Gamma^h_{\underline{sh}} \qquad \text{and} \qquad \omega, s = \omega \Gamma^h_{\underline{sh}}$$

hence the above expression simplifies to

$$\begin{aligned} &\tfrac{1}{2} \mathfrak{g}^{ik} g_{\underset{\vee}{ki},s} + \tfrac{1}{2} g_{ik} \mathfrak{g}^{\underset{\vee}{ki}} \Gamma^h_{\underline{sh}} - \tfrac{1}{2} \mathfrak{g}^{\underset{\vee}{mn}} g_{nm,s} - \tfrac{1}{2} \mathfrak{g}^{\underset{\vee}{mn}} g_{nm} \Gamma^h_{\underline{sh}} = \\ &\qquad = \tfrac{1}{4} \{ \mathfrak{g}^{ik} (g_{ki} - g_{ik})_{,s} - (\mathfrak{g}^{ik} - \mathfrak{g}^{ki}) g_{ki,s} \} = 0. \end{aligned}$$

Thus we obtain

$$^*\mathfrak{T}^r_{s,r} + \tfrac{1}{2}\, ^*\mathfrak{T}_{ik} g^{ik}{}_{,s} = \mathfrak{T}^r_{s,r} + \tfrac{1}{2} \mathfrak{T}_{ik} g^{ik}{}_{,s} \tag{1.14}$$

and so the identity

$$\boxed{\mathfrak{T}^{r}_{s,r} + \tfrac{1}{2}\mathfrak{T}_{ik}g^{ik}{}_{,s} = 0} \qquad \text{I}(a)$$

(1.15)

also holds in the Bonnor's field.

2. – Our object is now to change the second term in the conservation identity I into a sum of derivatives with respect to the coordinates—what is sometimes called a « plain divergence ». We begin by exhibiting that the integrand

$$\mathfrak{H}(= \mathfrak{g}^{ik}R_{ik} + p^2\mathfrak{g}^{ik}g_{k\underset{\vee}{i}}) ,$$

is in a certain sense equivalent to another integrand, H, which contains no higher than the first derivatives of g_{ik}. The equivalence rests on this that the difference $\mathfrak{H} - H$ is a plain-divergence, the variation (that vanishes at the boundary) of the four dimensional integral of which vanishes.

Take

$$H = \mathfrak{g}^{ik}\Lambda_{ik} - p^2\mathfrak{g}^{ik}g_{k\underset{\vee}{i}} , \qquad (2.1)$$

where

$$\Lambda_{ik} = \Gamma^{\alpha}_{\beta\alpha}\Gamma^{\beta}_{ik} - \Gamma^{\beta}_{\alpha k}\Gamma^{\alpha}_{i\beta} . \qquad (2.2)$$

We shall consider such variations which conserve the condition (1.2), and hence (0.3).

Now

$$\begin{aligned}\mathfrak{H} &= \mathfrak{g}^{ik}\Gamma^{\alpha}_{ik,\alpha} - \mathfrak{g}^{ik}\Gamma^{\alpha}_{i\alpha,k} + H + 2p^2\mathfrak{g}^{ik}g_{k\underset{\vee}{i}} \\ &= (\mathfrak{g}^{ik}\Gamma^{\alpha}_{ik})_{,\alpha} - (\mathfrak{g}^{ik}\Gamma^{\alpha}_{i\alpha})_{,k} - \mathfrak{g}^{ik}{}_{,\alpha}\Gamma^{\alpha}_{ik} + \mathfrak{g}^{ik}_{,k}\Gamma^{\alpha}_{i\alpha} + H + 2p^2\mathfrak{g}^{ik}g_{k\underset{\vee}{i}} \\ &= (\mathfrak{g}^{ik}\Lambda^{\alpha}_{ik})_{,\alpha} + (\mathfrak{g}^{\beta k}\Gamma^{i}_{\beta\alpha} + \mathfrak{g}^{i\beta}\Gamma^{k}_{\alpha\beta} - \mathfrak{g}^{ik}\Gamma^{\beta}_{\alpha\beta})\Gamma^{\alpha}_{ik} - (\mathfrak{g}^{\beta k}\Gamma^{i}_{\beta k})\Gamma^{\alpha}_{i\alpha} + H + 2p^2\mathfrak{g}^{ik}g_{k\underset{\vee}{i}} ,\end{aligned}$$

in virtue of (0.3), where

$$\Lambda^{\alpha}_{ik} = (\Gamma^{\alpha}_{ik} - \delta^{\alpha}_{k}\Gamma^{\sigma}_{i\sigma}) .$$

This can further be simplified to

$$\mathfrak{H} = (\mathfrak{g}^{ik}\Lambda^{\alpha}_{ik})_{,\alpha} - (\mathfrak{g}^{\beta k}\Lambda_{\beta k} - p^2\mathfrak{g}^{\beta k}g_{k\underset{\vee}{\beta}}) - (\mathfrak{g}^{ik}\Lambda_{ik} - p^2\mathfrak{g}^{ik}g_{k\underset{\vee}{i}}) + H ,$$

i.e.

$$\mathfrak{H} = (\mathfrak{g}^{ik}\Lambda^{\alpha}_{ik})_{,\alpha} - H . \qquad (2.3)$$

Now $(\mathfrak{g}^{ik}\Lambda^{\alpha}_{ik})_{,\alpha}$ is a plain divergence, hence its four dimensional integral can be turned into a surface integral, which suffers no change under variation that vanishes at the boundry, i.e.

$$\delta\int(\mathfrak{g}^{ik}\Lambda^{\alpha}_{ik})_{,\alpha}\mathrm{d}\tau = 0\,. \tag{2.4}$$

We thus obtain

$$\delta\int\mathfrak{H}\,\mathrm{d}\tau = -\,\delta\int H\,\mathrm{d}\tau\,. \tag{2.5}$$

Thus we have shown that the integrands $\mathfrak{H}$ and $-H$ are equivalent in the sense that their Hamiltonian derivatives are equal. From (2.5) and (1.6) it follows that

$$\delta\int H\,\mathrm{d}\tau = \int{}^{*}\mathfrak{T}_{ik}\,\delta g^{ik}\,\mathrm{d}\tau\,, \tag{2.6}$$

i.e. the Hamiltonian derivative of H w.r.t. g^{ik} is ${}^{*}\mathfrak{T}_{ik}$ i.e.

$${}^{*}\mathfrak{T}_{ik} = \frac{\delta H}{\delta g^{ik}} = \frac{\partial H}{\partial g^{ik}} - \frac{\partial}{\partial x^{\alpha}}\left(\frac{\partial H}{\partial g^{ik}_{,\alpha}}\right).$$

Therefore

$${}^{*}\mathfrak{T}_{ik}g^{ik}_{,s} = \frac{\partial H}{\partial x^{s}} - \frac{\partial}{\partial x^{\alpha}}\left(\frac{\partial H}{\partial g^{ik}_{,\alpha}}g^{ik}_{,s}\right) = \left(\delta^{\alpha}_{s}H - \frac{\partial H}{\partial g^{ik}_{,\alpha}}g^{ik}_{,s}\right)_{,\alpha}$$

We put

$${}^{*}\mathfrak{T}^{\alpha}_{s} = \frac{1}{2}\left(\delta^{\alpha}_{s}H - \frac{\partial H}{\partial g^{ik}_{,\alpha}}g^{ik}_{,\alpha}\right). \tag{2.7}$$

Then the conservation law I takes the form

$$\boxed{({}^{*}\mathfrak{T}^{r}_{s} + {}^{*}\mathfrak{T}^{r}_{s})_{,r} = 0}\,. \tag{2.8}$$ II

This is the result which we aimed at in the beginning of Sect. 2, i.e. the plain divergence form of conservation law; an identity under restriction (1.2). It is obviously seen that ${}^{*}\mathfrak{T}^{r}_{s}$ is not a tensor-density. Yet the relation II holds in every frame, though it does not treat of tensors only. This leads us to call ${}^{*}\mathfrak{T}^{r}_{s}$ a « Pseudo-tensor density ».

Now we wish to express ${}^{*}\mathfrak{T}^{\alpha}_{s}$ in terms of $\mathfrak{g}^{ik}$, Γ^{α}_{ik} and their derivatives. It has been shown while proving the result (2.3) that

$$\mathfrak{g}^{ik}_{,s}\Gamma^{\alpha}_{ik} - \mathfrak{g}^{ik}_{,k}\Gamma^{\alpha}_{is} = 2\mathfrak{g}^{ik}\Lambda_{ik}\,(=2\Lambda)\,. \tag{2.9}$$

Hence we want to use the partial derivative of H w.r.t. $\mathfrak{g}^{ik}_{,\alpha}$ instead of $g^{ik}_{,\alpha}$.

We know that

$$\delta\int H\,\mathrm{d}\tau = \int\frac{\delta H}{\delta g^{ik}}\,\delta g^{ik}\,\mathrm{d}\tau$$

also

$$= \int\frac{\delta H}{\delta \mathfrak{g}^{ik}}\,\delta\mathfrak{g}^{ik}\,\mathrm{d}\tau = \int\frac{\delta H}{\delta\mathfrak{g}^{ik}}\frac{\partial\mathfrak{g}^{ik}}{\partial g^{lm}}\,\delta g^{lm}\,\mathrm{d}\tau\,.$$

Hence

$$\frac{\delta H}{\delta g^{lm}} = \frac{\delta H}{\delta\mathfrak{g}^{ik}}\frac{\partial\mathfrak{g}^{ik}}{\partial g^{lm}}\,.$$

Now

$$^{*}\mathfrak{T}_{lm}g^{lm}_{,s} = \frac{\delta H}{\delta\mathfrak{g}^{lm}}g^{lm}_{,s}$$

$$= \frac{\delta H}{\delta\mathfrak{g}^{ik}}\frac{\partial\mathfrak{g}^{ik}}{\partial g^{lm}}\cdot\frac{\partial g^{lm}}{\partial x^{s}} = \frac{\delta H}{\delta\mathfrak{g}^{ik}}\mathfrak{g}^{ik}_{,s}$$

and proceeding as in the case of (2.7) we obtain

$$^{*}\mathfrak{T}^{\alpha}_{s} = \frac{1}{2}\left(\delta^{\alpha}_{s}H - \frac{\partial H}{\partial\mathfrak{g}^{ik}_{,\alpha}}\mathfrak{g}^{ik}_{,\alpha}\right). \tag{2.10}$$

It remains now to evaluate $\partial H/\partial\mathfrak{g}^{ik}_{,\alpha}$. Since

$$H = \Lambda - p^{2}\mathfrak{g}^{ik}g_{kj}\,,$$

it follows that

$$\frac{\partial H}{\partial\mathfrak{g}^{ik}_{,\alpha}} = \frac{\partial\Lambda}{\partial\mathfrak{g}^{ik}_{,\alpha}}\,. \tag{2.11}$$

Differentiating relation (2.9) we get

$$\mathfrak{g}^{ik}_{,\alpha}\mathrm{d}\Gamma^{\alpha}_{ik} - \mathfrak{g}^{ik}_{,k}\mathrm{d}\Gamma^{\alpha}_{i\alpha} + \Gamma^{\alpha}_{ik}\mathrm{d}(\mathfrak{g}^{ik}_{,\alpha}) - \Gamma^{\alpha}_{i\alpha}\mathrm{d}(\mathfrak{g}^{ik}_{,k}) = 2\,\mathrm{d}\Lambda\,.$$

The first two terms can be written as

$$-(\mathfrak{g}^{\beta k}\Gamma^{\prime}_{\beta\alpha} + \mathfrak{g}^{i\beta}\Gamma^{k}_{i\beta} - \mathfrak{g}^{ik}\Gamma^{\beta}_{i\beta})\mathrm{d}\Gamma^{\alpha}_{ik} - \mathfrak{g}^{\beta k}\Gamma^{\prime}_{\beta k}\mathrm{d}\Gamma^{\prime}_{\alpha} = \mathfrak{g}^{\beta k}\mathrm{d}\Lambda_{\beta k} = \mathrm{d}\Lambda - \Lambda_{\beta k}\mathrm{d}(\mathfrak{g}^{\beta k})\,.$$

Hence we obtain

$$\Gamma^{\alpha}_{ik}\mathrm{d}(\mathfrak{g}^{ik}_{,\alpha}) - \Gamma^{\alpha}_{i\alpha}(\mathrm{d}\mathfrak{g}^{ik}_{,k}) - \Lambda_{\beta k}\mathrm{d}(\mathfrak{g}^{\beta k}) = \mathrm{d}\Lambda\,.$$

Therefore

$$\frac{\partial \Lambda}{\partial \mathfrak{g}^{ik}_{,\alpha}} = \Lambda^{\alpha}_{ik} = \frac{\partial H}{\partial \mathfrak{g}^{ik}_{,\alpha}}. \tag{2.12}$$

Thus an alternative expression for $^{*}\mathfrak{F}^{\alpha}_{s}$ is

$$^{*}\mathfrak{F}^{\alpha}_{s} = \tfrac{1}{2}(\delta^{\alpha}_{s} H - \Lambda^{\alpha}_{ik}\mathfrak{g}^{ik}_{,s}) . \tag{2.13}$$

This can be written as

$$^{*}\mathfrak{F}^{\alpha}_{s} = \mathfrak{F}^{\alpha}_{s} - \tfrac{1}{2}\delta^{\alpha}_{s} p^{2}\mathfrak{g}^{ik}\underset{\vee}{g}_{ki}, \tag{2.14a}$$

where

$$\mathfrak{F}^{\alpha}_{s} = \tfrac{1}{2}(\delta^{k}_{\alpha}\Lambda - \Lambda^{\alpha}_{ik}\mathfrak{g}^{ik}_{,s}) . \tag{2.14b}$$

From (1.13) and (2.14) we see that

$$^{*}\mathfrak{T}^{r}_{s} + {}^{*}\mathfrak{F}^{r}_{s} = \mathfrak{T}^{r}_{s} + \mathfrak{F}^{r}_{s} \tag{2.15}$$

and thus the identity

$$\boxed{(\mathfrak{T}^{r}_{s} + \mathfrak{F}^{r}_{s})_{,r} = 0} . \tag{2.16}$$ II(a)

also holds in the Bonnor's field.

Part II.

3. – These conservation laws can also be obtained in the same way as SCHRÖDINGER [4] has deduced them in the case of purely affine field or Einstein's unified field. We do not propose to give the whole working here, as it is similar to that in the above mentioned paper [4], except that we start with the invariant integral of

$$\mathfrak{g}^{ik}R_{ik} + p^{2}\mathfrak{g}^{ik}\underset{\vee}{g}_{ki} \tag{3.1}$$

instead of $\mathfrak{g}^{ik}R_{ik}$ and the non-invariant integral, with the integrand

$$H = \Lambda - p^{2}\mathfrak{g}^{ik}\underset{\vee}{g}_{ki} \tag{3.2}$$

instead of .1 and some obvious minor changes here and there. We have adopted practically the same nomenclature, the relations between ${}^*\mathfrak{T}_{ik}$, ${}^*\mathfrak{F}_s^r$ and $\mathfrak{T}_{ik}$, $\mathfrak{F}_s^r$—the corresponding quantities in purely affine field—are given by (1.12), (1.13), and (2.14).

Working as in the above mentioned paper, we get the final form of the expression from which all the identities follow, as

$$\delta^* \int H \, d\tau = -2 \int \{ {}^*\mathfrak{T}^\alpha_{r,\alpha} + \tfrac{1}{2} {}^*\mathfrak{T}_{ik} g^{ik}_{,r} \} \xi^r \, d\tau + \int \{ H \xi^\alpha - \Lambda^\alpha_{ik} \delta^* g^{ik} + 2 {}^*\mathfrak{T}^\alpha_r \xi^r \}_{,\alpha} d\tau, \tag{3.3}$$

where the variation δ^* refers to the infinitesimal change of frame

$$\bar{x}^k = x^k + \xi^k(x) .$$

From the integral (3.3) by specializing the change of frame in different ways (SCHRÖDINGER (4)), the identities

$${}^*\mathfrak{T}^s_{r,s} + \tfrac{1}{2} {}^*\mathfrak{T}_{ik} g^{ik}_{,r} = 0 , \tag{3.4}$$

$$({}^*\mathfrak{T}^\alpha_r + {}^*\mathfrak{F}^\alpha_r)_{,\alpha} = 0 \tag{3.5}$$

and

$$\boxed{ {}^*\mathfrak{F}^s_r - {}^*\mathfrak{T}^s_r = \tfrac{1}{2} (\Lambda^\alpha_{rk} g^{sk} - \Lambda^\alpha_{kl} g^{ks} \delta^s_r \Lambda^\alpha_{ik} g^{ik})_{,\alpha} } \tag{3.6}$$

III

follow.

The first two are the invariant and non-invariant forms of the conservation law, as already deduced in (1.10) and (2.8). The third is a new set of sixteen identities expressing the components of ${}^*\mathfrak{F}^s_r + {}^*\mathfrak{T}^s_r$ as a plain divergence.

4. – From (3.4), (3.5) and (1.14), (2.15) it follows that

$$\mathfrak{T}^s_{r,s} + \tfrac{1}{2} \mathfrak{T}_{ik} g^{ik}_{,r} = 0 \tag{1.15}$$

and

$$(\mathfrak{F}^s_r + \mathfrak{T}^s_r)_{,s} = 0 , \tag{2.16}$$

which shows that the conservation identities which hold in the Schrödinger's purely affine field or Einstein's unified field also hold in Bonnor's field and vice-versa.

Again from (3.6) and (2.15) it follows that

$$\boxed{\mathfrak{H}_r^s + \mathfrak{T}_r^s = \tfrac{1}{2}(A^a_{rk}\mathfrak{g}^{sk} + A^a_{kr}\mathfrak{g}^{ks} - \partial_r^s A^a_{ik}\mathfrak{g}^{ik})_{,s}} \qquad (4.1)$$

which is the same identity that holds in Schrödinger's or Einstein's field.

* * *

In the end I wish to express my gratefulness to Dr. R. S. Mishra for his very kind and helpful guidance.

RIASSUNTO (*)

Si considerano le equazioni di campo della teoria unificata dei campi date da W. B. Bonnor e si studiano le leggi di conservazione nel campo. Il lavoro è diviso in due parti, nella prima delle quali si studiano le forme invarianti e non invarianti delle leggi di conservazione; nella seconda parte si delinea un procedimento in sostituzione del precedente, analogo a quello adottato da Schrödinger nei suoi campi puramente affini. Si dimostra che le leggi di conservazione valevoli nei campi di Schrödinger e di Einstein valgono anche nel presente caso. Si dimostra che i tensori momento-energia nel nostro caso soddisfano sedici identità che risultano analoghe a quelle ottenute da Schrödinger.

(*) *Traduzione a cura della Redazione.*

IL NUOVO CIMENTO Vol. IV, N. 4 1° Ottobre 1956

On the Dynamics of a Non-Uniform Electrically Conducting Fluid.

G. H. A. Cole

University College London, England

(ricevuto il 28 Giugno 1956)

Summary. — First steps are taken at building up a kinetic theory of ionised fluids under non-uniform conditions. The Boltzmann-Maxwell, and Fokker-Planck equations are related to molecular data, and in this way the approximations involved in their use are made clear.

1. – Introduction.

The microscopic theory of an ionized fluid, possibly immersed in an externa electromagnetic field, has been developed from the Liouville equation generalized to include the effect of simple binary encounters [1,2] (the Boltzmann equation), or alternatively to include the Coulomb interaction [3] (the Fokker-Planck equation). The macroscopic theory of hydromagnetics has been developed from a fusion of the equations of electromagnetism and of classical hydrodynamics [1,5]. The latter equations are derived from the microscopic equations of motion by invoking successively the conservation theorems of mass, momentum, and energy. A complete kinetic theory of conducting media under non-uniform conditions must provide a derivation of these initial equations

(1) S. Chapman and T. G. Cowling: *Mathematical Theory of Non-Uniform Gases* (C.U.P., 1952).

(2) L. Spitzer Jr.: *Physics of Fully Ionized Gases* (New York, 1956).

(3) S. Gasiorowicz, M. Newmann and R. J. Riddell: *Phys. Rev.*, **101**, 922 (1956).

(4) G. H. A. Cole: *Advances in Physics* (in press).

(5) W. Elsasser: *Am. Journ. Phys.*, **23**, 590 (1955).

in terms of molecular variables on the basis of molecular dynamics alone. In the present introductory note it is indicated how this can be achieved by applying the arguments of kinetic theory recently developed for non-uniform liquids ([6-8]). The theory will be applied in detail to the derivation of transport coefficients for ionized media in further papers.

2. – Premises.

The conducting fluid is represented by N charged particles contained in a volume V, immersed in an electromagnetic field $(\boldsymbol{E}_0, \boldsymbol{H}_0)$. Classical theory is invoked throughout so that it is not necessary to account for particle interaction effects of the ionization and recombination type. The charge and mass of the i-th particle are written respectively as e_i and m_i: the total force acting on the particle is assumed to be the sum of an external (hydrodynamic-electromagnetic) force $\boldsymbol{X}_i$, and an intermolecular force $\boldsymbol{F}_i$. $\boldsymbol{F}_i$ is itself assumed to be the sum of a short range force of the van der Waals type, $\boldsymbol{F}_{0i}$, and the Lorentz force arising from neighbour interaction. Radiation effects are neglected at present.

3. – Distribution Functions.

If $f^{(N)}(\boldsymbol{p}, \boldsymbol{r}, t)$ is the probability for the simultaneous occurrence of particle momenta and co-ordinates at time t, then $f^{(N)}$ is a solution of the Liouville equation

$$\frac{\partial f^{(N)}}{\partial t} + \sum_{i=1}^{N} \left[\frac{\boldsymbol{p}_i}{m_i} \cdot \nabla_{\boldsymbol{r}_i} f^{(N)} + (\boldsymbol{X}_i + \boldsymbol{F}_i) \cdot \nabla_{\boldsymbol{p}_i} f^{(N)} \right] = 0 , \tag{1}$$

which expresses the canonical form. Reduced distribution functions describing small groupings of molecules are derived from (1) by averaging over the partial phase $(\boldsymbol{P}, \boldsymbol{R})$ of the remainder. The simplest member of the set of $(N-1)$ equations so derived involves $f^{(1)}$, which may be interpreted alternatively as the singlet distribution, or the doublet distribution in relative co-ordinates. $f^{(1)}$ is a solution of the equation

$$\frac{Df^{(1)}}{Dt} = -\sum_{i=2}^{N} \int\int \left[\frac{\boldsymbol{p}_i}{m_i} \cdot \nabla_{\boldsymbol{r}_i} + \boldsymbol{X}_i \cdot \nabla_{\boldsymbol{p}_i} \right] f^{(N)} \, \mathrm{d}\boldsymbol{P} \, \mathrm{d}\boldsymbol{R} - \sum_{i=1}^{N} \int\int \boldsymbol{F}_i \nabla_{\boldsymbol{p}_i} f^{(N)} \, \mathrm{d}\boldsymbol{P} \, \mathrm{d}\boldsymbol{R} , \tag{2}$$

([6]) J. G. KIRKWOOD: *Journ. Chem. Phys.*, **14**, 180 (1946).
([7]) R. EISENSCHITZ: *Proc. Roy. Soc.*, A **215**, 29 (1952).
([8]) G. H. A. COLE: *Rep. Prog. Phys.*, **19**, 1 (1956).

where D/Dt is the conventional Stokes' operator, including terms involving $\boldsymbol{E}_0$ and $\boldsymbol{H}_0$. $\boldsymbol{X}_i$ and $\boldsymbol{F}_i$ are given by:

$$(3)\quad \begin{cases} (a) & \boldsymbol{X}_i = \dfrac{e_i}{m_i}\left\{\boldsymbol{E}_{0i} + \dfrac{1}{m_i c}[\boldsymbol{p}_i \cdot \boldsymbol{H}_{0i}]\right\} \\ (b) & \boldsymbol{F}_i = \boldsymbol{F}'_{0i} + \dfrac{e_i}{m_i}\left\{\boldsymbol{E}_i^{(i)} + \dfrac{1}{m_i c}[\boldsymbol{p}_i \cdot \boldsymbol{H}_i^{(i)}]\right\} \end{cases}$$

$\boldsymbol{E}_i^{(i)}$ and $\boldsymbol{X}_i^{(i)}$ are respectively the electric and magnetic fields in the neighbourhood of the i-th particle due to neighbours, and are to be interpreted as plasma linkage.

Equations analogous to (2) but involving successively the higher order functions $f^{(2)}$, $f^{(3)}$, $f^{(4)}$, ..., $f^{(N-1)}$ on the left hand side form the complete set of equations. Each equation provides less information about the physical system than does (1), but we assert that a knowledge of the pair function alone is sufficient to enable significant conclusions to be drawn in our case. It may, however, be necessary later to appeal to higher order functions in some cases.

4. – Irreversibility.

Equations (1) and (2) have a range of solutions applying to uniform or non-uniform conditions. Only the latter solutions are of interest here; they belong to a group not satisfying time reversal, and so cannot be obtained by a formal procedure such as a transformation to extended phase space. For deriving non-uniform distribution functions it is necessary to invoke a new hypothesis analogous to that of molecular chaos in the theory of dilute gases. Recently KIRKWOOD ([6]) has formulated such an hypothesis for liquids, and we now extend its validity to apply to ionized media. The Kirkwood hypothesis places a time condition on the autocorrelation coefficient ξ:

$$(4)\qquad \xi = \overline{\boldsymbol{F}_1(t)\cdot\boldsymbol{F}_1(t+\tau)} = 0 \qquad |\tau| > \tau_c .$$

The bar in (4) denotes a phase average over the remaining particles: τ_c is a time interval which is microscopically large (i.e. large compared to the time of extended molecular interaction) and yet macroscopically small (i.e. small compared to the Poincaré period). The existence of such a time interval in ionized fluids, where the forces are partly long ranged, is a direct consequence of the Debye shielding radius.

On the validity of (4), then, the time average of ξ over an interval $\tau > \tau_c$ leads to a constant: this has been interpreted for liquids ([6]) in terms of a friction tensor of the macroscopic Stokes' type, and this interpretation is

applicable also for ionized fluids. The existence of such a constant controlling the irreversible approach to uniformity is now regarded as characteristic. In the theory, then, solutions of (2) applicable to non-uniform conditions will be isolated by coarse-graining in time: the utility of coarse-graining in connection with non-equilibria was first recognized by Gibbs, and carried through for liquids by KIRKWOOD.

5. – Selection of Non-Uniform Distribution Functions.

If a steady state condition exists for projections on the subspaces of singlet and doublet distributions then on coarse-graining (2) over the time interval τ:

$$\left\{\frac{Df^{(1)}}{Dt} + \boldsymbol{\epsilon}\cdot\nabla_p f^{(1)} + \boldsymbol{h}\cdot\nabla_p f^{(1)}\right\}\tau = -\int_{\tau}^{0}\mathrm{d}t\iint(\boldsymbol{X}+\boldsymbol{F})\cdot\nabla_p f^{(2)}\,\mathrm{d}\boldsymbol{P}\,\mathrm{d}\boldsymbol{R}\,, \tag{5}$$

with

$$\begin{cases} (a) & \iint \boldsymbol{E}^{(i)}\cdot\nabla_p f^{(2)}\,\mathrm{d}\boldsymbol{P}\,\mathrm{d}\boldsymbol{R} = \boldsymbol{\epsilon}\cdot\nabla_p f^{(1)} \\ (b) & \dfrac{1}{mc}\iint[\boldsymbol{p}\cdot\boldsymbol{H}_i^{(i)}]\cdot\nabla_p f^{(2)}\,\mathrm{d}\boldsymbol{P}\,\mathrm{d}\boldsymbol{R} = \boldsymbol{h}\cdot\Delta_p f^{(1)}\,. \end{cases} \tag{6}$$

The total momentum change of a particle during τ due to its neighbours is

$$\Delta\boldsymbol{p} = \int_{\tau}^{0}(\boldsymbol{X}+\boldsymbol{F})\,\mathrm{d}t\,.$$

If $\nabla_p f^{(2)}$ is sensibly time independent the right hand side of (5) becomes:

$$-\iint\Delta\boldsymbol{p}\cdot\nabla_p f^{(2)}\,\mathrm{d}\boldsymbol{P}\,\mathrm{d}\boldsymbol{R}\,, \tag{7}$$

a form first given for liquids by EISENSCHITZ [7]. Using (7), (5) becomes explicitly:

$$\tau\left\{\frac{\partial f^{(1)}}{\partial t} + \frac{\boldsymbol{p}}{m}\cdot\nabla_r f^{(1)} + (\boldsymbol{E}_0+\boldsymbol{\epsilon})\cdot\nabla_p f^{(1)} + (\boldsymbol{H}_0+\boldsymbol{h})\cdot\nabla_p f^{(1)}\right\} = \iint\nabla\boldsymbol{p}\cdot\nabla_p f^{(2)}\,\mathrm{d}\boldsymbol{P}\,\mathrm{d}\boldsymbol{R}\,. \tag{8}$$

By averaging (8) over the invariants of the system the equations of macroscopic hydrodynamics result. If the external electromagnetic field is absent the terms

$\boldsymbol{\epsilon}$ and $\boldsymbol{h}$ still remain. The evaluation of $\boldsymbol{\epsilon}$ and $\boldsymbol{h}$ from (6) involves a knowledge of the spectral distribution of neighbours: this distribution can be expected to be affected by the presence of the field $(\boldsymbol{E}_0, \boldsymbol{H}_0)$ so that $\boldsymbol{\epsilon}$ and $\boldsymbol{h}$ are to be associated with the increments of interest in hydromagnetics.

In order to base a macroscopic theory on (8) it is necessary to rearrange the right hand side. Such a rearrangement will depend upon the magnitude of $\Delta\boldsymbol{p}$: the two limiting cases provide familiar forms. If $\Delta\boldsymbol{p}$ is large (corresponding to an angular deflection greater than 90°), and the time between such encounters is very large in comparison with the time of an encounter (density of such collisions small) then the arguments of KIRKWOOD [9] for short-ranged forces apply here also, and the right hand side of (8) takes the form of the Boltzmann-Maxwell collision integral. Alternatively if $\Delta\boldsymbol{p}$ is small (corresponding to an angular deflection of less than about 40°) the arguments of EISENSCHITZ [7] for short-ranged forces again apply since τ_c exists. In this case $\Delta\boldsymbol{p}\cdot\nabla_p f^{(N)}$ can be written $[f^{(N)}(\boldsymbol{p} - \Delta\boldsymbol{p}) - f^{(N)}(\boldsymbol{p})]$, which allows the right hand side of (8) to be expanded:

$$-f^{(1)}(\boldsymbol{p}) + \int f^{(1)}(\boldsymbol{p} - \Delta\boldsymbol{p})\chi(\Delta\boldsymbol{p})\,\mathrm{d}(\Delta\boldsymbol{p})\,. \tag{9}$$

This form is well known in the theory of stochastic processes [10]. On further expansion it leads to the Fokker-Planck equation, (9) containing mean, mean square, and mean component products of $\Delta\boldsymbol{p}$. By the standard procedure [10,11], it is found that $\Delta\boldsymbol{p}$ and $\Delta\boldsymbol{p}^2$ are of order τ, and that $\Delta\boldsymbol{p}_r\Delta\boldsymbol{p}_s$ and all higher moments are of order τ^2, and so can be neglected:

$$\tau\left\{\frac{\partial f^{(1)}}{\partial t} + \frac{\boldsymbol{p}}{m}\cdot\nabla_r f^{(1)} + (\boldsymbol{E}_0 + \boldsymbol{\epsilon})\cdot\nabla_p f^{(1)} + (\boldsymbol{H}_0 + \boldsymbol{h})\cdot\nabla_p f^{(1)}\right\} = -\frac{\partial}{\partial\boldsymbol{p}}(\overline{\Delta\boldsymbol{p}} f^{(1)}) + \frac{1}{2}\frac{\partial^2}{\partial\boldsymbol{p}^2}(\overline{\Delta\boldsymbol{p}^2} f^{(1)}) + 0(\tau^2)\,. \tag{10}$$

The associated friction constant is given by:

$$\beta = \int_0^\tau \overline{\{(\boldsymbol{F}_0(t) + \boldsymbol{X}(t))\cdot(\boldsymbol{F}_0(t+s) + \boldsymbol{X}(t+s))\}}\,\mathrm{d}s \tag{11}$$

the bar denoting an average over the remaining particles. By simple expansion (11) can be separated into three components: one involves $\boldsymbol{F}_0(t)\cdot\boldsymbol{F}_0(t+s)$

(9) J. G. KIRKWOOD: *Journ. Chem. Phys.*, **15**, 72 (1947).
(10) S. CHANDRASEKHAR: *Rev. Mod. Phys.*, **15**, 2 (1943).
(11) E. EISENSCHITZ: *Nature*, **167**, 216 (1951).

and arises from the short-range forces; another involves $\boldsymbol{X}(t)\cdot\boldsymbol{X}(t-s)$ and arises from the long-ranged forces. The evaluation of the former distribution involves problems notorious in the theory of liquids; the latter can be evaluated by trajectory methods [2] familiar in gas theory. The remaining contribution involves mixed autocorrelation terms of the form $F_0(t)\cdot\boldsymbol{X}(t-s)$. The different time fluctuation of the two components will not allow this last contribution to be significant. The form of (11) to be used in a particular case will, accordingly, depend on the density. If the density is high the short-ranged forces will predominate, and if low the long-ranged forces will predominate: for these cases the hydrodynamical Stokes' friction constant will usually be adequate, appropriate respectively to liquids and dilute gases.

If the friction constant is high enough, as in a highly compreszed ionised medium, the Fokker-Planck equation can be replaced to sufficient accuracy by the Smoluchowski equation [10] at all points except possibly in the neighbourhood of the origin. In first calculations this diffusion equation will be more amenable to solution than the full Fokker-Planck equation.

6. – Discussion.

From the argument of Sect. 5 the approximations involved in applying the Boltzmann equation alone, or the Fokker-Planck equation alone, are clear. In particular it is seen that a combination of Fokker-Planck and Boltzmann interaction terms still neglects a contribution from medium range molecular interaction which may be significant. For example it is likely that the neglect of this contribution caused the difficulties described by Cohen, Spitzer, and McRoulty [3] in the calculation of electrical conductivity. The effect of these medium ranged terms is expressible by the introduction of component correlations into (10). In any case the correct equation (8) should be used in the calculation of the distribution functions: the way in which this is to be done will be considered in a further paper.

A definite gap in the argument is our present inability to evaluate the expression for the friction tensor, or to evaluate the magnetic increment $\boldsymbol{h}$ occurring in (6). The problems raised in each case are essentially analogous. The electric increment $\boldsymbol{\epsilon}$ can be evaluated by the method of Holtzmark: unfortunately it is $\boldsymbol{h}$ that is of importance in hydromagnetics. It would seem, however, that approximate expressions can be derived for β and $\boldsymbol{h}$ which will be sufficient at least at first: the whole problem will be treated elsewhere.

Once the friction constant has been evaluated the coefficient of self-diffusion follows from the known relation $D_s = kT/2\beta$. Further, the fluxes of momentum and of energy may be explicitly evaluated leading respectively to the coefficients of viscosity and thermal conduction. It can be expected that

the temperature dependence of these two coefficients will be different: while the thermal conduction of the ionized medium can be expected to be weakly dependent on temperature, the viscosity can be expected to be strongly dependent. In this respect an ionized gas will differ markedly from an un-ionized gas. These questions will be considered in a later paper.

* * *

This work was performed during the tenure of an I. C. I. fellowship.

RIASSUNTO (*)

Si muovono i primi passi nella costruzione di una teoria cinetica di fluidi ionizzati in condizioni non uniformi. Le equazioni di Boltzmann-Maxwell e Fokker-Planck si riferiscono a dati molecolari ed in tal modo si precisano le approssimazioni insite nel loro impiego.

(*) *Traduzione a cura della Redazione.*

IL NUOVO CIMENTO Vol. IV, N. 4 1° Ottobre 1956

Phenomenological Equations for Superconductors.

M. R. Schafroth and J. M. Blatt

The F.B.S. Falkiner Nuclear Research and Adolph Basser Computing Laboratories School of Physics (*), The University of Sydney - Sydney, N. S. W., Australia

(ricevuto il 9 Luglio 1956)

Summary. — The requirement of a finite correlation length excludes the conventional London equations for superconductors. Alternative equations are proposed and discussed. Some of the consequences are: 1) a magnetic field is not completely expelled from a superconductor; the field at a large depth x is proportional to x^{-1}, rather than dropping off exponentially. 2) The Pippard effect follows as a natural consequence from the equations proposed here. 3) London's correlation between the Meissner field expulsion and persistent currents in superconducting rings depends on an infinite correlation length, and must hence be abandoned; the « persistent » ring currents must be interpreted as relaxation phenomena. The explanation of the enormously long lifetime is not possible within the framework of a purely phenomenological approach, but remains one of the tasks of a future microscopic theory of superconductivity.

1. – Introduction.

It is well known [1,2] that superconductivity is not merely a limiting case of ordinary electrical conductivity, in which the conductivity coefficient becomes infinitely large, but rather must be described by an entirely different set of macroscopic equations. A particular set of equations was proposed by London [1] and it has been shown that most of the observed electromagnetic properties of superconductors can be understood by means of the London

(*) Also supported by the Nuclear Research Foundation within the University of Sydney.

(1) F. London and H. London: *Physica*, **2**, 341 (1935).

(2) F. London: *Superfluids*, vol. I (New York, 1950).

equations. Changes in the London equations have been proposed in connection with recent experimental results [3], however, and it should perhaps be emphasized that the early experiments supporting the London equations were necessarily fairly crude, and the more recent detailed experiments have disagreed with the London equations quite often .

We have shown recently that the first London equation (λ = penetration depth)

$$-(4\pi\lambda^2/c)\,\mathrm{curl}\,\boldsymbol{j}_s = \boldsymbol{B}\,, \tag{1.1}$$

is unacceptable on purely theoretical grounds, because it violates the requirement of a finite « correlation length » [4,5]. That is, one of the consequences of equation (1.1) is that the charged particles responsible for the supercurrent have statistical correlated momentum vectors in thermal equilibrium, even in the absence of electromagnetic fields, no matter how far they are from each other in the solid. The fact is noted independently by CASIMIR [6] who points out very forcefully that London's picture of a superconductor implies the existence of « stable wave functions extending over a mile or so of dirty lead wire ». On the other hand, if we insist that coherence extends only over distances of the order of 10^{-4} cm. say, Casimir points out that « the existence of persisting currents (in rings) would remain unexplained ». Casimir makes no decision as to which horn of this dilemma should be taken.

We feel strongly that « stable wave functions extending over a mile or so of dirty lead wire » are out of the question at any non-zero temperature, and any equation which demands such a thing is a wrong equation and must be modified. The purpose of this paper is to develop a new set of *phenomenological* equations to replace the London equations, the new equations being consistent with a finite correlation length. We find, in full agreement with CASIMIR, that the new equations fail to give the correlation between persistent ring currents and the MEISSNER field expulsion which is a prominent feature of the original London theory. But this negative aspect is compensated somewhat by a positive feature of the theory: the new equations give a direct and natural explanation of the Pippard effect [3], which then allows us to estimate the size of the « correlation length » in superconductors. The correlation length is, in our opinion, the quantity needed to make Pippard's « coherence concept in superconductivity » [7] more precise and amenable to direct theoretical attack. On the other hand, Pippard's suggested modification of the London

---

(3) A. B. PIPPARD: *Proc. Roy. Soc.*, A **216**, 547 (1953).
(4) J. M. BLATT, S. T. BUTLER and M. R. SCHAFROTH: *Phys. Rev.*, **100**, 481 (1955).
(5) M. R. SCHAFROTH: *Phys. Rev.*, **100**, 502 (1955).
(6) H. B. G. CASIMIR: *Niels Bohr and the Development of Physics* (London, 1955).
(7) A. B. PIPPARD: *Physica*, **19**, 765 (1953).

equation (3) has the fault that it still implies an infinite correlation length. While it is quite possible that completely separate modifications of the London equations are required to account for the Pippard effect and for the finiteness of the correlation length, we believe that it is highly suggestive that a reasonable modification of the London equations for the finite correlation length already automatically gives a reasonable fit to the observations of PIPPARD.

The limitations of any purely phenomenological approach are of course considerable. Assumptions must be introduced at various stages in order to limit the (otherwise hopelessly large) range of possibilities. If the true theory of superconductivity is very complicated, it is very unlikely that phenomenological guesses will turn out to be correct in the end. Nevertheless, phenomenology is useful, for several reasons. First, a number of data can be correlated within a fairly simple framework; second, and more important, light is thrown on the requirements which a future microscopic theory of superconductivity will have to fulfil. In particular it is no longer necessary to construct a microscopic theory which leads to an *infinite* (as large as the solid body) correlation length, and from this point of view the construction of a microscopic theory of superconductivity has been made much easier. On the other hand, a microscopic theory which explains the Meissner field expulsion will *not* automatically explain the persistent ring currents, and separate theoretical investigation of the non-equilibrium properties of the superconducting state will be required. London's concept of « macroscopic metastability » (2) is dependent on an infinite correlation length, and can therefore not be used for actual physical superconductors.

Although the phenomenological equations developed in this paper may have an influence in the development of a future microscopic theory of superconductivity, we emphasize that our present considerations are independent of any detailed picture of the superconducting state. For most of the work in this paper, we do not need to know the nature of the charge carriers responsible for superconductivity, or the nature of the interaction responsible for the transition to the superconducting state. Only in the discussion of the Pippard effect do we make some simple assumptions about the microscopic phenomena underlying the macroscopic, phenomenological equations.

2. – Generalization of the First London Equation.

The first London equation, (1.1), involves no time derivatives and therefore applies to the state of thermodynamic equilibrium. In Sections **2**, **3** and **4** we shall be concerned with the study of the Meissner effect, i.e., the expulsion of a static magnetic field from the superconductor. We shalll therefore find it convenient to introduce, instead of the supercurrent density vector $\boldsymbol{j}_s$,

the magnetization vector $\boldsymbol{M}$ which yields the same current distribution: the relation between them is:

$$\boldsymbol{j}_s = c \operatorname{curl} \boldsymbol{M} . \tag{2.1}$$

We shall make the assumption that mathematical surface currents do not exist (*); if $\boldsymbol{M}$ has a non-zero tangential component just inside the surface of the superconductor, equation (2.1) implies that there is a true surface current. Hence we impose the boundary condition ($\boldsymbol{n}$ is a unit vector normal to the surface of the superconductor)

$$\boldsymbol{n} \times \boldsymbol{M} = 0 \text{ at the surface}, \tag{2.2}$$

The current distributions $\boldsymbol{j}_s$ which can be generated from equation (2.1) do not exhaust all possible current distributions, but they are adequate for a discussion of the Meissner effect. We shall return to this point in Sect. 7.

Usually there is, in addition to the supercurrent density $\boldsymbol{j}_s$, also a « normal current » density $\boldsymbol{j}_n$ given by Ohm's law

$$\boldsymbol{j}_n = \sigma \boldsymbol{E} , \tag{2.3}$$

where $\boldsymbol{E}$ is the local electric field. However, in thermodynamic equilibrium there is no electric field and hence no normal current inside the specimen: the supercurrent $\boldsymbol{j}_s$ is then the only current.

Substitution of (2.1) into the London equation (1.1) gives

$$\operatorname{curl} \operatorname{curl} \boldsymbol{M} = - (4\pi\lambda^2)^{-1} \boldsymbol{B} . \tag{2.4}$$

For comparison, we also write the relation between $\boldsymbol{M}$ and $\boldsymbol{B}$ for an ordinary diamagnet, of magnetic susceptibility χ:

$$\boldsymbol{M} = \frac{\chi}{1 + 4\pi\chi} \boldsymbol{B} . \tag{2.5}$$

We now look for a formalism which includes both (2.4) and (2.5) as special cases, and which can be applied to volumes of general shape. To do this, we first introduce, for each definite volume V, a complete orthonormal set of

(*) The same assumption is made quite generally also for normal conductors; it should not be confused with the question of surface charge densities, which in general do form on a conductor. The question of true surface currents in an ordinary diamagnet will be discussed later on.

vector functions $\boldsymbol{u}_k(\boldsymbol{r})$. These functions are defined as follows:

$$\text{curl curl } \boldsymbol{u}_k = q_k^2 \boldsymbol{u}_k \tag{2.6a}$$

$$\text{div } \boldsymbol{u}_k = 0 \tag{2.6b}$$

$$\boldsymbol{n} \times \boldsymbol{u}_k = 0 \text{ on the surface} \tag{2.6c}$$

$$\int \boldsymbol{u}_k \cdot \boldsymbol{u}_{k'} \, \mathrm{d}V = \delta_{k,k'} . \tag{2.6d}$$

These functions are familiar in electromagnetic theory: if we imagine the surface of the superconductor replaced by a perfect mirror, and the inside by vacuum, then the different values of k correspond to the different normal modes of the electromagnetic field in this cavity. The eigenvalue q_k^2 is proportional to the square of the frequency of normal mode number k, and the function $\boldsymbol{u}_k(\boldsymbol{r})$ defines the electric field pattern in this mode. For non-zero q_k equation (2.6*b*) is a consequence of (2.6*a*); (2.6*b*) was inserted explicitly in order to exclude the possibility $q_k = 0$. We see this as follows: multiply (2.6*a*) by $\boldsymbol{u}_k$ and integrate over the volume. Using vector identities, we get

$$\int \boldsymbol{u}_k \cdot \text{curl curl } \boldsymbol{u}_k \, \mathrm{d}V = \int (\text{curl } \boldsymbol{u}_k)^2 \, \mathrm{d}V - \int (\boldsymbol{u}_k \times \text{curl } \boldsymbol{u}_k) \cdot \boldsymbol{n} \, \mathrm{d}S . \tag{2.7}$$

The surface integral vanishes because of (2.6*c*). Hence the integral on the left, and with it q_k, is zero if and only if curl $\boldsymbol{u}_k$ vanishes everywhere in the volume. But it is well-known that there is no non-zero vector field which satisfies the boundary condition (2.6*c*) and has curl $\boldsymbol{u}_k = \text{div } \boldsymbol{u}_k = 0$.

The set $\boldsymbol{u}_k$ is complete for vector fields with div $(\boldsymbol{u}) = 0$; that is, any square integrable divergence-free vector function $\boldsymbol{u}(\boldsymbol{r})$ can be expanded as a linear superposition of the $\boldsymbol{u}_k$, and this expansion converges in the sense of least squares. In the case of a brick-shaped volume this reduces to an assertion about the completeness of ordinary Fourier expansions.

We now expand both $\boldsymbol{M}$ and $\boldsymbol{B}$ in terms of the $\boldsymbol{u}_k$:

$$\boldsymbol{M}(\boldsymbol{r}) = \sum_k M_k \boldsymbol{u}_k(\boldsymbol{r}) \tag{2.8}$$

$$\boldsymbol{B}(\boldsymbol{r}) = \sum_k B_k \boldsymbol{u}_k(\boldsymbol{r}) . \tag{2.9}$$

Since we assume linearity of the relation between $\boldsymbol{M}$ and $\boldsymbol{B}$, the most general relation is of the form

$$M_k = \sum_{k'} \varkappa_{kk'} B_{k'} . \tag{2.10}$$

We now observe that the London equation (2.4) and the diamagnetic relation (2.5) have this in common: $\alpha_{kk'}$ is a *diagonal* matrix. The various cavity modes are not mixed up. In attempting to generalize the London equation, we shall assume that this property is preserved. We write therefore

$$M_k = -(4\pi\lambda^2)^{-1}K(q_k)B_k\,, \tag{2.11}$$

where the «kernel» $K(q)$ is an, as yet undetermined, function of the real variable q. The London equation (2.4) is obtained through the choice

$$K(q) = 1/q^2 \quad \text{(London equation)}, \tag{2.12}$$

whereas the diamagnetic equation (2.5) is obtained from

$$K(q) = \frac{4\pi\lambda^2\chi}{1 - 4\pi\chi} \qquad \text{(diamagnetic)}, \tag{2.13}$$

that is, $K(q)$ is independent of q. Of course, the quantity λ is superfluous in (2.13) and could have been absorbed into the definition of $K(q)$, equation (2.11). However, since we shall be dealing mostly with superconductors, this choide would not be convenient.

The reduction from (2.10) to (2.11) is the basic assumption of this phenomenological approach, and a few words of discussion may be in order. From general principles one can see that α_{kk} must be a symmetric, real matrix; hence there exists a set of base functions $\boldsymbol{w}_k(\boldsymbol{r})$ which diagonalize this matrix. Our assumption can therefore be rephrased by saying that the particular orthonormal set $\boldsymbol{u}_k(\boldsymbol{r})$ defined by (2.6) is this set. The main reason for choosing the set $\boldsymbol{u}_k$ is the fact that it does diagonalize the matrix α for the London equation (since α for an ordinary diamagnet is a multiple of the unit matrix, it is diagonal in all base sets). We want to find a simple phenomenological generalization of the London equation; without a microscopic theory of superconductivity, we must make a guess of some sort, and the assumption (2.11) represents this guess. We still have considerable freedom through various choices of the kernel $K(q)$, but we shall see that there are conditions on $K(q)$ which restrict its choice and hence make the phenomenological approach reasonably definite. On the other hand, the general matrix α_{kk} would allow so many choices that it would be well-nigh hopeless to determine it in a purely phenomenological way.

It should be realized that our basic equation (2.11) cannot apply to non-isotropic media. Thus the phenomenological equations derived here must still be generalized to non-isotropic media. This generalization will not be attempted here.

A word of caution is in order about the nature of the expansions (2.8) and (2.9). The base functions $\boldsymbol{u}_k$ are normal to the surface of the superconductor, whereas the magnetic induction vector $\boldsymbol{B}$ is in general not normal to the surface. Thus the expansion (2.9), although it converges in the sense of least squares, does not converge uniformly and can not be differentiated term by term. On the other hand, if the kernel $K(q)$ decreases sufficiently rapidly for large values of q, the expansion for the magnetization $\boldsymbol{M}(\boldsymbol{r})$ does converge uniformly, and defines an $\boldsymbol{M}(\boldsymbol{r})$ which is normal to the surface everywhere. The London kernel (2.12) satisfies this condition, but the diamagnetic kernel (2.13) does not. Indeed, in the usual description of diamagnetism, true surface currents appear at the surface of the material when it is put into a magnetic field. Actually, of course, the transition at the surface of the diamagnetic material is not infinitely sharp, but takes place over distances of a few atomic layers. Hence the kernel (2.13) is an idealization, and should be replaced by one which approaches zero for values of q larger than about 10^8 cm^{-1}. A possible choice would be

$$K(q) = -\frac{4\pi\lambda^2\chi}{1+4\pi\chi}\,\frac{\mu^2}{q^2+\mu^2} \qquad \text{(modified diamagnet)}\,, \tag{2.14}$$

where μ is of the order of 10^8 cm^{-1}. Such a kernel would yield diamagnetic currents concentrated in a surface layer of thickness μ^{-1}, rather than mathematical surface currents. For practical purposes, of course, (2.13) and (2.14) are equivalent to each other.

3. – Condition on $K(q)$ from the Rotating Bucket Theorem.

The following condition has been obtained [5], as the result of the assumption of a finite correlation length: put a superconducting cylinder into a longitudinal magnetic field, and « polarize the neutrons » in such a way that the magnetic induction vector $\boldsymbol{B}$ is constant throughout the cylinder; then the total magnetic moment of the cylinder can increase with the radius R of the cylinder no faster than R^3. The purpose of this section is to translate this theorem into a condition on $K(q)$.

Take a cylindrical volume of radius R and height L. For the purpose of this discussion we do not need to determine the entire set of functions $\boldsymbol{u}_k(\boldsymbol{r})$ defined by (2.6); it is sufficient to restrict ourselves to $\boldsymbol{u}_k$ which are parallel to the z-direction everywhere, and independent of z and the angle θ. The z-component of $\boldsymbol{u}_k$ will be denoted by $u_k(r)$ and is given by

$$u_k(r) = N_k J_0(z_k r/R) \tag{3.1}$$

where z_k is the k'th positive zero of the Bessel function $J_0(z)$, and the normalization constant N_k is equal to

$$N_k = \frac{1}{V^{\frac{1}{2}} J_1(z_k)} \qquad (V = \pi R^2 L). \tag{3.2}$$

Next we expand the constant vector $\boldsymbol{B}$ as a superposition of the $\boldsymbol{u}_k$. Let B denote the magnitude of $\boldsymbol{B}$, then B_k in (2.9) is given by

$$B_k = BLN_k \int_0^R J_0(z_k r/R)\, 2\pi r \,\mathrm{d}r = \frac{2BV^{\frac{1}{2}}}{z_k} . \tag{3.3}$$

The total magnetic moment of the cylinder is the volume integral of the magnetization vector $\boldsymbol{M}$ which is given by (2.8) and (2.11). The calculation gives

$$\mathcal{M} = \int M_z \,\mathrm{d}V = -\frac{VB}{\pi\lambda^2} \sum_{k=1}^{\infty} \frac{K(z_k/R)}{z_k^2} . \tag{3.4}$$

Since the volume V is proportional to R^2, the rotating bucket condition asserts that, in the limit of very large R, the infinite sum in (3.4) must not increase with R faster than linearly.

We first take the two special cases of a diamagnet and a London superconductor. The first is defined by (2.13) and gives the expected result (*)

$$\mathcal{M} = VB \frac{\chi}{1 + 4\pi\chi} 4 \sum_{k=1}^{\infty} \frac{1}{z_k^2} = VB \frac{\chi}{1 + 4\pi\chi} . \tag{3.5}$$

The London superconductor is defined by (2.12) and gives (*)

$$\mathcal{M} = -\frac{R^2 VB}{\pi\lambda^2} \sum_{k=1}^{\infty} (z_k)^{-4} = -\frac{R^2 VB}{32\pi\lambda^2} . \tag{3.6}$$

This result is proportional to R^1 and therefore violates the rotating bucket theorem; the same conclusion was arrived at more directly in reference [1].

Let us now consider (3.4) for a general kernel $K(q)$. Since the sum over k converges even for constant $K(q)$, it is clear that the limiting behaviour for large values of R is related to the analytic behaviour of $K(q)$ in the neighbourhood of $q = 0$. Let us suppose, therefore, that $K(q)$ near $q = 0$ is pro-

(*) See Appendix I for the evaluation of the sum, and other mathematics in connection with this Fourier-Bessel expansion.

portional to q^{ν}. The diamagnet has $\nu = 0$, the London superconductor has $\nu = 2$. For arbitrary ν, the sum in (3.4) becomes proportional to R^{ν}, and the total magnetic moment proportional to $R^{2+\nu}$. According to the rotating bucket theorem, the exponent cannot exceed 3. We therefore obtain the following *condition on the kernel* $K(q)$:

$$\lim_{q \to 0} [qK(q)] < \infty . \tag{3.7}$$

This condition excludes the London kernel, but does *not* exclude a kernel with a singularity at $q = 0$; indeed, $K(q)$ may have a q^{-1} singularity at $q = 0$. It is often supposed that superconductivity is merely a particularly strong type of diamagnetism; in terms of our formalism this would mean that the kernel $K(q)$ stays finite (but large) at $q = 0$. A simple example would be the kernel (2.14) with $4\pi\chi$ very close to -1, and μ^{-1} appreciably larger than the observed penetration depths in superconductors.

4. – The Law of Field Penetration.

We now turn to the Meissner effect, i.e., the expulsion of the magnetic field from the superconducting material. We shall use two kernels $K(q)$, both of which are consistent with the condition (3.7). The first kernel is the « modified diamagnet », equation (2.14), but with simplified notation:

$$K_1(q) = (q^2 + \mu^2)^{-1} . \tag{4.1}$$

The quantity μ is to be interpreted as the inverse of the « correlation length ». Another length enters the field penetration law through the factor $(4\pi\lambda^2)^{-1}$ in the fundamental law (2.11); this second length, λ, will turn out to govern the law of field penetration very near the surface, whereas μ^{-1} becomes important only some distance into the material.

The London superconductor is included in (4.1) as a special case, namely $\mu = 0$; of course, this case violates condition (3.7).

The other standard kernel is meant to be representative of the class of kernels $K(q)$ which have the strongest singularity at $q = 0$ consistent with condition (3.7), i.e., which go like q^{-1} for very small q. For ease of calculation we shall choose

$$K_2(q) = [q(q + \mu)]^{-1} . \tag{4.2}$$

It is understood, of course, that K_1 and K_2 are each only one possibility out of a very large class of functions; however, the main features of the law

of field penetration are not strongly dependent on the detailed shape of the function $K(q)$, but do depend significantly on whether $K(q)$ behaves like q^{-1} or like a constant as q approaches zero.

For the purpose of the Meissner effect, we can simplify the problem by considering a plane slab of superconductor of thickness L, and then let L go to infinity. This is permissible provided only that the radius of curvature of the surface of the actual superconductor is much larger than both the London depth λ and the correlation length $\Lambda = \mu^{-1}$. Let the left surface of the slab coincide with the y-z plane, and consider an external field $\boldsymbol{B}$ in the y-direction applied outside the slab at $x = 0$ and $x = L$. The set of functions $\boldsymbol{u}_k(\boldsymbol{r})$ reduces for our purpose to vector functions with x- and z-components equal to 0, and

$$[\boldsymbol{u}_k(\boldsymbol{r})]_y = (2/L)^{\frac{1}{2}} \sin(k\pi x/L) \qquad k = 1, 2, 3, \ldots \tag{4.3}$$

In order to find the law of field penetration, we notice that the time-independent Maxwell equation for a superconductor with unit permeability

$$c \operatorname{curl} \boldsymbol{B} = 4\pi \boldsymbol{j}_s = 4\pi c \operatorname{curl} \boldsymbol{M}, \tag{4.4}$$

implies that the formal vector field $\boldsymbol{H}(\boldsymbol{r})$ defined by

$$\boldsymbol{H} = \boldsymbol{B} - 4\pi \boldsymbol{M}, \tag{4.5}$$

has zero curl inside the superconductor. The divergence of $\boldsymbol{B}$ is zero, and our expansion of $\boldsymbol{M}$ in terms of the vector eigenfunctions (2.6) ensures that $\boldsymbol{M}$ also has zero divergence. Hence $\boldsymbol{H}(\boldsymbol{r})$ is a constant vector field in our slab, equal to the boundary value B_0, since $\boldsymbol{M}$ is constructed so that it vanishes at the boundary. We expand this constant field in our vector eigenfunctions $\boldsymbol{u}_k$ and find

$$\boldsymbol{H} = \sum_{k=1}^{\infty} H_k \boldsymbol{u}_k(\boldsymbol{r}), \tag{4.6a}$$

$$\begin{cases} H_k = B_0(8L)^{\frac{1}{2}}/k\pi & k \text{ odd}, \\ H_k = 0 & k \text{ even}. \end{cases} \tag{4.6b}$$

Combination of (4.5), (4.6a), (2.8), (2.9), and (2.11) gives the following expansion coefficients for the field $\boldsymbol{B}(\boldsymbol{r})$:

$$B_k = \frac{H_k}{1 + \lambda^{-2} K(q_k)}. \tag{4.7}$$

We substitute this together with (4.6*b*) into the expansion (2.9) and let L go to infinity; the resulting law of field penetration for a general kernel $K(q)$ becomes

$$B(x) = B_0(2/\pi)\int_0^\infty \frac{\sin(qx)}{q[1 - \lambda^{-2}K(q)]}\,dq\,. \tag{4.8}$$

This integral is easily evaluated for $K_1(q)$ and gives

$$B_1(x) = B_0\,\frac{\exp[-\sigma x] + (\mu\lambda)^2}{1 + (\mu\lambda)^2}\,, \qquad \sigma = \lambda^{-1}[1 + (\mu\lambda)^2]^{\frac{1}{2}}\,. \tag{4.9}$$

This curve is shown in Fig. 1 for the special case $\mu\lambda = 0.1$, i.e., a correlation length 10 times the London depth λ. For small depths x we get the

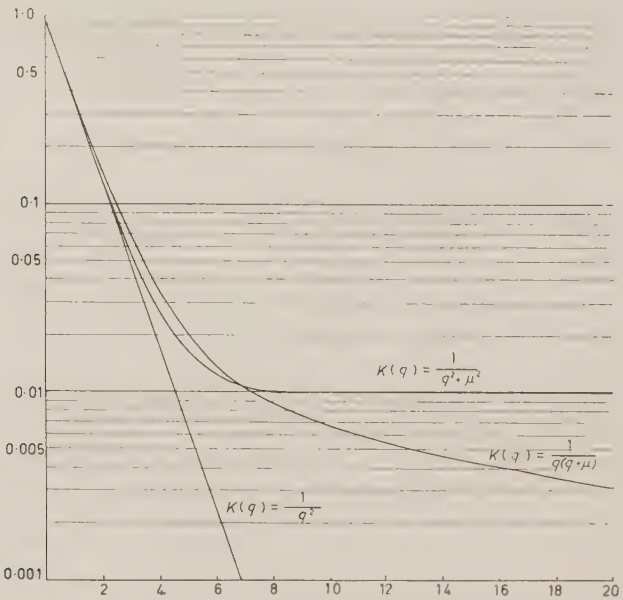

Fig. 1. – The law of field penetration. Ordinate: Magnetic field, in units of the field applied to the surface of the slab; abscissa: distance into the slab, in units of the London penetration depth λ. The three cases illustrated are: (*a*) The London kernel $K(q) = q^{-2}$, leading to an exponential penetration. (*b*) The « diamagnetic » kernel $K(q) = (q^2 + \mu^2)^{-1}$, leading to a constant field in the interior of the specimen. (*c*) The « singular » kernel $K(q) = [q(q + \mu)]^{-1}$, leading to a penetration inversely proportional to the distance into the specimen, for large distances. The quantity μ was chosen to equal $1/10\lambda$ in cases (*b*) and (*c*), i.e., the correlation length $\Lambda = 10\lambda$.

usual exponential penetration law; however, at large depths the field approaches a finite value, rather than zero.

The corresponding integral for the kernel $K_2(q)$ can not be done in closed form in terms of tabulated functions (it involves exponential integrals of complex arguments); however, if $\mu\lambda \ll 1$ (i.e., if the correlation length is much larger than the London depth), it is possible to find a good approximation (see Appendix II for the mathematics):

$$\frac{B(x)}{B_0} = \left[\cos\left(\frac{1}{2}\mu x\right) - \frac{1}{2}\mu\lambda \sin\left(\frac{1}{2}\mu x\right)\right] \exp\left[-x/\lambda\right] + (\mu\lambda/2\pi)\, F(x/\lambda)\,, \tag{4.10a}$$

$$F(z) = (1+z)e^{-z}\bar{E}i(z) - (1-z)e^{z}\dot{E}i(-z)\,, \tag{4.10b}$$

where the exponential integral functions are defined in JAHNKE and EMDE [8]. The penetration law (4.10) is shown graphically in Fig. 1, again for $\mu\lambda = 0.1$. The deviation from a simple exponential decay starts somewhat sooner than with the kernel $K_1(q)$; however, the most important difference is the behaviour for large x. The asymptotic expansions for the exponential integrals in (4.10*b*) give

$$\frac{B(x)}{B_0} = \frac{2\mu\lambda^2}{\pi x} \qquad \text{for large } x\,. \tag{4.11}$$

That is, unlike the regular kernel (4.1), the kernel (4.2) does lead to a real expulsion of the magnetic field: as we go farther and farther into the material, the field becomes smaller and smaller and approaches zero like x^{-1}. This is characteristic of all kernels with a q^{-1} singularity at $q = 0$.

While a superconductor with a kernel of type $K_2(q)$ does expel a magnetic field completely, the penetration of the field into the superconductor is much deeper than in the London case. PIPPARD [3] defines a quantity which we shall call the «formal penetration depth» by

$$\lambda_P = \frac{\int_0^\infty B(x)\,\mathrm{d}x}{B_0}\,. \tag{4.12}$$

It is clear from (4.9) and (4.10) that this quantity diverges for the two kernels we have used. The same can be shown quite generally from (4.8) for any kernel $K(q)$ which satisfies the rotating bucket condition (3.7). Thus Pippard's definition of the penetration depth is inapplicable to physical superconductors.

---

[8] E. JAHNKE and F. EMDE: *Tables of Functions* (New York, 1943).

Experimentally, the static penetration depth is determined by a combination of two measurements, the first of which measures the ratio of the penetration depths at two different temperatures, the second the difference between the same two quantities. The first measurement determines the magnetic susceptibility of very fine-grained colloidal suspensions of the superconducting material ([9]). The individual « grains » are supposed to be spheres of radius R much smaller than the London depth λ. It is immediately obvious that the behaviour of the kernel $K(q)$ near $q = 0$ does not enter in such a measurement; our two standard kernels, (4.1) and (4.2), have been chosen so that they agree with the London kernel $K(q) = q^{-2}$ for values of q in the neighbourhood of λ^{-1}. Hence there is no need to modify the conventional analysis of this experiment ([2]), unless the London form of the penetration law is changed radically even for values of x near λ (values of q near λ^{-1}). The rotating bucket condition (3.7), which forms the main basis of this paper, is quite irrelevant.

The second measurement involved in finding the static penetration depth consists in measuring the total magnetization of a superconducting cylinder, of radius $R \gg \lambda$. This is done in two ways: 1) a thin cylindrical rod is suddenly removed from a magnetic field, and the change in flux is detected ([10]); 2) two coils are wound on a cylindrical core of superconducting material, and the mutual inductance of the two coils is measured ([11]). In both cases only differences between the magnetization at two different temperatures can be determined accurately.

We now derive a formula for the total magnetization of a cylinder when a magnetic field B_0 is applied to it, parallel to the cylinder axis. This formula differs from (3.4) because we no longer « polarize the neutrons » so as to cancel the Meissner field expulsion. Our base functions $\boldsymbol{u}_k$ are again given by (3.1) and (3.2), and the expansion coefficients of a *constant* field are given by (3.3); however, this constant field, according to (4.5), must be interpreted as $\boldsymbol{H}$, not $\boldsymbol{B}$. We thus have

$$H_k = B_k - 4\pi M_k = -\frac{2B_0 V^{\frac{1}{2}}}{z_k} . \tag{4.13}$$

We combine this with the fundamental relation (2.11) and solve for the Fourier coefficient of the magnetization density, M_k, to obtain

$$M_k = -\frac{K(q_k)H_k}{4\pi[\lambda^2 + K(q_k)]} , \tag{4.14}$$

([9]) D. SHOENBERG: *Proc. Roy. Soc. London*, A **175**, 49 (1940).

([10]) M. DESIRANT and D. SHOENBERG: *Proc. Phys. Soc. London*, **60**, 413 (1948).

([11]) E. LAURMAN and D. SHOENBERG: *Proc. Roy. Soc. London*, A **198**, 560 (1949); H. B. G. CASIMIR: *Physica*, **7**, 887 (1940).

where

$$q_k = z_k/R \,. \tag{4.15}$$

Integration of the magnetization density over the volume of the cylinder then gives the following result for the total magnetic moment

$$\mathcal{M} = -\frac{B_0 V}{\pi} \sum_{k=1}^{\infty} \frac{K(q_k)}{z_k^2[\lambda^2 + K(q_k)]}$$

or, for the magnetic moment per unit length of the cylinder

$$\frac{L}{\mathcal{M}} = -B_0 R^2 \sum_{k=1}^{\infty} \frac{K(z_k R)}{z_k^2[\lambda^2 - K(z_k/R)]} \,. \tag{4.16}$$

The evaluation of these sums is discussed in Appendix I; here we quote the results. If the magnetic field were expelled completely from the cylinder, the magnetization per unit length of the cylinder would be given by

$$\frac{\mathcal{M}_0}{L} = -B_0 R^2/4 \,, \tag{4.17}$$

where B_0 is the field at the surface of the cylinder. Let $\mathcal{M}$ be the actual magnetization, and define the « effective penetration depth » D by

$$\frac{\mathcal{M}}{L} = -B_0 (R - D)^2/4 \,. \tag{4.18}$$

We assume that the radius R of the cylinder is much larger than D. The London kernel then gives the well-known result ([2])

$$D \cong \lambda \quad \text{(London)}, \tag{4.19}$$

whereas the kernel $K_1(q)$ (modified diamagnet) gives

$$D \cong \lambda(1 + \tfrac{1}{2}\mu^2 R\lambda) \tag{4.20}$$

and the singular kernel $K_2(q)$ leads to

$$D \cong \lambda[1 + (2\mu\lambda/\pi) \ln (R/\lambda) - 0.369\,\mu\lambda - \tfrac{1}{2}\lambda/R] \,. \tag{4.21}$$

Of the two ways of determining the total magnetization of a cylinder, the mutual inductance method ([11]) has been employed with cylinders of large

radius (of the order of 1 cm), whereas the other method ([10]) was used with much thinner cylinders. It is obvious that the correction to the London value is much bigger with $K_1(q)$ than with $K_2(q)$, the more so the larger the radius R of the specimen. (This is of course a direct consequence of the difference between the penetration laws (4.9) and (4.11) well inside the specimen). Since we want to study the effect of the correction to the London values, we shall use the results from the mutual inductance method for our comparison.

Before we can compare against experiment, we need to known the correlation length $\Lambda = \mu^{-1}$, at least by order of magnitude. We shall show in the next two sections that the Pippard effect can be used to estimate Λ for specimens of controlled amounts of impurity; the values of Λ so found are of the same order of magnitude as the mean free path of electrons in the normal (non-superconducting) state at the same temperature, i.e., between 10^{-5} and 10^{-4} cm. Since the correlation length increases as the material is purified, and care was taken in SHOENBERG's experiment ([11]) to work with high-purity specimens, we shall use the estimate $\Lambda < 10^{-3}$ cm. To the extent that this estimate might be too low, the following conclusions are still somewhat doubtful. However, a correlation length of the order of 10^{-2} cm would be needed to upset the conclusions below; this is very much larger than the qualitative estimates of the « coherence length » in superconductors made by PIPPARD and others. Since the point is of considerable importance for the theory of superconductivity, we suggest that the CASIMIR-SHOENBERG experiment ([11]) be redone with specimens of controlled amounts of impurity, such that the mean free path is of the order of 10^{-4} cm or somewhat less. This should settle the matter beyond all doubt.

Now to the conclusion, assuming that the correlation length is no longer than 10^{-3} cm. With λ of the order of 10^{-5} cm and R of the order of 1 cm, (4.20) leads to a huge correction (factor of 6) whereas (4.21) gives a 7 percent effect. Since the experimental value of D agrees reasonably well with the microwave determination by PIPPARD ([3]), we conclude that *the « regular » kernel $K_1(q)$ is excluded by the data* (subject to the qualifications in the preceding paragraph).

Although our calculations have been done with only two kernels, it can be seen qualitatively that the nature of the singularity (if any) of $K(q)$ at $q = 0$ is the determining factor in the difference between (4.20) and (4.21). We conclude that *superconductivity is characterized by a kernel $K(q)$ with a q^{-1} singularity at $q = 0$*. Thus a superconductor is *not* merely a particularly effective diamagnet, but is qualitatively different from any diamagnetic substance.

5. – Generalization of the Second London Equation.

Some of the most interesting measurements on superconductors have been carried out at microwave frequencies (3). The time-independent equation (1.1) or its generalization (2.11) are insufficient to discuss such measurements. LONDON postulated a second equation:

$$\frac{4\pi\lambda^2}{c^2}\frac{\partial \boldsymbol{j}_s}{\partial t} = \boldsymbol{E}\,, \tag{5.1}$$

which relates the time rate of change of the supercurrent density $\boldsymbol{j}_s$ to the electric field $\boldsymbol{E}$. In addition, there is a normal current density $\boldsymbol{j}_n$ which is given by Ohm's law

$$\boldsymbol{j}_n = \sigma\boldsymbol{E}\,, \tag{5.2}$$

where σ is the conductivity. The total current density is the sum

$$\boldsymbol{j} = \boldsymbol{j}_s + \boldsymbol{j}_n\,. \tag{5.3}$$

It is well known that the second London equation (5.1) can not be derived from (1.1). However, a partial derivation can be made which is sufficient for the discussion of microwave measurements. We assume that all relaxation times of interest are small compared to the time intervals involved in the experiments (i.e., to the period of the microwave oscillation). We are then allowed to differentiate the equilibrium equation (1.1) with respect to the time. This differentiation will not give us the complete relation (5.1) between the fields $\boldsymbol{j}_s$ and $\boldsymbol{E}$, but only its projection on to the space R of vector fields orthogonal to the potential-flow fields. In the case of singly connected volumes (*) this projection is defined as follows: consider any divergence-free vector field $\boldsymbol{w}$,

$$\operatorname{div}\boldsymbol{w} = 0\,. \tag{5.4}$$

We define the projection $\hat{\boldsymbol{w}}$ of $\boldsymbol{w}$ on to R by the relation

$$\operatorname{curl}\hat{\boldsymbol{w}} = \operatorname{curl}\boldsymbol{w} \tag{5.5}$$

(*) For multiply connected volumes, one has to postulate in addition that $\boldsymbol{w}$ be orthogonal to the finite number of potential flows satisfying (5.6).

and the vanishing of its normal component at the surface Σ of the volume:

$$\hat{\boldsymbol{w}}_{\perp} = 0 . \tag{5.6}$$

To actually construct $\hat{\boldsymbol{w}}$ from a given $\boldsymbol{w}$ one puts

$$\hat{\boldsymbol{w}} = \boldsymbol{w} - \operatorname{grad} \varphi , \tag{5.7}$$

where

$$\nabla^2 \varphi = 0 \tag{5.8}$$

and

$$\left(\frac{\partial \varphi}{\partial n}\right)_{\Sigma} = w_{\perp} \tag{5.9}$$

(5.8) and (5.9) determine φ and, therefore, $\hat{\boldsymbol{w}}$ uniquely. In particular, if $\operatorname{curl} \boldsymbol{w} = \operatorname{curl} \hat{\boldsymbol{w}} = 0$, the solution is $\hat{\boldsymbol{w}} = 0$.

With this definition, we are going to derive from (1.1) by differentiation with respect to time the relation

$$\frac{4\pi\lambda^2}{c^2} \frac{\partial \hat{\boldsymbol{j}}_s}{\partial t} = \hat{\boldsymbol{E}} . \tag{5.1'}$$

The projections of $\boldsymbol{j}_s$ and $\boldsymbol{E}$ on to the potential flow fields remain unlinked. The relation linking them in the London theory,

$$\frac{4\pi\lambda^2}{c^2} \frac{\partial (\boldsymbol{j}_s - \hat{\boldsymbol{j}}_s)}{\partial t} = \boldsymbol{E} - \hat{\boldsymbol{E}} \tag{5.1''}$$

is a new assumption over and above the first London equation and the assumption of small relaxation time (5.1′) is, however, sufficient for the discussion of microwave measurements. The derivation of (5.1′) from (1.1) can easily be generalized to our modified equation (2.11); we then get a basis for the discussion of microwave measurements on our modified theory. The question of meaning and generalization of (5.1″) will be dealt with in Sect. 7.

Let us now take the time-derivative of (1.1). We get

$$-\frac{4\pi\lambda^2}{c} \operatorname{curl} \frac{\partial \boldsymbol{j}_s}{\partial t} = \frac{\partial \boldsymbol{B}}{\partial t} = -c \operatorname{curl} \boldsymbol{E}, \tag{5.10}$$

or

$$\operatorname{curl} \left[\boldsymbol{E} - \frac{4\pi\lambda^2}{c^2} \frac{\partial \boldsymbol{j}_s}{\partial t}\right] = 0 \tag{5.11}$$

and, by definition,

$$\text{curl}\left[\hat{\boldsymbol{E}} - \frac{4\pi\lambda^2}{c^2}\frac{\partial\hat{\boldsymbol{j}}_s}{\partial t}\right] = 0 \tag{5.12}$$

from which (5.1′) follows.

In the case of a singly-connected suerconductor into which no current is fed, we have for the supercurrent

$$(\boldsymbol{j}_{s\perp})_\Sigma = 0 \tag{5.13}$$

and for the Ohm's current:

$$(\boldsymbol{j}_{n\perp})_\Sigma = 0\,. \tag{5.14}$$

We are assuming here separate conservation laws for $\boldsymbol{j}_s$ and $\boldsymbol{j}_n$ at the surface.

Therefore

$$\boldsymbol{j}_s = \boldsymbol{j}_s \tag{5.15}$$

and, since

$$\boldsymbol{E} = \frac{1}{\sigma}\boldsymbol{j}_n\,,$$

also

$$\boldsymbol{E} = \hat{\boldsymbol{E}}\,. \tag{5.16}$$

(5.1′) is, therefore, adequate to describe any such set-up.

In order to generalize the second London equation, we now rephrase the same argument in terms of an expansion in vector eigenfunctions. The set $\boldsymbol{u}_k$, equation (2.6), is a complete set, but is awkward for our present purpose because of the boundary condition (2.6*c*). This boundary condition is appropriate for an expansion of the magnetization density $\boldsymbol{M}$, whose tangential component vanishes at the surface, but inappropriate for an expansion of the supercurrent density $\boldsymbol{j}_s$, whose *normal* component vanishes at the surface (unless there is another metal, e.g., a normal conductor, adjacent to the superconductor, and charge transport occurs from one to the other; we shall exclude this case for the moment). Consider now the set of functions $\boldsymbol{v}_k$ defined by

$$\boldsymbol{v}_k = (q_k)^{-1}\,\text{curl}\,\boldsymbol{u}_k\,. \tag{5.17}$$

These functions correspond to the magnetic field in a cavity in which the

electric field pattern is given by the function $\boldsymbol{u}_k$. Applying the operators curl and curl curl to both sides of (5.17) and using (2.6*a*) we get

$$\boldsymbol{u}_k = (q_k)^{-1} \operatorname{curl} \boldsymbol{v}_k \tag{5.17a}$$

and

$$\operatorname{curl}\operatorname{curl} \boldsymbol{v}_k = q_k^2 \boldsymbol{v}_k \,. \tag{5.18a}$$

Forming the divergence of both sides of (5.17) gives directly

$$\operatorname{div} \boldsymbol{v}_k = 0 \,. \tag{5.18b}$$

Consider now a small closed curve C drawn on the surface of the volume V, and form the closed line integral $\int \boldsymbol{u}_l \cdot \mathrm{d}\boldsymbol{s}$. According to (2.6) this integral vanishes. Using Stokes' theorem, we get from (5.17)

$$\int_C \boldsymbol{u}_k \cdot \mathrm{d}\boldsymbol{s} = (q_k) \int_S \boldsymbol{v}_k \cdot \boldsymbol{n} \, \mathrm{d}S = 0 \,.$$

Since this must be true for all closed curves C on the surface, we conclude that

$$\boldsymbol{n} \cdot \boldsymbol{v}_k = 0 \qquad \text{on the surface.} \tag{5.18c}$$

Finally, combination of (2.7), (2.6*a*) and (2.6*d*), together with the definition (5.27), give the result

$$\int \boldsymbol{v}_k \cdot \boldsymbol{v}_{k'} \, \mathrm{d}V = \delta_{k,k'} \,. \tag{5.18d}$$

Thus the functions v_k form an orthonormal set, all of whose members are eigenfunctions of the operator curl curl, are divergence-free, and have vanishing normal component at the surface. This set is complete in the space R defined above; it is normal to all potential flow fields. The latter statement is verified simply by computing

$$\int \mathrm{d}^3x (\operatorname{grad} \varphi) \cdot \boldsymbol{v}_k = \int \mathrm{d}^3x \operatorname{div} (\varphi \boldsymbol{v}_k) - \int \mathrm{d}^3x \varphi \operatorname{div} \boldsymbol{v}_k = \tag{5.19}$$

$$= \int \mathrm{d}S \, \boldsymbol{n} \cdot \boldsymbol{v}_k \varphi - \int \mathrm{d}^3x \varphi \operatorname{div} \boldsymbol{v}_k = 0,$$

where use has been made of (5.18*b*) and (5.18*c*).

The completeness in R can be proved from the completenes of the set $\boldsymbol{u}_k$ in the following way: we wish to show that any $\hat{\boldsymbol{w}}$ can be expanded in terms of the $\boldsymbol{v}_k$. Expand $\boldsymbol{W} = \operatorname{curl}\hat{\boldsymbol{w}}$ terms of the set $\boldsymbol{u}_k$:

$$\boldsymbol{W} = \operatorname{curl}\hat{\boldsymbol{w}} = \sum_k W_k \boldsymbol{u}_k = \sum_k \frac{W_k}{q_k} \operatorname{curl} \boldsymbol{v}_k \,. \tag{5.20}$$

Integrating term by term, which is permissible, we get an expansion for a certain solution $\boldsymbol{w}$ of the equation $\operatorname{curl}\boldsymbol{w} = \boldsymbol{W}$:

$$\boldsymbol{w} = \sum_k \frac{W_k}{q_k} \boldsymbol{v}_k \,. \tag{5.21}$$

The expansion (5.20) being convergent for any field $\hat{\boldsymbol{w}}$ of interest, (5.21) will even be uniformly convergent due to the additional factor $1/q_k$, and, therefore, $\boldsymbol{w}$ is continuous. For the case of a rectangular box, these statements reduce to well-known theorems about Fourier series.

Therefore

$$(\boldsymbol{w}_1)_2 \qquad 0, \tag{5.22}$$

which implies

$$\boldsymbol{w} = \hat{\boldsymbol{w}} \tag{5.23}$$

and this proves the completeness of the set $\boldsymbol{v}_k$.

In terms of the set $\boldsymbol{v}_k$, the projection $\hat{\boldsymbol{w}}$ of a vector field $\boldsymbol{w}$ can be constructed as follows:

$$\hat{\boldsymbol{w}} = \sum_k w_k \boldsymbol{v}_k, \tag{5.24}$$

with

$$w_k = \int \mathrm{d}^3x \, \boldsymbol{v}_k(x) \cdot \boldsymbol{w}(x) \,. \tag{5.25}$$

Now we can proceed to generalize (5.1′). We have

$$\operatorname{curl}\boldsymbol{E} - \frac{1}{c}\frac{\partial \boldsymbol{B}}{\partial t} = \sum_k' \left(-\frac{1}{c}\frac{\partial B_k}{\partial t} \right) \boldsymbol{u}_k \tag{5.26}$$

and following the reasoning leading from (5.20) to (5.21), (5.23) we get

$$\hat{\boldsymbol{E}} = \sum_k E_k \boldsymbol{v}_k \,, \tag{5.27a}$$

$$E_k = -\frac{1}{cq_k}\frac{\partial B_k}{\partial t} \,. \tag{5.27b}$$

On the other hand, the series (2.8) converges uniformly and can be differentiated term by term. This gives

$$c \operatorname{curl} \boldsymbol{M} = \sum_k c q_k M_k \boldsymbol{v}_k = \sum_k j_{sk} \boldsymbol{v}_k \,. \tag{5.28}$$

We see that this field always belongs to the space R, and that, therefore, (2.1) must strictly read

$$\hat{\boldsymbol{j}}_s = c \operatorname{curl} \boldsymbol{M} \,. \tag{5.29}$$

This is another way of formulating the fact that a magnetization current can never lead to charge transport.

(5.27) and (5.28) together with (2.11), now yield the required generalization of (5.1′):

$$\frac{\partial j_{sk}}{\partial t} = \frac{c^2 q_k^2}{4\pi\lambda^2} K(q_k) E_k \,. \tag{5.30}$$

6. – The Pippard Effect.

In a very interesting series of papers, PIPPARD ([3,12]) has explored the surface impedance of superconductors at microwave frequencies. The surface impedance Z is proportional to the (complex) ratio of the component of $\boldsymbol{E}$ parallel to the surface, to the component of $\boldsymbol{H}$ parallel to the surface. We assign a time factor $\exp[i\omega t]$ to all quantities; furthermore we treat again a slab of thickness L and let L go to infinity at the end; this is permitted because the field penetrates into the specimen only to a small distance, even if the specimen is not superconducting (skin effect); the two sides of the slab are given by $x = 0$ and $x = L$. Then the surface impedance is given by ([13])

$$Z = R + iX = -\frac{4\pi}{c}\left(\frac{E_z}{B_y}\right)_{x=0} \,. \tag{6.1}$$

In a superconductor obeying London's equations, the surface impedance can be found simply (reference ([2]), page 85, equations (3) and (4)) and is

$$R = \frac{4\pi\lambda\omega}{c^2}\left(\frac{\alpha - 1}{2\alpha^2}\right)^{\frac{1}{2}}, \qquad X = \frac{4\pi\lambda\omega}{c^2}\left(\frac{\alpha + 1}{c^2}\right)^{\frac{1}{2}} . \tag{6.2a}$$

$$\alpha = [1 + (\lambda/\delta)^4]^{\frac{1}{2}} , \tag{6.2b}$$

$$\delta = c/(4\pi\sigma\omega)^{\frac{1}{2}} = \text{classical skin depth} . \tag{6.2c}$$

([12]) A. B. PIPPARD: *Proc. Roy. Soc.*, A **191**, 370, 400 (1947); A **203**, 98, 195, 210 (1950).
([13]) E. MAXWELL, P. M. MARCUS and J. C. SLATER: *Phys. Rev.*, **76**, 1332 (1949).

The surface resistance R leads to energy dissipation, whereas the surface reactance X leads to a change in the resonance frequency of a resonant cavity into which a superconducting substance is introduced. If the penetration depth λ is much smaller than the skin depth δ, the parameter α is close to 1 and the reactance X gives a direct measure of λ. It is conventional to define the « inductive skin depth » δ_i of the surface by the equation

$$\delta_i = c^2 X / 4\pi\omega \,. \tag{6.3}$$

We see that for $\lambda \ll \delta$ equations (6.2) and (6.3) lead to

$$\delta_i \cong \lambda \quad \text{(London equation).} \tag{6.4}$$

For this reason it has become customary to refer to a measurement of the inductive skin depth in the superconducting state as a measurement of the superconducting penetration depth λ. Experimentally ([3]) the quantity determined directly is the difference between the inductive skin depth δ_i in the superconducting and in the normal state, at the same temperature (the specimen is made normal by superimposing a constant magnetic field larger than critical). By various indirect methods the inductive skin depth in the *normal* state is determined; this determination is complicated by the existence of the « anomalous skin effect » ([14]). The inductive skin depth δ_i in the superconducting state is then found by subtraction, and is the quantity of interest here.

In his fundamental paper, PIPPARD ([3]) shows that this inductive skin depth is highly impurity dependent, in spite of the fact that the transition temperature of the specimen is almost independent of impurity content. He infers that this implies the existence of another characteristic length ξ in a superconductor, in addition to the penetration depth λ (which he calls λ_∞). PIPPARD suggests a modification of the London equations to include this additional length.

Pippard's equation can not be written in terms of our formalism, because he assumes « diffuse scattering » of his « superconducting electrons » at the surface of the specimen; in terms of our equation (2.10), this implies the existence of non diagonal terms $\alpha_{kk'}$. However, Pippard's equation leads to an essentially exponential expulsion of the magnetic field from the superconducting specimen, and therefore is inconsistent with a finite correlation length. It is of course possible that two separate modifications in the London equations are necessary: one to give a finite correlation length, and a second modific-

---

([14]) A. B. PIPPARD: *Proc. Roy. Soc.*, A **191**, 385 (1947); G. E. H. REUTER and E. H. SONDHEIMER: *Proc. Roy. Soc.*, A **195**, 336 (1948).

ation to yield the impurity dependence of the inductive skin depth of a superconductor at microwave frequencies.

However, we now go on to show that the very same modification in the London equation which is required to yield a finite correlation length automatically implies a dependence of the inductive skin depth on the correlation length, and that this dependence is in the right direction and of the right order of magnitude to explain the Pippard effect if we assume that the correlation length in an impure specimen is of the same order of magnitude as the mean free path.

For the slab of thickness L, the functions $\boldsymbol{v}_k$ are given by (5.7) and (4.3); $\boldsymbol{v}_k$ has only a z component, given by

$$[\boldsymbol{v}_k(\boldsymbol{r})]_z = (2/L)^{\frac{1}{2}} \cos(k\pi x/L) \qquad k = 1, 2, 3, \ldots \tag{6.5}$$

The Maxwell equations are

$$c \operatorname{curl} \boldsymbol{E} = -i\omega \boldsymbol{B} , \tag{6.6}$$

$$c \operatorname{curl} \boldsymbol{B} = 4\pi(\boldsymbol{j}_s + \boldsymbol{j}_n) + i\omega\varepsilon \boldsymbol{E} . \tag{6.7}$$

In equation (6.7) we can neglect the displacement current (last term on the right side) and we integrate from $x = 0$ to $x = x$, to get

$$B(x) = B(0) + (4\pi/c)\int_0^x [j_s(x') + j_n(x')]\,\mathrm{d}x' . \tag{6.8}$$

We multiply both sides by $u_k(x)$, (4.3), and integrate from $x = 0$ to $x = L$. We also interchange the orders of integration over x and x' to get [H_k is defined by (4.6a)]

$$B_k = H_k + (4\pi/c)\left\{(L/k\pi)j_k \quad (-)^k(2L)^{\frac{1}{2}}(k\pi)^{-1}\int_0^L [j_s(x') + j_n(x')]\,\mathrm{d}x'\right\} . \tag{6.9}$$

By equation (6.8) the last integral in (6.9) is equal to $(c/\pi)[B(L) - B(0)]$. We assume that there is no field applied to the other side of the slab, and that the slab is thick enough so that the field applied at $x = 0$ effectively does not penetrate to $x = L$, i.e., L is much larger than the classical skin depth (6.2c). Then $B(L) = 0$, and we get, by combining terms,

$$B_k = \frac{(2/L)^{\frac{1}{2}}B(0) + (4\pi/c)j_k}{q_k} - \frac{(2/L)^{\frac{1}{2}}B(0) + (4\pi/c)(j_{sk} + j_{nk})}{q_k} . \tag{6.10}$$

Next we use (5.2) and (5.17) to get

$$j_{nk} + j_{sk} = \left[\sigma - \frac{ic^2 q_k^2 K(q_k)}{4\pi\omega\lambda^2}\right] E_k \,. \tag{6.11}$$

Finally, we use the Maxwell equation (6.6) in the form

$$E_k = -(i\omega/cq_k)B_k \tag{6.12}$$

and combine (6.10), (6.11) and (6.12) to get

$$B_k = \frac{(2/L)^{\frac{1}{2}} B(0)}{q_k[1 + \lambda^{-2}K(q_k) + i(q_k\delta)^{-2}]} \,. \tag{6.13}$$

The electric field at depth x is given by (5.15a) with E_k defined by (6.12) and (6.13). We are interested in the value of the field at $x = 0$. Substitution of (6.5) and insertion into the definition (6.1) gives

$$Z = (8\pi i\omega/Lc^2) \sum_k [q_k^2 + (q_k/\lambda)^2 K(q_k) + i\delta^{-2}]^{-1} \,.$$

Now we let L approach infinity and replace the sum over k by an integral. The result for the surface impedance of the superconductor is

$$Z = R + iX = \frac{8i\omega}{c^2} \int_0^\infty \frac{\mathrm{d}q}{q^2 + (q/\lambda)^2 K(q) + i\delta^{-2}} \tag{6.14}$$

and the inductive skin depth δ_i of the superconductor is, according to (6.3),

$$\delta_i = (2/\pi) \int_0^\infty \frac{q^2 + (q/\lambda)^2 K(q)}{[q^2 + (q/\lambda)^2 K(q)]^2 + \delta^{-4}} \,\mathrm{d}q \,. \tag{6.15}$$

It is an easy matter to check that the London kernel (2.12), inserted into (6.14) and (6.15), yields the results (6.2). The approximate result (6.4) is obtained by neglecting the quantity δ^{-4} in the denominator of (6.15).

In the derivation of (6.15) we have used the law (5.2) for the « normal » current. As is well-known, this fails when the field varies over distances small compared to an electron mean free path ([14]). However, it is shown in Appendix III that the correction for the anomalous skin effect produces entirely insignificant changes in the formula (6.15), and can hence be ignored.

Although the integral (6.15) can be evaluated exactly for the kernel (5.1), the answer is too complicated to be very informative. We shall make the

assumptions (which are adequately satisfied in practice) that

$$\lambda \ll \Lambda \qquad \text{and} \qquad \lambda \ll \delta \,. \tag{6.16}$$

In that case the kernel (4.1) gives the result

$$\delta_i \cong \lambda + \frac{\lambda\delta}{2^{\frac{1}{2}}\Lambda} \,, \tag{6.17}$$

whereas the kernel (4.2) gives (see Appendix II for the calculation)

$$\delta_i \cong \lambda + \frac{2\lambda^2}{\pi\Lambda}\left[\ln\left(\Lambda\delta^2/\lambda^3\right) - \frac{1}{2} - \frac{3\pi\lambda}{16\Lambda}\right] . \tag{6.18}$$

We see that the inductive skin depth of the superconductor exceeds λ by an amount which goes to zero as the correlation length Λ becomes very large. It is now necessary to make some kind of estimate of the correlation length. Without a microscopic theory of superconductivity this is difficult. However, in *impure* metals we feel it is reasonable to assume that Λ is proportional to, and not very much different from, the mean free path l of electrons in the *normal* state of the specimen. The argument for this is the following: the mean free path for electrons in the normal state is determined by the presence of foreign atoms in the lattice. Such foreign atoms may be expected to affect the « superconducting electrons » also. For example, if superconductivity is due to the formation of electron pair states which act like Bose-Einstein particles ([15]), then such a pair would be broken up in a collision with an impurity atom in the lattice. The break-up of such a pair state presumably destroys momentum correlations associated with the presence of such states, and hence we expect the correlation length Λ to be of the same order of magnitude as the mean free path for normal electrons. We shall therefore assume that Λ is a constant times l, the constant being expected to be within an order of magnitude of 1.

Whereas this assumption is reasonable for impure specimens, it carries little conviction for pure specimens. There the mean free path of the normal electrons is determined by collisions with lattice vibrations rather than with impurity atoms. Without a microscopic theory of superconductivity, there is no convincing reason to believe that the superconducting particles suffer similar collisions. Hence not much weight can be put on the curve which we shall obtain in the region corresponding to the very pure specimens. It is fortunate that the experimental uncertainties are also worst in that same region.

([15]) M. R. SCHAFROTH: *Phys. Rev.*, **96**, 1442 (1954).

With the assumption $\Lambda \sim l$ we have an immediate qualitative explanation of the Pippard effect. PIPPARD observed an increase in the inductive skin depth δ_i by roughly a factor 2 as the mean free path l is shortened (by addition of impurities) to about 10^{-5} cm. If we deduce λ from the δ_i of the very pure specimens, λ is of the order of $5 \cdot 10^{-6}$ cm. In order to get an effect of this order of magnitude from equation (6.17) or (6.18), the value of the correlation length Λ needed is a few times 10^{-5} cm, which is indeed quite comparable to the mean free path l of conduction electrons in the normal state of the specimen.

We emphasize that this order-of-magnitude agreement has been obtained without adding new parameters to the theory. The necessity for a correlation length Λ follows from purely theoretical arguments ([4,5]) having nothing to do with the Pippard effect, and in fact the application to the Pippard effect was recognized by us only later on.

For a more detailed comparison we assume precise proportionality between Λ and l, i.e.,

$$\Lambda = gl\,, \tag{6.19}$$

where g is a constant. Let us see what formulas (6.17) and (6.18) predict concerning the dependence of δ_i on the mean free path l. Since the classical

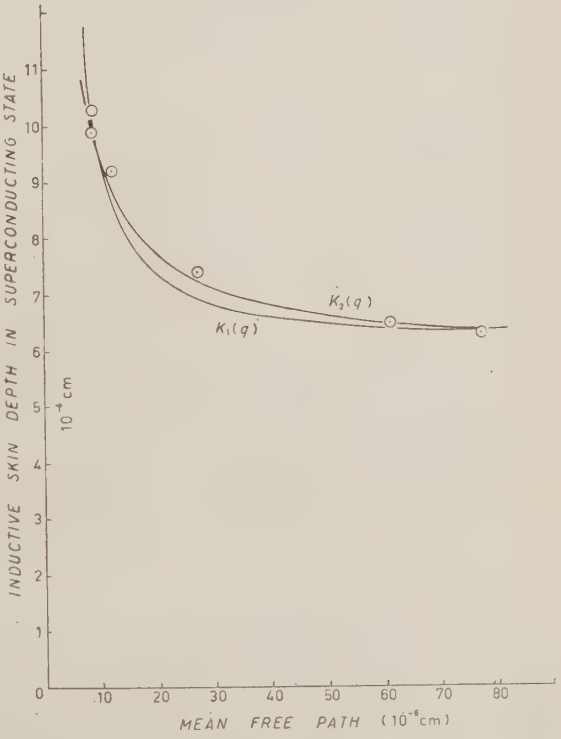

Fig. 2. – The Pippard Effect. Ordinate: Inductive skin depth in the superconducting state, in 10^{-6} cm. Abscissa: Mean free path l of the electrons in the normal state of the specimen, also in 10^{-6} cm. The points represent Pippard's measured values, the two theoretical curves correspond to the « diamagnetic » kernel $K_1(q)$ and the « singular » kernel $K_2(q)$, respectively. The « singular » kernel gives a somewhat better fit to the data, but the difference is probably not significant.

skin depth δ is proportional to $l^{-\frac{1}{2}}$, we get $\delta_i - \lambda$ proportional to $l^{-\frac{3}{2}}$ from (6.17), proportional to l^{-1} from (6.18). In the latter case, the argument of the logarithm is independent of l, and the last term in the bracket is a small correction.

In Fig. 2 we have plotted the experimental data of PIPPARD together with some theoretical curves. The agreement is better with formula (6.18), i.e., the singular kernel $K_2(q)$. This is of course to be expected: we have already seen, in Sect. **4**, that kernel $K_1(q)$ is inconsistent with other experiments unless the correlation length A is considerably in excess of 10^{-3} cm for pure specimens. Although the Pippard effect measurements concern mostly impure specimens, they tend to support shorter values for the correlation length. It is reasonable, therefore, that the same kernel, $K_2(q)$, which gives consistent results for the static measurements, also gives a better fit to the microwave measurements of PIPPARD.

A more detailed study of the integral (6.15), given in Appendix II, shows that the region of q important for the Pippard effect is $q \sim A^{-1}$, not $q \sim 0$. Thus the Pippard effect can be used to find an estimate for the correlation length A, but can not be used by itself to decide whether $K(q)$ approaches a finite limit as $q \to 0$, or has a q^{-1} behaviour there. This is also the reason why formulas (6.17) and (6.18) give roughly the same estimate for A.

On the other hand, the Pippard effect, by providing us with an estimate of A, does constitute one essential link in the chain of reasoning used in Sect. **4** to exclude the regular kernel $K_1(q)$ in favour of the singular kernel $K_2(q)$.

We call attention to the fact that both formulas (6.17) and (6.18) lead to a *frequency-dependent* inductive skin depth δ_i in the superconducting state, through the dependence on the classical skin depth δ, (6.2*c*). PIPPARD ([3]) gives an argument, based on the Kramers-Kronig relation, to show that δ_i is very nearly equal to the « formal » penetration depth (4.12) at zero frequency. In our theory the formal penetration depth is infinite, whereas δ_i is finite and frequency dependent.

Although it will be of interest to look for a frequency dependence of δ_i experimentally, we would like to stress that the detailed frequency dependences of equation (6.17) and (6.18) depend not merely, indeed not even mainly, upon the behaviour of the kernel $K(q)$ near $q = 0$, but are affected by the behaviour of $K(q)$ for much larger values of q, including even values comparable to λ^{-1}, the inverse of the London depth. Thus changes in the kernel for large values of q, with which we are not concerned in this paper, may very well alter the details of formulas (6.17) and (6.18), both as regards frequency dependence and temperature dependence. Hence experiments to test the ideas proposed in this paper should be carried out at zero frequency, not in the microwave region.

In concluding this section, we emphasize that our interpretation of the Pippard effect, if correct, automatically validates our use of the rotating bucket

theorem for superconductivity. The main question in using the rotating buckett theorem is the actual size of the correlation length, in particular whether the correlation length is smaller than the size of the usually employed specimens. From the Pippard effect we get an order of magnitude for the correlation length which is indeed small enough compared to usual laboratory dimensions to make the rotating bucket condition meaningful.

7. – Charge Transport and Persistent Currents in Rings.

LONDON ([1,2]) first suggested that the apparently vanishing electrical resistance of superconducting segments of a circuit and the persistent currents in superconducting rings can be understood by reference to the Meissner effect, as essentially diamagnetic currents. This « diamagnetic approach to superconductivity » has since been generally adopted with only occasional exceptions.

We shall now show that the diamagnetic approach to superconducting charge transport depends upon the implicit assumption of an infinite correlation length.

We start with a purely formal argument: if any mathematical meaning is to be attached to the statement that supercurrents are of diamagnetic origin, it surely is that the supercurrent density $\boldsymbol{j}_s$ can be expressed as the curl of a magnetization vector $\boldsymbol{M}$ i.e., our equation (2.1). We assert that any current density of this form fails to lead to charge transport across a complete cross-section of the material. The proof is straightforward: consider a volume V of superconducting material (for example a superconducting wire segment or a superconducting ring); let S be a surface which cuts through this volume, so that it intersects the surface of the superconductor in a closed curve C (for example, S may be a cross-section through the wire, C the boundary of this cross-section). Let us compute the rate at which charge is transported across the cut. We get

$$\mathrm{d}e/\mathrm{d}t = \int_S \boldsymbol{j}_s \cdot \boldsymbol{n}\, \mathrm{d}S = c\int_S (\mathrm{curl}\, \boldsymbol{M}) \cdot \boldsymbol{n}\, \mathrm{d}S = c\int_C \boldsymbol{M} \cdot \mathrm{d}\boldsymbol{s} = 0\,. \tag{7.1}$$

The last integral vanishes because the magnetization vector $\boldsymbol{M}$ is normal to the surface of the specimen; if this condition is violated, it means true mathematical surface currents, which would again not be « diamagnetic », and would be contrary to the spirit of the London approach.

If one were to describe a current distribution with non-vanishing charge transport as if it were a diamagnetic current, the resultant magnetization density $\boldsymbol{M}$ would either violate the boundary condition at the surface of the specimen, or $\boldsymbol{M}$ would become singular somewhere inside the superconducting

volume V, or both. Thus the London argument from the Meissner field expulsion (which *is* representable in terms of an acceptable magnetization density $\boldsymbol{M}$) to the superconducting charge transport phenomena is by no means obvious, and is in fact linked to the particular form which LONDON assumes for his electrodynamic equations.

Let us understand the physical reason for the difficulty we have encountered. The standard proof of the relation (2.1) between the magnetization and the diamagnetic current density, as given for example in Vol. II of ABRAHAM and BECKER ([16]), assumes that the diamagnetic currents are small ring currents of the kind envisaged by AMPÈRE. It is intuitively obvious that a sum of small rings currents can never give a net charge transport across a complete cross-section of the specimen, simply because each individual ring current fails to do so.

The crucial word here is « small » ring currents. Let us now assume that the ring current can become large, indeed as large as the whole cross-section in question. Let us start with a disc shaped superconductor, in which a ring current is induced which travels parallel to the outer edge of the disc, within a small distance from that edge. This ring current is supposed to shield the inside of the disc, so that there is no magnetic field inside. We can then imagine that we cut out a portion from the centre of the disc, thereby making a superconducting ring, without changing anything essential to the problem — the magnetic field and the currents are both zero in the part we have just cut out. This, we believe, is qualitatively the basis of LONDON's success in relating the currents in superconducting rings to the diamagnetic currents in the Meissner effect.

If this interpretation is correct, then LONDON's success is crucially dependent on the existence of macroscopic diamagnetic currents, i.e., current loops which are as large as the whole cross-section of the specimen; ordinary amperian current loops, which are supposed to be of microscopic dimensions, can never lead to such a result. Indeed LONDON himself recognized this point and talked in terms of « macroscopic quantum states ». In our terminology, the correlation between diamagnetic currents and superconducting charge transport depends crucially upon the assumption of an infinite (as large as the specimen) correlation length Λ. If the correlation length is finite and much smaller than the size of the specimen, macroscopic ring currents are impossible except as superpositions of microscopic ring currents, and we have shown that superposition of microscopic ring currents can never give charge transport.

Thus the « diamagnetic approach to superconductivity » is inconsistent with a finite correlation length. The currents which occur in the Meissner effect

([16]) *Theorie der Elektrizität*, Band II (Leipzig, 1933), see paragraph 21.

are indeed of diamagnetic type, but currents of a different type are needed to explain charge transport phenomena, and the conclusion from the Meissner effect to the frictionless charge transport is invalid for any system with a finite correlation length, i.e., for any actual physical system.

The same conclusion was reached independently by CASIMIR [6] who says: « If London's equation would only hold in cells of the order of for instance 10^{-4} cm, ... the existence of persisting currents would remain unexplained ». We are in full agreement with this remark.

Let us now show the same thing in terms of the mathematical formalism which we have developed in earlier sections. The nearest we could get to a general relation between the current and the electric field was equation (5.30), which connects the « projections » $\hat{\boldsymbol{E}}$ and $\mathrm{d}\hat{\boldsymbol{j}}_s/\mathrm{d}t$. We recall that these « projections » were on to the incomplete set of vector eigenfunctions $\boldsymbol{v}_k(\boldsymbol{r})$ defined by (5.17). In the discussion of this set, we remarked that the additional functions necessary to complete it are the « potential flow » fields in the volume. These are just the vector fields which give rise to non-vanishing charge transport. Equation (5.30) says nothing at all about precisely these crucial components.

We may attempt to get around this difficulty by a « continuity » argument as follows. The eigenvalues q_k form a set which gets denser and denser as the volume is increased. We have assumed all along that the values of the kernel $K(q_k)$ evaluated at the eigenvalues q_k define a continuous function $K(q)$ of the real variable q. Let us now assume that relation (5.30) should be extrapolated straightforwardly to the limit $q_k \to 0$, thereby giving relations for the charge transport components (which indeed correspond to $q_k = 0$). This yields

$$\frac{\mathrm{d}j_{s0}}{\mathrm{d}t} = (c^2/4\pi\lambda^2) \lim_{q\to 0} [q^2 K(q)] E_0 \,, \tag{7.2}$$

where j_{s0} and E_0 are the coefficients of $\boldsymbol{j}_s$ and $\boldsymbol{E}$ with respect to one of the hitherto omitted vector base functions with $q = 0$. We believe that this « continuity » argument is equivalent to the assumption of a « localized » relation between $\mathrm{d}\boldsymbol{j}_s/\mathrm{d}t$ and the electric field $\boldsymbol{E}$, but we have not succeeded in proving this equivalence mathematically in the 3-dimensional case. The relationship between « localizability » of the kernel in x-space and continuity at $q_k = 0$ in k-space is well-known in one dimension, however.

We now see that equation (7.2) is crucially different for the London kernel $K(q) = q^{-2}$ and all the kernels which we have considered, and which diverge no more strongly than q^{-1}. The London kernel extrapolates naturally to the relation

$$\mathrm{d}j_{s0}/\mathrm{d}t = (c^2/4\pi\lambda^2) E_0 \quad (\text{LONDON}), \tag{7.3}$$

which asserts that zero electric field inside the superconductor, i.e., $E = 0$, implies no change in the charge-transporting current j_{s0}, but electric fields induced, say, by changing magnetic fields, will alter this current.

On the other hand, all kernels which satisfy the rotating bucket condition (3.7) extrapolate naturally to the relation

$$\mathrm{d}j_{s0}/\mathrm{d}t = 0 \qquad \text{(Finite correlation length).} \tag{7.4}$$

At first sight this appears to imply unchanging charge transporting supercurrents; but it also implies that such currents can never be set up! For example, consider a ring placed between the poles of a magnet, and then cooled down below the superconducting transition temperature, thereby obtaining a Meissner effect. As long as the ring remains in its initial position, $j_{s0} = 0$ both in the London theory and in our present approach. Now remove the ring from between the poles of the magnet. In the London case, the electric field produced by the change in flux sets up a charge transporting ring current through equation (7.3), in such a way as to counteract and in fact completely cancel the change in flux. No such thing is implied by equation (7.4). Whatever currents may be set up by the changing flux are purely ohmic in character and die away; supercurrents are never set up in this way if equation (7.4) holds.

At first sight, this is a contradiction to the experimental fact that supercurrents are indeed set up by just such an experiment. However, we recall how equation (5.30), and hence (7.2) and (7.4), were derived. We took the equilibrium equation (2.11) and differentiated both sides with respect to time. This is valid for quasi-equilibrium processes only, i.e., for processes which proceed slowly compared to all relevant relaxation times of the system. Since we get into a contradiction by this procedure, we are forced to conclude that *the « persistent » currents in superconducting rings must be understood as relaxation phenomena, i.e., that they are not « really persistent » but eventually die away.*

This conclusion makes it more difficult to construct a microscopic theory of superconductivity. No longer is it sufficient to find a microscopic theory of the Meissner effect, but it is also necessary to construct a separate theory of the quasi-persistent currents in rings and the other charge transport phenomena associated with superconductivity. Since the Meissner effect, unlike the quasi-persistent currents, is an equilibrium phenomenon, it is logical to look for an explanation of that effect first.

This situation is very similar to the one for liquid helium; there, also, it was believed until recently that the superflow is truly reversible, i.e., an equilibrium phenomenon, so that an explanation of the thermodynamic properties of liquid helium (the λ-transition) would automatically yield the superfluid

properties as well. Recently it has been shown ([3,17]) that the superflow can not be truly reversible in a system with finite correlation length, and in particular can not be truly reversible for liquid helium. Hence, even after the nature of the λ-transition is understood, it is still necessary to make a separate theory of the superfluid properties. It is only natural that the finite correlation length should lead to entirely similar consequences for superconductivity.

Although a phenomenological approach of the kind used here can not lead directly to a microscopic understanding of such tremendously long relaxation times, there is one point worth emphasizing on the basis of even a phenomenological approach (*). At least part of this long relaxation time is almost surely a consequence of the nearly complete expulsion of the magnetic field from a superconductor. For example, consider a superconducting slab of thickness L. If a constant magnetic field H_0 is applied to both sides of the slab, we get a Meissner effect, so that the field at the centre of the slab is very much smaller than H_0. With H_0 the same on both sides, there is no net current in the slab. Now suppose that we reverse the sign of the magnetic field on one side of the slab but not on the other. The Maxwell equation (6.8) then implies that there exists a net charge transport parallel to the slab. In an ordinary diamagnet, this charge transport is by means of an ohmic current, and the magnetic field quickly collapses unless an electric field is applied so as to maintain the ohmic current. The magnetic field distribution inside a *diamagnet* under the two conditions (equal field on both sides, equal and opposite fields on both sides) is shown schematically in Fig. 3*a*

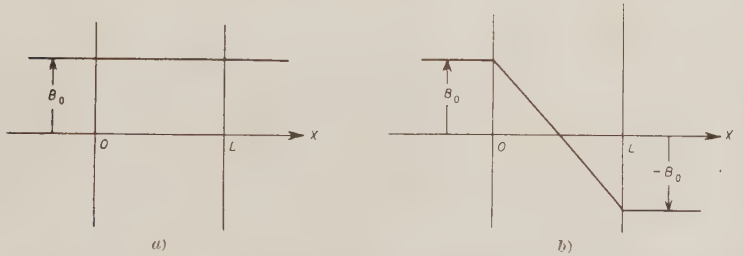

Fig. 3. – Magnetic field inside a diamagnetic slab. (*a*) The same field applied to both sides of the slab; (*b*) Equal and opposite fields applied to the two sides of the slab.

and 3*b*. We see that these magnetic fields are very different from each other. Now, on the other hand, suppose the same is done with our superconducting slab. The magnetic field distributions inside the superconductor are shown schematically in Fig. 4*a* and 4*b*. Since we assume a finite correlation length, the « information » from one side of the slab cannot get directly to the other side, but must travel by means of the conditions at intermediate points. Near the centre of the slab, the magnetic field is very

([17]) S. T. Butler and J. M. Blatt: *Phys. Rev.*, **100**, 495 (1955).

(*) A very similar argument was communicated to us by Dr. G. Kuper (private communication).

small anyway, in Fig. 4*a* as well as in Fig. 4*b* (where it is actually zero). It is reasonable to suppose, therefore, that the rate of transmission of information from one side of the slab to the other is cut down, compared to a diamagnet, by a factor of the order of the ratio of the magnetic field at the centre of the slab (in the Meissner case) to the magnetic field applied outside. According to equation (4.11), this ratio is

$$\frac{B(L/2)}{B_0} \simeq \frac{4\mu\lambda^2}{\pi L} . \tag{7.5}$$

Reasonable orders of magnitude might be: $\lambda \sim 10^{-5}$ cm, $\mu^{-1} \sim 10^{-3}$ cm, $L \sim 10^{-1}$ cm; this gives a factor of the order of 10^{+6} to lengthen the effective relaxation time.

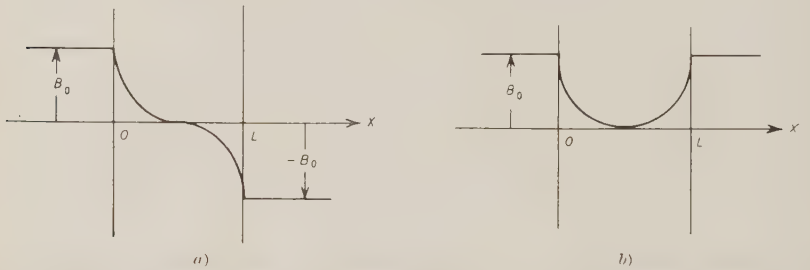

Fig. 4. Magnetic field inside a superconducting slab. (*a*) The same field applied to both sides of the slab; (*b*) Equal and opposite fields applied to the two sides of the slab.

Of course, such a factor is by no means enough to account for the observed persistence of ring currents; but it should certainly be a help in the construction of a future microscopic theory of superconductivity that a factor of this order of magnitude is almost surely there, as a result of *electromagnetic* effects, so that the specific « intrinsic » relaxation time does not need to be quite as large as one would have supposed otherwise.

The same qualitative reasoning also suggests that it would be worth while to investigate the persistence of ring currents in very thin superconductors, i.e., to cut down on the « slab thickness » L, and in impure rather than very pure superconductors, to cut down on the correlation length $\Lambda \simeq \mu^{-1}$.

Beyond this the phenomenological approach cannot go. Furthermore, we believe that it will not be possible to use the conventional methods of non-equilibrium statistical mechanics, i.e., the Boltzmann transport equation, to understand the very long relaxation times involved in superfluid helium and in quasi-persistent superconducting ring currents. It is very likely that a new, more general approach to non-equilibrium quantum statistical mechanics is required before these problems can be treated effectively. On the other hand, the equilibrium properties (Meissner effect in superconductors and λ-transition in liquid helium) should be understandable within the present framework of equilibrium statistical mechanics, and the construction of such microscopic theories is obviously the next step.

* * *

We would like to thank Dr. S. T. BUTLER for innumerable valuable discussions about the subject of this paper, and Dr. A. B. PIPPARD for some helpful discussions concerning his experiments. We are indebted to Dr. M. BUCKINGHAM for some cogent comments on an earlier draft of this manuscript.

APPENDIX I

Mathematics of Fourier-Bessel Expansion.

In Sections 3 and 4 we encountered sums of the type

$$S = \sum_{k=1}^{\infty} G(z_k) , \tag{I.1}$$

where $G(z)$ is some known function which is regular for real positive z, and z_k is the k-th positive zero of the Bessel function $J_0(z)$. We now describe a general method for handling such sums, which is a slight generalization of the method used by WATSON [18] to derive the expansion of $J_\nu(z)$ as an infinite product.

Consider the function $J_1(z)/J_0(z)$. The poles of this function are the zeros of $J_0(z)$, i.e., the numbers z_k, and the residue at each pole is -1, since $J_1(z)$ is the negative derivative of $J_0(z)$. Since $G(z)$ is by assumption regular for real positive z, the poles of the function $G(z)J_1(z)/J_0(z)$ along the positive real z-axis are again the numbers z_k, and the residues at these poles are equal to $-G(z_k)$. Thus if we take a contour integral along the contour indicated in Fig. 5, we obtain the result

$$S = (2\pi i)^{-1} \int_C \frac{G(z)J_1(z)}{J_0(z)} \, dz . \tag{I.2}$$

At this stage, we are in a position to use all the methods possible in transforming contour integrals. For example, if the value of $G(z)$ on a semi-circle far out is sufficiently small, we can transform the contour into the contour C' shown in Fig. 5; we then get one contribution from the little semi-circle around $z = 0$, and another

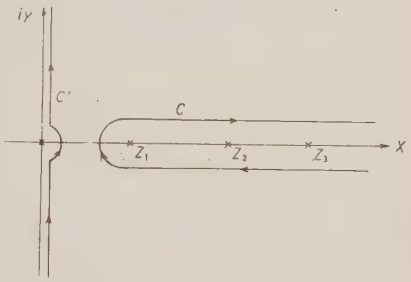

Fig. 5. – Paths for contour integration in the complex z-plane. The real numbers z_1, z_2, ... are the zeroes of the Bessel function $J_0(z)$.

[18] G. N. WATSON: *Theory of Bessel Functions* (Cambridge, 1948).

contribution from the integral over the imaginary axis. The latter contribution vanishes if $G(-iy) = G(iy)$.

As an example, consider the case $G(z) = z^{-2}$, i.e., the sum which appears in (3.5). The contour C can be transformed to C', the only contribution comes from the little semi-circle around $z = 0$, and we get

$$S = -\frac{1}{2}\left[\text{residue of } \frac{J_1(z)}{z^2 J_0(z)} \text{ at } z = 0\right] = \frac{1}{4}\,. \tag{I.3}$$

By the same method, we get

$$\sum_{k=1}^{\infty} z^{-4} = \frac{1}{2}\left[\text{residue of } \frac{J_1(z)}{z^4 J_0(z)} \text{ at } z = 0\right] = \frac{1}{32}\,. \tag{I.4}$$

The expression (4.16) for the magnetization per unit length of a cylinder of radius R leads to the integral

$$\frac{\mathcal{M}}{L} = -B_0 R^2 (2\pi i)^{-1} \int_C \frac{K(z/R)}{\lambda^2 + K(z/R)} \frac{J_1(z)}{z^2 J_0(z)}\, dz\,. \tag{I.5}$$

The London kernel $K(q) = q^{-2}$ gives rise to poles at $z = \pm iR/\lambda$; these two poles together with the pole at zero give the only contribution to the integral if the contour is transformed into C' in Fig. 5. The result is

$$\frac{\mathcal{M}}{L} = -\frac{B_0 R^2}{4}\left[1 - \frac{2\lambda}{R}\frac{I_1(R/\lambda)}{I_0(R/\lambda)}\right], \tag{I.6}$$

where $I_n(z)$ is the Bessel function of imaginary argument, as defined in WATSON [18]. For $R \gg \lambda$, the usual case, the ratio of the two Bessel functions approaches 1, and we get the usual London result (4.19).

The « diamagnetic » kernel $K_1(q) = (q^2+\mu^2)^{-1}$ gives rise to poles at $z = \pm i\sigma R$ where

$$\sigma = [1 + (\mu\lambda)^2]^{\frac{1}{2}} = [1 + (\lambda/\Lambda)^2]^{\frac{1}{2}}\,. \tag{I.7}$$

These two poles together with the pole at $z = 0$ again give the whole result, which is

$$\frac{\mathcal{M}}{L} = -\frac{B_0 R^2}{4}\,\frac{1}{1 + (\mu\lambda)^2}\left[1 - \frac{2}{\sigma R}\frac{I_1(\sigma R)}{I_0(\sigma R)}\right]. \tag{I.8}$$

The approximate result (4.20) is obtained by assuming $\mu\lambda \ll 1$, i.e., a correlation length $\Lambda \simeq \mu^{-1}$ much larger than the London depth λ, and also $\sigma R = R/\lambda \gg 1$, i.e., a cylinder of radius much larger than the London depth.

The kernel $K_2(q)$ substitute into (I.5) gives

$$\frac{\mathcal{M}}{L} = -\frac{B_0 R^2}{4}\,(1 - X)\,, \tag{I.9a}$$

where

$$X = \frac{4\mu\lambda^2}{\pi R}\int_0^\infty \frac{I_1(Rx/\lambda)}{I_0(Rx/\lambda)}\,\frac{1}{(1-x^2)^2+(\mu\lambda x)^2}\,\frac{\mathrm{d}x}{x}\,. \tag{I.9b}$$

In order to evaluate this integral approximately, we note that the ratio $I_1(y)/I_0(y)$ is essentially unity for large y, i.e., over most of the range of integration over x. We therefore break the range into two parts, $Rx/\lambda < 3$ and $Rx/\lambda > 3$. In the lower range, we can replace the quantity $(1 - x^2)^2 + (\mu\lambda x)^2$ by 1, and are left with the integral

$$\int_0^3 \frac{I_1(y)}{yI_0(y)}\,\mathrm{d}y = 1.186\,. \tag{I.10}$$

In the region $y = Rx/\lambda > 3$, the following approximation is sufficient (better than 3 percent):

$$\frac{I_1(y)}{I_0(y)} \cong 1 - (2y)^{-1}\,. \tag{I.11}$$

Substitution into (I.9b) leads to elementary integrals, which are then further simplified by using the fact that $\mu\lambda \ll 1$ and the lower limit of integration, $x_1 = 3\lambda/R$, is also much less than 1. The result is

$$\int_{3\lambda/R}^\infty \left(1 - \frac{\lambda}{2Rx}\right)\frac{1}{(1-x^2)^2+(\mu\lambda x)^2}\,\frac{\mathrm{d}x}{x} \simeq \tag{I.12}$$

$$\cong \frac{\pi}{2\mu\lambda} - \ln(3\lambda/R) - \frac{1}{2} - \frac{\pi}{4R\mu} - \frac{1}{6} + \cdots\,.$$

Formula (4.21) then follows by noticing that, to the accuracy of our approximations, the X in (I.9) and the effective penetration depth D in (4.18) are related by

$$X \cong 2D/R\,. \tag{I.13}$$

Appendix II

Evaluation of Some Integrals.

The kernel $K_2(q) = [q(q+\mu)]^{-1}$ leads to rather awkward integrals, two of which are discussed below. A third integral, (I.5), has been done in Appendix I.

The law of field penetration, (4.8), becomes

$$\frac{B(x)}{B_0} = \frac{2}{\pi}\,\mathrm{Im}\int_0^\infty \frac{(q+\mu)\exp[iqx]}{q(q+\mu)+\lambda^{-2}}\,\mathrm{d}q\,. \tag{II.1}$$

We swing the contour around to coincide with the positive imaginary axis in the q-plane; letting $q = iy$, we get

$$\frac{B_0(x)}{B_0} = \frac{2\mu}{\pi\lambda^2}\int_0^\infty \frac{\exp[-xy]}{(y^2 - \lambda^{-2})^2 + (\mu y)^2}\,dy\,. \tag{II.2}$$

Interpreting this as the real part of a complex integral, we now swing the contour in the y-plane to coincide with the positive imaginary y-axis; there is a pole of the integrand at the position y_1 given by

$$y_1^2 = \lambda^{-2} - \tfrac{1}{2}\mu^2 + i\mu[\lambda^{-2} - (\tfrac{1}{2}\mu)^2]^{\frac{1}{2}} \tag{II.3}$$

where the square root of y_1^2 is in the first quadrant. The quantity $(\mu\lambda)^2 = (\lambda/\Lambda)^2$ is by assumption small (correlation length Λ much larger than London depth λ) and we are justified in neglecting terms of this order of magnitude compared to 1, provided that they do not have large numerical coefficients. It is easily seen that the numerical coefficients are indeed less than 1 for the cases of interest to us. We then get, approximately

$$\lambda_1 \cong \lambda^{-1} + i\tfrac{1}{2}\mu\,. \tag{II.4}$$

Making corresponding simplifications for the residue at this pole, we get, with the notation $y = + iq'$

$$\frac{B(x)}{B_0} = \left[\cos\left(\frac{1}{2}\mu x\right) - \frac{1}{2}\mu\lambda\sin\left(\frac{1}{2}\mu x\right)\right]\exp[-x/\lambda] + \tag{II.5}$$

$$+ \frac{2\mu}{\pi\lambda^2}\int_0^\infty \frac{\sin(q'x)}{(q'^2 + \lambda^{-2})^2 - (\mu q')^2}\,dq'\,.$$

Consistent with our approximation so far, we can now neglect the term $(\mu q')^2$ in the denominator; the largest relative error occurs for $q' = \lambda^{-1}$, and the fractional error at this point equals $(\frac{1}{2}\mu\lambda)^2$, which is negligible. The resulting integral can be recovered by differentiation with respect to σ^2 of the well-known integral

$$\int_0^\infty \frac{\sin(q'x)}{q'^2 + \sigma^2}\,dq' = (2\sigma)^{-1}(\exp[-\sigma x]\,\overline{Ei}(\sigma x) - \exp[+\sigma x]\,Ei(-\sigma x))\,, \tag{II.6}$$

where the exponential integral functions occurring here are defined in JAHNKE and EMDE ([8]). The result is equation (4.10).

We now turn to the integral for the inductive skin depth at microwave frequencies (Pippard effect), formula (6.15). Using the notation

$$\alpha = \mu\lambda = \lambda/\Lambda\,, \qquad \beta = \lambda/\delta\,, \qquad x = q\lambda\,, \tag{II.7}$$

we obtain

$$\frac{\delta_i}{\lambda} = \frac{2}{\pi}\int_0^\infty \frac{x^2 - \dfrac{x}{x-\alpha}}{\left(x^2 - \dfrac{x}{x-\alpha}\right)^2 - \beta^4}\,\mathrm{d}x\,. \tag{II.8}$$

This is in principle an elementary integral, but the straigthforward evaluation is too complicated to be worth while. Instead we make use of the fact that both α and β are small compared to 1. We divide the range of integration into two regions. In region i, small x, we can neglect x^2 compared to $x/(x-\alpha)$; in region ii, large x, we can ignore the β^4 in the denominator. Let x_1 be the dividing point between these two regions. We determine the optimum value of x_1 by the condition that the fractional error made in the two regions is the same for $x = x_1$. This leads to the equation

$$x^4 + \frac{2x^3}{x-\alpha} = \beta^4\,, \tag{II.9}$$

which we solve approximately under the assumption $x_1 \ll \alpha$ to get

$$x_1 \cong (\tfrac{1}{2}\alpha\beta^4)^{\frac{1}{3}}\,. \tag{II.10}$$

The relative error made at this point is of the order of $(\alpha^5\beta^4)^{\frac{1}{3}}$ which is quite small enough. The error in the integral (II.8) is of course even smaller, since this is the worst point.

From here on the evaluation is straightforward; we simplify the results by ignoring terms which contribute less than 1 percent, under the assumptions $\alpha < \frac{1}{3}$, $\beta < \frac{1}{10}$. This gives the following contributions

Region i: $(2/\pi)[x_1 - \alpha \ln (x_1/\alpha\beta^2)]$

Region ii: $1 - 3\alpha^2/8 - (2/\pi)[x_1 + \alpha \ln (x_1) + \tfrac{1}{2}\alpha]\,.$

When we add these results, the quantity x_1 drops out, showing that the precise value of the breaking point between the two regions is unimportant and therefore justifying a posteriori our appropriate solution of (II.9). The final result is

$$\frac{\delta_i}{\lambda} = 1 - (2\alpha/\pi)[\ln (\alpha\beta^2) + \tfrac{1}{2}] - 3\alpha^2/8\,, \tag{II.11}$$

which is formula (6.18) of the text, except for notation.

We have spent some time going into the details of this evaluation, because a physical point is involved here as well. In region ii, large x, we ignored the quantity β^4 in the denominator of (II.8). This quantity β, according to (II.7), involves the classical skin depth δ. We conclude that *the classical skin effect enters into the calculation of the Pippard effect only for small values of* $x \sim q\lambda$.

i.e. for values of q less than

$$q_1 = x_1/\lambda = (\lambda^2/2\Lambda\delta^4)^{\frac{1}{3}} . \tag{II.12}$$

For larger values of q, the classical skin effect can be ignored altogether. In the limit of a London superconductor, $\Lambda \to \infty$, q_1 approaches 0 and the microwave inductive skin depth is a direct measure of the London depth λ, independent of the classical skin depth δ in the normal state of the specimen.

Appendix III

The Reuter-Sondheimer Correction to the Pippard Effect.

It is well-known ([14]) that the classical theory of the skin effect fails when the classically computed skin depth δ becomes comparable to the mean free path l of the electrons in the specimen. Since the classical skin depth δ enters into our calculation of the Pippard effect, and for Pippard's specimens δ is quite comparable to l, we must investigate the importance of this correction. We shall first give a physical argument why the correction is unimportant, and shall then indicate briefly how the formula (6.15) for the microwave inductive skin depth of a superconductor would be changed by this correction.

At the end of Appendix II, we pointed out that the classical skin effect is important only for low values of the integration variable q, namely q less than q_1, formula (II.12). Qualitatively, q_1^{-1} is therefore the smallest distance over which we need to consider the classical skin effect. Phenomena which are associated with faster distance variations are not influenced significantly by the skin effect.

On the other hand, the Reuther-Sondheimer correction is important only for effects which vary rapidly with distance. Hence if the non-dimensional quantity $q_1 l$ is smaller than or comparable to unity, the Reuther-Sondheimer correction may be expected to be unimportant: in the region $q < q_1$, where the skin effect matters, it is given correctly by the classical expressions: in the region $q > q_1$ the skin effect doesn't matter anyway, and hence a correction to it matters even less.

A typical « impure » specimen of Pippard has, order of magnitude wise: $\lambda \sim 5 \cdot 10^{-6}$ cm, $l \sim 10^{-5}$ cm, $\delta \sim 5 \cdot 10^{-5}$ cm, $\Lambda \sim 2 \cdot 10^{-5}$ cm. This gives $q_1^{-1} \sim 2 \cdot 10^{-4}$ cm and $q_1 l \sim 0.05$. The corresponding numbers for a typical « pure » specimen would be: $\lambda \sim 5 \cdot 10^{-6}$ cm, $l \sim 10^{-4}$ cm, $\delta \sim 2 \cdot 10^{-5}$ cm, $\Lambda \sim 2 \cdot 10^{-4}$ cm. This gives $q^{-1} \sim 10^{-4}$ cm and hence $q_1 l \sim 1$. Since there is no appreciable Pippard effect anyway for the pure specimens, we see that the Reuter-Sondheimer correction is unimportant for our purposes.

In order to make this argument more mathematical, let us now turn to the modifications which the Reuter-Sondheimer correction introduces into the analysis of Sections 5 and 6. Reuter and Sondheimer ([14]) consider two possibilities, « specular reflection » and « diffuse reflection » of the electrons at the boundary of the specimen. Since there is no significant qualitative differences between these two cases, we choose the one that is easier to work with, namely

the specular reflection. This has the advantage that the operators remain diagonal in our representation in terms of vector eigenfunctions $\boldsymbol{v}_k$. The only change is in the relation between normal current $\boldsymbol{j}_n$ and electric field $\boldsymbol{E}$; the classical relation (5.2) gives, after expansion of both fields in eigenfunctions $\boldsymbol{v}_k$:

$$j_{nk} = \sigma E_k \,, \tag{III.1}$$

whereas the Reuter-Sondheimer formalism leads to

$$j_{nk} = \sigma(q_k) E_k \,, \tag{III.2}$$

where

$$\sigma(q) = \sigma \frac{3}{2} \frac{[1 + (ql)^2] \operatorname{arctg}(ql) - ql}{(ql)^3} = \sigma S(ql) \,. \tag{III.3}$$

For small values of q, $ql \ll 1$, (III.3) reduces to $\sigma(q) = \sigma$, and hence (III.2) becomes equivalent to (III.1), as expected.

By following through the analysis of Sect. 6 leading to equation (6.15), we see that the only change is the replacement of the term δ^{-4} in the denominator by $[\delta^{-2} S(ql)]^2$. That is, formula (6.15) becomes

$$\delta_i = (2/\pi) \int_0^\infty \frac{q^2 + (q/\lambda)^2 K(q)}{[q^2 + (q/\lambda)^2 K(q)]^2 + [\delta^{-2} S(ql)]^2} \, \mathrm{d}q \,. \tag{III.4}$$

In « region ii » of Appendix II, i.e., q large, the term δ^{-4} in (6.15) was so small that it could be ignored compared to the rest of the denominator. Since $S(ql)$ decreases with increasing q, this term is now even smaller and can hence be ignored even more thoroughly.

We have estimated the boundary q_1 between « region i » and « region ii » for the particular kernel $K_2(q)$, which is also the type of kernel which we believe represents a superconductor correctly. A very similar estimate can be made for the kernel $K_1(q)$.

RIASSUNTO (*)

La richiesta di una lunghezza di correlazione finita esclude le equazioni convenzionali di London per i superconduttori. Si propongono e si discutono altre equazioni. Alcune delle conseguenze sono: 1) un campo magnetico non si può espellere completamente da un superconduttore: il campo, a grande profondità x, è proporzionale a x^{-1} anzichè affievolirsi esponenzialmente. 2) L'effetto Pippard segue come conseguenza naturale dalle equazioni già proposte. 3) La correlazione di London tra l'espulsione del campo di Meissner e le correnti persistenti negli anelli superconduttori dipende da una lunghezza di correlazione infinita e deve pertanto essere abbandonata; le correnti anulari « persistenti » debbono essere interpretate come fenomeni di rilassamento. La spiegazione della vita enormemente lunga non è possibile nel quadro di un attacco puramente fenomenologico del problema, e resta uno dei compiti di una futura teoria microscopica della superconduttività.

(*) *Traduzione a cura della Redazione.*

High Energy Nuclear Interactions in Lead by Cosmic Ray Protons at 3500 m.

R. Giacconi, A. Lovati, A. Mura and C. Succi

Istituto di Scienze Fisiche dell'Università - Milano
Istituto Nazionale di Fisica Nucleare - Sezione di Milano

(ricevuto il 12 Luglio 1956)

Summary. — A multiplate cloud chamber, triggered by G.M. counters, has been operated at 3500 metres a.s.l. to collect high energy nuclear interactions in lead by cosmic ray protons. A study is made of the development of the nuclear cascade in lead. The angular distribution of the secondary interacting particles, the characteristics of the successive interactions of the cascade, the mean free path for nuclear interaction of the secondary ionizing particles have been analyzed. For the shower particles produced in high energy interactions (by protons of mean energy 50 GeV) similar to the *jets* of nuclear emulsions, the mean free path is found to be geometrical. Associated with the 786 interactions seen in the chamber, 15 V^0 and 3 $V^{\pm}$ particles have been observed. The distribution of the angles between the production plane and the decay plane of the V^0 is given.

In previous researches [1,2] we have studied, by means of a multiplate cloud chamber operated at random, some aspects of cosmic radiation at 3500 m. In the present experiment some of those questions have been further investigated, in a higher energy region, using at the same altitude the same cloud chamber triggered by G.M. counters. The study refers in particular to the development of the nuclear cascade in lead, the mean free path for nuclear interaction of secondary ionizing particles and the production of V^0 particles.

---

(1) A. Lovati, A. Mura, G. Tagliaferri and S. Terrani: *Nuovo Cimento*, **9**. 946 (1952).

(2) A. Lovati, A. Mura, C. Succi and G. Tagliaferri: *Nuovo Cimento*, **12**. 526 (1954).

While the energy region of the nuclear interactions analyzed in [1] and in [2] was of a few GeV, the one of the present experiment ranges from a few GeV to a few tens GeV.

1. – Experimental.

The chamber, of useful dimensions 60 · 50 · 15 cm³, contained 5 lead plates, each 18 g cm⁻² thick. The chamber was expanded whenever a coincidence occurred between *one and only one* counter of a tray of ten above the chamber and *at least two* of another tray of ten counters below. The latter were sheltered with lead to avoid triggering by μ-mesons accompanied by knock-on electrons.

From 10000 photographs we have chosen the 786 ones containing at least one nuclear interaction in lead produced by an unnaccompanied ionizing primary. Since the material above the chamber (top of the chamber, thermostatic box and roof of the laboratory) was only 5 g cm⁻², it may be assumed that practically all the interactions selected are produced by protons. The selection of the counters and the thickness of the plates provide a strong bias against the observation of interactions with 0, 1 and 2 penetrating particles; on the contrary the events with electronic component or associated with some other interactions are lightly favoured. Some of the 786 « primary » interactions were associated with one or more « secondary » interactions in lead or with stars or decay events in gas. In Table I all the events developped in lead have been classified according to the different types of association observed.

TABLE I. - *Classification of the events developped in lead.*
(I means primary interaction, II secondary interaction, etc.).

Type of event	I	I II	I II II	I II III	I II III	Total
No. of events	655	109	18	2	2	786
No. of interactions	655	218	54	6	8	941

In Table II the interactions occurred in the upper four plates of the chamber have been distributed according to the number of penetrating shower particles (p.s.p.) [3]. This distribution may give a rough indication of the energy range

[3] Penetrating shower particle (p.s.p.) has been defined the penetrating particle which could be seen to ionize near the minimum (< twice the minimum) before and after crossing the plate just close to the one where the interaction took place. The corres-

of the interactions. According to DEUTSCHMANN (4), for instance, a 10 GeV proton produces a nuclear interaction in lead with a mean multiplicity of 3-4 p.s.p., while a 30 GeV proton gives interactions with mean multiplicity 5-7.

TABLE II. – *Distribution of the nuclear interactions in lead according to the number of p.s.p.*

No. of p.s.p. per interaction	0	1	2	3	4	5	6	7	⩾8	Total
Primary interactions:										
No. of interactions	77	81	101	144	96	77	46	36	21	679
No. of p.s.p.	0	81	202	432	384	385	276	252	189	2201
Secondary interactions:										
No. of interactions	62	16	10	6	9	0	1	0	0	104
No. of p.s.p.	0	16	20	18	36	0	6	0	0	96

2. – Development of the Nuclear Cascade in Lead.

Links between primary and secondary interactions. – Nuclear cascades in lead were observed in 131 photographs (see Table I). In these photographs the total number of secondary interactions is 151. These secondary interactions were thought to be associated to the primary ones either because an ionizing link was observed (68 cases) or because the position and age of the secondary interaction indicated a probable, but not identified, link with the primary one. In 31 cases it was possible to attribute the probable link between primary and secondary interaction to a neutral particle. In the remaining 52 cases, since the primary event developped with many p.s.p. and (or) with rich electronic cascades, any attempt to recognize the link failed.

Angular distribution of the links. – The angular distribution of the p.s.p. produced in primary interactions, with respect to the direction of the incident proton, has been determined in order to have some information on the direction of the cascade development. In Fig. 1 the hystograms (*a*) and (*b*) show the angular distribution of the p.s.p. produced in the primary interactions which are associated with a secondary interaction: (*a*) and (*b*) refer respectively to the p.s.p. that produce a secondary interaction and to the other p.s.p. Hystogram (*c*) shows the distribution of the neutral links. The

ponding energies for protons and π-mesons are at least 270 and 60 MeV respectively. Lightly ionizing particles that connect two interactions in two adjacent plates are also considered as p.s.p.

(4) M. DEUTSCHMANN: *Zeits. f. Naturf.*, **9***a*, 477 (1954).

distributions (*a*) and (*c*) appear very similar. The fact that the angular distribution of the interaction-producing particles is much narrower than that of the non interacting p.s.p. indicates that the particles produced in the core of the disintegrations, with higher energy, produce more secondary interactions. In consequence the nuclear cascade develops mainly in the forward direction.

Characteristics of the primary and secondary interactions. – From the analysis of the photographs, primary interactions (produced by protons) and secondary interactions (produced by π-mesons and nucleons) look very similar. However the mean multiplicity of p.s.p. (see Table II) is very different: 3.2 and 0.9 respectively. The primary interactions have also a higher yield of electronic component.

A more direct comparison is shown in Table III, where the cascades are distributed according to the total numbers of p.s.p.$+\pi^0$ of the primary and secondary interaction (5). The mean multiplicity of p.s.p.$+\pi^0$ of the primary and secondary interactions of the cascade is 5.5 and 1.2 respectively.

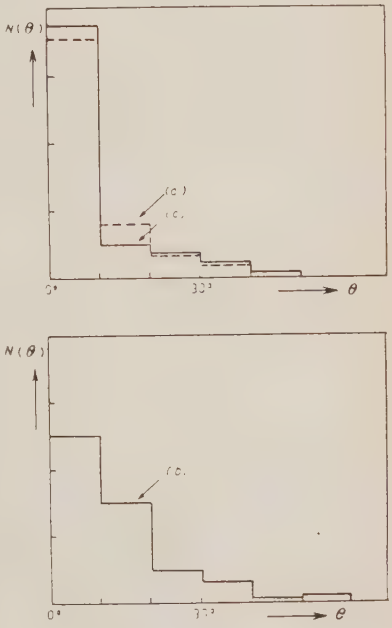

Fig. 1. – Angular distribution $N(\theta)$ of the particles produced in the primary interactions associated with secondary interactions: (*a*) p.s.p. that produce secondary interactions, (*b*) p.s.p. that do not produce secondary interactions, (*c*) neutral links between primary and secondary interactions. The angles θ shown in the hystogram are the projected angles between the direction of the incident proton and that of the particle considered.

(5) As to the number of π^0-mesons, interactions with one or two electron showers, each of these with at least two particles emerging from the plate just close to the one in which the interaction took place, were said to have one π^0-meson; interactions with three or four electron showers were said to have two π^0-mesons; etc. In the present experimental conditions the minimum energy required for a π^0-mesons in order to be detected is of the order of 300 MeV.

TABLE III. – *Distribution of the nuclear cascades according to the numbers of p.s.p.+π^0 of the primary and secondary interaction.*

No. of p.s.p.+π^0 per interaction		Primary interactions								Secondary interactions	
		0	1	2	3	4	5	6	$\geqslant 7$	total no. of interact.	total no. of p.s.p.+π^0
Secondary interactions	0	0	0	4	6	11	10	14	15	60	0
	1	0	1	2	3	0	3	1	1	11	11
	2	0	0	2	4	1	0	1	3	11	22
	3	0	0	1	1	3	0	2	2	9	27
	4	0	0	0	0	0	3	1	2	6	24
	5	0	0	2	1	0	2	1	1	7	37
										(104)	(121)
Primary interactions	total no. of interactions (*)	0	1	9	11	13	16	18	23	(91)	
	total no. of p.s.p.+π^0	0	1	18	35	52	80	108	207	(502)	

(*) The numbers of interactions quoted in this row do not correspond to the sum of the numbers of the columns above, due to the fact that some of the primary interactions are associated with two secondary interactions.

3. - Mean Free Path for Nuclear Interaction of the Penetrating Shower Particles.

The *apparent* mean free path (m.f.p.) for nuclear interaction in lead of the p.s.p. produced in the primary interactions has been determined and found to be 780 g cm^{-2}, with an error of about 10%. This value is close to the one obtained in an early experiment ([6]) and corresponds to a *true* m.f.p. nearly geometric.

In order to obtain a rough estimate of the variation of the m.f.p. with the multiplicity of the primary interaction—observed by DULLER and WALKER ([7]) for production of penetrating showers in lead—the ratio of the number of interaction-producing ionizing particles to the total number of p.s.p. produced in primary interactions has been evaluated for different groups of multiplicities. Roughly the same value was found (5.6, 5.3 and 4.6% for multiplicities of 2–3, 4–5 and $\geqslant 6$ p.s.p. respectively). This result does not support the idea that the m.f.p. for nuclear interaction of the p.s.p. decreases at high values of multiplicity of the primary event.

([6]) A. LOVATI, A. MURA, C. SUCCI and G. TAGLIAFERRI: *Nuovo Cimento*, **8**, 271 (1951).

Since high multiplicity of the primary interaction does not always imply high energy of the p.s.p., we have evaluated the m.f.p. of the p.s.p. for events with high energy primary and high multiplicity of p.s.p. These events were selected among the primary interactions with $\geqslant 5$ p.s.p., requiring the angle containing one half of the p.s.p. produced in the collision to be less than 15°. We have found 30 such events. From the spacial reconstruction of the events, we have calculated the mean energy of the incident proton following the method of Duller and Walker (7). In Fig. 2 the characteristic plot of the method $F/(1-F)$ *versus* $\operatorname{tg}\theta$ is shown. The experimental points seem to fit well with a straight line, thus confirming the hypotheses of the method (in particular the single nucleon-nucleon collision). The mean energy of the incident proton was found to be about 50 GeV with an error of 10%. The hypothesis of a single collision seems to be confirmed by the fact that the mean multiplicity of evaporation tracks of this group of interactions results to be only 1.5 against 4.2 found for the other interactions with $\geqslant 5$ p.s.p. The high number of shower particles, their narrow angular distribution and the low multiplicity of heavily ionizing particles are roughly the conditions required for a shower seen in emulsion to be classified as a *jet*. The mean free path for nuclear interaction of the p.s.p. of high multiplicity and high energy interactions under study has been found to be nearly geometric (the *apparent* m.f.p. was 800 g cm^{-2} of lead with an error of about 20%). The result of the present analysis is therefore in good agreement with the conclusions obtained with nuclear emulsions for the shower particles of *jets* (8).

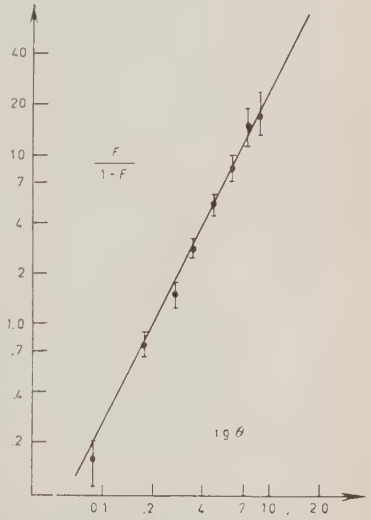

Fig. 2. - F plot of the angular distribution of the p.s.p. of the events of high energy selected according to the criteria described in Sect. **3** (mean energy of the interactions about 50 GeV). F is the fraction of particles that are emitted within the angle θ in the laboratory system: θ is the angle between the direction of the incident proton and that of the p.s.p. produced in the interaction.

(7) N. M. Duller and W. D. Walker: *Phys. Rev.*, **93**, 215 (1954).

(8) U. Haber-Schaim, F. T. Hoang, L. Scarsi and M. Teucher: *Suppl. Nuovo Cimento*, **12**, 472 (1954).

4. – V^0-Particles.

Associated with the 786 primary interactions in lead we have found 15 V^0 and 3 $V^{\pm}$ decays. In one case, shown in Fig. 3, the production of one V^0 and one $V^{\pm}$ has been observed.

The ratio of the number of V^0 particles to the total number of p.s.p. produced in primary interactions is 0.7%, in close agreement with the *uncorrected* value reported by GAYTHER and BUTLER (9). Following the method of PODOLANSKI (10) we have been able to identify 4 Λ^0 and 6 θ^0. In the remaining cases the identification failed.

As known, the distribution of the angles between the production plane and the decay plane is of great interest for the determination of the spin of the V^0 particles. The analysis of the V^0 events has given in the present research an experimental distribution practically isotropic (5, 4 and 6 events in the regions 0°–30°, 30°–60° and 60°–90°). Previous data have been reported by GAITHER and BUTLER (9) for 42 cases and by DEUTSCHMANN *et al.* (11) for 34 ones.

* * *

It is a pleasure to thank Professors G. POLVANI and P. CALDIROLA for their interest in this experiment.

We are indebted to the Directors of the Laboratorio della Testa Grigia (Professors BALLARIO and FIDECARO) for granting us laboratory facilities and to Drs. DE PETRIS and RIVA for their help in the analysis of the photographs. We are particularly grateful to Mr. NICOLAI for valuable assistance in running the apparatus.

Financial helps have been provided by the Istituto di Scienze Fisiche (with the contribution of the Amici dell'Istituto and of the A.N.I.D.E.L.) and by the I.N.F.N., Sezione di Milano.

(9) D. B. GAYTHER and C. C. BUTLER: *Phil. Mag.*, **46**, 467 (1955).

(10) J. PODOLANSKI and R. ARMENTEROS: *Phil. Mag.*, **45**, 13 (1954).

(11) M. DEUTSCHMANN, M. CRESTI, W. D. B. GREENING, L. GUERRIERO, A. LORIA and G. ZAGO: *Nuovo Cimento*, **3**, 566 (1956).

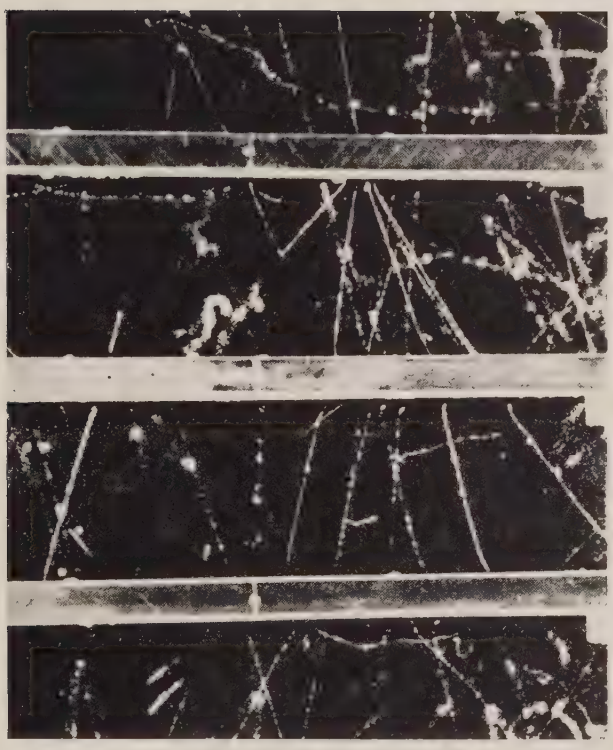

Fig. 3. - Nuclear interaction in lead that produces a pair of V particles.

RIASSUNTO

Con una camera di Wilson a lastre di piombo sono state raccolte fotografie di interazioni nucleari di alta energia prodotte da protoni della radiazione cosmica a 3 500 metri. Vengono studiati diversi aspetti della cascata nucleare in piombo: in particolare la distribuzione angolare delle particelle interagenti, le caratteristiche delle interazioni successive ed il libero cammino medio per interazione nucleare dei secondari ionizzanti. Per le particelle di sciame prodotte nelle interazioni più energiche (da protoni di energia media intorno ai 50 GeV) simili ai *jets* delle emulsioni nucleari, il cammino medio libero è risultato quello geometrico. Associate alle 786 interazioni in piombo rivelate nella camera si sono osservate 15 particelle V^0 e 3 $V^{\pm}$. Viene data la distribuzione degli angoli tra il piano di produzione ed il piano di decadimento delle V^0.

Decay Characteristics and Masses of Positive K Mesons Produced by the Bevatron.

R. W. Birge, D. H. Perkins, J. R. Peterson
D. H. Stork and M. N. Whitehead

University of California, Radiation Laboratory - Berkeley, California

(ricevuto il 14 Luglio 1956)

Summary. — A large emulsion stack exposed to the positive K beam at the Berkeley 6 GeV Bevatron has been used to measure the mass of the K-particles and their abundances. The masses for the decay modes $K_{\mu 2}$, $K_{\pi 2}$ and τ were obtained by measurement of the mean range of the secondaries. In addition, masses for all modes compared to the proton mass were measured by the range-momentum method. The abundances were determined by following and blob-counting secondaries. The data are:

Type	Abundances %	Primary Mass (m_e)	Mass from Secondary Range (m_e)
τ	5.56 ± 0.41	966.3 ± 2.1	966.1 ± 0.7
τ'	2.15 ± 0.47	967.7 ± 4	—
$K_{\mu 2}$	58.2 ± 3.0	967.2 ± 2.2	965.8 ± 2.4
$K_{\pi 2}$	28.9 ± 2.7	966.7 ± 2.0	962.8 ± 1.8
$K_{\mu 3}$	2.83 ± 0.95	969 ± 5	
K_{e3}	3.23 ± 1.30	967 ± 8	—

1. – Introduction.

In previous communications [1] we have reported on measurements of the masses of positive K-mesons by use of the strong-focusing spectrometer of the Berkeley Bevatron. The decay modes of a few of the K_L's were identified

[1] R. W. Birge, J. R. Peterson, D. H. Stork and M. N. Whitehead: *Phys. Rev.*, **100**, 430 (1955); R. W. Birge, R. P. Haddock, L. T. Kerth, J. R. Peterson, J. Sandweiss, D. H. Stork and M. N. Whitehead: *Pisa Conference Report* (1955).

by blob-counting the secondaries a few centimeters from the decay point. The masses of these identified K's were then measured by the range-momentum method.

It soon became obvious that any mass difference between the various types of K-mesons was so small as to be detectable only by more precise measurements on identified particles. At the same time the small mass differences became of increasing interest as evidence indicated that the $K_{\tau 2}(0^-)$ and the τ-meson could not have the same spin and parity configuration (2). This result indicated that they must either be different particles or be genetically related, as in the cascade scheme (3), wherein either particle might be the decay product of the other. In the latter scheme a range-momentum-type measurement would give the mass of the parent particle only. The half life of the daughter particle is presumed to be so short as to be undetectable.

From the range measurements of the secondaries from each of the modes $K_{\pi 2}$, $K_{\mu 2}$, τ, we have calculated the Q's of the decays, and therefore the mass of the possible « daughter » particle in the cascade scheme. In following and blob-counting the decay secondaries we have also obtained the relative abundance of the various modes of decay and the decay spectra of the three-body modes involving a single charged secondary, viz. $K_{\mu 3}$, $K_{e 3}$, and τ'. The details of the range-momentum method of measuring the masses of the primary K-particles are to be published separately (4). The analysis of the τ-decays obtained in this work has been described previously (5).

The ranges of the secondaries from $K_{\mu 2}$ and $K_{\tau 2}$ particles, the identification of the decay modes, the relative abundances, and the significance of the mass measurements are discussed here. These data are compared with those given by other experimenters.

2. – General Method.

2·1. *Exposure.* – A nuclear emulsion stack of 95 pellicles, each of thickness 600 μm and area 9 by 17.5 inches, was exposed at the Bevatron to a K-meson beam produced in a copper target at 90° to the primary 6.2 GeV protons. Details of the strong-focusing spectrometer used to form the K beam have

(2) R. Dalitz: *Proceedings of the Fifth Annual Rochester Conference* (New York, 1956).

(3) S. B. Treiman and H. W. Wyld, Jr.: *Phys. Rev.*, **99**, 1039 (1955); T. D. Lee and J. Orear: *Phys. Rev.*, **100**, 932 (1955).

(4) J. R. Peterson: *The Masses of Identified Positive Heavy Mesons* (Thesis), UCRL-3368, April 1956.

(5) R. P. Haddock: *Nuovo Cimento*, **4**, 240 (1956); also *Analysis of One Hundred Bevatron τ^+ Particles*, UCRL-3284, Feb. 1956.

been given elsewhere [1,4]), but the general features are as follows. A strong-focusing quadrupole magnetic lens forms an image of the target in the stack, of at a point about 1 foot behind a bending magnet that serves to separate particles different momenta (see Fig. 1). The momentum resolution of the system is determined by the magnification of the lens system and dispersion of the bending magnet. In our experiment, this resolution was $\pm 1.2\%$ in momentum, which, when combined with the K-meson range straggling, resulted in a standard deviation of $\pm 19\ m_e$ in the determination of the mass of a single K-particle by range-momentum measurements. The average proper time of flight was $1.4 \cdot 10^{-8}$ s.

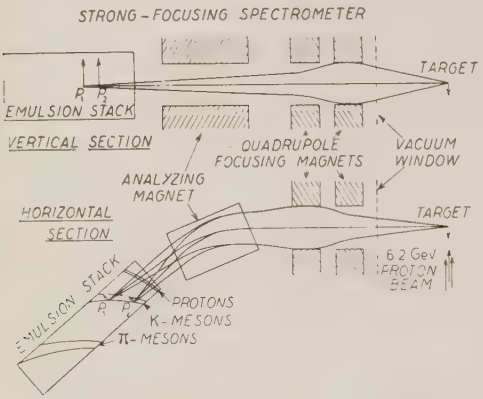

Fig. 1. – Diagram of strong-focusing spectrometer.

2·2. *Scanning.* – A swath was scanned in each emulsion just beyond the proton range and perpendicular to the beam direction. Each track of appropriate grain density and direction was followed to its end. Observation of one or more tracks of secondary particles at the end point identified the primary as a heavy meson. The distribution in range of such primary particles shows a sharp peak; that of particles with no observed decay is more diffuse but also shows a distinct peak at the same range. The areas under the peaks indicate that about 15% of the secondaries of K-particles escaped detection. See Appendix A for discussion of the effect of this loss on relative abundances.

The heavy mesons thus found were classified by the scanners as τ's or K-particles with light or dark secondary tracks. The subjective category « dark » includes roughly all secondary tracks of ionization greater than twice the minimum value.

2·3. *Identification of Secondaries.*

1) Systematic following. – The track of each decay secondary was followed if its direction indicated that it had 21 cm of emulsion path available. In this way it was possible not only to follow to rest secondaries from the $K_{\mu 2}$ mode, but also to obtain an unbiased sampling of the decay modes. The secondary particles to be distinguished were the π^- from $K_{\pi 2}$-decay, (R=range ≈ 12 cm); μ^+ from $K_{\mu 2}$, ($R \approx 21$ cm); π^+ from alternative decay of the τ,

TABLE I. – *Path length of non-stopped particles obtained from systematic following of secondaries.*

Events identified $K_{\mu 2}$	Secondary Range (cm)	Type of ending	Events identified $K_{\pi 2}$	Secondary Range (cm)	Type of ending
1	6		1	1	*
2	6	–	2	2	*
3	6	0	3	3.5	*
4	7	0	4	4	*
5	7	0	5	5	§
6	7	–	6	6	*
7	9	0	7	6.5	+
8	9	0	8	7	0
9	9	–	9	7	*
10	9	–	10	9	*
11	10	0	11	11.5	0
12	10	0			
13	10	§			
14	11	0			
15	11	§			
16	11	–			
17	11	–			
18	11	0			
19	12	0			
20	12	§			
21	12	0			
22	13	–			
23	13	+			
24	14	0			
25	14	0			
26	15	0			
27	15	0			
28	16	0			
29	17	+			
30	17	0			
31	17	0			
32	17	0			
33	17	0			
34	18	0			
35	19	0			
36	19	0			
37	19	0			
38	20	0			
39	20	0			
40	21	0			

* = star in flight
0 = out of stack
⊥ = lost
§ = stopped following

($R_{max} = 3.8$ cm); e^+ from K_{e3}; and the μ^+ from $K_{\mu 3}$, ($R_{max} \approx 17$ cm, assuming the decay mode $K_{\mu 3} \to \mu^+ + \pi^0 + \nu$)

Of course not all tracks could be followed to the ends of their ranges, because some of the π-mesons interacted in flight, some tracks of all varieties were lost out of the stack by accumulated Coulomb scattering, and a few very flat tracks were lost between pellicles. All secondary tracks not stopped were blob-counted as far along the track as possible, and are listed in Table I.

For tracks not stopped, the separation of the remaining modes was based on the blob count and on the following arguments. The relative yield of K's decaying into the three-body modes such as the $K_{\mu 3}$ and K_{e3} is about 6% (*), and in addition only a fraction of their secondary energies are high enough to be confused in this analysis with a $K_{\mu 2}$ or $K_{\pi 2}$ secondary. Hence, tracks satisfying the ionization criterion for $K_{\pi 2}$ secondaries when leaving the stack have been listed as π's even though they might have been μ's from $K_{\mu 3}$ decay.

Only four secondaries were classified as $K_{\pi 2}$ in this manner, and therefore it is unlikely that one could have been a μ. Secondaries making a star in flight are also listed as π's from $K_{\pi 2}$ decay, having been separated from τ' secondaries on the basis of blob count.

The forty tracks leaving the stack at nearly minimum ionization have been called μ's from $K_{\mu 2}$. All had path lengths in the stack greater than 6 cm. Of these, 25 had path lengths less than 14 cm. We estimate that about 1% of these could be μ's from $K_{\mu 3}$, and the only other alternative, the e^+, should have been easily recognized after 6 cm by its characteristic energy loss and associated scattering. Considerable attention was given to the possibility of the incorrect identification of those secondaries that left the stack at 6 to 9 cm, which could have been high-energy electrons rather than μ-mesons from

TABLE II. – *Numbers of particles identified by systematic following of secondaries.*

Primary	Secondaries			Total
	Ending in stack	Stars in flight	Not stopped	
$K_{\mu 2}$	20	0	40	60
$K_{\pi 2}$	20	7	4	31
$K_{\mu 3}$	2	0	0	2
K_{e3}	2	0	0	2
τ'	2	0	0	2
				97

(*) See Sect. 3.

$K_{\mu 2}$-decay. The data indicate that the possibility of such misinterpretation is remote.

The number of events in each category obtained from the systematic following of secondaries as described above is shown in Table II.

Three additional $K_{\pi 2}$ secondaries were stopped out of a group of 75 secondaries described in Sect. 3·1.

2) Blob-Counting of Secondaries.

a) Introduction. – The proportion of K_{μ}-particles that could be identified by following the secondary particles was only of the order of 2.5%, and it was felt desirable to attempt the identification of further K-particles by other methods. Information regarding the velocity of emission of the secondary particles can be obtained by measurement of the track density close to the point of decay. It is known, from the foregoing results, that of those secondaries of $\beta \geq 0.7$, corresponding to values of the specific ionization below 1.3 times the minimum value, the great majority ($\sim 87\%$) result from the $K_{\mu 2}$ and $K_{\pi 2}$ modes of decay. In both cases, the secondary is monoenergetic, the ratio of the values of specific ionization being $I_{\pi 2}/I_{\mu 2} \simeq 1.15$. If the statistical fluctuations associated with the measurement of track density can be made sufficiently small, the secondaries may be resolved into one or other category with fairly high efficiency.

In order to specify the ionization of a secondary particle, it was decided to measure the blob density in the tracks. The blob density is the number, per unit track length, of clearly resolved grains or clusters of grains, and is also therefore the total number of visible gaps per unit length. Blob counting is particularly suited to tracks produced by particles of ionization close to the minimum value, and has the advantages of rapidity of measurement and minimum subjective errors.

b) Calibration. – In order that the measured blob density b may be interpreted in terms of the ionization of the particle, it is necessary to refer it to that of the track of a particle of known ionization, occurring in the same region of the emulsion. The momentum of the particles entering the stack was $\simeq 360$ MeV/*c*. Pions of this momentum have a range of 35 cm of emulsion. In order to calibrate the emulsions, it was convenient to make blob counts on the tracks of these pions at a depth of 7 cm into the stack, i.e., at about the same depth as the end points of the K-particle tracks. At this depth, the pions, with a residual range of the order of 28 cm, have practically the same velocity—and hence tracks of the same blob density—as the $K_{\mu 2}$ secondaries. For convenience, the mean blob density in the track of these pions or of the $K_{\mu 2}$ secondaries will be called the standard blob density and denoted by b_0.

The emulsion stack was developed in several batches, each batch containing 12 consecutive emulsion sheets. All emulsions in a given batch were processed simultaneously under identical conditions. Counts were made on pion tracks in each emulsion of the development batches used for the blob-count measurements. The blob densities at different emulsion depths were recorded, and hence the variation of development with depth was obtained. Within the statistical errors of the observations, this depth dependence appeared to be much the same in the different emulsions, and the depth variation assumed in the subsequent analysis was that obtained by combining the data from all the emulsions calibrated. It was found that the blob density varied trough the emulsion depth by some $\pm 6\%$ about the mean value. Relative to this mean value, that at any particular depth was determined within a statistical error of $\pm 1\%$.

The fluctuations of development between individual emulsions of a given batch were next investigated. These fluctuations comprise not only variations in sensitivity and degree of development from one emulsion to another, but also variations over the surface area of a particular emulsion. In each emulsion, b_0 was found within a statistical error of 2.5%, and internal fluctuations of b_0 between emulsions in a particular batch were consistent with this value. If real variations within such a batch existed, they were undetectable and cannot have been greater than 1%.

In the absence of such fluctuations, the value of b_0 for a particular emulsion was assumed to be equal to the mean value of b_0 for the batch. As the analysis proceeded, more $K_{\mu 2}$ secondaries were identified by tracing them to rest, and counts were made on the tracks of these particles in order to check the values of b_0 obtained from the pion tracks. The secondaries were traced from emulsion to emulsion in a batch, for distances up to ~ 3 cm from the origin, small corrections being applied to take account of the effect of slowing down. In Table III, the values of b_0 are given for four development batches in which both types of calibration were employed; the data from the pions and from $K_{\mu 2}$ secondaries are displayed separately. The two sets of data are in fair

TABLE III. – *Values of b_0 for four development batches.*

Batch No.	Emulsion No.	Calibration pions		$K_{\mu 2}$ secondaries		Mean b_0
		No. blobs	b_0	No. blobs	b_0	
2	15 – 27	13307	151.5 ± 1.3	10711	151.3 ± 1.5	151.4
3	28 – 36	6453	161.3 ± 2	8023	154.4 ± 2	157.5
5	50 – 60	10686	158.0 ± 1.5	5722	161.3 ± 2	159.6
6	61 – 66	6496	174 ± 2	5297	178 ± 2.5	176.0

agreement, and the mean, shown in the last column, is the final value of b_0 adopted for a particular batch. The statistical error on this value of b_0 is of the order of 1 %, and the variations of b_0 between different development batches greatly exceed this figure. This can presumably be accounted for by the fact that the various batches were processed at different times and in some cases were made up from different manufacturer's batches of emulsion. The processing procedure was as nearly as possible the same for the different development batches.

c) Blob counts of K secondaries. During the scanning of the emulsion stack, the approximate angles of dip of the K secondaries were recorded. From the events observed in the development batches previously calibrated, those K secondaries were selected which had recorded dip angles less than 22°, corresponding to projected track lengths $l_p > 1.5$ mm per emulsion. Blob counts were made on these, totaling 183 tracks. It is convenient to group the tracks into two categories as follows.

Class A consists of secondaries of $l_p < 5$ mm. The track was followed from the point of decay, and blob-counted along its entire length in the next emulsion. If necessary further counts were made in succeeding emulsions, until at least 600 blobs were obtained. For the track densities and lengths in this category, counts had in practice to be made in one, two, or three emulsions. Since the tracks are approximately rectilinear, the blob densities found in this way are practically independent of the variation of development with depth. The blob density was calculated from the total number of blobs and true track length calculated from l_p and assuming an emulsion thickness of 600 μm. The average number of blobs counted on Class A tracks was 855.

Class B contains the remaining secondaries, of $l_p > 5$ mm. It will be clear that, for very flat tracks, the total angle of multiple scattering may become comparable with the initial angle of dip. Flat tracks are therefore not even approximately rectilinear, and the mean blob density taken over the entire length is dependent on the depth variation. The procedure adopted for Class B tracks was to count at least 700 blobs, either in the emulsion containing the point of decay, if the track length in this emulsion was sufficient, or in the next emulsion if it was not. Counting near the top surfaces of the emulsions was avoided, since there the depth variation was most rapid. The required number of blobs was obtained in practice over a length of about 5 mm, and in this interval, as for Class A tracks, the path of the secondary was assumed to be rectilinear. The depths in the emulsion of the end points of the count were determined, and from the measured blob density and the standard value b_0 appropriate to the mean track depth and development batch, the ratio $b^* = b/b_0$ was calculated. The average number of blobs on Class B tracks was 750.

d) Total distribution. – The distribution in the values of b^* so obtained is shown in Fig. 2. In addition, the secondaries were divided into three groups: Class A secondaries of length $1.5 < l_p < 3$ mm (dip angle $22^\circ > \theta > 11^\circ$); the remaining Class A secondaries of $3 < l_p < 5$ mm (dip angle $11^\circ > \theta > 6^\circ$); and Class B secondaries of $l_p > 5$ mm and $\theta < 6^\circ$. The mean values of b^* for the three histograms were $1.03 \pm .01$; $1.05 \pm .01$; and $1.04 \pm .01$ respectively. Thus, within the limits of dip angle considered (0° to 22°), systematic errors in b^* arising from possible change in the blob-count convention with angle of dip appear to be of the order of 1% or less. This result is in strong contrast with that of BARKAS, HECKMANN and SMITH [6], who obtain a 10% increase in blob density as θ increases from 0° to 16°. A comparison of the histograms for Class A tracks and for Class B tracks also indicates that systematic errors in the assumed variation of blob density with depth in the emulsion are equally negligible.

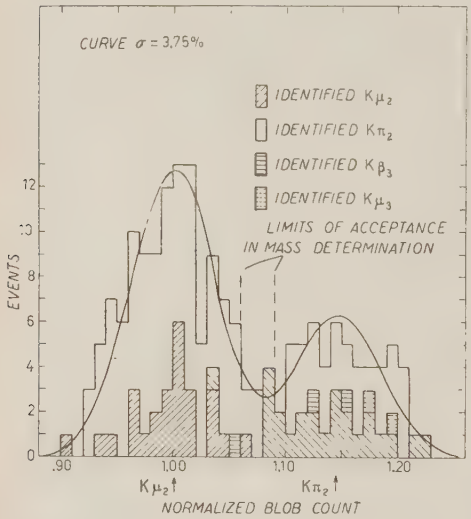

Fig. 2. – Distribution of normalized blob density for flat secondaries. Normalization is to π tracks of 210 MeV in the emulsion stack and to identified $K_{\mu 2}$ secondaries.

Included in the histogram shown in Fig. 2, and shown shaded, are the values of b^* for a few secondaries that were identified independently by following them to rest. In order to obtain results of greater statistical weight some of the $K_{\mu 2}$ secondaries so identified were also blob-counted in several emulsions (the $K_{\mu 2}$ calibration tracks described above), and the resulting distribution is shown separately in Fig. 3. The average number of blobs counted for each point in Fig. 2 was 815; in Fig. 3, 825.

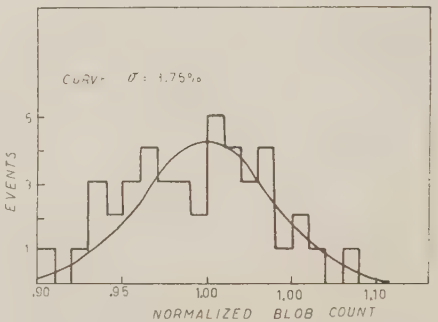

Fig. 3. – Distribution of normalized blob density for identified $K_{\mu 2}$ secondaries.

(6) W. H. BARKAS, H. H. HECKMAN and F. M. SMITH: *Nuovo Cimento*, **3**, 85 (1956).

The standard deviation of the histogram in Fig. 3 is $\simeq 4\%$. The curves in Fig. 2 show the expected Gaussian distributions in b^* for 180 tracks, for an assumed standard deviation of 4%, a mean value of b^* for the tracks of $K_{\tau 2}$ secondaries of 1.145, and a ratio of the frequencies of the two modes of decay $N_{K_{\mu 2}} N_{K_{\tau 2}}$ of 2.0. For this choice of parameters, the observed and expected distributions are in good agreement. It will be seen that the expected number of μ secondaries of $b^* > 1.07$ is about equal to the expected number of π secondaries of $b^* < 1.07$. The observed ratio of numbers of events of b^* less than and greater than 1.07, excluding identified $K_{\mu 3}$'s, in 118/62 = 1.90 ± 0.30.

3. - Relative Abundances of the Various Modes of Decay.

In computing the relative abundances of the various modes of decay, it must be borne in mind that the samples used change with the manner in which the secondaries are identified. For example, a blob count at the decay point does not distinguish between the $K_{\mu 2}$ and the K_{e3} modes, or between a $K_{\tau 2}$ secondary and a μ secondary of energy ~ 80 MeV from the $K_{\mu 3}$ mode.

The data from which the final abundances are derived are displayed in Table IV. For each mode of decay, the actual number of events found, and the correct sample size, are given. The latter is derived in a manner discussed below.

The total percentages of the τ' and $K_{\mu 3}$ types have been obtained by adding the percentage found by the scanners to the percentage found in systematically following or blob-counting secondaries. The procedure thus utilizes all available data and gives a result independent of the variation of efficiency or dark-track recognition with secondary ionization. This combining procedure requires, however, that the efficiency of dark-secondary recognition and the efficiency for finding any secondary both have the same distribution in dip angle (since only flat secondaries were systematically studied). The dip angles of all dark secondaries were measured and compared to the dip-angle distribution of 100 other secondaries randomly selected. The distributions were found to be the same and corresponded to spatial isotropy.

As described in Sect. 2.2, the over-all efficiency for detecting a K secondary during scanning is 85%. It will be assumed that the efficiency for detecting secondaries of ionization greater than 1.3 × minimum (though not necessarily recognizing them as such) is 100%.

3·1. τ, τ', *and* $K_{\mu 3}$ *Secondaries.*

1) Dark secondaries. – Those τ, τ', and $K_{\mu 3}$ secondaries recognized by the scanners as being darkly ionizing, were found among a total of

TABLE IV. - *Corrected abundances.*

K-particle Type	Secondary energy interval	Stack 20			Stack 16A			Combined data		
		No. Found	Sample	Percent	No. Found	Sample	Percent	No. Found	Sample	Percent
τ		112	2272	4.93 ± 0.46	59	803	7.35 ± 0.96	171	3075	5.56 ± 0.41
τ'	D.S. (*)	32	2272	1.41	16	803	1.99	48	3075	1.56
	Systematic following and blob count	2	320	0.63	0	20	0	2	340	0.59
	All	—	—	2.04 ± 0.51	—	—	1.99 ± 0.50	—	—	2.15 ± 0.47
$K_{\mu 3}$	D.S. (*)	7	2272	0.31	2	803	0.25	9	3075	0.29
	0–60	4	320	1.25	1	20	5.00	5	340	1.47
	60–80	2	186	1.07	—	—	—	2	186	1.07
	80–90	0	124	0	—	—	—	0	124	0
	90–110	0	91	0	—	—	—	0	91	0
	110–135	0	71	0	—	—	—	0	71	0
	All	—	—	2.63 ± 0.97	—	—	—	—	—	2.83 ± 0.99
K_{e3}	Systematic following	6	186	3.23 ± 1.30	—	—	—	6	186	3.23 ± 1.30
$K_{\mu 2}$	—	See Text			—	—	—	—	—	58.5 ± 3.0
$K_{\pi 2}$	—				—	—	—	—	—	27.7 ± 2.7

(*) D.S. represents dark secondaries recognized by scanners.

1930 K-meson endings. Correcting for the over-all scanning efficiency, we have a total 2272 K-mesons. In this sample, there were found 112 examples of τ, 37 of τ', and 7 of $K_{\mu 3}$.

2) Secondaries blob-counted and followed. – Ninety-seven secondaries were systematically followed and 183 blob-counted as described in Sect. 2·3-1 and 2·3-2. In addition, a further 75 secondaries were followed for a distance of between 5 and 8 cm (a mean of 6.5 cm), in order to find additional examples of $K_{\mu 3}$ and K_{e3}. Of the 183 secondaries blob-counted, 107 were duplicated in the systematic following. The cases of τ' and low-energy $K_{\mu 3}$ (0 to 60 MeV) systematically found came therefore from a sample of 248 K secondaries. The samples studied excluded cases of τ and τ', and of $K_{\mu 3}$ found by dark-secondary recognition, which amount to 7.1% of all K's, and therefore represented 92.6% of an unselected sample of K-mesons. After correction for scanning efficiency and for τ's and initially recognized dark secondareis, the sample number becomes 320. This correction has been made in Table IV.

3) High-energy $K_{\mu 3}$ secondaries. – Those $K_{\mu 3}$'s of secondary energy exceeding 60 MeV (ionization below 1.3 times minimum) could be found only by systematic following. For example, 172 secondaries were followed a distance such that a 70-MeV muon would have been identified. After correction for K's with recognized dark secondaries, the sample number becomes 186. The $K_{\mu 3}$ data have been grouped in Table IV for several secondary energy intervals. The number of K-mesons in the sample diminishes at higher muon energies, as the number of secondaries followed out to sufficiently great distances to ensure identification becomes progressively smaller.

3·2. K_{e3} secondaries. – K_{e3} secondaries were found only by following 162 K-meson secondaries, or in a sample of 186 K-mesons of all types. The shortest distance followed, for which the secondary remained near minimum ionization, was 5 cm. Ninety-three percent of the secondaries were followed 6 cm or otherwise identified, and 76% of the secondaries were followed at least 9 cm or otherwise identified (i.e., observation of star in flight, or ionization above plateau). Such K_{e3} secondaries as were found were readily identified by observing the increase in multiple scattering of their tracks, which typifies large energy losses. At 6 cm, 90% of the electrons will lose more than $\frac{3}{4}$ of their energy, while at 9 cm essentially all lose $\frac{3}{4}$ of their energy. Thus, we estimate that our over-all efficiency for discriminating between 250 MeV electron secondaries and $K_{\mu 2}$ secondaries was better than 96%. The six electron secondaries in the above samples had $p\beta$ = 73, 75, 80, 100, 183, and 200 MeV/c.

3·3. $K_{\mu 2}$ *and* $K_{\pi 2}$ *secondaries.* – One hundred forty-nine $K_{\mu 2}$ and 77 $K_{\pi 2}$ were found by the methods described in Sects. 2·3-1 and 2·3-2. From their

ratio, corrected for scanning efficiency (Appendix A), and the total percentage of $K_{\mu 2}$ and $K_{\pi 2}$, the percentage of each was determined.

Additional data obtained from a smaller stack [1] (16A) are shown in Table IV. The data from both stacks have been combined in the last column.

3·4. *Comparison with other data.* – In Table V our results are compared with nuclear-emulsion-stack results from other laboratories [7-12]. The abundances for the τ' and the $K_{\mu 3}$ in the first three columns have been derived from the published data by means of the methods described in Sections 3·1 and 3·2. The data of columns 2 and 3 have been corrected for scanning efficiencies derived by assuming 100% efficiency for τ's and a τ abundance of 5.6%. The numbers in columns 4, 5 and 6 are as quoted in the references except that we have computed the uncertainties on the Rochester results on the basis of the number of events of each type found. Statistics in the table are based upon the square root of the number of events and therefore have the significance of standard deviations only for those cases with large numbers of events.

In the last five rows of Table V are given the conditions of exposure of the nuclear emulsion stacks. With one possible exception there are no significant variations in the relative yield of K-mesons of different types under the different exposure conditions. The one possible exception is the K_{e3}, which appears from Table V to be found less frequently under conditions of longer flight time. Specifically, the combined short time-of-flight data of GS and EP give 10 K_{e3} compared to 94 $K_{\pi 2}$ and $K_{\mu 2}$. The combined long time-of-flight results from M.I.T., Dublin, our work give 13 K_{e3} compared to 326 $K_{\pi 2}$ and $K_{\mu 2}$. With these data and the equal lifetimes of $1.2 \cdot 10^{-8}$ s for the $K_{\pi 3}$ and $K_{\mu 2}$ [13] we can determine the K_{e3} lifetime, assuming the abundances at production to be the same under all conditions of exposure. The result for the K_{e3} mean lifetime is $0.62 \cdot 10^{-8}$ s, with a 90% probability of its lying between 0.47 and $0.94 \cdot 10^{-8}$ s. Conversely, if we assume both that the relative production abun-

(7) G-Stack Collaboration: *Nuovo Cimento*, **2**, 1063 (1955).

(8) D. Ritson, A. Pevsner, S. Fung, M. Widgoff, G. T. Zorn, G. Goldhaber and S. Goldhaber: *Phys. Rev.*, **101**, 1085 (1956).

(9) J. Crussard, V. Fouché, J. Hennessy, G. Kayas, L. Leprince-Ringuet, D. Morellet and F. Renard: *Nuovo Cimento*, **3**, 731 (1956).

(10) F. M. Smith, H. H. Heckman and W. H. Barkas: *Composition of a Secondary-Particle Beam from the Bevatron*, UCRL-3289, March, 1956.

(11) T. F. Hoang, M. F. Kaplon and G. Yekutieli: *Phys. Rev.*, **102**, 1185 (1956).

(12) C. O'Ceallaigh, Alexander and R. H. W. Johnston: *Proceedings of Sixth Annual Rochester Conference on High-Energy Physics*, 1956.

(13) V. Fitch and R. Motley: *Phys. Rev.*, **101**, 496 (1956). L. W. Alvarez, F. C. Crawford, M. L. Good and M. L. Stevenson: *Phys. Rev.*, **101**, 503 (1596).

TABLE V. – *Comparison of abundances from different laboratories.*

	G.S. [7]	E.P. [8]	MIT [9]	S.H.B. [10]	Rochester [11]	Dublin [12]	Our data
τ	(5.6)	(5.6)	(5.6)	7.8 ± 1.4	5.2 ± 1.6	6.5 ± 0.6	5.56 ± 0.41
τ'	1.1 ± 0.6	0.8 ± 0.4	1.6 ± 0.8	1.9 ± 0.8	3.5 ± 1.4	3.9 ± 1.6	2.15 ± 0.47
$K_{\mu 2}$	63 ± 8	57 ± 6	60 ± 10	65.2 ± 10.3	59 ± 8	51.0 ± 5.7	58.5 ± 3.0
$K_{\pi 2}$	19 ± 5	25 ± 5	20 ± 10	21.4 ± 5.6	21 ± 6	27.5 ± 4.2	27.7 ± 2.7
$K_{\mu 3}$	2.5 ± 1.2	3.8 ± 2.3	1.3 ± 0.7	1.1 ± 0.7 *	$6 \pm ?$ *	7.2 ± 2.1	2.83 ± 0.95
K_{e3}	9.1 ± 4.1	$7.9 + 3.5$	2 ± 2	$2.6 + 2.2$ * 1.7	$5 + 3.5$ *	3.9 ± 1.6	3.23 ± 1.30
Primary Beam	Cosmic rays	6.2 GeV protons (Bevatron)	6.2 GeV protons (Bevatron)	4.8 GeV protons (Bevatron)	2.9 GeV protons (Cosmotron)	6.2 GeV protons (Bevatron)	6.2 GeV protons (Bevatron)
Target	Emulsion stack	Emulsion stack	Ta	Ta	Cu	Cu	Cu
K production angle	0-180°	90° favored	90°	90°	60°	90°	90°
K energy (MeV)	Various	100-240	100	126	63	114	114
Proper time of flight (seconds)	$> 5 \cdot 10^{-10}$	$3\text{-}9 \cdot 10^{-10}$	$1.5 \cdot 10^{-8}$	$1.2 \cdot 10^{-8}$	$2.16 \cdot 10^{-8}$	$1.35 \cdot 10^{-8}$	$1.35 \cdot 10^{-8}$

(*) Based on a fraction of the complete spectrum.

dances under all conditions are equal and that the K_{e3}, $K_{\pi 2}$, and $K_{\mu 2}$ have the same lifetime, the purely statistical probability of obtaining such poor agreement between the short- and long-flight-time K_{e3} abundances is less than 0.02. Further study is required to resolve this discrepancy or to verify the difference in the K_{e3} behavior.

4. – Range Measurements on $K_{\mu 2}$ and $K_{\pi 2}$ Secondaries.

4·1. *Method.* – The measurement of the range of each particle consisted of adding the chords between points where the track made large single scatters or accumulated multiple scatters of at most 10°. This range includes the air gaps between pellicles and therefore, when multiplied by the gross density of the stacked emulsion, gives the range in g cm^{-2}.

The gross density was measured by the following procedure. The emulsion stack was first clamped tightly, with no tissue paper spacers, between $\frac{3}{4}$-in. bakelite plates by means of bolts going through holes punched in the pellicles. All outside edges were machined smooth. The stack density was then determined by over-all weight and dimensions to be 3.80 ± 0.02 g cm^{-3}. The error is derived from the fluctuations in the thickness of the stack as measured at twelve different places.

The projected distances (Δx, Δy) between points were obtained by taking differences between the microscope stage screw readings. For each chord, Δz was taken equal to the number of plates traversed multiplied by the average apparent plate thickness before development obtained from the over-all thickness of the stack. Thus the air gaps are included in both the range and the density measurements. The individual plates were aligned by brass tabs which were glued on the corners with respect to X-ray fiducial marks.

The range-energy curve used ([14]) was calculated for an emulsion density of 3.815 g cm^{-3}, and the measured ranges must be transformed correspondingly. If the difference between this value and our measured density was due only to the air gaps in the stack the ranges in centimeters would transform inversely as the ratio of the densities. If part of the difference was due to water content of the emulsions—an exact calculation would have allowed for the change in stopping power with water content—that is, if the pellicle density, assumed to be 3.815, was actually 3.825. For example, in this humidity region the density ratios must be corrected by addition of a quantity that is equal to 0.05 times the relative difference in density ($\Delta\varrho/\varrho$) ([5]).

([14]) W. H. BARKAS and D. M. YOUNG: *Emulsion Tables. I. Heavy-Particle Functions*, UCRL-2579 (Rev.), Sept. 1954.

In order to estimate the actual emulsion density, and hence the stopping power of our stack, we have measured the ranges of 46 nearly flat secondaries from π-μ decays, each contained within a single pellicle. These tracks were picked with a dip angle such that a 10% uncertainty in the shrinkage factor would lead to an error of less than 0.25% in the range of the muon. The average muon range obtained was (596.4 ± 6) μm, which agrees with that obtained by the G-Stack Collaboration [7] of (597.8 ± 2.1) μm for a density of 3.825 g cm^{-3}. Thus the uncertainty in stopping power due to the uncertainty of water content is less than 0.05%. This represents a negligible contribution to the errors in the $K_{\mu 2}$ and $K_{\pi 2}$ secondary ranges.

4·2. *Mass of the* $K_{\mu 2}$ *and* $K_{\pi 2}$ *from ranges of the secondaries.* – The range distributions of the 20 muons and 23 pion secondaries that stopped in the stack are given in Fig. 4. Shown also are the standard deviations of the experimental distributions, which agree well with the theoretical range straggling. The mean ranges for the stack density of 3.80 g cm^{-3} are

$$R_\mu = (20.90 \pm 0.13) \text{ cm},$$

$$R_\pi = (11.70 \pm 0.065) \text{ cm}.$$

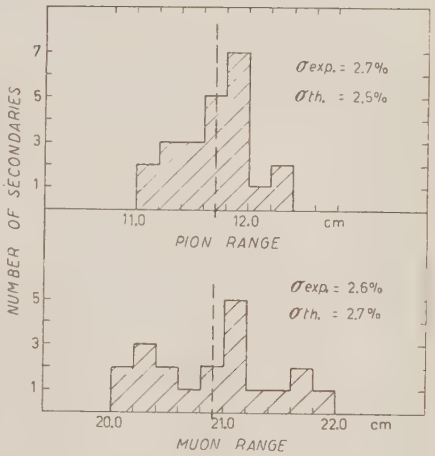

Fig. 4. – Distribution of $K_{\mu 2}$ and $K_{\pi 2}$ secondary ranges. The dashed line shows the position of the mean of the distribution. σ_{exp} is the experimental standard deviation and σ_{th} is the theoretical straggling.

These ranges have been converted to a density of 3.815 g cm^{-3}, and the energies computed corresponding to these ranges, assuming the decay schemes

$$K_{\mu 2} \rightarrow \mu^+ + \nu,$$

$$K_{\pi 2} \rightarrow \pi^+ + \pi^0,$$

and are shown in Table VI.

TABLE VI. – *Ranges and energies of* $K_{\mu 2}$ *and* $K_{\pi 2}$.

	Secondary range Density = 3.815 g cm^{-3}	Secondary energy
$K_{\mu 2}$	20.84 ± 0.13 cm	152.36 MeV
$K_{\pi 2}$	11.65 ± 0.067 cm	107.67 MeV

The K-particle masses are computed from these energies by use of the following pion and muon masses ([15,16]):

$$M_{\pi^+} = 273.3\ m_e\ ,$$

$$M_{\pi^-} = 272.8\ m_e\ .$$

$$M_{\pi^-} - M_{\pi^0} = 8.8\ m_e\ ,$$

$$M_{\mu^+} = 206.9\ m_e\ .$$

The results are:

$$M_{K_{\mu 2}} = (964.8 \pm 2.4)\ m_e\ .$$

$$M_{K_{\pi 2}} = (964.2 \pm 1.8)\ m_e\ .$$

where the errors given are due only to the standard deviation of the mean of the experimental range straggling.

Listed for comparison are the mass values from other laboratories, computed by use of the Barkas and Young range-energy curves ([14]).

	$K_{\mu 2}$	$K_{\pi 2}$
G-Stack ([7])	962.8 ± 4	969.3 ± 3
E.P. ([8])	952 ± 4	969 ± 4
M.I.T. ([9])	962.4 ± 5	963.6 ± 4.3

The curves from Baroni *et al.* ([17]) give consistent values for the $K_{\pi 2}$ mass but raise the $K_{\mu 2}$ mass about 13 m_e.

4·3. *Discussion of Results.* – Besides the quoted statistical errors the uncertainty in the value of the π mass contributes to an error of the order of $\pm 1\ m_e$ in the K mass. The $\frac{1}{2}\%$ uncertainty in the density becomes $\pm 1.2\ m_e$ for the $K_{\pi 2}$ mass nad $\pm 2\ m_e$ for the $K_{\mu 2}$ mass.

As a check for further systematic errors, we remeasured all the pion secondaries, and found a negligible change in the mean range caused by the measurement procedure.

([15]) W. H. BARKAS, W. F. BIRNBAUM and F. M. SMITH: *Phys. Rev.*, **101**, 778 (1956).

([16]) W. CHINOWSKY and J. STEINBERGER: *Phys. Rev.*, **93**, 586 (1954).

([17]) G. BARONI, C. CASTAGNOLI, G. CORTINI, C. FRANZINETTI and A. MANFREDINI: *CERN Report BS9.*

There is also the question as to the reliability of the range-energy relation. Recently BARKAS *et al.* [18] have made an experimental determination of the ranges of pions of known energy for five values of energy up to about 100 MeV. They have recalculated the Barkas-Young values normalized to these experimental points. In the region above the last experimental point, the curve is extrapolated theoretically as before. With this new relation our mass values become

$$M_{K_{\mu 2}} = (965.8 \pm 2.4)\ m_e\ ,$$

$$M_{K_{\pi 2}} = (962.8 \pm 1.8)\ m_e\ .$$

For comparison, the mass of the τ [5] computed from the Q of the decays in this stack, and from one other stack treated in a similar manner, is

$$M_\tau = 966.1 \pm 0.7\ .$$

5. – Primary Mass.

The masses of the various types of K particles have also been measured by the primary range-momentum method. Measurements were made only on those tracks whose secondaries had been identified. Ranges of the K particles were measured along the track by the same method as were the secondaries. The momentum of each particle was determined from its entrance position in the stack, by measurement of the range of the protons entering the same position and hence their momentum. In the case of the protons, the measured ranges were actually projected ranges, and a correction to account for the range shortening due to multiple scattering effectively increased the K-meson

TABLE VII. – *Masses by Range-Momentum Method.*

Type	Mass (m_e)	No. Measured
τ	966.3 ± 2.1	77
τ'	967.7 ± 4	21
$K_{\mu 2}$	967.2 ± 2.2	96
$K_{\pi 2}$	966.7 ± 2.0	54
$K_{\pi 3}$	969 ± 5	12
K_{e3}	967 ± 8	6

[18] W. H. BARKAS, P. H. BARRETT, P. CÜER, H. H. HECKMAN, F. M. SMITH and H. TICHO: *High-Velocity Particle Ranges in Emulsion*, UCRL-3254, Jan. 1956, and W. H. BARKAS: private communication.

mass by about $2\,m_e$. In addition, the different energy loss of K's and protons in the air path through the deflecting magnet and subsequent field-free region ahead of the stack required a mass correction of from 6 to $8\,m_e$ on each particle, varying slightly with the incident momentum. Details of these and other corrections appear elsewhere [4].

The final corrected values of the masses, with the number of particles measured for each variety, are shown in Table VII.

6. – Conclusions.

We have measured the masses of the various decay modes of positive K-mesons by two independent methods. The first is the measurement of the Q of the decay for the $K_{\mu 2}$, $K_{\pi 2}$, and τ; the second is the range-momentum method applied to the primaries. In the first method, the largest mass difference, that of $M_\tau - M_{K_{\pi 2}}$, is $(3.3 \pm 2.4)\,m_e$. The error includes (*a*) $\pm 1.9\,m_e$, statistical standard deviation; (*b*) $\pm 1.4\,m_e$, for possible variation in stack density; and (*c*) $\pm 0.6\,m_e$, for the uncertainty in pion masses. If the uncertainty of the range-energy relation is included the significance of the small mass difference decreases.

In the second method the masses are all the same within experimental error. In particular $M_\tau - M_{K_{\pi 2}}$, is $(-0.4 \pm 2.9)\,m_e$.

It is shown in Sect. 3 that our data on the relative abundances are the same as those taken under entirely different conditions of exposure and flight time, with the possible exception of the K_{e3}. If we also consider the equality of the masses it appears that we are observing different decay modes of the same particle.

However, this conclusion is in strong contradiction with the most likely spin and parity assignments of the τ-meson (0^- or 2^-), which configurations are not possible for a $K_{\pi 2}$. Various theoretical and phenomenological descriptions have been proposed in order to resolve this dilemma, none of which are really satisfactory. For example, the cascade scheme [3] demands at least $10\,m_e$ difference between the τ and $K_{\pi 2}$ to account for the observed half life for a $0 \to 0$ spin transition. This mass difference is well outside our experimental errors. Furthermore, neither the $K_{\pi 2}$ [19] nor the τ is believed to have spin one, hence transition $0 \to 1$ and $1 \to 0$ are not considered.

Transitions from $0 \to 2$ or $2 \to 0$ demand about $3\,m_e$ to account for the observed half lives. The experiment of ALVAREZ *et al.* [20] shows that any

[19] B. J. MOYER and J. OSHER: Private communication.

[20] L. W. ALVAREZ, N. C. CRAWFORD, M. L. GOOD and M. L. STEVENSON: *Proceeding of Sixth Annual Rochester Conference on High-Energy Physics*, 1956.

γ-rays accompanying the transition $\tau \to K_{\pi 2}$ must be less than $1\,m_e$ total energy, thus ruling out spin changes of ≥ 2. The possibility of the reverse transition, viz. $K_{\pi 2} \to \tau + \gamma$, is not excluded by the above experiment. In addition, a $2^- \to 2^-$ transition requires only a 6 keV mass difference to give the observed half life, and no experiment to date has had sufficient sensitivity to detect a mass difference this small. However, we believe that the zero spin assignments are the most probable and therefore the cascade scheme is unsatisfactory.

Other suggestions [21-23], while accounting for the mass degeneracy, must rely on an accident of nature to explain the half-life degeneracy. A more recent proposal, now being studied by BLUDMAN and RUDERMAN [24], has been to postulate the existence of a scalar π^0 in addition to the usual pseudoscalar π^0, with the result that the neutral and positive K particles have different parity. Then the positive τ and $K_{\pi 2}$ could both be 0^-.

The reader is referred to the proceedings of the 1956 Rochester Conference [25] for discussions of other theories that would have the τ and $K_{\pi 2}$ be the same particle.

* * *

This experiment has been carried out with the guidance and encouragement of Professor CHAIM RICHMAN. It could not have been successfully completed without the help of many other people. Our thanks are due to Mr. C. WALLER and the group at Ilford Ltd. for their co-operation in making the large emulsion stack used. Dr. EDWARD LOFGREN and the members of the Bevatron staff aided in the successful exposure of the stack. Mr. LEROY KERTH aided in the design and setup of the strong-focusing spectrometer

The emulsion were mounted on glass supplied with a grid co-ordinate system developed by Mr. PHILIP CARNAHAN. The processing of the stack was a group effort, with many late shifts taken by Mr. JACK SANDWEISS.

Some of the secondaries were followed by Dr. LUDWIG VAN ROSSUM and Dr. STANLEY LEONARD.

One of the most important phases of the work, that of scanning the stack, was done by Mrs. BEVERLY BALDRIDGE, Miss IRENE D'ARCHE, Mrs. EDITH GOODWIN, Mrs. MARILYNN HARBERT, and Miss KATHRYN PALMER. Range measu-

(21) T. D. LEE and C. N. YANG: *Phys. Rev.*, **102**, 290 (1956); M. GELL-MANN: private communication.

(22) S. BLUDMAN: *Interpretation of K-Meson Decays*, UCRL-3217, Jan. 1956.

(23) M. LYNN STEVENSON: *The Ratios of Lifetimes of Heavy Mesons and Hyperons as Predicted by Phase Space*, UCRL-3275, Feb. 1956.

(24) S. BLUDMAN and M. RUDERMAN: private communication.

(25) *Proceedings of Sixth Annual Rochester Conference on High-Energy Physics*, 1956.

rements of primaries and τ and π-μ decays were done by Mr. Victor Cook, Mr. George Preston, and Mr. Norman Thomas. We are grateful for the patient and careful work of all of this group.

This work was done under the auspices of the U. S. Atomic Energy Commission.

Appendix

Effect of Efficiency of Detection of K Secondaries on the Relative Abundances.

As mentioned in Sect. 2·2, the over-all efficiency for detection of K secondaries by the scanners is 85%. Since 8% of the K-particles yield secondaries of ionization exceeding twice the minimum value, for which the efficiency is presumably 100%, this implies that 16% of the lightly ionizing secondaries escape detection. We shall consider how this loss affects the relative abundances of the predominant decay modes $K_{\pi 2}$ and $K_{\mu 2}$. (The statistical errors on the frequencies of the rare modes K_{e3} and $K_{\mu 3}$ are at present so large that small effects due to scanning inefficiency will not be considered).

A $K_{\pi 2}$ or $K_{\mu 2}$ secondary may escape detection for two main reasons. (*a*) Fluctuations in grain density occur, and a chance absence of grains close to the point of decay can lead to failure to pick up the track. (*b*) The stopping point of the primary particle may be close to the emulsion surface, so that if the secondary is directed outwards, its track may be missed because of its shortness, or the somewhat lower grain density near the top surface of the emulsion, or the presence of surface markings at the glass interface.

In (*a*), the probability of detection depends on the mean grain density, which is 15% greater in the tracks of $K_{\pi 2}$ secondaries than for $K_{\mu 2}$. The scanners scrutinize a roughly spherical volume, of ~ 50 μm radius about the end point of each stopping particle, for evidence of a secondary. Assuming a random distribution of grains along the secondary tracks, we have calculated the expected detection efficiency for each decay mode, on the simplifying assumption that some minimum number of grains must occur along the first 50 μm of track in order for the secondary to be detected. For a given value of the true ratio $R_0 = N_{K\mu 2}/N_{K\pi 2}$, we can then find the expected ratio R in terms of the total efficiency ε for detecting both types of secondary. We find that $S = R/R_0$ varies almost linearly with ε, and that for the measured value of $\varepsilon = 84\%$, $S = 0.89$. Thus, for $R = 1.93 \pm 0.29$, the true ratio becomes $R_0 = 2.12 \pm 0.30$. We feel that this value of R_0 will be, if anything, an overestimate, for the reasons given above: (*a*) it is certain that fluctuations of grain density over distances less than 50 μm will (in many cases) be of importance in detecting the track; and since these fluctuations will be greater than those over 50 μm lengths, the bias in favor of $K_{\pi 2}$ secondaries will be correspondingly less. (*b*) surface effects may account for a 5% to 10% loss.

RIASSUNTO (*)

Per misurare la massa delle particelle K e la loro abbondanza si è esposto un grosso pacco di emulsioni al raggio di K positivi del bevatrone di 6 GeV di Berkeley. Le masse per i modi di decadimento $K_{\mu 2}$; $K_{\pi 2}$ e τ si sono ottenute misurando il range medio dei secondari. Si sono inoltre misurate col metodo range-momento per tutti i modi di decadimento le masse rispetto alla massa del protone. Le abbondanze si sono determinate seguendo le tracce dei secondari e col conteggio dei blob. I dati sono esposti nella seguente tabella:

Tipo	Abbondanze %	Massa del primario (m_e)	Massa del range del secondario (m_e)
τ	5.56 ± 0.41	966.3 ± 2.1	966.1 ± 0.7
τ'	2.15 ± 0.47	967.7 ± 4	—
$K_{\mu 2}$	58.2 ± 3.0	967.2 ± 2.2	965.8 ± 2.4
$K_{\pi 2}$	28.9 ± 2.7	966.7 ± 2.0	962.8 ± 1.8
$K_{\mu 3}$	2.83 ± 0.95	969 ± 5	—
K_{e3}	3.23 ± 1.30	967 ± 8	—

(*) *Traduzione a cura della Redazione.*

Evaluation of the Scattering Lengths in Pion-Nucleon Scattering. (*).

J. Orear

Columbia University - New York

(ricevuto il 16 Luglio 1956)

Summary. — All the pion-proton scattering data below 60 MeV which provide values and errors for the phase shifts have been used to obtain the s-wave scattering lengths. The results are $a_1 = 0.167 \pm .012$ and and $a_3 = -0.105 \pm .010$. The value $(a_1 - a_3) = 0.26 \pm .04$ as obtained from recent photoproduction results and Panofsky ratio values was also used. The scattering length for α_{33} becomes $a_{33} = 0.22 \pm .03$ if one assumes the linear Chew-Low energy dependence up to 170 MeV.

A considerable amount of new data relevant to the low energy phase shifts in pion-nucleon scattering were presented at the CERN Symposium, June 1956. The quantity of data is now sufficient to make an accurate determination of the s-wave phase shifts at low energy. In this determination we assume $\alpha_1 = a_1 \eta$ up to 42 MeV and $\alpha_3 = a_3 \eta$ up to 58 MeV where η is the pion momentum in the center of mass system in units of μc. The Carnegie Tech data [1] at 150, 170 and 220 MeV justify this assumption of linearity at low energies. In fact it appears that α_3 remains fairly linear up to 220 MeV, but that α_1 departs from linearity and becomes fairly constant with energy from 150 to 220 MeV [1,2].

A least squares determination of a_1 and a_3 is made to all pion-nucleon scattering data in this low energy region. Because the errors of the phase

---

(*) Supported by the joint program of the United States Office of Naval Research and the United States Atomic Energy Commission.

(1) J. Ashkin, J. P. Blaser, F. Feiner and M. O. Stern: *Phys. Rev.*, **101**, 1149 (1956) and private communication from J. Ashkin.

(2) J. Orear: *Proceedings of the CERN Symposium*, in press.

shifts must be known in order to obtain a least squares solution, we use only those data which quote both phase shifts and their errors. For an ideal least squares analysis, the various laboratories should use the same criteria in evaluating their errors. The 65 MeV Columbia π scattering results were not used because they are in need of revision due to the change in the Panofsky ratio and because no error analysis has been made ([3]).

In addition to the pion scattering results, we used the value of $(a_1 - a_3)$ at zero energy obtained from the most recent photoproduction and Panofsky ratio results. The evaluation was made at threshold by the same method described previously ([4]). The value $\sigma = (1.43 \pm .02) \cdot 10^{-28} \eta$ cm^2 was used for the s-wave total cross-section at threshold for $\gamma + P \to N + \pi^+$ ([5,6]). The value $r_0 = 1.87 \pm .13$ was used for the threshold ratio of π^- to π^+ photoproduction in deuterium ([5]). Unfortunately it is still a matter of guesswork how much Coulomb correction to use. This author prefers a $(10 \pm 10)\%$ threshold correction which raises r_0 to 2.08. BERNARDINI pointed out that a 10% correction at threshold means a Coulomb correction significantly less than 10% in the energy region where the deuterium experiments were performed ([6]). The value $1.42 \pm .20$ was used for the Panofsky ratio. This is the average of the two new values given at the CERN Symposium ([7,8]). An additional 10% error is given to the result $(a_1 - a_3) = 0.26$ because of the arguments of NOYES ([9]). He shows that if one chooses rather extreme models for the s-wave pion-nucleon potential, the failure of isotopic spin conservation can affect $(a_1 - a_3)$ by as much as 10%.

Table I shows the 9 experimental values ([10-17]) used in making the least

([3]) A. SACHS: private communication.

([4]) J. OREAR: *Phys. Rev.*, **96**, 176 (1954).

([5]) M. BENEVENTANO, G. BERNARDINI, D. CARLSON-LEE, G. STOPPINI and L. TAU: *Nuovo Cimento*, **4**, 323 (1956).

([6]) We wish to thank G. BERNARDINI for carefully checking this evaluation.

([7]) J. M. CASSELS: *Proceedings of the CERN Symposium*, in press.

([8]) A. W. MERRISON: *Proceedings of the CERN Symposium*, in press.

([9]) H. P. NOYES: *Phys. Rev.*, **101**, 320 (1956).

([10]) M. C. RINEHART, K. C. ROGERS and L. M. LEDERMAN: *Phys. Rev.*, **100**, 883 (1955).

([11]) D. NAGLE, R. HILDEBRAND amd R. PLANO: *Proceedings of the CERN Sympsium*, in press.

([12]) W. SPRY: *Phys. Rev.*, **95**, 1295 (1954); J. TINLOT and A. ROBERTS: *Phys. Rev.*, **95**, 137 (1954).

([14]) S. L. WHETSTONE and D. H. STORK: *Phys. Rev.*, **102**, 251 (1956).

([15]) J. OREAR, W. SLATER, J. J. LORD, S. L. EILENBERG and A. B. WEAVER: *Phys. Rev.*, **96**, 174 (1954).

([16]) J. OREAR, J. J. LORD and A. B. WEAVER: *Phys. Rev.*, **93**, 575 (1954).

([17]) D. BODANSKY, A. SACHS and J. STEINBERGER: *Phys. Rev.*, **90**, 996 (1953).

squares determination of a_1 and a_3. The result is

$$(1) \qquad a_1 = 0.167 \pm .012 , \qquad a_3 = -0.105 \pm .010 .$$

The least squares sum evaluated at the solution is $M = 3.24$. This agrees well with the expected mean value $M = 7$ in the case of 9 experimental values fitted with 2 independent parameters. The small value of M is an additional confirmation of the assumption of linearity.

TABLE I. – *List of all low energy* π-p *scattering data containing s-wave phase shifts with errors* a_1 is α_1/η and a_3 is α_3/η .

Energy	Reference	a_3	$(a_1 - a_3)$	$(2a_1 + a_3)$
0 MeV (π^- capture)	this paper	—	$0.26 \pm .04$	—
$2.5 \div 30$ MeV π^-	[10]	—	—	$0.25 \pm .05$
$10 \div 30$ MeV π^-	[11]	—	—	$0.23 \pm .04$
$10 \div 35$ MeV π^+	[12]	$-0.13 \pm .035$	—	—
20, 30, 40 MeV π^-	[13]	—	$0.27 \pm .03$	—
22 MeV π^+	[14]	$-0.098 \pm .0146$	—	—
26 MeV π^-	[15]	—	—	$0.152 \pm .087$
45 MeV π^+	[16]	$-0.138 \pm .03$	—	—
58 MeV π^+	[17]	$-0.10 \pm .02$	—	—

A least squares fitting of the level shifts in pi-mesic atoms gives $a_1 = 0.145 \pm .02$ and $a_3 = -0.11 \pm .014$ assuming the effects of individual nucleons are purely additive ([18]). These results were not used in the determination of a_1 and a_3 because they depend on the assumption of additivity. However, now that a_1 and a_3 are well known from the scattering data, a comparison can be made with the pi-mesic atom results to check the assumption of additivity. The assumption appears to pass the test quite well.

Our previous evaluation ([4]) of the scattering length for α_{33} assumed the energy dependence $\alpha_{33} = a_{33}\eta^3$ up to 80 MeV. This gave the result $a_{33} = 0.235$. However, if the two parameter energy dependence suggested by CHEW and LOW ([19])

$$(2) \qquad \frac{\eta^3}{\omega^*} \cot \alpha_{33} = \frac{3}{4f^2}\left(1 - \frac{\omega^*}{\omega_0^*}\right)$$

had been used with exactly the same data, a lower value for a_{33} would have

([18]) M. B. STEARNS and M. STEARNS: *Energies of* π-*Mesonic* X-*rays*, in *Phys. Rev.*, in press.

([19]) G. CHEW and F. LOW: *Phys. Rev.*, **101**, 1570 (1956).

resulted. From a purely empirical point of view the energy dependence given by Eq. (2) fits the values of α_{33} up to 170 MeV remarkably well when the values $f^2 = 0.087$ and $\omega_0 = 2.17$ are used. This is seen in Figure 1. The straight line of Fig. 1 corresponds to $a_{33} = 0.22 \pm .03$ at $\omega^* = 1$.

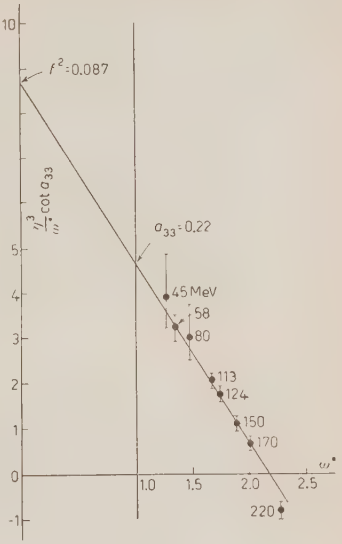

Fig. 1. - Chew-Low plot of α_{33} showing experimental values and their errors at 45, 58 80, 113, 124, 150, 170 and 220 MeV which are given in references ([16,17,20,21,20,2,2]) and ([2]) respectively. The line has the value 4.6 at $\omega^* = 1$ which corresponds to $\alpha_{33} = 0.22\eta^3$ at threshold.

* * *

The author wishes to thank Professors PUPPI, BERNARDINI and STANGHELLINI for helpful discussions and is grateful for the hospitality extended to him during his visit to the University of Bologna.

([20]) G. QUARENI: *Proceedings of the CERN Symposium*, in press.
([21]) J. OREAR: *Phys. Rev.*, **96**, 1417 (1954).

RIASSUNTO (*)

Tutti i dati sullo scattering pione-protone al disotto dei 60 MeV che forniscono valori ed errori per gli spostamenti di fase sono stati usati per ottenere le lunghezze di scattering delle onde *s*. I risultati sono $a_1 = 0.167 \pm .012$ e $a_3 = -0.105 \pm .010$. Si è anche usato il valore $(a_1 - a_3) = 0.26 \pm .04$ ottenuto da recenti risultati di fotoproduzione del rapporto di Panofsky. La lunghezza di scattering per α_{33} risulta $a_{33} = 0.22 \pm .03$ assumendo la dipendenza lineare dell'energia di Chew-Low fino a 170 MeV.

(*) *Traduzione a cura della Redazione.*

IL NUOVO CIMENTO Vol. IV, N. 4 1° Ottobre 1956

Quantentheorie der Felder als Distributionstheorie.

W. Schmidt und K. Baumann

Institut für theoretische Physik der Universität - Wien

(ricevuto il 16 Luglio 1956)

Zusammenfassung. — Die Distributionstheorie von L. Schwartz wird zu einer mathematisch konsistenten Formulierung der Quantenfeldtheorie verwendet. Die Einführung von Distributionen impliziter Funktionen gestattet es, viele Formeln mit geringfügigen Änderungen in den strengen Formalismus zu übernehmen. Die Annahme, daß es eine raumzeitliche Feldoperatordistribution gibt, führt auf einen von Wightman angegebenen Hilbertraum. Er ist durch eine Folge von Distributionen, die Vakuumerwartungswerte der Theorie, bestimmt. Diese werden für die freien Felder (Schrödinger-Gordon-Feld, Maxwellfeld, Diracfeld) aus einfachen Annahmen hergeleitet. Beim Maxwellfeld ergibt sich zwanglos, daß die Metrik nur in dem durch die Lorentzbedingung eingeschränkten Hilbertraum definit ist. Die Definition einer Dichte-Distribution, welche den üblichen Doppelpunktprodukten entspricht, erweist sich auch in dieser Fassung der Quantenfeldtheorie als möglich.

1. – Einleitung.

Es gibt bisher anscheinend keine allen Anforderungen mathematischer Strenge genügende Formulierung der Quantenfeldtheorie. Die Darstellung von Friedrichs [1] dürfte nicht leicht auf Felder mit Wechselwirkung zu verallgemeinern sein; auch wird der Distributionsbegriff nicht benützt und die Kovarianz geht durch die Verwendung von Raumintegralen verloren. Ähnliches gilt für eine Arbeit von Cook [2].

Eine befriedigende Fassung der Theorie gewinnt man, wenn man raum-

[1] K. O. Friedrichs: *Mathematical Aspects of Quantum Field Theory* (New York, 1953).

[2] J. M. Cook: *Trans. Am. Math. Soc.*, **74**, 122 (1953).

zeitliche Distributionen [3] von Feldoperatoren als Grundgrößen einführt. Man gelangt so dazu, eine Feldtheorie durch die Vakuumerwartungswerte der Produkte aus den Feldoperatoren, also ebenfalls gewisse Distributionen, zu definieren. Obwohl in dieser Arbeit diese Distributionen nur für die wichtigsten freien Felder tatsächlich aufgesucht werden, liegt damit ein für beliebige — auch wechselwirkende — Felder gültiger Rahmen vor. Es verbleibt noch die Aufgabe, Integralgleichungen zu finden, deren Lösungen die Vakuumerwartungswerte der wechselwirkenden Felder sind und in welchen keine unendlichen Renormierungskonstanten auftreten. Dieses Problem wurde ebenfalls schon behandelt [4].

2. – Der Begriff der gemäßigten Distribution.

Der von SCHWARZ eingeführte allgemeine Begriff der Distribution ist für uns zu weit, da er keine Fouriertransformation zuläßt. Wir wollen uns auf die gemäßigten Distributionen [5] (g. D.) beschränken, die eine Fouriertransformierte besitzen.

Der Raum $\mathfrak{S}$ der Testfunktionen. – Sei $f(x_1, x_2, ..., x_n)$ eine reelle oder komplexe Funktion der n reellen Variablen $x_1, x_2, ..., x_n$, die beliebig oft in beliebiger Reihenfolge differenzierbar ist. Wir schreiben

$$\frac{\partial^{p_1}}{\partial x_1^{p_1}} \frac{\partial^{p_2}}{\partial x_2^{p_2}} \cdots \frac{\partial^{p_n}}{\partial x_n^{p_n}} f = f^{(p)}, \qquad x_1^{q_1} x_2^{q_2} \ldots x_n^{q_n} = x^q .$$

Dann ist f eine Testfunktion (Tf.), wenn für alle $p = (p_1, ..., p_n)$, $q = (q_1, ..., q_n)$ von ganzen, nicht negativen Zahlen $x^q f^{(p)}$ beschränkt bleibt im ganzen R^n. Man kann in $\mathfrak{S}$ eine Pseudotopologie $P(\mathfrak{S})$ einführen durch die Festsetzung: eine Folge von Tf. f_n konvergiert gegen die Tf. f, wenn für alle p, q die Folge $x^q f_n^{(p)}$ im ganzen R^n gleichmäßig gegen $x^q f^{(p)}$ strebt. Man kann zeigen [6], daß es eine abzählbare Folge von Tf. g_n gibt, so daß es zu jedem $f \in \mathfrak{S}$ eine Teilfolge der g_n gibt, die im Sinne von $P(\mathfrak{S})$ nach f strebt. Daher kann man sagen, « g_n ist dicht in $\mathfrak{S}$, $\mathfrak{S}$ ist separabel im Sinne von $P(\mathfrak{S})$ », wenn man diese Ausdrücke für die Pseudotopologie benützen will.

[3] L. SCHWARTZ: *Théorie des distributions*, I, II (Paris, 1950); I. HALPERIN: *Introduction to the Theory of Distributions* (Toronto, 1952).

[4] J. G. VALATIN: *Proc. Roy. Soc., (London)*, A **222**, 93, 228 (1954); A **225**, 535 (1954); A **226**, 254 (1954); H. LEHMANN, K. SYMANZIK und W. ZIMMERMANN: *Nuovo Cimento*, **8**, 205 (1954).

[5] « Distributions tempérées », L. SCHWARZ, l. c., Kap. VII, insbes. §, 3, 4.

[6] Eine ausführliche Behandlung dieser Fragen wird in einer mathematischen Arbeit von W. SCHMIDT erscheinen.

Der Raum $\hat{\mathfrak{S}}$ der Fouriertransformierten der $f \in \mathfrak{S}$ besteht wieder aus genau allen Tf. Konvergiert $f_n \to f$ in $P(\mathfrak{S})$, so gilt für die Fouriertransformierten $\hat{f}_n \to \hat{f}$ in $P(\hat{\mathfrak{S}})$.

Beispiele für Tf. sind $g(x) = \exp[-x^2]$ oder

$$h(x) = \exp\left[\left(-\frac{1}{x-a} - \frac{1}{b-x}\right)\right]^{1/n}$$

für $a < x < b$, 0 sonst. Mit $f \in \mathfrak{S}$, $g \in \mathfrak{S}$ ist auch $af+bg \in \mathfrak{S}$.

Der Raum $\mathfrak{S}'$ der g. D. – $\mathfrak{S}'$ ist der zu $\mathfrak{S}$ duale Raum. Er besteht aus allen Funktionalen T, die den $f \in \mathfrak{S}$ eine komplexe Zahl $T[f]$ zuordnen und die Eigenschaft haben, daß $T[af+bg] = aT[f]+bT[g]$, sowie daß $T[f_n]$ gegen $T[f]$ konvergiert, wenn $f_n \to f$ in $P(\mathfrak{S})$.

Die Nullmenge einer Distribution T ist die Menge jener Punkte x, die im Inneren eines offenen Intervalls I liegen, so daß $T[f] = 0$ für alle $f \in \mathfrak{S}$, die $f(x) = 0$ für $x \notin I$ erfüllen. Die dazu komplementäre Menge heißt Stützmenge $M(T)$. Die Nullmenge ist offen, die Stützmenge abgeschlossen.

Distributionen über O. – Sei O eine konvexe offene Menge. $\mathfrak{S}_0$ soll der Raum der Funktionen g sein, die in O beliebig oft differenzierbar sind und für die $x^a g^{(\nu)}$ in O beschränkt ist. g_n konvergiert gegen g in der Pseudotopologie $P(\mathfrak{S}_0)$, wenn $x^a g_n^{(\nu)} \to x^a g^{(\nu)}$ gleichmäßig in O. Ohne Beweis bringen wir den Satz (6): Zu jedem $g \in \mathfrak{S}_0$ gibt es ein $f \in \mathfrak{S}$, das in O mit g übereinstimmt; strebt $g_n \to g$ in $P(\mathfrak{S}_0)$, so gibt es f_n und ein $f \in \mathfrak{S}$, so daß $f_n \to f$ in $P(\mathfrak{S})$ und f_n bzw. f in O mit g_n bzw. g übereinstimmen.

Ist $M(T) \subset O$, so kann man $T[g]$ für alle $g \in \mathfrak{S}_0$ durch $T[g] = T[f]$ definieren, wobei $f \in \mathfrak{S}$, $f = g$ in O. Ist also $g_n \to g$ in $\mathfrak{S}_O$, so gilt $T[g_n] \to T[g]$. Die Definition ist eindeutig.

Ableitung einer g. D. – Unter $\partial T/\partial x_i$ versteht man jene g. D., die der Testfunktion $f(x)$ die Zahl $T[-\partial f/\partial x_i]$ zuordnet. Ableitungen nach verschiedenen Koordinaten sind vertauschbar.

Jeder quadratisch-Lebesgueintegrierbaren Funktion $l(x)$ entspricht eine g. D. $l[f] = \int l(x) f(x)\,dx$. Ein anderes Beispiel ist die Diracsche Deltafunktion mit $\delta[f] = f(0)$.

Da $\mathfrak{S}$ mit $\hat{\mathfrak{S}}$ und auch $P(\mathfrak{S})$ mit $P(\hat{\mathfrak{S}})$ übereinstimmt, kann man jede g. D. auch als g. D. im Impulsraum ansehen. Zu jedem $T \in \mathfrak{S}'$ gibt es daher eine Fouriertransformierte $\hat{T} \in \hat{\mathfrak{S}}' = \mathfrak{S}'$, so daß $\hat{T}[\hat{f}] = T[f]$.

Direktes Produkt von g. D. – Seien S, T beide aus $\mathfrak{S}'$. Dann kann man $S(x) \times T(y)[f(x)g(y)] = S[f]T[g]$ definieren. Es ist möglich zu zeigen:

1) Die endlichen Summen $\sum f_n(x)g_n(y)$ liegen dicht im Raum $\mathfrak{S}_2$ der Tf. in 2 Variablen im Sinne von $P(\mathfrak{S}_2)$.

2) Aus diesem Grunde existiert eine eindeutig durch S, T bestimmte g. D. $S(x) \times T(y)$, die für alle $f(x, y) \in \mathfrak{S}_2$ erklärt ist und die für $f(x)g(y)$ gerade $S[f]\,T[g]$ ergibt. Analog sind direkte Produkte zu verstehen, wenn bereits x, y mehrdimensional sind. Zum Beispiel ist die Deltafunktion $\delta[f(x_1, \ldots, x_n)] = f(0, \ldots, 0)$ das direkte Produkt der eindimensionalen Deltafunktionen. Das direkte Produkt wird bei SCHWARTZ ausführlich behandelt.

Distributionen impliziter Funktionen (7). – Seien T eine Distribution in m Variablen und $g_1(x_1, \ldots, x_n), \ldots, g_m(x_1, \ldots, x_n)$ feste Funktionen. Wir wollen nun eine n-dimensionale Distribution $T(g_1, \ldots, g_m)[f(x_1, \ldots, x_n)]$ definieren. Wir bilden

$$d(y_1, \ldots y_m) = \int\limits_{g_j(x) \leqq y_j} f \,\mathrm{d}x_1 \ldots \mathrm{d}x_n \,. \tag{1}$$

Die g_j müssen so gewählt werden, daß d beliebig oft differenzierbar und $e(y_1, \ldots, y_m) = \partial/\partial y_1 \ldots \partial/\partial y_m \; d$ eine Tf. in $\mathfrak{S}_m$ ist, wenn $f \in \mathfrak{S}_n$. Weiter soll $e_n \to e$ in $P(\mathfrak{S}_m)$ aus $f_n \to f$ in $P(\mathfrak{S}_n)$ folgen. Diese Bedingung für die g_j soll hier nicht näher untersucht werden (6). $T(g_1, \ldots, g_m)$ ist nun durch

$$T(g_1, \ldots, g_m)[f] = T[e] \tag{2}$$

definiert. Jedes $T[f]$ kann man nach dieser Definition $T(x_1, \ldots, x_n)[f]$ schreiben. Ein triviales Beispiel ist $T = \delta$, $g = x - x'$, also $\delta(x - x')[f(x)] = f(x')$. Wir betrachten als weiteres Beispiel $T = \delta$, $g = x^2 - m^2$, wobei $x = (x^0, x^1, x^2, x^3)$, $x^2 = (x^0)^2 - \boldsymbol{x}^2$. Hier ist

$$d(y_1) = \int\limits_{g \leqq y_1} f \,\mathrm{d}x^0 \,\mathrm{d}x^1 \,\mathrm{d}x^2 \,\mathrm{d}x^3 = \iiint\limits_{\boldsymbol{x}^2 + m^2 + y_1 \geqq 0} \mathrm{d}x^1 \,\mathrm{d}x^2 \,\mathrm{d}x^3 \int\limits_{-(\boldsymbol{x}^2 + m^2 + y_1)^{\frac{1}{2}}}^{(\boldsymbol{x}^2 + m^2 + y_1)^{\frac{1}{2}}} f(x^0, \ldots x^3) \,\mathrm{d}x^0 \,. \tag{3}$$

Ist $m^2 + y_1 > 0$, so ist die Ungleichung $\boldsymbol{x}^2 + m^2 + y_1 \geqslant 0$ von selbst erfüllt, man muß nur noch nach den Grenzen der x^0-Integration differenzieren und hat

$$e(y_1) = \frac{1}{2} \int \frac{f(\boldsymbol{x}, \sqrt{\boldsymbol{x}^2 + m^2 + y_1})}{\sqrt{\boldsymbol{x}^2 + m^2 + y^1}} \,\mathrm{d}\boldsymbol{x} - \frac{1}{2} \int \frac{f(\boldsymbol{x}, -\sqrt{\boldsymbol{x}^2 + m^2 + y_1})}{\sqrt{\boldsymbol{x}^2 + m^2 + y_1}} \,\mathrm{d}\boldsymbol{x} \,. \tag{4}$$

Für $m^2 + y_2 < 0$ ist auch noch nach den Grenzen der $\boldsymbol{x}$-Integration zu dif-

(7) Ähnliche Betrachtungen bei S. ALBERTONI und M. CUGIANI: *Nuovo Cimento*. **8**, 874 (1951); **10**, 157 (1953).

ferenzieren. Das gibt Terme, für die $\boldsymbol{x}^2 + m^2 + y_1 = 0$ ist, so daß das x^0-Integral null wird. Somit ist (4) stets erfüllt und man sieht

$$\delta(x^2 - m^2)[f] = \frac{1}{2}\int \frac{f(\boldsymbol{x}, \mu)}{\mu}\,\mathrm{d}\boldsymbol{x} - \frac{1}{2}\int \frac{f(\boldsymbol{x}, -\mu)}{\mu}\,\mathrm{d}\boldsymbol{x}; \qquad \mu^2 = \boldsymbol{x}^2 + m^2. \tag{5}$$

Es ist klar, daß $\delta(x^2 - m^2)[f(\Lambda x)] = \delta(x^2 - m^2)[f(x)]$, wenn Λ eine Lorentztransformation bedeutet. Man kann endlich zeigen (8):

1) Alle lorentzinvarianten Distributionen, also solche mit $T[f(\Lambda x)] = T[f(x)]$, haben die Form $T = S(x^2) + R$, wobei R eine Linearkombination von Distributionen $(\Box^2)^k \delta$ ist $(k = 0, 1, 2, \ldots)$.

2) Alle gegen Lorentztransformationen ohne Zeitumkehr (o. Z.) invarianten Distributionen lassen sich schreiben $T = S(x^2) + \theta(x^0) S_1(x^2) + R$. Dabei hat $S_1(y)$ die Stützmenge in $y \geqslant 0$.

$\theta(x^0) = 1$ für $x^0 > 0$, 0 sonst, weiter schreiben wir $\varepsilon(x^0) = \theta(x^0) - \theta(-x^0)$. $\theta(x^0) S_1(x^2)$ bedeutet, daß man in (4) für $e(y_1)$ nur das erste Integral nimmt, $\theta(-x^0) S_1(x^2)$ heißt, daß nur der zweite Term einzusetzen ist.

Der Beweis (6) folgt am einfachsten durch die Tatsache (3), daß, wenn man nur Tf. betrachtet, die außerhalb eines festen beschränkten Intervalles verschwinden, jede g. D. als höhere Ableitung (im Distributionssinn) einer stetigen Funktion dargestellt werden kann.

Unter Distributionen $\delta_4(x_1 - x_2)\,\delta(x_1^2 - m^2)[f(x_1, x_2)]$ und ähnlichen Ausdrücken soll folgendes verstanden werden: Man bildet zuerst das direkte Produkt $\delta_4(y)\,\delta(z)$ und setzt die impliziten Funktionen $y = x_1 - x_2$ und $z = x^2 - m^2$ ein.

Konvergenz von Vektoren und Operatoren. – Sind u, v Vektoren im Hilbertraum, so bezeichnen wir mit (u, v) ihr inneres Produkt, mit $\|u\|$ die Norm. Eine Folge u_n konvergiert stark gegen u, wenn $\lim \|u_n - u\| = 0$. Eine Folge von linearen Operatoren O_n konvergiert gegen O, wenn es einen linearen, überall dichten Teilraum R gibt, der zum Definitionsbereich fast aller O_n und von O gehört, so daß $O_n u \to Ou$ im Sinne der starken Vektorkonvergenz für alle u aus R.

Gemäßigte Vektor- und Operatordistributionen. – Eine gemäßigte Vektor-(Operator)distribution ordnet jedem $f \subset \mathfrak{S}$ einen Vektor $u[f]$ (oder einen Operator $O[f]$) zu. Eine Vektor(Operator)distribution ist linear, d.h. $u[af + bg] -$

(8) Eine andere Methode zur Behandlung lorentzinvarianter Distributionen bei P. D. Methée: *Comment. Math. Helv.*, **28**, 225 (1954).

$-au[f]-bu[g]$ und stetig, d.h. aus $f_n \to f$ in $P(\mathfrak{S})$ folgt $u[f_n]$ stark konvergent nach $u[f]$ (bzw. $O[f_n] \to O[f]$).

3. – Die Δ-Distributionen.

Die Distributionen $\tilde{\Delta}[f]$, $\Delta_F[f]$, $\Delta^{ret}[f]$, $\Delta^{av}[f]$ in $f(x^0, x^1, x^2, x^3)$ sind gegeben durch Integrale

$$T[f] = \frac{1}{(2\pi)^2}\int \mathrm{d}k \frac{\hat{f}(k)}{-k^2+m^2}\,, \tag{6}$$

über $\mathrm{d}k = \mathrm{d}k^0\mathrm{d}k^1\mathrm{d}k^2\mathrm{d}k^3$. Dabei treten bei den beiden Hyperbelästen $-k^2+m^2=0$ Singularitäten auf. Man hat in der komplexen k^0-Ebene längs der durch Fig. 1 veranschaulichten Kurven zu integrieren. Die Integration über k^1, k^2, k^3 verläuft im Reellen. Die gegebene Integrationsvorschrift setzt voraus, daß $f(k)$ für komplexe k analytisch ist. Dies wird durch die Definition $\hat{f}(k) = (2\pi)^{-2}\int f(x)\exp[-ikx]\,\mathrm{d}x$ gewährleistet. Für Tf. $f \in \mathfrak{S}$ konvergiert das Integral, auch die Limeseigenschaften sind erfüllt.

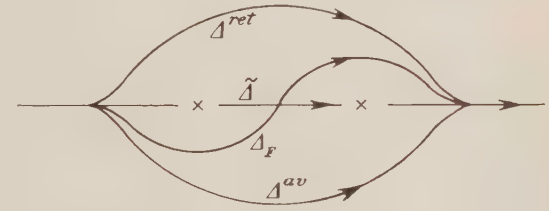

Fig. 1.

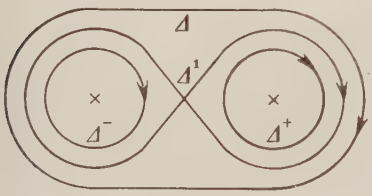

Fig. 2.

Die Distributionen Δ, Δ^1, Δ^+, Δ^- erklären wir ebenfalls durch Integrale der Form (6). In der komplexen k^0-Ebene werden die beiden Singularitäten nach Fig. 2 umfahren, während k^1, k^2, k^3 reell bleiben.

Folgende Relationen sind unter anderem leicht zu beweisen:

$$\begin{cases} \Delta^+[f] = \Delta[f^+]\,, \quad \Delta^-[f] = \Delta[f^-]\,, \quad \Delta^+[f] = -\Delta^-[f(-x)]\,, \\ \Delta[f] = \Delta[f^+ + f^-] = \Delta^+[f] + \Delta^-[f]\,. \end{cases} \tag{7}$$

Dabei ist

$$f^{\pm}(x) = (2\pi)^{-2}\int\limits_{k^0 \gtrless 0} \hat{f}(k)\,\mathrm{d}k\,. \tag{8}$$

An sich ist f^+ keine Tf., $\Delta[f^+]$ heißt nur, daß man f^+ in die oben erklärten Integrale einsetzen soll.

Direkte Auswertung von $\Delta^+[f]$ mit dem Residuensatz gibt

$$\Delta^+[f] = \frac{2\pi i}{(2\pi)^2} \cdot \frac{1}{2} \int \frac{\hat{f}(k, \sqrt{k^2+m^2})}{\sqrt{k^2+m^2}} \, \mathrm{d}k = \frac{i}{2\pi} \theta(k^0)\, \delta(k^2 - m^2)[\hat{f}(k)] \,. \tag{9}$$

Analog ist

$$(\hat{\Delta}^1, \hat{\Delta}, \hat{\Delta}^+, \hat{\Delta}^-) = \frac{i}{2\pi} \delta(k^2 - m^2)\,(1, \varepsilon(k^0), \theta(k^0), -\theta(-k^0)) \,. \tag{10}$$

Daraus sieht man, daß diese Distributionen lorentzinvariant sind. Auch $\tilde{1}$ ist lorentzinvariant, da man den Hauptwert als

$$\lim_{\substack{\eta \to 0 \\ |\, -k^2+m^2| > \eta}} \int \frac{\hat{f}(k)\, \mathrm{d}k}{-k^2+m^2}$$

invariant definieren kann. Da die restlichen J-Distributionen sich hievon nur um invariante Distributionen unterschieden, sind auch sie invariant. Direkt kann man die Invarianz so einsehen: Jeder Integrationsweg über k^0, k^1, k^2, k^3 im Komplexen, der durch Anwendung einer Lorentztransformation o.Z. aus dem angegebenen Weg entsteht, umfährt die Singularitäten $k^2 - m^2$ in topologisch gleicher Weise, so daß die Beiträge infolge des Residuensatzes gleich bleiben.

Gesucht sei eine Distribution G, die

$$(\Box^2 + m^2)\, G[f] = 0 \tag{11}$$

löst und die invariant gegen Lorentztransformationen o.Z. ist. Dies führt auf $G[(\Box^2+m^2)f] = 0$ bzw. $\hat{G}[(-k^2+m^2)\hat{f}] = 0$. Dies wird offenbar von den Distributionen (10) erfüllt. Umgekehrt: Ist G invariant gegen Lorentztransformationen o.Z., so auch $\hat{G}$. Also hat $\hat{G}$ die Gestalt $\hat{G} = G_1(k^2) + \theta(k^0) G_2(k^2) + R$. Soll noch die Schrödinger-Gordon-Gleichung erfüllt werden, so muß $\hat{G} = a_1 \delta(k^2 - m^2) + a_2 \theta(k^0)\, \delta(k^2 - m^2) + a_3 \delta$ sein ($a_3 = 0$, außer $m = 0$),

$$\hat{G} = \frac{i}{2\pi} \delta(k^2 - m^2)(c_1 \theta(k^0) - c_2 \theta(-k^0)) + a_3 \delta = c_1 \hat{\Delta}^+ + c_2 \hat{\Delta}^- + a_3 \delta \,.$$

Demnach hat die allgemeinste invariante Lösung der Schrödinger-Gordon-Gleichung die Gestalt [8])

$$G[f] = c_1 \Delta^+[f] + c_2 \Delta^-[f] + c_3 \int f(x)\, \mathrm{d}x \,. \tag{12}$$

c_3 muß Null sein, außer $m = 0$.

Die inhomogene Gleichung

$$(\Box^2 + m^2)\,G[f] = T[f] \tag{13}$$

kann u. a. dann gelöst werden, wenn T eine beliebig oft differenzierbare Punktfunktion ist. Da $\hat{T}$ eine g. D. ist, muß es ein Polynom als Majorante haben (3), so daß $\hat{f}(k)\hat{T}(-k) \in \hat{\mathfrak{S}}$. Nun setzen wir

$$G[f] = (2\pi)^2 \hat{\Delta}[\hat{f}(k)\,\hat{T}(-k)]\,. \tag{14}$$

Ist etwa $T = \delta$, also $\hat{T} = (2\pi)^{-2}$, so ist $G[f] = \hat{\Delta}[f]$.

An Stelle von Δ kann man auch Δ_F, Δ^{av}, Δ^{ret} nehmen, die sich nur um Lösungen der homogenen Gleichung von Δ unterscheiden.

Takahashi (9) hat die Δ-Distributionen nach anderen Gesichtspunkten betrachtet. Außer den Gleichungen (11), (12) wurden noch « Anfangsbedingungen » gestellt. Das heißt, es its möglich, die Δ-Distributionen für Funktionen f zu betrachten, welche die Form $f = g(\boldsymbol{x})\,\delta(x^0)$ oder $g(\boldsymbol{x})\,\delta'(x^0)$ haben, genauer, man kann $\hat{f}(k) = (2\pi)^{-\frac{1}{2}}\hat{g}(k)$ bzw. $ik^0(2\pi)^{-\frac{1}{2}}\hat{g}(k)$ formal in das Integral (10) einsetzen. Diese Integrale konvergieren und man erhält

$$\hat{\Delta}[\hat{g}(\boldsymbol{k})] = 0\,, \quad \frac{\partial \Delta}{\partial x^0} = \hat{\Delta}[\,\cdot ik^0(2\pi)^{-\frac{1}{2}}\hat{g}(\boldsymbol{k})] = (2\pi)^{-\frac{3}{2}}\int \hat{g}(k)\,\mathrm{d}k = g(0)\,. \tag{15}$$

Diese beiden Gleichungen entsprechen « $\Delta = 0$ für $x^0 = 0$, $\partial\Delta/\partial x^0 = \delta(\boldsymbol{x})$ für $x^0 = 0$ ». Das zusammen mit (11) legt aber Δ fest, da aus (11) folgt

$$\hat{\Delta}[\hat{f}(k)] = S[\hat{f}(\boldsymbol{k}, \sqrt{\boldsymbol{k}^2 + m^2})] + T[\hat{f}(\boldsymbol{k}, -\sqrt{\boldsymbol{k}^2 + m^2})]\,. \tag{16}$$

Man kann nun in den Anfangsbedingungen fur $f(\boldsymbol{k}, \pm\sqrt{\boldsymbol{k}^2 + m^2}) = (2\pi)^{-\frac{1}{2}}a(\boldsymbol{k})$ ein beliebiges $a(\boldsymbol{k})$ einsetzen, so daß die beiden Distributionen S, T festgelegt sind.

$\Delta(x-y)[f(x,y)]$ bedeutet offenbar $\Delta[e(z)]$, wobei $e(z) = \int f(x+t, t)\,\mathrm{d}t$. Man hat

$$\Delta(x-y)[f(x,y)] = (2\pi)^2 \hat{\Delta}[\hat{f}(k, -k)]\,, \tag{17}$$

weil $\hat{e} = (2\pi)^2 \hat{f}(k, -k)$. Es ist auch möglich,

$$\Delta(x-y)[f(x,y)] = (2\pi)^2 \hat{\Delta}(k)\,\delta(k+l)[\hat{f}(k,l)] \tag{18}$$

(9) T. Takahashi: *Progr. Theor. Phys.*, **11**, 1 (1954).

zu schreiben. Auch gilt

$$\Delta(x-y)[f(x)g(y)] = \Delta[f(x) * g(-y)] , \tag{19}$$

wobei der Stern das konvolutorische Produkt bedeutet. Offenbar ist

$$\Delta(x-y)[f(x+a, y+a)] = \Delta(x-y)[f(x, y)] . \tag{20}$$

Weiter gilt

$$\left\{\begin{aligned} &\Delta(x-y)[f^+g^-] &&= \Delta^+(x-y)[fg] , \\ &\Delta(x-y)[f^-g^+] &&= \Delta^-(x-y)[fg] = -\Delta^+(x-y)[gf] , \\ &\Delta^+(x-y)[\bar{g}f] &&= -\overline{\Delta^+}(x-y)[\bar{f}g] , \\ &\Delta(x-y)[fg] &&= \Delta(x-y)[f^+g^-] + \Delta(x-y)[f^-g^+] = \\ & &&= \Delta^+(x-y)[fg] - \Delta^+(x-y)[gf] . \end{aligned}\right. \tag{21}$$

In Abt. 6 wird gezeigt werden, daß $\Delta^+(x-y)$ eine Punktfunktion ist und $\Delta(x-y)$ verschwindet, wenn x und y raumartig zueinander liegen. Wegen $\Delta(x-y)[f(x, y)] = \Delta[\int f(z+t, t)\,\mathrm{d}t]$ folgt, daß $\Delta^+[f(x)]$ und folglich auch Δ^-, Δ, Δ^1 Punktfunktionen sind, wenn x raumartig ist, sowie daß Δ für raumartige x verschwindet, d.h. $\Delta[f] = 0$, wenn $f(x) = 0$ für $x^2 \geqslant 0$.

4. – Der Hilbertraum $\mathfrak{W}$ von Wightman. ([10])

Ein Punkt aus dem Teilraum $\mathfrak{V} \subset \mathfrak{W}$ ist gegeben durch eine abbrechende Folge

$$f = \{f_0, f_1(x_1), f_2(x_1, x_2), \ldots\} . \tag{22}$$

Dabei ist f_0 eine komplexe Zahl, f_r eine Tf. in $4r$ Variablen, x_j steht an Stelle von $x_j^0 = ct_j$, x_j^1, x_j^2, x_j^3. Addition und Multiplikation mit einer Zahl ist erklärt durch

$$\{f_0, f_1, \ldots, f_r, 0, 0 \ldots\} + \{g_0, g_1, \ldots, g_r, \ldots, g_s, 0, 0, \ldots\} = \\ = \{f_0 + g_0, f_1 + g_1, \ldots, f_r + g_r, \ldots, g_s, 0, 0 \ldots\} , \tag{23}$$

$$c\{f_0, f_1, \ldots, f_r, 0, \ldots\} = \{cf_0, cf_1, \ldots, cf_r, 0, \ldots\} . \tag{24}$$

([10]) A. S. WIGHTMAN: *Phys. Rev.*, **101**, 860 (1956).

Das innere Produkt ist durch eine Folge von Distributionen F_0, F_1, F_2, ... gegeben, wobei $F_0 = 1$ und F_r eine Distribution in $4r$ Variablen bedeutet; ist $f = \{f_0, f_1, ..., f_r, 0, ...\}$ und $g = \{g_0, ..., g_s, 0, ...\}$, so setzt man

$$(f, g) = \sum_{l=0}^{r} \sum_{m=0}^{s} F_{l+m}[\bar{f}_l(x_l, ..., x_1) g_m(x_{l+1}, ..., x_{l+m})] , \tag{25}$$

wobei $F_0[\bar{f}_0 g_0] = \bar{F}_0 \bar{f}_0 g_0 = \bar{f}_0 g_0$.

Damit $(f, g) = \overline{(g, f)}$, muß sein

$$F_n[f(x_1, ..., x_n)] = \bar{F}_n[\bar{f}(x_n, ..., x_1)] . \tag{A}$$

Damit $(f, f) \geqslant 0$, muß

$$\sum_l \sum_m F_{l+m}[\bar{f}_l(x_l, ..., x_1) f_m(x_{l+1}, ..., x_{l+m})] \geqslant 0 \tag{B}$$

sein für alle $f \in \mathfrak{V}$. Elemente f mit $(f, f) = 0$ sind Nullelemente. Elemente g, h, die sich um Nullelemente unterscheiden, sind als gleich zu betrachten. Das ist zulässig, weil dann alle ihre Skalarprodukte mit anderen Vektoren gleich sind: Wenn $g - h = f$, so ist

$$|(g, d) - (h, d)| = |(f, d)| \leqslant \|f\| \cdot \|d\| = 0 .$$

$\mathfrak{V}^k$ sei jener Teilraum aus $\mathfrak{V}$, dessen Folgen spätestens nach dem k-ten Glied abbrechen: $f_j = 0$ für $j > k$. $\mathfrak{V}^k$ ist die Erweiterung von $\mathfrak{V}^k$ zu einem vollständigen Raum, ebenso $\mathfrak{W}$ die Erweiterung von $\mathfrak{V}$. $\bigcup_k \mathfrak{W}^k$ heiße endlicher Teil von $\mathfrak{W}$.

$\mathfrak{W}^1$ ist separabel. Man braucht nur die Folge g_n zu nehmen, die «dicht ist in $P(\mathfrak{S})$». Falls eine Teilfolge $g_{n_k} \to f$ in $P(\mathfrak{S})$, so konvergiert $g_{n_k} \to f$ auch im Sinne der Metrik von $\mathfrak{W}$. Daher ist g_n dicht in $\mathfrak{W}^1$, daher auch in $\mathfrak{W}^1$, und $\mathfrak{W}^1$ ist separabel. Ebenso ist $\mathfrak{W}^k$ separabel für jedes k, so daß auch $\mathfrak{W}$ selbst separabel ist.

5. – Die physikalischen Postulate.

Wir formulieren die allgemeinen Postulate hier der Übersichtlichkeit halber zunächst für ein reelles Skalarfeld.

1) Raumzeitliche Mittelwerte des Feldskalars sind Observable. Es gibt Operatoren $\varphi[f]$ in dem zu bestimmenden Hilbertraum, die der Messung des

« Mittels von φ mit der Gewichtsfunktion f » zugeordnet sind [11]). $\varphi[f]$ möge eine gemäßigte Operatordistribution sein. Es muß hermitisch sein für reelle f, woraus man

$$\varphi^{+}[f] = \varphi[\bar{f}] \tag{26}$$

folgert.

2) Es gibt eine Darstellung der Gruppe der inhomogenen Lorentztransformationen (a, Λ). Dabei bedeutet (a, Λ) die Ausübung einer homogenen Transformation Λ, gefolgt von einer Translation a. Jedem (a, Λ) ohne Zeitumkehr wird eine unitäre (d.h. $U^{+} = U^{-1}$ oder $(Uf, Ug) \quad (f, g)$) Transformation $U(a, \Lambda)$ zugeordnet, jedem (a, Λ) mit Zeitumkehr eine antiunitäre (d. h. $(Uf, Ug) = (f, g)$). Zwischen $\varphi[f]$ und $U(a, \Lambda)$ besteht die Relation

$$U(a, \Lambda)\varphi[f]U^{-1}(a, \Lambda) = \varphi[f(\Lambda^{-1}(x - a))] . \tag{27}$$

3) Es gibt einen Vakuumzustand Ω, für welchen gilt

$$U(a, \Lambda)\Omega = \Omega . \tag{28}$$

4) Die Kausalitätsbedingung: $\varphi[f]$ und $\varphi[g]$ sind vertauschbar, wenn f und g raumartig zueinander liegen, d.h. wenn $f(x)g(y) = 0$ für $(x - y)^2 \geqslant 0$.

5) Energie-Impuls-Operator P_k und Drehimpulsoperator J_{mn} sind die mit i multiplizierten Erzeugenden von Translationen bzw. homogenen Lorentztransformationen. Es soll keinen Zustand negativer Energie geben.

Aus den Postulaten folgt, daß es neben Ω noch Zustände $\varphi[f]\Omega$, $\varphi[f_1]\varphi[f_2]\Omega$, $\ldots \varphi[f_1] \ldots \varphi[f_n]\Omega$ und Summen darüber gibt. Der Zustand $f_0\Omega + \varphi[f_1^1]\Omega + \varphi[f_1^1]\varphi[f_2^2]\Omega + \ldots \varphi[f_n^1] \ldots \varphi[f_n^n]\Omega$, wobei f_0 eine komplexe Zahl ist, soll in der Form

$$f = \{f_0, f_1^1(x_1), f_2^1(x_1)f_2^2(x_2), \ldots, f_n^1(x_1) \ldots f_n^n(x_n), 0, 0, \ldots\}$$

geschrieben werden. Konvergiert

$$\sum_{k=1}^{\infty} f_k^1(x_1) \ldots f_k^n(x_n)$$

[11]) Genau gesagt handelt es sich um Messungen mit Hilfe eines Probekörpers mit der « Raumzeitdichte » $f(x)$; s. N. BOHR und L. ROSENFELD: *Phys. Rev.*, **78**, 794 (1950).

in $P(\mathfrak{S}_n)$ gegen $f_n(x_1, ..., x_n)$, so setzen wir

$$\sum_k \{0, 0, ..., f_k^1(x_1) ... f_k^n(x_n), ...\} = \{0, ..., f_n(x_1, ..., x_n), 0, ...\} .$$

An Stelle von $\{0, 0, ... f_n(x_1, ... x_n), 0, ...\}$ wollen wir kurz $f_n(x_1, ... x_n)$ schreiben.

Das innere Produkt im Hilbertraum können wir

$$(29) \qquad (f_n(x_1, ... x_n), f_m(x_1, ... x_m)) = F_{nm}[\bar{f}_n(x_n ... x_1) f_m(x_{n+1} ... x_{n+m})]$$

schreiben, wobei F_{nm} eine Distribution in $4(n+m)$ Variablen ist und $F_{nm}[\bar{f}_n f_m] = \bar{F}_{mn}[\bar{f}_m f_n]$. Da offenbar

$$(30) \qquad \varphi[f] f_n(x_1 ... x_n) = f(x_1) f_n(x_2 ... x_{n+1})$$

und wegen (26) gilt

$$(31) \qquad (f_n, \varphi[f] g_m) = (\varphi[\bar{f}] f_n, g_m)$$

und

$$(32) \qquad F_{n,m+1}[\bar{f}_n(x_n ... x_1) f(x_{n+1}) g_m(x_{n+2} ... x_{n+m+1})] = \\ = F_{n+1,m}[f(x_{n+1}) \bar{f}_n(x_n ... x_1) g_m(x_{n+2} ... x_{n+m+2})] .$$

Daher ist $F_{n,m+1} = F_{n+1,m}$ und man kann $F_{nm} = F_{n+m}$ setzen. Wir haben daher einem Raum $\mathfrak{P}$ vor uns, der zu $\mathfrak{W}$ zu erweitern ist. Die F_n müssen den Bedingungen (A) und (B) von Abt. 4 gehorchen. Weitere Bedingungen (C), (D), (E) können aus den Postulaten gefolgert werden:

Aus 2), 3) folgt

$$(33) \qquad U(a, \Lambda) \varphi[f_1] ... \varphi[f_n] \Omega = \varphi[f_1(\Lambda^{-1}(x_1 - a))] ... \varphi[f_n(\Lambda^{-1}(x_n - a)] \Omega .$$

Dasselbe gilt auch für Summen darüber und somit allgemein

$$(34) \qquad U(a, \Lambda) f_n(x_1 ... x_n) = f_n(\Lambda^{-1}(x_1 - a) ... \Lambda^{-1}(x_n - a)) .$$

Wegen der Unitarität von U ist

$$(35) \qquad (U\Omega, U\varphi[f_1] ... \varphi[f_n] \Omega = (\Omega, \varphi[f_1(\Lambda^{-1}(x_1 - a))] ... \varphi[f_n(\Lambda^{-1}(x_n - a))] \Omega) = \\ = (\Omega, \varphi[f_1] ... \varphi[f_n] \Omega)$$

und wir erhalten die notwendige, aber, wie man leicht sieht, auch hinreichende

Bedingung

$$\text{(C)} \qquad F_n[f(\Lambda^{-1}(x_1 - a) \dots \Lambda^{-1}(x_n - a))] = F_n[f(x_1 \dots x_n)] \quad \text{für } \Lambda \text{ o. Z.}$$

Falls Λ eine Transformation mit Zeitumkehr ist, muß

$$\text{(C')} \qquad F_n[f(\Lambda^{-1}(x_1 - a) \dots \Lambda^{-1}(x_n - a))] = \overline{F}_n[f(x_1 \dots x_n)]$$

sein, damit U antiunitär ist.

Aus $F[f(x_1 - a, \dots x_n - a)] = F[f(x_1 \dots x_n)]$ folgt $F(x_1 \dots x_n)[f] = F(x_1 + a, \dots x_n + a)[f]$. Es gibt ein H, so daß $F(x_1, x_2, \dots x_n)[f] = H(x_1, x_2 - x_1, \dots x_n - x_1)[f]$. Dieses H erfüllt $H(x_1 + a, x_2 - x_1, \dots x_n - x_1)[f] = H(x_1, x_2 - x_1, \dots x_n - x_1)[f]$, so daß $H(x_1, x_2 - x_1, \dots x_n - x_1)[f] = G(x_2 - x_1, \dots x_n - x_1)[f]$. Also ist

$$(36) \qquad F[f] = G(x_2 - x_1, x_3 - x_1, \dots x_n - x_1)[f] .$$

Direkte Berechnung ergibt hier $c(y_1 \dots y_{n-1}) = \int f(t, t + y_1, \dots t + y_{n-1})\, dt$, somit ist $F[f] = G[\int f(t, t + y_1, \dots t + y_{n-1})\, dt]$.

Falls $f(x_1 \dots x_n) = h(x_1) g(x_2 \dots x_n)$, ist $F[f] = G[\int h(t) g(t + y_1, \dots t + y_{n-1})\, dt] = \int h(t)\, G[g(t + y_1, \dots t + y_{n-1})]\, dt$, wie aus der Stetigkeit in t von $g(t + y_1, \dots, t + y_{n-1})$ und $G[g(t + y_1, \dots t + y_{n-1})]$ folgt. Aus diesem Grund ist $F_n[h(x_1) g(x_2 \dots x_n)]$ bei festem g eine Punktfunktion in x_1. Ähnlich sieht man ein, daß $F_n[h(x_j) \cdot g(x_1 \dots x_{j-1} x_{j+1} \dots x_n)]$ eine Punktfunktion in x_j ist. *Folglich kann man die Matrix $\varphi(x)$ durch*

$$(37) \qquad (f_n, \varphi(x) g_m) = F_{n+m+1}[\overline{f}_n(x_n \dots x_1) g_m(x_{n+2} \dots x_{n+m+1}), x_{n+1}]$$

definieren. Doch ist $\varphi(x)$ (im allgemeinen) kein Operator.

Die Bedingung 4) besagt jetzt, daß, wenn $g(x) h(y) = 0$ für $(x - y)^2 \geqslant 0$, so

$$(38) \qquad F[f(\dots)\{g(x_j) h(x_{j+1}) - h(x_j) g(x_{j+1})\} l(\dots)] = 0$$

oder

$$\text{(D)} \qquad F[f(x_1 \dots x_j x_{j+1} \dots x_n)] = 0 ,$$

falls 1) f antysimmetrisch in x_j, x_{j+1} ist, 2) $f = 0$ für $(x_j - x_{j+1})^2 \geqslant 0$.

Aus 5) folgt

$$(39) \qquad P_k f_n(x_1 \dots x_n) = i \sum_{j=1}^{n} \frac{\partial f_n}{\partial x_j^k} , \qquad P_k \Omega = 0 ,$$

$$(40) \qquad J_{kl} f_n(x_1 \dots x_n) = i \sum_{j=1}^{n} \left(x_j^k \frac{\partial}{\partial x_j^l} - x_j^l \frac{\partial}{\partial x_j^k} \right) f_n , \qquad J_{kl} \Omega = 0 .$$

Es gilt $[P_\nu, q[f]] = -iq[\partial f/\partial x^\nu]$ oder in dem in Abt. 6 noch zu besprechenden Impulsraum

$$[\boldsymbol{P}, \varphi[\hat{f}]] = -\varphi[\boldsymbol{k}\hat{f}], \qquad [P_0, \varphi[\hat{f}]] = \varphi[k_0\hat{f}], \tag{41}$$

$$\boldsymbol{P}\hat{f}_n = -\sum_{\nu=1}^{n} \boldsymbol{k}_j \hat{f}_n, \qquad P_0\hat{f}_n = \sum_{\nu=1}^{n} k_j^0 \hat{f}_n. \tag{42}$$

Fragen wir nach den Eigenzuständen von P_ν. Zunächst ist Ω ein Eigenzustand mit dem Eigenwert Null. Weitere Eigenzustände können nur auftreten, wenn $\hat{F}$ eine δ-artige Singularität bei irgendeinem k-Wert besitzt. Wegen der Lorentzinvarianz kann dies höchstens bei $k = 0$ eintreten.

Weiter sagt die Bedingung 5), daß die F_n so beschaffen sein müssen, daß zu negativen Energien gehörende f die Norm 0 haben.

Sowohl die Zustände f als auch die Operatoren P_k, J_{kl} sind unabhängig von der Zeit, so daß die Erhaltungssätze gelten.

Die Operatoren U, P_k J_{kl}, $\varphi[f]$ sind im in $\mathfrak{W}$ dichten Bereich $\mathfrak{V}$ erklärt, man kann sie abgeschlossen machen. Ist neben $C = (f_k^0, f_k^1, \ldots f_k^r, 0 \ldots)$ auch $C_\tau = (0, ff_k^0, ff_k^1, \ldots ff_k^r, 0 \ldots)$ eine Cauchyfolge, so ist für das abgeschlossene $q[f]$: $q[f]C = C_\tau$. Aus den Stetigkeitseigenschaften der F_n folgt, daß die $f_n(x_1 \ldots x_n)$ Vektordistributionen und die $q[f]$ Operatordistributionen sind.

Die Existenz aller Zustände aus $\mathfrak{W}$ folgt aus den Postulaten. Doch kann es weitere Zustände geben und $\mathfrak{V}$ Teilraum eines umfassenderen Raumes sein.

6. – Übergang zum Impulsraum.

Wie schon in Abt. 2 erwähnt, ist mit $f \in \mathfrak{S}$ auch die Fouriertransformierte [12] $\hat{f} \in \mathfrak{S}$ und umgekehrt. Zu jeder g. D. F gibt es eine Fouriertransformierte $\hat{F}$, die $\hat{F}[\hat{f}] = F[f]$ erfüllt. Man kann daher jeden Zustand $f \in \mathfrak{V}$,

$$f = \{f_0, f_1, \ldots f_n, 0, 0, \ldots\}$$

auch durch die Folge der Fouriertransformierten

$$\hat{f} = \{\hat{f}_0, \hat{f}_1, \ldots \hat{f}_n, 0, 0, \ldots\}$$

[12] Wir setzen für die Fouriertransformierte

$$\hat{f}(k^0, \ldots k^3) = (2\pi)^{-2} \int f(x^0, \ldots x^3) \exp[ikx]\, \mathrm{d}^4x,$$
$$f(x) = (2\pi)^{-2} \int \hat{f}(k) \exp[-ikx]\, \mathrm{d}^4k.$$

Etwa $\hat{\delta}(x - x') = (2\pi)^{-2} \exp[ikx']$; $\hat{\delta}(x^0) = \hat{1} \cdot \hat{1} \cdot \hat{1} \cdot \hat{\delta}(x^0) = (2\pi)^{\frac{3}{2}} \delta(\boldsymbol{x})(2\pi)^{-\frac{1}{2}} = 2\pi\delta(\boldsymbol{x})$ wegen $\hat{1} = (2\pi)^{\frac{1}{2}}\delta$.

charakterisieren. Das innere Produkt ist durch

$$\hat{F}_0, \quad \hat{F}_1, \quad \hat{F}_2, \ \ldots$$

und

$$(\hat{f}_n, \hat{g}_m) = \hat{F}_{n+m}[\hat{f}_n(-k_n \ldots - k_1)\hat{g}_m(k_{n+1} \ldots k_{n+m})] \tag{43}$$

gegeben, weil

$$\hat{\bar{f}}(k_1 \ldots k_n) = \bar{\hat{f}}(-k_1 \ldots - k_n) . \tag{44}$$

Einige der Bedingungen (A) bis (E) sollen nun auf den Impulsraum übertragen werden. So lautet jetzt (A)

$$\hat{F}[\hat{f}(k_1 \ldots k_n)] = \bar{\hat{F}}[\bar{\hat{f}}(-k_n \ldots - k_1)] . \tag{A}$$

Es wurde gezeigt, daß $F[f] = G[e(y_1 \ldots y_{n-1})]$. Man findet $\hat{e}(k_1 \ldots k_{n-1}) = (2\pi)^2 \hat{f}(-k_1 - \ldots - k_{n-1}, k_1, \ldots, k_{n-1})$, daher

$$\hat{F}[\hat{f}(k_1 \ldots k_n)] = (2\pi)^2 \hat{G}[\hat{f}(-k_1 - \ldots - k_{n-1}, k_1, k_2, \ldots k_{n-1})] . \tag{45}$$

Man kann dafür auch schreiben

$$\hat{F} = \delta(k_1 + \ldots + k_n) T(k_1 \ldots k_n) . \tag{46}$$

Eine hinreichende Bedingung für Lorentzinvarianz o.Z. ist: $\hat{F}_n$ ist eine Summe von Distributionen der Gestalt

$$\hat{T}_n = \delta(k_1 + \ldots + k_n) \prod_t \delta(a_1^t k_1 + \ldots + a_n^t k_n) S(k_l \cdot k_m, \varepsilon(k_1^0)) . \tag{47}$$

f_n soll Nullelement sein, wenn es nur Frequenzen mit $\sum_{j=1}^{m} k_j^0 < 0$ besitzt. Für solche f_n wird daher bei beliebigem g_m

$$\hat{F}_{m+n}[\hat{g}(-k_1 \ldots - k_m)\hat{f}(k_{m+1} \ldots k_{m+n})] = 0 . \tag{E}$$

Die Distribution F_l hat daher ihre Stützmenge nur in $k_j^0 + k_{j+1}^0 + \ldots + k_l^0 > 0$, oder, was wegen (46) auf das selbe hinauskommt, in $k_1^0 + \ldots + k_{j-1}^0 < 0$. Aus der Lorentzinvarianz schließt man, daß $\hat{F}_l$ nur dort die Stützmenge hat, wo

$$\begin{cases} k_1 + \ldots + k_{j-1} & \text{im positiven Lichtkegel,} \\ k_j + \ldots + k_l & \text{im negativen Lichtkegel.} \end{cases} \tag{48}$$

Sei $\{\eta\} = \{\eta_1, \eta_2, \dots \eta_n\}$ eine Folge von Vierervektoren, so daß

(49) $\qquad \eta_{j+1} - \eta_j$ im positiven Lichtkegel.

Die Funktion

(50) $$\hat{h} = (2\pi)^{-2n} \exp[-ik_1(x_1 - i\eta_1) - \dots - ik_n(x_n - i\eta_n)]$$

ist keine Tf., da aber $k_1\eta_1 + \dots + k_n\eta_n > 0$ für alle k_j, die (48) erfüllen, verhält sie sich auf der Stützmenge von F_n wie eine solche. Die Menge der $(x_1 \quad i\eta_1, \dots x_n \quad i\eta_n)$ mit (49) ist konvex und es gibt offenbar eine sie enthaltende offene Menge O, so daß $\hat{h} \in \mathfrak{S}_o$ und man $\hat{F}_n[\hat{h}]$ definieren kann. Wir erklären nun

(51) $$F(z_1, \dots z_n) = F(x_1 - i\eta_1, \dots x_n - i\eta_n) = \hat{F}[\hat{h}] .$$

$F(z_1 \dots z_n)$ ist eine Punktfunktion, wenn die η_j (49) erfüllen und ist, da der Differenzenquotient von $\hat{h}$ in $P(\mathfrak{S}_o)$ gegen die Ableitung von $\hat{h}$ strebt, analytisch in diesem Gebiet.

Es ist

(52) $$\int F(x_1 \quad i\eta_1 \dots x_n \quad i\eta_n) f(x_1 \dots x_n)\, dx_1 \dots dx_n - \int \hat{F}[\hat{h}] f(x_1 \dots x_n)\, dx_1 \dots dx_n =$$
$$= \int \hat{F}[\hat{h} f(x_1 \dots x_n)\, dx_1 \dots dx_n] = \hat{F}(\hat{f} \exp[\quad k_1\eta_1 \quad \dots \quad k_n\eta_n]) .$$

Das Integral kann man in die Distribution hineinnehmen, weil $\hat{h}$ in $\mathfrak{S}_o$ stetig in den x_j ist. Da $\hat{f} \exp[-(k_1\eta_1 + \dots + k_n\eta_n)\lambda] \to \hat{f}$ in $P(\mathfrak{S}_o)$ für $\lambda \to 0$, ist

(53) $$\begin{cases} F[f] = \hat{F}[\hat{f}] = \lim\limits_{\lambda \to 0} \hat{F}[\hat{f} \exp[-\lambda(k_1\eta_1 + \dots + k_n\eta_n)]] \\ \qquad = \lim\limits_{\lambda \to 0} \int F(x_1 - \lambda\eta_1, \dots, x_n - \lambda\eta_n) f(x_1 \dots x_n)\, dx_1 \dots dx_n . \end{cases}$$

F ist genau dann lorentzinvariant, wenn $F(\Lambda z_1 \dots \Lambda z_n) = F(z_1 \dots z_n)$. Aus der Translationsinvarianz folgt $F(z_1 \dots z_n) = L(\zeta_1, \zeta_2, \dots \zeta_{n-1})$ mit $\zeta_j = z_{j+1} - z_j$. L ist analytisch, wenn $-\operatorname{Im} \zeta_j$ im positiven Lichtkegel liegt. Es gilt der Satz ([10]): Ist $L(\zeta_1 \dots \zeta_{n-1})$ analytisch, wenn $\operatorname{Im} \zeta_j$ im positiven Lichtkegel liegt, und invariant gegenüber Lorentztransformationen o.Z., dann ist L eine analytische Funktion in den Skalarprodukten $\zeta_l \cdot \zeta_m$ in dem Gebiet, über welches $\zeta_l \cdot \zeta_m$ variiert, wenn ζ_l, ζ_m im obigen Bereich variiert.

Dann ist aber L eine analytische Funktion in den Quadraten von Summen aufeinanderfolgender ζ_j, also ist L eine analytische Funktion in den $(z_l - z_m)^2$ auf jenem Gebiet G, über dem $(z_l \quad z_m)^2$ variiert, wenn die z (49) befriedigen. Das ist gerade der Bereich, in dem $-\operatorname{Im}(z_l - z_m)$ im positiven Lichtkegel liegt.

G besteht aus allen Punkten der komplexen Ebene außer der positiven reellen Achse.

Sei nun f eine Funktion, die verschwindet, wenn zwei ihrer Argumente raumartig zueinander liegen. Es gilt

$$(54)\qquad \begin{cases} F[f] = \lim\limits_{\lambda\to 0}\int f(x_1 \dots x_n)\, F(x_1 - i\lambda\eta_1 \dots x_n - i\lambda\eta_n)\,\mathrm{d}x \dots \mathrm{d}x_n \\ \quad = \lim\limits_{\lambda\to 0}\int f(x_1 \dots x_n)\, L\big((x_l - x_m - i\lambda(\eta_l - \eta_m))^2\big)\mathrm{d}x_1 \dots \overset{\cdot}{\mathrm{d}}x_n\,. \end{cases}$$

Ist nun $x_l \dots x_m$ raumartig, so liegt $(x_l - x_m)^2$ auf der negativen reellen Achse, wo L analytisch ist, daher existiert $\lim\limits_{\lambda\to 0} L\big((x_l - x_m - i\lambda(\eta_l - \eta_m))^2\big) = L\big((x_l - x_m)^2\big)$ und

$$(55)\qquad F[f] = \int f(x_1, \dots x_m)\, L\big((x_l - x_m)^2\big)\,\mathrm{d}x_1 \dots \mathrm{d}x_n\,.$$

Für paarweise raumartig gelegene Punkte ist daher F eine beliebig oft differenzierbare Punktfunktion.

Für reelle, raumartige $z_l - z_m$ bleibt $L\big((z_l - z_m)^2\big)$ wegen der Kausalität bei Vertauschen zweier Indizes gleich. Nach dem Identitätssatz muß daher $L\big((z_l \dots z_m)^2\big)$ überall bei Vertauschen zweier Indizes unverändert bleiben. Die F_2 erfüllen daher, wenn die übrigen Bedingungen gelten, (D) identisch.

$F_2[fg] = -i\,\Delta^+(x-y)[fg]$ erfüllt alle Bedingungen. $F_2[fg] = \overline{F_2[\bar{g}\bar{f}]}$ (A) gilt nach (21). (B), (C) und (E) folgen aus der Impulsraumdarstellung. Daher ist $\Delta^+(x-y)$ für raumartiges $x - y$ eine Punktfunktion und die Vertauschungsregeln (D) werden automatisch erfüllt. Das bedeutet, daß

$$(56)\qquad \Delta(x-y)[fg] = \Delta^+(x-y)[fg] - \Delta^+(x-y)[gf] = 0\,,$$

wenn $f(x)g(y) = 0$ für $(x-y)^2 > 0$. $\Delta(x-y)$ verschwindet daher für raumartiges $x - y$.

7. – Das Schrödinger-Gordon-Feld.

Um die Theorie des freien Schrödinger-Gordon-Feldes zu erhalten, fordern wir zusätzlich zu den in Abt. 5 gemachten Annahmen:

1) $[\varphi[f], \varphi[g]]$ ist eine Zahl $T[fg]$.

2) $(\Box^2 + m^2)\varphi[f] = 0$.

Aus Abt. 5 schließt man, daß wegen $(\Omega, [\varphi[f], \varphi[g]]\Omega) = T[fg]$ die g. D. $T[fg]$ lorentz- und translationsinvariant ist. Aus der Translationsinvarianz folgt

wie früher $T[f(x,y)] = H[\int f(x+t,t)\,dt]$. Da H eine invariante Lösung der Schrödinger-Gordon-Gleichung sein muß, ist wegen Abt. 3 $H[l(x)] = c_1 1^-[l] - c_2 1^-[l] + c_3 \int l(x)\,dx$. Nun muß aber mit T auch H schiefsymmetrisch sein, so daß $H = c\Delta$, $T = c\Delta(x_1 - x_2)$ sein muß. T erfüllt nur dann die Bedingung (B), wenn c auf der negativen imaginären Achse liegt. Wir normieren so, daß $T = -i\Delta(x-y)$. Folglich ist

$$T[fg] = F_2[fg] - F_2[gf] = -i\Delta(x-y)[fg]\,. \tag{57}$$

Da $F_2[\hat{f}(k_1)\hat{g}(k_2)]$ seine Stützmenge wegen (48) innerhalb $k_1 > 0$ und $k_2 > 0$ haben muß, ist $F_2[fg] = -i\Delta^+(x_1 - x_2)[fg] + a\hat{f}(0)\hat{g}(0)$. Für $m > 0$ muß wegen 2) $a = 0$ sein. Im Falle $m = 0$ muß man die zusätzliche Annahme machen, daß man stets

3) $\varphi[f] = \varphi[f^+] + \varphi[f^-]$

setzen kann, d.h. daß φ in $k^a = 0$ keine δ-artige Singularität besitzt. Dies wird bei $m \neq 0$ durch 2) von selbst garantiert. Daraus folgt.

$$F_0 = 1\,, \quad F_1 = 0\,, \quad F_2[f(x_1,x_2)] = -i\Delta^+(x_1 - x_2)[f(x_1,x_2)]\,. \tag{58}$$

Allgemein gilt

$$F_{2j+1} = 0\,, \quad F_{2j}[f_1 \dots f_{2j}] = \sum F_2[f_{k_1} f_{l_1}] F_2[f_{k_2} f_{l_2}] \dots F_2[f_{k_j} f_{l_j}]\,. \tag{59}$$

Die Summe ist über alle Paarbildungen $k_h < l_h$, $k_h < k_{h+1}$ der ersten $2j$ natürlichen Zahlen zu bilden. Für beliebige $f(x_1 \dots x_{2j})$ ist F_{2j} durch das direkte Produkt gegeben; im allgemeinen Fall kann man die Integrale in den 1^--Distributionen nicht mehr unabhängig ausführen, sondern es treten mehrfache Integrale auf. Der Beweis für (59) folgt durch Induktion nach n:

$$F_n[f_1 \dots f_n] = F_n[f_1^- f_2 \dots f_n]\,;$$

wegen

$$F_n[f_2 f_3 \dots f_{j-1} f_1^+ f_j \dots f_n] =$$
$$= F_n[f_2 \dots f_{j-1} f_j f_1^- f_{j+1} \dots f_n] - i\Delta^+(x_1 - x_j)[f_1 f_j] F_{n-2}[f_2 \dots f_{j-1} f_{j+1} \dots f_n]$$

und $F_n[f_2 \dots f_n f_1^-] = 0$ kann man f_1 nach rechts durchziehen und erhält

$$F_n[f_1 \dots f_n] = \sum_{j=2}^{n} F_2[f_1 f_j] F_{n-2}[f_2 \dots f_{j-1} f_{j+1} \dots f_n]\,, \tag{60}$$

woraus (59) folgt. Die Fouriertransformierten kann man schreiben

$$F_{2j} = (2\pi)^j \sum \delta(k_{k_1}^2 + m^2)\,\delta(k_{k_1} + k_{l_1}) \ldots \delta(k_{k_j}^2 + m^2)\,\delta(k_{k_j} + k_{l_j})\,. \tag{61}$$

Prüfen wir nun die Bedingungen (A) bis (E) nach. (A) folgt aus (61), (C) und (E) sind offenbar. In Abt. **8** wird gezeigt werden, daß jedem Zustand aus $\mathfrak{H}$ ein abbrechende Folge $f = \{f_0, \ldots f_r, 0, \ldots\}$ entspricht, deren f_j nur negative Frequenzen enthalten. Für solche f ist

$$(f, f) = \sum_{j=0}^{r} (f_j, f_j)\,. \tag{64}$$

Um (B) einzusehen, genügt daher $F_{2j}[\bar{f}_j \bar{f}_{j-1} \ldots \bar{f}_1 f_1 \ldots f_j] \geqslant 0$, wobei $f_r^- = f_r$, $\bar{f}_r^- = \bar{f}_r$. Funktionen mit negativen Frequenzen darf man untereinander vertauschen, ebenso solche mit positiven. Aus diesem Grund ist es hinreichend, zu zeigen, daß $F_{2j}[\bar{f}(x_j \ldots x_1)\, f(x_1 \ldots x_j)] \geqslant 0$, wenn f nur negative Frequenzen besitzt und symmetrisch in den x_i ist. Ein Term aus (64) hat aber für solche f die Gestalt

$$(2\pi)^j \left(\frac{1}{2}\right)^j \int \frac{\hat{f}(-\boldsymbol{k}_1, -\sqrt{\boldsymbol{k}_1^2+m^2}, \ldots -\boldsymbol{k}_j, -\sqrt{\boldsymbol{k}_j^2+m^2})\, \hat{f}(-\boldsymbol{k}_1, -\sqrt{\boldsymbol{k}_1^2+m^2}, \ldots)}{\sqrt{\boldsymbol{k}_1^2+m^2} \ldots \sqrt{\boldsymbol{k}_j^2+m^2}}\, \mathrm{d}\boldsymbol{k}_1 \ldots \mathrm{d}\boldsymbol{k}_j\,.$$

Da $I(x_1 \ldots x_2)[fg] = 0$, wenn f und g raumartig zueinander liegen, ist auch die Kausalitätsbedingung erfüllt.

8. – Die Partikeldarstellung.

Jedes $f = \{f_0, \ldots f_j, 0, \ldots\}$ ist äquivalent einem $g = \{g_0, \ldots g_j, 0, \ldots\}$, dessen g_r nur negative Frequenzen besitzen. Am einfachsten beweist man dies durch Induktion nach j. Ist $g_j = h_1(x_1) \ldots h_j(x_j) = \varphi[h_1]h_2(x_2) \ldots h_j(x_j)$, so darf man voraussetzen, daß $h_2, h_3, \ldots, h_j$ nur negative Frequenzen enthalten. Daher ist

$$g_j = \{\varphi[h_1^+] + \varphi[h_1^-]\}\varphi[h_2]h_3^- \ldots h_j^- =$$

$$= h_1^- h_2^- \ldots h_j^- + h_2^-(h_1^- h_3^- \ldots h_j^-) + F_2[h_1 h_2]h_3^- \ldots h_j^-\,.$$

Der erste und dritte Term der rechten Seite ist in der gewünschten Form, den mittleren kann man nach Voraussetzung in einen äquivalenten mit negativen Frequenzen umwandeln. Jedes f_j kann man daher als Summe von g_k^- darstellen, wobei k die ganzen Zahlen von gleicher Parität wie j zwischen 0 und j durchläuft.

Ein Zustand $g_j(x_1 \dots x_j)$ ist als einer mit j Teilchen zu deuten. Die Distribution $F_{2j}[f(x_1 \dots x_j) g_j^-(x_{j-1} \dots x_{2j})]$ ist in $x_1, \dots x_j$ eine Punkfunktion, sobald die $x_1, \dots x_j$ paarweise raumartig zueinander liegen. Die Funktion

$$\Phi(x_1, \dots x_j) = F_{2j}[x_1, \dots x_j, g_j^-(x_{j+1} \dots x_{2j})] \tag{62}$$

ist die Wellenfunktion von $g_j^-(x_1, \dots x_j)$. Es gilt

$$(\Box_i^2 - m^2)\Phi = 0\,, \tag{63}$$

Φ ist symmetrisch in den x_l.

In der Partikeldarstellung ist das innere Produkt besonders einfach:

$$(f, g) = \sum F_{2r}[\overline{f_r^-} g_r^-]\,. \tag{64}$$

Nicht abbrechende Folgen f liegen in $\mathfrak{W}$, wenn $\sum F_{2r}[\overline{f_r} f_r]$ konvergiert. Es gibt also Zustände, die aus Zuständen mit beliebig hoher Teilchenzahl zusammengesetzt sind.

Man kann einen Teilchenzahloperator N einführen durch

$$N f_n^- = n f_n^-\,. \tag{65}$$

N ist für den ganzen endlichen Teil von $\mathfrak{W}$ erklärt.

Zunächst liegen alle f in $\mathfrak{Z}$. Dadurch, daß man den Raum vollständig macht, kommen alle f_r hinzu, für welche die $3r$-fachen Integrale in $F_{2r}[\overline{f_r} f_r]$ existieren. Es gibt Elemente in $\mathfrak{W}'$, die man durch Punktfunktionen nicht mehr darstellen kann. Eine Darstellung aller Elemente aus $\mathfrak{W}'$ geben die $\{\hat{f}_0, \hat{f}_1^-, \dots \hat{f}_l^-, 0, \dots\}$, deren $\hat{f}_l$ auf $k^2 = m^2$ definiert und Lebesgue-integrierbar sind, und für die $\hat{F}_{2l}$ konvergiert. Dementsprechend ist $q[f]$ für solche f erklärt ($l = 1$).

9. – Das elektromagnetische Feld.

Zur Beschreibung des elektromagnetischen Feldes haben wir unter sinngemäßer Verallgemeinerung der in Abt. 5 aufgestellten Forderungen 1) und 2) zu verlangen, daß es vier Operatordistributionen $\varphi^\mu[f_\mu(x)]$ gibt, die bei Lorentztransformationen in

$$U(a, \Lambda)\varphi^\mu[f_\mu(x)]U^{-1}(a, \Lambda) = \sum_\nu \Lambda_{\mu\nu}\varphi^\nu[f_\mu(\Lambda^{-1}(x - a))] \tag{66}$$

übergehen. Es ist sinnvoll, die Feldoperatoren nun als Linearform im Raum

der Quadrupel $f_\mu(x)$ darzustellen:

$$\varphi[f_\mu(x)] = \sum_\mu \varphi^\mu[f_\mu(x)] \,. \tag{67}$$

Diese transformiert sich gemäß

$$U(a, \Lambda)\varphi[f_\mu(x)]U^{-1}(a, \Lambda) = \varphi[(\Lambda^{-1}f)_\mu(\Lambda^{-1}(x-a))] \,. \tag{68}$$

Durch wiederholte Anwendung von (67) auf Ω und durch Summation gelangt man zu einer Darstellung der Zustände durch 4^n Testfunktionen in $4n$ Variablen, und es gilt

$$U(a, \Lambda)\{f, f_\mu, f_{\mu\nu}, \ldots\} = \{f, (\Lambda^{-1}f)_\mu(\Lambda^{-1}(x-a)), \ldots\}. \tag{69}$$

Ergänzen wir die in Abt. 7 gemachte Annahme 1) durch die Forderung, daß der Kommutator nicht nur dem Einheitsoperator im Hilbertraum proportional sein soll, sondern auch dem «Einheitstensor» $g^{\mu\nu}$, und behalten wir 2) und 3) bei, so wird

$$[\varphi[f_\mu], \varphi[g_\nu]] = iD(x_1 - x_2)[f_\mu g^\mu]. \tag{70}$$

Die Metrik ergibt sich dadurch zu $F_0 = 1$, $F_1 = 0$,

$$F_n[f_{1\mu_1} \ldots f_{n\mu_n}] = i \sum_l D^+(x_1 - x_l)[f_1^{\mu_1} f_{1\mu_l}] F_{n-2}[f_2^{\mu_2} \ldots f_{l-1}^{\mu_{l-1}}, f_{l+1}^{\mu_{l+1}} \ldots f_n^{\mu_n}] \tag{71}$$

und ist offenbar indefinit.

Zum Einbau der Lorentzbedingung in die Theorie rechnen wir mit einer Partikeldarstellung im Impulsraum. Wir verlangen

$$\varphi[k_\mu \hat{f}^+(k)] g^-_{\nu_1 \ldots \nu_n} = 0 \,. \tag{72}$$

Die linke Seite von (72) wäre für beliebige $\hat{g}^-_{\nu_1 \ldots \nu_n}$ irgendeinem $\hat{h}^-_{\lambda_1 \ldots \lambda_{n-1}}$ gleich. (72) heißt also

$$\begin{aligned} 0 &= (\hat{h}^-_{\lambda_1 \ldots \lambda_{n-1}}(k_1 \ldots k_{n-1}),\ k'_{1\mu} \hat{f}^+(k'_1) \hat{g}_{\nu_1 \ldots \nu_n}(k'_2 \ldots k'_{n+1})) = \\ &= \sum_\nu \hat{F}_{2n}[\hat{h}^-_{\lambda_1 \ldots \lambda_{n-1}}(-k_{n-1} \ldots k_1) k_{n\mu} \hat{f}^+(k_n) \hat{g}_{\nu_1 \ldots \nu_n}(k_{n+1} \ldots k_{2n})] = \\ &= (-)^n (2\pi)^n \theta(k_1^0)\, \delta(k_1^2) \ldots \theta(k_n^0)\, \delta(k_n^2) [\bar{\hat{h}}^{\mu_1 \ldots \mu_{n-1}}(-k_{n-1} \ldots -k_1) \cdot \\ &\qquad \cdot f(k_n) \sum_{P(l)} k_n^{\mu_n} \hat{g}^-_{\mu_{l_1} \ldots \mu_{l_n}}(-k_{l_1} \ldots -k_{l_n})] \,, \end{aligned} \tag{73}$$

wobei $P(l)$ alle Permutationen $(l_1, \ldots l_n)$ von $(1, \ldots n)$ durchläuft. Da h und f

beliebig sind, bedeutet (73), daß neben Ω nur solche $\hat{g}_{\nu_1 \dots \nu_n}(k_1 \dots k_n)$ zugelassen sind, welche die 4^{n-1} Gleichungen

$$k_n^{\mu_n} \sum_{P(l)} \hat{g}^-_{\mu_{l_1} \dots \mu_{l_n}}(k_{l_1} \dots k_{l_n}) = 0 \tag{74}$$

zu den 4^{n-1} $(n-1)$-tupeln $(\mu_1, \dots, \mu_{n-1})$ erfüllen.

In dem durch (74) eingeschränkten Raum ist die Metrik definit. Es ist nämlich

$$\begin{aligned} (-)^n \theta(k_1^0)\, \delta(k_1^2) \dots \theta(k_n^0)\, \delta(k_n^2) [\overline{\hat{g}^{-\mu_1 \dots \mu_n}}(-k_n \dots -k_1) \sum_{P(l)} \hat{g}^-_{\mu_{l_1} \dots}(-k_{l_1} \dots)] = \\ = (-)^n \frac{1}{n!} \theta(k_1^0)\, \delta(k_1^2) \dots [\sum_{P(m)} \overline{\hat{g}^{-\mu_{m_1} \dots}}(-k_{m_1} \dots) \sum_{P(l)} \hat{g}^-_{\mu_{l_1} \dots}(-k_{l_1} \dots)] = \\ = (-)^n \theta(k_1^0)\, \delta(k_1^2) \dots [\overline{G}^{\mu_1 \dots \mu_n}(-k_1 \dots -k_n) G_{\mu_1 \dots \mu_n}(-k_1 \dots -k_n)] ; \end{aligned} \tag{75}$$

(74) bedeutet

$$k_n^{\mu_n} G_{\mu_1 \dots \mu_n}(-k_1 \dots -k_n) = 0 .$$

Da G symmetrisch ist, folgt hieraus

$$k_j^{\mu_j} G_{\mu_1 \dots \mu_n}(-k_1 \dots -k_n) = 0 , \qquad j = 1, \dots n. \tag{76}$$

Wir behaupten nun

$$(-)^n \overline{G}^{\mu_1 \dots \mu_n} G_{\mu_1 \dots \mu_n} > 0 \quad \text{für} \quad k_i^2 = 0 \tag{77}$$

und beweisen es durch vollständige Induktion. Es sei

$$(-)^l \overline{G}^{\mu_1 \dots \mu_l}{}_{\mu_{l+1} \dots \mu_n} G_{\mu_1 \dots \mu_n} > 0 .$$

Das Koordinatensystem sei so gewählt, daß $\boldsymbol{k}_{l+1}$ in die x_1-Achse fällt. Dann sagt (76) für $j = l+1$

$$G_{\mu_1 \dots \mu_l 0 \mu_{l+2} \dots \mu_n} = G_{\mu_1 \dots \mu_l 1 \mu_{l+2} \dots \mu_n}$$

und wir bekommen

$$(-)^{l+1} \overline{G}^{\mu_1 \dots \mu_{l+1}}{}_{\mu_{l+2} \dots \mu_n} G_{\mu_1 \dots \mu_n} > 0 .$$

Der durch die Lorentzbedingung eingeschränkte Teilraum ist daher ein echter Hilbertraum [13]. Durch wiederholte Anwendung der Feldoperatoren

[13] Er muß erst vollständig gemacht werden.

$F_{\mu\nu}[f] = q_\mu[\partial f/\partial x^\nu] - q_\nu[\partial f/\partial x^\mu]$ kann man diesen Raum aufbauen. In ihm werden die Maxwellgleichungen für die $F_{\mu\nu}$ als Operatorgleichungen erfüllt. Die Anwendung der $q_\mu[f]$ führt aus dem Hilbertraum hinaus; sie sind also keine Operatoren im Hilbertraum.

10. – Das Diracfeld.

Wir führen Operatordistributionen $\psi[f]$, $\psi^\dagger[f]$ ein, die den Integralen

$$\psi[f] \sim \int \psi_\alpha^\dagger(x) f_\alpha(x)\,\mathrm{d}x\,, \qquad \psi^\dagger[f] \sim \int \psi_\alpha(x) f_\alpha(x)\,\mathrm{d}x$$

entsprechen sollen. Wir nehmen im Integranden stets den hermitisch konjugierten Operator, weil dies dem Skalarprodukt im Hilbertraum entspricht. Ist A ein beliebiger auf Koordinaten oder Indizes wirkender Operator, so ist

$$(A\psi)[f] = \psi[A^\dagger f]\,, \qquad (A\psi^\dagger)[f] = \psi^\dagger[A^\dagger f]\,. \tag{78}$$

Folglich ist

$$\psi^*[f] = (\psi^\dagger\beta)[f] = \psi^\dagger[f\beta] \sim \int \psi_\alpha(x) f_\beta(x)\beta_{\beta\alpha}\,\mathrm{d}x\,, \tag{79}$$

wobei $\beta = \beta^\dagger$, $\beta^{-1}\gamma^\dagger\beta = \gamma$, und

$$\psi^\dagger[f] = \psi^*[f\beta^{-1}]\,. \tag{80}$$

Es gilt

$$\psi[f]^\dagger = \psi^\dagger[\bar{f}]\,. \tag{81}$$

Das Postulat 2) aus Abt. 5 ist für A o.Z. durch

$$\begin{cases} U(a, A)\psi[f]U^{-1}(a, A) &= \psi[S^\dagger f(A^{-1}(x-a))]\,, \\ U(a, A)\psi^*[f]U^{-1}(a, A) &= \psi^*[f(A^{-1}(x-a))S^{-1\dagger}] \end{cases} \tag{82}$$

zu ersetzen, wobei $S^\dagger = \beta S^{-1}\beta^{-1}$, $S^{-1}\gamma S = A\gamma$. Für A mit Zeitumkehr ist rechts $\bar{f}$ zu nehmen. An Stelle von 4) sollen nun die Antikommutatoren verschwinden, die man aus ψ und ψ^* bilden kann, wenn die Tf. raumartig zueinander liegen. 3) und 5) werden übernommen.

Wir nennen

$$\psi[f]\Omega = f^{(-)}\,, \qquad \psi^*[f]\Omega = f^{(-)}\,. \tag{83}$$

Durch fortgesetzte Anwendung von ψ und ψ^* erhalten wir die Elemente eines

Raumes $\mathfrak{B}$ [14] in der Gestalt

$$f = \{f_0, f_1^{(s_1)}(x_1), f^{(s_1,s_2)}(x_1, x_2), \ldots\},$$

wobei $s_j = \pm$; f_n ist noch eine Matrix $f_{\alpha_1 \ldots \alpha_n}(x_1 \ldots x_n)$, $\alpha_j = 1, \ldots, 4$. Für das innere Produkt machen wir den Ansatz

$$(\Omega, g_n^{(s_1 \ldots s_n)}) = F_n[g_n^{(s_1 \ldots s_n)}]\,. \tag{84}$$

Wegen (80) und (81) ist

$$\begin{aligned}(f^{(+)}, g_n^{(s_1 \ldots s_n)}) &= (\psi[f]\Omega, g_n^{(s_1 \ldots s_n)}) = \\ &= (\Omega, \psi^*[\bar{f}\beta^{-1}] g_n^{(s_2 \ldots s_{n+1})}) = F_{n+1}[(\bar{f}\beta^{-1})^{(-)} g_n^{(s_2 \ldots s_{n+1})}]\,.\end{aligned}$$

Ähnlich sind alle inneren Produkte durch die F_n gegeben. Diese haben wieder (A) bis (E) analoge Bedingungen zu erfüllen.

Nach den Bedingungen des Abt. 5 sind nun jene aus Abt. 7 zu modifizieren:

1) Die Antikommutatoren sind Zahlen und Skalare.

2) $(\partial - m)\psi[f] = 0$, $\psi^*(\partial + m)[f] = 0$ oder $\psi[(\partial^\dagger - m)f] = 0$, $\psi^*[f(\partial^\dagger + m)] = 0$.

Daraus schließt man ähnlich wie in Abt. 7 und Abt. 9 auf

$$\left\{\begin{aligned}&\{\psi[f], \psi[g]\} = \{\psi^*[f], \psi^*[g]\} = 0\,,\\ &\{\psi[f], \psi^*[g]\} = iS[fg]\,,\\ &S[fg] = -\Delta(x-y)[g(y)(\partial_x^\dagger + m)f(x)] = -\Delta(x-y)[g(y)(-\partial_y^\dagger + m)f(x)]\,.\end{aligned}\right. \tag{85}$$

Tatsächlich ist

$$\begin{aligned}(\partial_x - m)S[f(x)g(y)] &= S[(\partial_x^\dagger - m)f(x)g(y)] = 0\,,\\ S[f(x)g(y)](\partial_y + m) &= S[f(x)g(y)(\partial_y^\dagger + m)] = 0\,.\end{aligned}$$

Aus dem Fehlen von Zuständen negativer Energie schließt man

$$F_2[f^{(s)}g^{(s)}] = 0\,, \quad F_2[f^{(+)}g^{(-)}] = iS^+[fg]\,, \quad F[_2f^{(-)}g^{(+)}] = iS^-[gf]\,. \tag{86}$$

---

[14] Wir behalten trotz der Unterschiede gegenüber Abt. 4 der Einfachheit halber die Bezeichnungen $\mathfrak{B}$, $\mathfrak{B}^k$, $\mathfrak{W}$ ... bei.

Allgemein schließt man durch Induktion auf

$$F_{2j}[f_1^{(s_1)} \dots f_{2j}^{(s_{2j})}] = \sum \eta_{k_1 l_1 \dots k_j l_j} F_2[f_{k_1}^{(s_{k_1})} f_{l_1}^{(s_{l_1})}] \dots F_2[f_{k_j}^{(s_{k_j})} f_{l_j}^{(s_{l_j})}] \tag{87}$$

analog (59). $\eta_{m_1 \dots m_n}$ ist 1 für gerades $P(m)$, -1 für ungerades. Man kann zeigen, daß die F_n allen Forderungen genügen.

Jeder Zustand $f(x_1 \dots x_n)$ kann als Summe von Vektoren mit Tf. in höchstens $4n$ Variablen mit nur negativen Frequenzen dargestellt werden. Der Teilchenzahloperator N und der Gesamtladungsoperator Q sind in dieser Darstellung gegeben durch

$$Nf^{(s_1 \dots s_n)}(x_1 \dots x_n) = nf^{(s_1 \dots s_n)}(x_1 \dots x_n)\,, \tag{88}$$

$$Qf^{(s_1 \dots s_n)}(x_1 \dots x_n) = \sum_{j=1}^{n} (s_j e) f^{(s_1 \dots s_n)}(x_1 \dots x_n)\,. \tag{89}$$

$\psi[f]\Omega$ ist ein Elektronenzustand, $\psi^*[f]\Omega$ ein Positronenzustand, umgekehrt wie bei $\psi(x)$ und $\psi^*(x)$.

Wenden wir uns nun der Einführung eines Stromdichteoperators $j[h]$ zu, der für alle aus Tf. gebildeten Vierervektoren $h = (h_0(x), \dots h_3(x))$ definiert werden soll. $j[h]$ entspricht dem Ausdruck $e\int \psi^*(x)\gamma^\mu h_\mu(x)\psi(x)\,\mathrm{d}x$ der herkömmlichen Theorie. Da es kein $\psi(x)$ und $\psi^*(x)$ gibt, muß man indes anders vorgehen. Man kann formal schreiben

$$\begin{aligned} j[h] &= \int e\psi^*(x_1)\gamma^\mu h_\mu(x_1)\,\delta(x_1 - x_2)\,\psi(x_2)\,\mathrm{d}x_1\,\mathrm{d}x_2 = \\ &= e\int \psi^\dagger(x_1)\beta\gamma^\mu h_\mu(x_1)\,\delta(x_1 - x_2)\,\psi(x_2)\,\mathrm{d}x_1\,\mathrm{d}x_2 = \\ &= e\psi\psi^\dagger[\beta\gamma^\mu h_\mu(x_1)\,\delta x_1 - x_2)] = e\psi\psi^*[\gamma^\dagger h(x_1)\,\delta(x_1 - x_2)\,)\,. \end{aligned}$$

Diese heuristischen Überlegungen sind die Richtschnur für die Definition der Matrixelemente von $j[h]$ durch folgende Vorschrift:

1) Man bildet die Matrixelemente von $\psi[u]\psi^*[v] - (\Omega, \psi[u]\psi^*[v]\Omega)$, das sind die Matrixelemente von $\psi[u]\psi^*[v]$ ohne jene Terme, in welchen $S^-[uv]$ vorkommt.

2) Man geht mit $u(x_1)v(x_2) \to eh(x_1)\delta(x_1 - x_2)\gamma^\dagger$ bzw. $\hat{u}(k_1)\hat{v}(k_2) \to$ $\to (2\pi)^2 e\hat{h}(k_1 - k_2)\gamma^\dagger$. $\gamma^\dagger$ hat die nötigen 16 Komponenten. $\hat{h}(k_1 + k_2)$ ist keine Tf., doch existieren die Impulsraumintegrale, wenn nur $\hat{h}(k)$ bzw. $h(x)$ Tf. ist.

Als Illustration berechnen wir $(\Omega, \psi^*[f]j[h]\psi[g]\Omega)$. Zunächst ist

$$(\Omega, \psi^*[f]\psi[u]\psi^*[v]\psi[g]\Omega) = -S^-[uf]S^-[gv] - S^-[gf]S^+[uv]\,.$$

Der zweite Term ist wegzulassen, der erste ergibt

$$(2\pi)^2\theta(-k_1^0)\theta(\quad k_2^0)\delta(k_1^2\quad m^2)\delta(k_2^2\quad m^2)[f(\quad k_1)(k_1\gamma^\nu - m)\dot{u}(k_1)c(\quad k_2)(k_2\gamma^\nu\quad m)\dot{g}(k_2)].$$

Setzen wir an Stelle von $u_\lambda(k_1)c_{\cdot\beta}(\quad k_2)$ hier $(2\pi)^2 e\hat{h}(k_1\quad k_2)\gamma^\nu_{\lambda\beta}$, so erhalten wir

$$e\theta(\quad k_1^0)\theta(\quad k_2^0)\,\delta(k_1^2\quad m^2)\,\delta(k_2^2\quad m^2)[f(\quad k_1)(k_1\gamma^\nu\; - m)\,\dot{h}(k_1\quad k_2)\gamma^\nu(k_2\gamma^\nu\; - m)\dot{g}(k)] -$$

$$e\int \frac{f(\quad k_1)(k_1\gamma^\nu\; - m)\,\dot{h}(k_1\quad k_2)\gamma^\nu(k_2\gamma^\nu\quad m)\dot{g}(k_2)}{4k_1^0k_2^0}\,\mathrm{d}\boldsymbol{k}_1\,\mathrm{d}\boldsymbol{k}_2.$$

Hierbei ist $k_j^0 = -(\boldsymbol{k}_j^2 + m^2)^{\frac{1}{2}}$ einzusetzen.

Man überzeugt sich leicht, daß $(f_n^{\alpha_1\cdots\alpha_{n'}}, j[h]g_m^{\beta_1\cdots\beta_{m'}})$ gleich $(f_n'^{\alpha_1\cdots\alpha_{n'}}, j[h]g_m'^{\beta_1\cdots\beta_{m'}})$ ist, wenn f_n mit f_n' und g_m' mit g_m äquivalent ist. Durch die Vorschrift, daß $(f, j[h]g)$ linear in g, antilinear in f ist, kann man $(f, j[h]g)$ für alle $f, g \in \mathfrak{V}$ erklären. Zusammenfassend gilt für diese Matrix:

a) $(f, j[h]g) = (f', j[h]g')$, sobald f mit f' und g mit g' äquivalent ist.

b) $(f, j[h]g)$ läßt sich auf alle Elemente f, g übertragen, die in $\mathfrak{W}^r$ liegen und ist stetig in $\mathfrak{W}^r$ in der Metrik von $\mathfrak{W}^r$.

c) $(f_n^{\cdot}, j[h]g_m^{\cdot}) = 0$, außer die Zahl der Elektronen in f unterscheidet sich von der Zahl der Elektronen in g um ± 1, und ebenso die der Positronen.

Es soll angedeutet werden, wie man zeigt, daß $j[h]$ nicht nur eine Matrix ist, sondern auch ein Operator. *b*) bedeutet, daß (f, jg) für alle f, g aus dem endlichen Teil von $\mathfrak{V}$ erklärt werden kann. Nach *c*) kann aber f beliebig in $\mathfrak{V}$ sein, wenn nur g im endlichen Teil liegt, da es, wenn $g \in \mathfrak{W}^r$, nur auf die Komponenten von f in $\mathfrak{W}^{r+2}$ ankommt. Aus dem gleichen Grund ist $(f, j[h]g)$ stetig in f. Jede stetige, antilineare Funktion in f hat die Form (f, d). Daher ist $j[h]$ ein über dem endlichen Teil von $\mathfrak{V}$ definierter Operator, der dem Element g das Element d zuordnet: $j[h]g = d$.

Im Grenzfall $h(x) \to (\delta(x^0), 0, 0, 0)$ bzw. $\hat{h}(k) \to (2\pi\delta(\boldsymbol{k}), 0, 0, 0)$ existieren die Matrixelemente, wie man sich durch Einsetzen überzeugt. Einige Rechnung zeigt, daß sie mit den Matrixelementen von Q übereinstimmen.

RIASSUNTO

Viene applicata la teoria delle distribuzioni di L. SCHWARTZ nella formulazione della teoria quantistica dei campi onde risulti matematicamente consistente. L'introduzione di funzioni di distribuzione permette di ottenere molte formule nel formalismo rigoroso e con cambiamenti semplicissimi rispetto alla formulazione corrente. Facendo l'ipotesi dell'esistenza di un operatore di campo spazio-temporale avente l'aspetto distribuzionale, si arriva alla formulazione di uno spazio Hilbertiano introdotto dal WIGHTMAN: tale spazio è metricamente definito da una successione di distribuzioni le quali altro non sono che i valori medi del vuoto risultanti dalla teoria. Tali valori vengono ottenuti con semplici ipotesi per i campi di Schrödinger-Gordon, di Maxwell, di Dirac. A proposito del campo elettromagnetico si osserva che la metrica è definita solo in un sottospazio dell'intero spazio di Hilbert definito dalla condizione di Lorentz. Infine si rende possibile la definizione di densità di corrente nella struttura della teoria, densità che corrisponde all'abituale.

Étude de la dissolution des grains d'argent des plaques nucléaires épaisses dans le fixateur.

G. Thuro et M. Paić

Institut Ruder Bošković
et Institut de Physique de la Faculté des Sciences - Zagreb (Yougoslavie)

(ricevuto il 18 Luglio 1956)

Resumé. — Par suite d'un grand nombre d'expériences il a été constaté que l'oxygène atmosphérique facilite considérablement la dissolution des grains d'argent dans le fixateur. C'est pourquoi la dissolution des grains d'argent des plaques photographiques dans les solutions d'hyposulfite de sodium contenant des réducteurs — soit du bisulfite de sodium, soit du sulfite de sodium en présence d'acide acétique — a été étudiée. Sous condition de diminuer, par ébullition prolongée de l'eau, la quantité d'oxygène dans les solutions, il est possible d'empêcher, par de faibles concentrations de ces additions, la dissolution de l'argent. Ces résultats ont été appliqués au fixage des plaques nucléaires de 400 et 600 μm d'épaisseur. Des domaines de concentration en bisulfite de sodium, ou en sulfite de sodium en présence d'acide acétique, pour lesquels il n'y a ni dissolution de l'argent ni turbidité gênante des plaques nucléaires, ont été déterminés. Un fixateur contenant, en plus de l'hyposulfite de sodium, du sulfite de sodium et de l'acide acétique, est proposé.

1. – Introduction.

La dissolution, dans le bain de fixage des grains d'argent qui forment les traces des particules ionisantes des émulsions nucléaires est un phénomène fréquent, lorsqu'il s'agit des émulsions épaisses, particulièrement gênant et jusqu'à présent incontrolable [1-4]. Ayant eu nous mêmes des déboires avec

[1] A. Bonetti et G. Occhialini: *Suppl. Nuovo Cimento*, **11**, 222 (1954).
[2] R. W. Birge, L. T. Kerth, Ch. Richman, D. H. Stork et S. L. Whetstone: Berkeley, California, *UCRL* - 2690 (1954).
[3] G. Meulemans: *Suppl. Nuovo Cimento*, **12**, 410 (1954).
[4] M. Teucher: *Ergebnisse d. exakt. Naturwiss.*, **28**, 407 (1955).

le fixage des émulsions nucléaires, nous avons décidé d'élucider ce phénomène, de trouver, si possible, sa cause et d'y remédier.

Nous avons étudié d'abord l'action du fixateur sur l'argent finement divisé des plaques photographiques ordinaires. Ces plaques ont été préalablement développées et fixées suivant le procédé habituel en photographie. La dissolution de l'argent a été appréciée photométriquement. Ayant trouvé la composition des bains de fixage dans lesquels l'argent ne se dissout pas, nous avons fixé dans ces bains des plaques nucléaires épaisses. L'examen de l'image microscopique nous a permis de choisir la composition du fixateur qui tout en ne dissolvant pas les grains d'argent n'altère pas la qualité de l'image microscopique.

2. Appréciation photométrique de la dissolution de l'argent.

Des plaques photographiques panchromatiques (FK Univerzal Pan) ont été exposées à la lumière, développées, fixées, lavées et séchées suivant la pratique photographique habituelle. La dimension moyenne des grains d'argent de telles plaques a été de 0.5 μm environ. La densité optique $\log (I_0/I)$ de chaque plaque a été déterminée à l'aide d'un microphotomètre. Elle était de 0.7 environ. Les plaques photographiques ont été ensuite immergées dans des solutions à étudier et abandonnées là pendant 4 jours, à la température de 5 °C. C'est le temps nécessaire pour terminer l'opération du fixage d'une emulsion nucléaire de 600 μm d'épaisseur. Après ce laps de temps les plaques ont été lavées à l'eau courante, séchées et photométrées. La quantité d'argent mise en contact avec le fixateur a été toujours très faible par rapport au volume de fixateur: 250 cm^3 environ de fixateur pour une plaque de (3×3) cm^2, déjà fixée.

Dans le cas où la même densité optique a été retrouvée, il n'y avait pas de dissolution d'argent, et le rapport δ des densités optiques après et avant l'action du bain est égal à 1. La valeur δ inférieure à 1 indique une dissolution de l'argent et δ supérieure à 1 montre l'augmentation de l'opacité de la plaque consécutive à la formation d'un depôt ou à la coloration de la gélatine.

3. – Action de l'oxigène atmosphérique.

Pour dégager les facteurs essentiels qui influent sur la dissolution de l'argent dans la solution d'hyposulfite de sodium un grand nombre d'expériences a été effectuée. Dans celles que nous allons mentionner il s'agissait de l'action, dans des conditions de température et de durée déjà indiquées, d'une solution d'hyposulfite de sodium ($Na_2S_2O_3 \cdot 5H_2O$) « pur pour analyse » de 360 g/l, dans l'eau distillée. Voici les résultats de ces expériences.

Lorsque la solution d'hypolsfite de sodium est préparée avec de l'eau distillée froide et l'action a lieu dans un récipient ouvert il se produit une forte dissolution de l'argent ($\delta = 0.21 \pm 0.12$). Si la solution remplit entièrement le récipient fermé, moins d'argent se dissout ($\delta = 0.44 \pm 0.14$). Le remplacement de l'air atmosphérique par l'azote a pour effet une certaine diminution de la dissolution ($\delta = 0.29$ au lieu de 0.21 en présence d'air). Si l'azote est barboté de temps à autre à travers la solution, δ augmente de 0.29 à 0.37.

La solution étant préparée avec de l'eau distillée, bouillie 30 min environ, dans un ballon en verre chimiquement résistant, l'action dissolvante de la solution en récipient ouvert est plus faible ($\delta = 0.28 \pm 0.14$) que lorsque l'eau n'est pas bouillie.

L'amélioration devient nette si la solution remplit entièrement ou presque le récipient ($\delta = 0.91\ ^{0.06}_{0.17}$). Un faible courant d'air à travers la solution ainsi préparée, maintenu pendant l'action sur la plaque, fait tomber δ à 0.1, ce qui correspond à une dissolution presque complète de l'argent de la plaque. Si l'on ne dissout pas le fixateur dans l'eau chaude, immédiatement après l'ébullition, mais seulement après l'avoir laissé refroidir, bien que le récipient dans lequel l'action a lieu soit entièrement rempli, il y a dissolution ($\delta = 0.1 \pm 0.14$). Le filtrage de la solution d'hyposulfite encore chaude détruit l'avantage de l'ébullition préalable, même si l'action se fait en récipient clos et rempli entièrement ($\delta = 0.46 \pm 0.2$).

Ces expériences montrent que c'est l'oxygène de l'air qui favorise la dissolution de l'argent et que l'ébullition préalable de l'eau, servant à la préparation du fixage, la diminue considérablement, bien qu'insuffisament.

Le milieu oxydant favorisant la dissolution de l'argent on pouvait espérer de l'empêcher en ajoutant à la solution d'hyposlfite de sodium des réducteurs entrant habituellement dans la composition du fixateur, à savoir le bisulfite de sodium ($Na_2S_2O_5$) et le sulfite de sodium (Na_2SO_3).

4. – Action du bisulfite et du sulfite de sodium.

En ajoutant des quantités croissantes de bisulfite de sodium à des solutions d'hyposulfite de sodium préparées à partir d'eau distillée n'ayant pas été préalablement bouilli, la dissolution de l'argent de la plaque photographique a été favorisée dans quatre cas sur cinq et entravée dans un cas (Fig. 1). L'inconstance de l'action du bisulfite a été signalée par Meulemans [3].

Pour diminuer la quantité d'oxygène dissous, nous avons préparé le bain de fixage avec de l'eau distillée bouillie pendant 30 minutes. Cette eau, retirée du feu est immédiatement versée sur la quantité nécessaire d'hyposulfite de sodium placée dans des flacons à poudre de 250 cm³, pour obtenir une teneur de 360 g/l. A cette solution on ajoutait, au besoin, du bisulfite et du sulfite

de sodium, préalablement dissous dans l'eau chaude bouillie. Les flacons sont bouchés à l'émeri et placés dans le frigidaire à +5 °C. Lorsque la solution a atteint cette température, les plaques à examiner y ont été immergées.

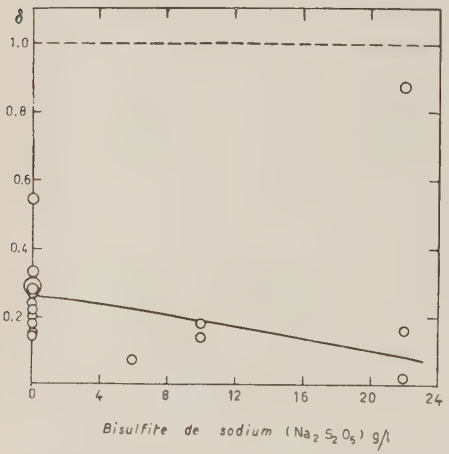

Fig. 1. – Rapport δ des densités optiques des plaques photographiques développées, après et avant l'action à 5 °C, des solutions de l'hyposulfite de sodium ($Na_2S_2O_3 \cdot 5H_2O$: 360 g/l), en fonction de la teneur en bisulfite de sodium. Durée de l'action: 4 jours. L'eau servant à la préparation des solutions *n'a pas été bouillie.*

Les résultats obtenus avec les plaques photographiques déjà fixées, de dimensions (3×3) cm² en présence de bisulfite de sodium sont representés sur la Fig. 2*a*. On voit que la solution d'hyposulfite pur tout en étant préparée à partir d'eau bouillie, dissout des quantités notables d'argent. Dès que l'on ajoute une faible quantité de bisulfite de sodium (0.3 g/l) la dissolution de l'argent est complètement empêchée, sous condition d'opérer en flacon plein et bouché, ce qui a été surtout réalisé dans les expériences à faible teneur de bisulfite. Il semble que des quantités élevées de bisulfite de sodium (30 g/l) favorisent la dissolution de l'argent.

Si en plus du bisulfite de sodium on ajoute une quantité constante de sulfite de sodium, 5 g/l (Fig. 2*b*) ou 10 g/l (Fig. 2*c*), on observe une augmentation de l'opacité des plaques qui n'est pas souhaitable.

Pour nous rendre compte de l'influence du bisulfite et du sulfite de sodium sur la qualité de l'image microscopique des émulsions nucléaires, nous avons utilisé des émulsions pelées Ilford G5 de 600 et 400 μm d'épaisseur, préalablement collées sur verre et développées suivant le procédé de Dilworth, Occhialini et Vermaesen [5].

Les émulsions nucléaires ont été soumises à l'action du fixateur de la même manière que les plaques photographiques. Il y avait toujours un grand excès de fixateur: 1 cm³ environ d'émulsion nucléaire pour 1 l de fixateur. Après lavage à l'eau courante et séchage à l'air libre calme, les émulsions nucléaires ont été examinées au microscope. Les résultats de l'examen microscopique au grossissement 1000 sont représentés sur le Figs. 3 *a b c*. Sur l'axe des or-

[5] C. C. Dilworth, G. Occhialini et L. Vermaesen: *Bull. du Centre de Phys. Nucl., Bruxelles*, **23** (1950).

données sont portées les valeurs se rapportant à la qualité de l'image microscopique des traces, exprimée en « notes » allant de 0 à 10, données par deux observateurs. Les notes ont les significations suivantes: 0, plaque complètement opaque, inutilisable; 1, presque complètement opaque, inutilisable; 2, très opaque, pratiquement inutilisable; 3, les traces près de la surface de

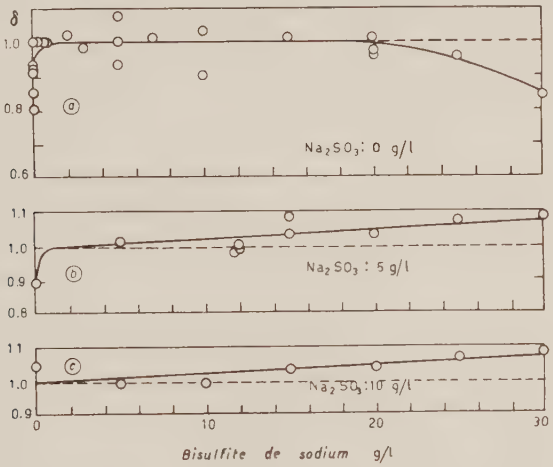

Fig. 2. – Valeur δ des plaques photographiques développées immergées quatre jours, à 5 °C, dans des solutions de $Na_2S_2O_3 \cdot 5H_2O$ (360 g/l), en fonction de la teneur en bisulfite et sulfite de sodium. L'eau servant à la préparation des solutions *a été bouillie pendant* $\frac{1}{2}$ h.

a plaque peuvent être distinguées; 4, les traces peuvent être discernées aussi dans les régions plus profondes, mais il est difficile de compter les grains; 5, la plaque peut être utilisée pour les mesures, mais dans les régions profondes l'image microscopique des grains n'est pas très nette, l'observation et les mesures sont fatiguantes; 6 et 7, les caractères généraux de la plaque restent pareils à ceux mentionnés en liaison avec la « note » 5, mais le travail d'observation et de mesure devient plus facile qu'avec une plaque ayant cette « note »; 8, 9, 10, les plaques caractérisées par ces « notes » élevées ont des qualités optiques très satisfaisantes: l'image près du fond de la plaque est presque, ou tout à fait aussi nette et contrastée que près de la surface et ces qualités ne sont pas dues à une clarification de l'image due à la « corrosion ». L'interval des notes allant de 8 à 10 est hachuré sur les graphiques.

Des faibles additions de bisulfite de sodium, allant de 0.3 à 2 g/l permettent d'obtenir des images de bonne qualité (Fig. 3*a*), sans apparition de la « corrosion ». Des teneurs plus grandes de bisulfite de sodium provoquent la turbidité et rendent difficile l'observation microscopique.

L'addition de 5 g/l et de 10 g/l de sulfite de sodium (Fig. 3*b* et *c*) en plus des quantités croissantes de bisulfite de sodium augmente la turbidité et n'est pas à recommander.

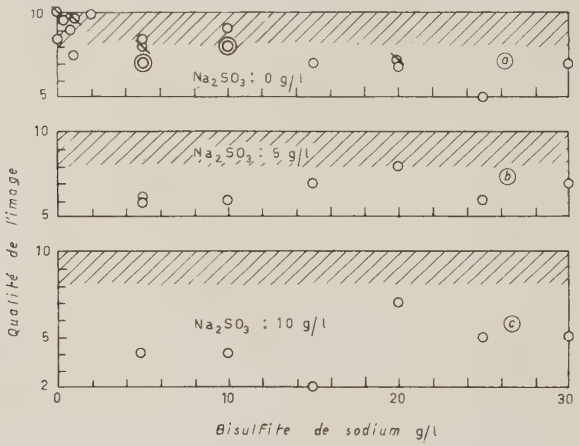

Fig. 3. – Qualité, notée de 0 à 10, de l'image microscopique des traces nucléaires dans les plaques nucléaires, fixées à 5 °C dans des solutions de $Na_2S_2O_3 \cdot 5H_2O$ (360 g/l), en fonction de la teneur en bisulfite et sulfite de sodium. Rapport du volume de l'émulsion nucléaire et du volume de fixateur: 1/1000 environ. Pas d'agitation. L'eau servant à la préparation des solutions *a été bouillie pendant* ½ h. Les cercles barrées se rapportent aux plaques de 600 μm d'épaisseur les autres cercles aux plaques de 400 μm.

5. – Action du sulfite de sodium en présence de l'acide acétique.

Des additions de sulfite de sodium à la solution d'hyposlfite de sodium préparée avec de l'eau distillée non bouillie, peuvent empêcher la dissolution des grains d'argent des plaques photographiques comme le montre la Fig. 4. Malheureusement la turbidité des plaques nucléaires augmente considérablement avec la quantité de sulfite de sodium ajoutée. Lorsque cette quantité est suffisante pour protéger complètement l'argent de la dissolution, la plaque nucléaire devient opaque, donc inutilisable. Cette observation est en accord avec une remarque de WALLER (6).

Si l'on prépare les solutions d'hyposulfite de sodium à partir d'eau distillée

(6) BRAUN, CORNIL, G. MEULEMANS: *Congrès International sur le Rayonnement cosmique, Bagnères de Bigorre* (1953).

bouillie, des plus faibles quantités de sulfite de sodium sont suffisantes pour empêcher une forte dissolution de l'argent (Fig. 5). Toutefois la protection n'est pas complète, à moins d'ajouter jusqu'à 10 g/l de Na_2SO_3 ce qui augmente la turbidité des émulsions nucléaires.

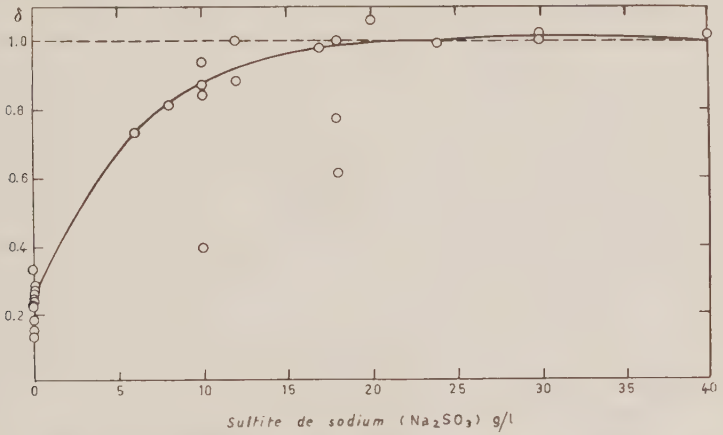

Fig. 4. Valeur δ des plaques photographiques développées immergées 4 jours, à 5 °C, dans des solutions de $Na_2S_2O_3 \cdot 5H_2O$ (360 g/l), en fonction de la teneur en sulfite de sodium. L'eau servant à la préparation des solutions *n'a pas été bouillie*.

En acidifiant, même très légèrement, la solution d'hyposulfite de sodium additionnée de sulfite de sodium, la protection contre la dissolution de l'argent devient très bonne: déjà 0.2 cm³ d'acide acétique glacial par litre en présence de 0.25 g/l de Na_2SO_3 agissent nettement dans ce sens (Fig. 6*a*). La quantité d'acide acétique que l'on peut ajouter à la solution d'hyposulfite de sodium (360 g/l), croît avec la quantité de sulfite de sodium préalablement ajoutée. En absence de sulfite la moindre quantité d'acide acétique décompose déjà l'hyposulfite. La plus forte teneur en sulfite de sodium ajoutée a été 10 g/l en présence de 16 cm³ d'acide acétique par litre. Dans cet interval étendu de teneurs en sulfite de sodium et en acide acétique la dissolution de l'argent a été empêchée, comme le montre la Fig. 6.

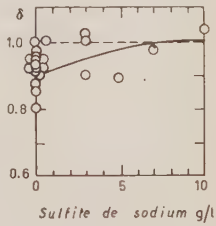

Fig. 5. – Valeur δ des plaques photographiques développées, traitées de la manière indiquée sur la Fig. 4, mais les solutions ont été préparées à partir d'eau distillée *bouillie pendant* ½ h.

La Fig. 7 permet de relever la composition des fixateurs donnant de bons résultats, dans les conditions où nous avons opéré, à savoir:

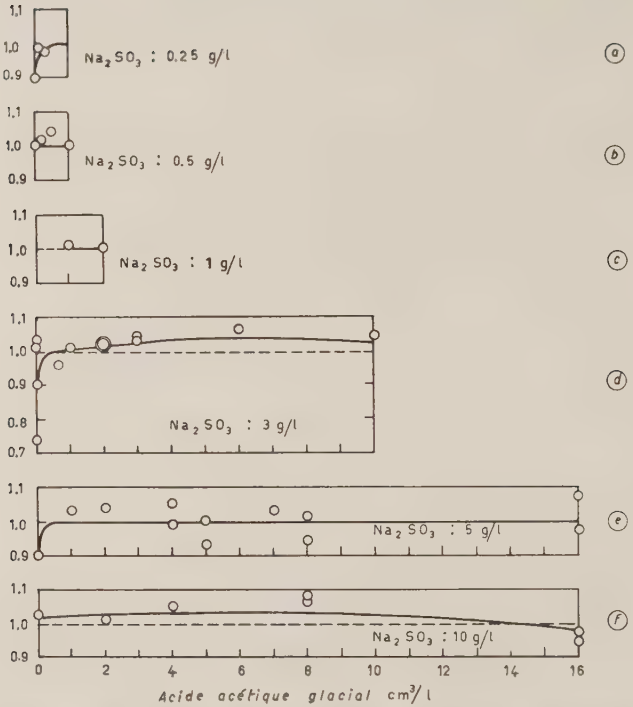

Fig. 6. – Valeur δ des plaques photographiques développées, immergées 4 jours, à 5 °C, dans des solutions de $Na_2S_2O_3 \cdot 5H_2O$ (360 g/l), en fonction de la teneur en sulfite de sodium et en acide acétique glacial. L'eau servant à la préparation des solutions *a été bouillie pendant* $\frac{1}{2}$ h.

$Na_2S_2O_3 \cdot 5H_2O$ (g/l)	Na_2SO_3 (g/l)	$CH_3 \cdot COOH$ (cm³/l)
360	0.5	0.4 à 1
360	1	(0.4) à 2
360	3	0.6 à 3
360	5	1 à 8

La quantité de 0.25 g/l de sulfite de sodium n'empêche pas complètement la dissolution de l'argent, tandis que 10 g/l de sulfite de sodium provoquent la turbidité.

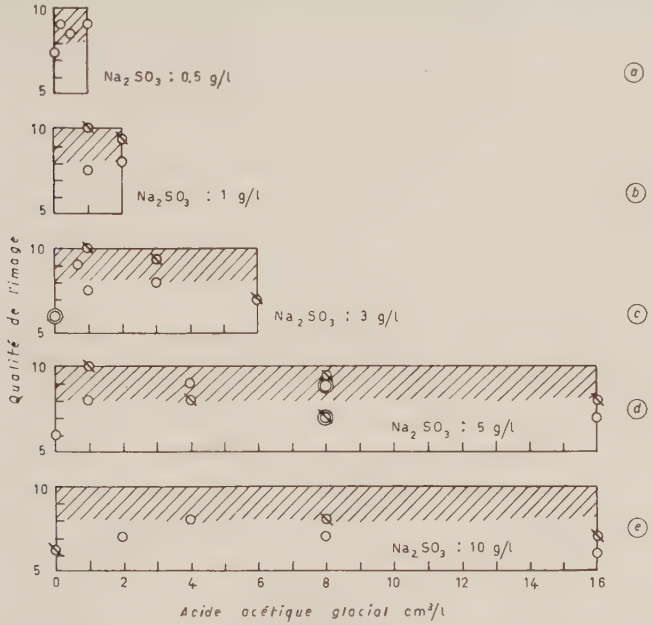

Fig. 7. – Qualité, notée de 0 à 10, de l'image microscopique des traces nucléaires dans les plaques nucléaires, fixées dans des solutions de $Na_2S_2O_3 \cdot 5H_2O$ (360 g/l), en fonction de la teneur en sulfite de sodium et en acide acétique glacial. Rapport du volume de l'émulsion nucléaire et du volume de fixateur: 1/1000 environ. Pas d'agitation. L'eau servant à la préparation des solution *a été bouillie pendant* ½ h.

6. – Influence du récipient.

Les essais décrits jusqu'à présent ont été effectués avec des plaques de petites dimensions ((2×2) cm²), sans agitation du fixateur et dans des récipients en verre bouchés à l'émeri. Toutefois le plus souvent on utilise des plaques nucléaires beaucoup plus grandes et le traitement a généralement lieu dans un récipient métallique à travers lequel circule le fixateur.

Un essai avec 6 plaques nucléaires ((5×10) cm²) de 600 μm d'épaisseur en récipient entièrement en acier inoxydable, avec circulation du fixateur, préparé avec de l'eau bouillie, contenant $Na_2S_2O_3 \cdot 5H_2O$: 360 g/l, Na_2SO_3: 6 g/l et $CH_3 \cdot COOH$: 5 cm³/l, et en atmosphère d'azote a donné des résultats satisfaisants, bien qu'il y ait eu une faible diminution de la valeur δ (0.92). Le rapport du volume de l'émulsion nucléaire et du volume de fixateur était 1/500 environ. Deux autres essais, avec des plaques nucléaires (400 μm) et des plaques photographiques de petites dimensions, dans le même récipient entièrement

plein et fixateur immobile, contenant $Na_2S_2O_3 \cdot 5H_2O$: 360 g/l, $Na_2S_2O_5$: 0.6 g/l, ont montré que le récipient métallique peut favoriser la dissolution de l'argent. En effet, la valeur δ des plaques photographiques ainsi traités a été de 0.37 dans un essai et 0.23 dans l'autre, tandis que les traces dans les plaques nucléaires ont disparu sur une épaisseur de 15 μm environ. Dans des récipients en verre bouchés à l'émeri le même fixateur ne provoquait pas de « corrosion ».

7. – Quelques remarques complémentaires.

Les plaques nucléaires ont été en général exemptes de coloration rougeâtre, sauf dans le cas où le lavage, après le bain d'arrêt, a été prolongé pendant une nuit.

La transparence des plaques nucléaires traitées ne dépend pas seulement du traitement subi, mais aussi de leur fabrication. Ainsi des plaques de 600 μm étaient parfois plus transparentes que des plaques de 400 μm traitées simultanément (Fig. 3 et 7).

Lorsque la plaque photographique ne montre aucune dissolution des grains d'argent, la plaque nucléaire traitée simultanément n'en montre pas non plus: la densité linéaire des grains d'une trace nucléaire ne diminue pas lorsqu'elle atteint la surface libre de l'émulsion.

8. – Conclusions.

Les expériences que nous avons effectuées nous permettent de conclure, qu'il est possible d'empêcher la dissolution des grains d'argent des plaques nucléaires sous condition d'éliminer autant que possible la présence d'oxygène atmosphérique et de protéger le bain de fixage soit avec des faibles quantités de bisulfite de sodium, soit, en présence d'acide acétique, avec des petites quantités de sulfite de sodium. Il est alors possible d'obtenir des plaques nucléaires transparentes, sans dissolution des grains d'argent.

Puisqu'il est difficile d'opérer en absence complète d'air et puisque le sulfite de sodium en milieu acide protège mieux contre la dissolution de l'argent que le bisulfite de sodium, nous proposons d'utiliser le bain de fixage contenant du sulfite de sodium en quantité aussi grande qu'elle ne provoque pas la turbidité de l'image. Dans ces conditions le récipient métallique ne paraît pas particulièrement gênant.

9. – Fixateur proposé.

Nous proposons le fixateur suivant:

Hyposulfite de sodium ($Na_2S_2O_3 \cdot 5H_2O$) . .	360	g
Sulfite de sodium anhydre (Na_2SO_3) . . .	5	g
Acide acétique glacial	4	cm^3
Eau distillée bouillie . . . . . q. s. p.	1000	cm^3

Tous les produits chimiques « purs pour analyse ».

Pour préparer un litre de ce fixateur on procède de la manière suivante. Un litre d'eau distillée est chauffé dans un ballon de verre à l'ébullition pendant $\frac{1}{2}$ h environ. L'hyposulfite de sodium est mis dans le récipient d'un litre faisant partie du dispositif de fixage. Le sulfite de sodium et l'acide acétique sont mis chacun dans un bécher. L'eau bouillante (600 cm^3 environ) est versée sur l'hyposulfite et sur les deux autres produits (50 cm^3 environ sur le sulfite de sodium et 100 cm^3 sur l'acide acétique) dans chaque bécher. Dès que l'hyposulfite et le sulfite sont dissous, les deux solutions sont mélangées (on évitera toute agitation superflue des liqueurs). L'acide acétique et la quantité d'eau nécessaire pour faire un litre sont ajoutés. Le fixateur ainsi préparé est placé immédiatement dans la glacière à 4-5 °C. Dès qu'il est froid il est prêt à être utilisé.

RIASSUNTO (*)

In seguito a un gran numero di esperienze si è constatato che l'ossigeno atmosferico facilita considerevolmente il dissolvimento dei granuli d'argento nel fissatore. Per questo motivo si è studiato il dissolvimento dei granuli d'argento delle lastre fotografiche nelle soluzioni d'iposolfito di sodio contenenti riduttori - bisolfito di sodio, o solfito di sodio in presenza di acido acetico. A condizione di diminuire per ebollizione prolungata dell'acqua la quantità d'ossigeno nelle soluzioni, è possibile di impedire, con deboli aggiunte di tali additivi, il dissolvimento dell'argento. Questi risultati sono stati applicati al fissaggio delle lastre nucleari di 400 e 600 μm di spessore. Si sono determinati dei tassi di concentrazione del bisolfito di sodio, o del solfito di sodio in presenza di acido acetico, per i quali non si ha nè dissolvimento dell'argento nè torbidità fastidiosa delle lastre nucleari. Si propone un fissatore contenente, oltre l'iposolfito di sodio, solfito di sodio e acido acetico.

(*) *Traduzione a cura della Redazione.*

IL NUOVO CIMENTO Vol. IV, N. 4 1° Ottobre 1956

On Gravitational Motion.

B. Bertotti (*)

Dublin Institute for Advanced Studies - Dublin

(ricevuto il 30 Luglio 1956)

Summary. – The problem of gravitational motion can be fruitfully tackled by using an alternative perturbation method, in which the « quasi-stationary » assumption is replaced by a more general one, fast motion being allowed, although the field is still weak. A simple rigorous property of spherical symmetry is assumed for each body, which is described by a suitable distribution of energy and momentum. The equations of motion which one gets for the two-body problem at the *first* approximation are nothing but Einstein's equations [see (1)], except for the two terms which are non linear in the masses.

1. – On the Approximation Procedure.

The approximation technique usually adopted in general relativity is based on the « quasi-stationary » assumption, which demands that the time-derivative of any field quantity be much smaller than the space-derivatives; that is to say, physically, bodies move slowly with respect to light signals (1).

We propose first to comment systematically on an alternative procedure in which a more general condition replaces the ordinary assumption, as one will see later, and is *fully* Lorentz-invariant. Although of course the usual method seems to be quite sufficient for any astronomical problem, a full use

(*) On leave of absence from the Istituto Nazionale di Fisica Nucleare, Sezione di Milano.

(1) We quote here the main papers concerning the problem of gravitational interaction: A. Einstein and L. Infeld: *Can. Journ. of Mat.*, **1**, 209 (1949) (here quoted as EI); A. Papapetrou: *Proc. Phys. Soc.*, A **64**, 57 (1951); L. Infeld: *Acta Phys. Pol.*, **13**, 187 (1954).

of the concepts of restricted relativity is certainly more suitable to approximate generally covariant equations, and allows for more general results.

The gravitational equations

$$R_{\mu\nu} + 4\pi k(2T_{\mu\nu} - g_{\mu\nu}T) = 0 \quad (1) \tag{1}$$

[2]

can be solved in successive approximation by assuming the metric tensor to be an analytical function of the *gravitational constant* k:

$$g_{\mu\nu} = \underset{0}{g_{\mu\nu}} + k\underset{1}{g_{\mu\nu}} + k^2\underset{2}{g_{\mu\nu}} + \dots . \tag{2}$$

A similar development is also assumed for $T^{\mu\nu}$, or for the quantities as a function of which $T^{\mu\nu}$ is defined. In general, the number written underneath a symbol shall mean the corresponding coefficient in the k-series.

The Galileian metric with signature -2 will be taken as zero-order approximation:

$$\underset{0}{g_{\mu\nu}} = \eta_{\mu\nu} \quad (3) \tag{3}$$

[3]

(no natural curvature!). Denoting with $N_{\mu\nu}$ the terms in the contracted curvature tensor $R_{\mu\nu}$ which are non-linear in

$$h_{\mu\nu} = g_{\mu\nu} - \eta_{\mu\nu} , \tag{4}$$

(1) can be written

$$h_{\mu\nu,\sigma\underline{\sigma}} - h_{\mu\sigma,\nu\underline{\sigma}} - h_{\nu\sigma,\mu\underline{\sigma}} + h_{\sigma\underline{\sigma},\mu\nu} = -8\pi k(2T_{\mu\nu} - g_{\mu\nu}T) - 2N_{\mu\nu} . \tag{5}$$

Equating the coefficients of k in both sides, the problem is reduced to the successive solution of sets of *linear* equations:

$$\underset{n}{h}_{\mu\nu,\sigma\underline{\sigma}} - \underset{n}{h}_{\mu\sigma,\nu\underline{\sigma}} - \underset{n}{h}_{\nu\sigma,\mu\underline{\sigma}} + \underset{n}{h}_{\sigma\underline{\sigma},\mu\nu} = -8\pi(2\underset{n-1}{T}_{\mu\nu} - \underbrace{g_{\mu\nu}T}_{n-1}) - 2\underset{n}{N}_{\mu\nu} ; \tag{5'}$$

in each set unknown quantities and quantities known from the previous approximations are separated in the two members.

---

[2] The notation: Greek indices run from 0 to 3; the comma and the stroke (/) signify respectively ordinary and covariant derivatives.

[3] We agree that we underline an index when we want to « raise » or « lower » it with the η-symbol:

$$v^{\mu}\, v^{\varrho} \equiv \eta_{\mu\varrho} .$$

It is easily seen that the left-hand side of (5)′—call it $2\underset{n}{L}_{\mu\nu}$—satisfies identically

$$2\underset{n}{L}_{\mu\nu,\nu} - \underset{n}{L}_{\nu,\mu} = 0 \; ; \tag{6}$$

therefore the right-hand side must fulfil the same relationship. It can be shown that this is so when the field equations (5) and the *conservation law*

$$\underset{/\nu}{T^{\mu\nu}} = 0 \tag{7}$$

are satisfied up to the order $n-1$. The proof runs very much on the same lines as Einstein's proof of analogous relations (see EI, § 7). Remembering the identities

$$(2R^{\mu\nu} - g^{\mu\nu}R)_{/\nu} = 0 \, , \tag{8}$$

one envisages

$$(8) + 16\pi k \, (7)$$

at the n-th order, for which (7) is required only up to the order $n-1$. The theorem easily follows from taking into account the field equations (5) up to the order $n-1$. We skip further details, and conclude that each approximation step—the n-th, say—consists in

a) solving the field equations (5′) for which $T^{\mu\nu}$ and $h_{\mu\nu}$ are needed only up to the $(n-1)$-th order, and

b) restricting the choice of $\underset{n}{T^{\mu\nu}}$ with the condition

$$\underbrace{\underset{n}{T^{\mu\nu}}}_{n}{}_{/\nu} = 0 \, , \tag{7′}$$

which insures the integrability of the next order field equations.

The integration of (5′) is easily performed in a frame in which

$$2\underset{n}{h}_{\mu\nu,\nu} - \underset{n-1}{h}_{\nu,\mu} = 0 \; ; \tag{9}$$

(5′) then acquires the well known form

$$\underset{n}{h}_{\mu\nu,\sigma\sigma} = -8\pi(2\underset{n-1}{T}_{\mu\nu} - \underbrace{g_{\mu\nu}T}_{n-1}) + 2\underset{n}{N}_{\mu\nu} \, , \tag{10}$$

and its general solution is a superposition of waves and retarded potentials. The condition (9) has to be imposed on the free waves; but the retarded (or advanced) potentials—to which we will confine ourselves—necessarily fulfil (9), since the right-hand side of (10)—the «source»—fulfils, because of (7), the same relation.

A generic frame of reference can be restored by an n-th order change of co-ordinates:

$$x^\varrho \to x'^\varrho = x^\varrho + \underset{n}{a^\varrho}\,, \tag{11}$$

tha $\underset{n}{a^\varrho}$ being arbitrary functions. The new $\underset{n}{h}$'s are

$$\underset{n}{h'_{\mu\nu}} = \underset{n}{h_{\mu\nu}} - \underset{n}{a_{\mu,\nu}} - \underset{n}{a_{\nu,\mu}}\,. \tag{12}$$

In order that this formal procedure should be useful at all, the order of magnitude of any quantity occurring here must correspond to its order in the k-development: that is to say, an n-th order quantity must be much smaller than a quantity of the order $n-1$. We require this to be true at least in *one inertial frame*; since any Lorentz-transformation is allowed, it might not hold in all the other ones. k being a constant, this hypothesis has the important consequence that if a quantity and its co-ordinate derivatives occur in the scheme, they must be of the same order of magnitude. Moreover, the very recurrent nature of the approximation process tells us then that our condition holds good if simply

$$|\underset{n}{h_{\mu\nu}}| \ll 1 \tag{13}$$

at least in one inertial frame.

2. – The Structure of the Body.

We will be concerned with bodies represented by a suitable, regular distribution of energy and momentum, following Papapetrou's line (see [1]). In this respect Infeld's work shows clearly that Einstein's approach, based on the empty space field equations with singular metric, is equivalent to postulating sources of the field, endowed with a definite structure, and obeying the conservation law. In the present incomplete state of the theory we deem the matter-tensor but a necessary and very useful evil.

The usual expression for a perfect fluid

$$T^{\mu\nu} = (\varrho + p)v^\mu v^\nu - pg^{\mu\nu} \tag{14}$$

will be assumed to describe each body; here ϱ and p are taken positive in the interior and nil outside; and v^μ is a time-like unit vector field (the « stream lines »). They shall also be endowed with the following rudimentary property of spherical symmetry. We assume that a « central » stream-line

$$l : x^\mu = y^\mu(s) \tag{15}$$

exists such that the pressure p, in every three-dimensional infinitesimal neighbourhood orthogonal to l, is a function of the Riemannian distance from l alone. If p is continuous with its first derivatives at l, this means

$$p_{,\mu} - p_{,\varrho} v^\varrho v_\mu = 0 \quad \text{on} \quad l\,, \tag{15}$$

since the distance from l is a quadratic function of the differentials dx^μ.

A simple calculation now shows that the conservation of (13) implies

$$(\varrho + p) v^\mu{}_{/\varrho} v^\varrho - (p^{,\mu} - p_{,\varrho} v^\varrho v^\mu) = 0\ ; \tag{16}$$

therefore our assumption (15) has as a consequence the geodesic character of l, and vice-versa.

One might wonder whether it is always possible to demand on each body this property (15). Let us notice that our power-series procedure is such that the conservation law (7) is imposed at *each* step on the quantities ϱ, p and v^μ *alone*, the g-field being known already with the necessary approximation: one has therefore only to demand at each stage that l be any geodesic of the known field.

Furthermore, once (15) is agreed upon, the motion of the « centre » and hence the motion of the body if its size is negligible, depends at each step on its structure only as far as the previous approximations are concerned. In this way the drawback in this formulation, of dragging in academic complications of structure, is partially relieved. Moreover (15) brings about a simplification in the calculations: at the last step, instead of going through the explicit form of (7′), one has only to demand for l the geodesic principle at that order of approximation. We choose for it the form:

$$\delta \int g_{\mu\nu}(y^\varrho(\tau)) \frac{dy^\mu}{d\tau} \frac{dy^\nu}{d\tau} d\tau = 0\,, \tag{17}$$

τ being an arbitrary parameter (1). To complete the scheme, we add that the bodies shall be very small relatively to the reciprocal distance, and their

(1) See T. Levi-Civita: *Absolute Differential Calculus* (London, 1927), p. 330.

density ϱ shall be low enough to allow for the condition (13) to be true everywhere. Moreover, according to the actual astronomical conditions, the pressure p will be taken as small as of the first order.

The uncertainty in the frame described by (11) can be taken into account simply by considering the world-line l of each body as undefined by the small amounts a^μ at each order.

3. – The First Order Approximation.

As an elementary and illustrative application we now go over to the first approximation step for the case of two bodies. Denoting them with the indices 1 and 2, and writing for simplicity $h_{\mu\nu}$ for $kh_{\mu\nu}$, ϱ and r^μ for $\underset{0}{\varrho}$ and $\underset{0}{r^\mu}$, the field equations (10) read, for $n=1$:

$$h_{\mu\nu,\sigma\sigma} = -8\pi k[\varrho_1(2v_1^\mu v_1^\nu - \eta_{\mu\nu}) + \varrho_2(2v_2^\mu v_2^\nu - \eta_{\mu\nu})] . \tag{18}$$

We must remember that now whenever k appears no corrections of any sort are needed: geometrical terms—distance, orthogonality, etc.—can be written with their usual Minkowskian meaning, and the pressure can be neglected. The integrability conditions (7′), now reading

$$(\varrho_1 v_1^\mu v_1^\nu + \varrho_2 v_2^\mu r_2^\nu)_{,\nu} = 0 ,$$

amount to saying that the constituent particles are conserved and move uniformly. We agree to take r^μ constant throughout the bodies, and for ϱ a function of the orthogonal distance from l alone. The solution of (18) is then:

$$h_{\mu\nu} = -2\varphi_1(2\dot{y}_1^\mu \dot{y}_1^\nu - \eta_{\mu\nu}) - 2\varphi_2(2\dot{y}_2^\mu \dot{y}_2^\nu - \eta_{\mu\nu}) , \tag{19}$$

where

$$\dot{y}_1^\mu = \frac{\mathrm{d}y_1^\mu}{\mathrm{d}s_1}$$

are four numbers and φ_1 is the potential solution of

$$\varphi_{1,\sigma\sigma} = 4\pi k\varrho_1 ; \tag{20}$$

that is, the Lorentz-transform of the ordinary Newtonian potential km_1/r_1 (and similarly for the other body).

We see now the meaning of our condition (13): in the rest-frame of l, for

instance, we must have:

$$|h_{\mu\nu}\dot{y}_1^\mu \dot{y}_1^\nu| = 2\varphi_1 + 2\varphi_2(2q^2 - 1) \ll 1 ,$$

where

$$q \equiv \dot{y}_1^\mu \dot{y}_2^\mu \tag{21}$$

is the (hyperbolic) cosine between the zero-order velocities. This condition suffices for averring (13): if a time-like vector, like the $\dot{y}$'s, has a very small time component, the spatial part must be very small too. We conclude that everywhere 1) the potential φ_1 must be very small and 2) the potential of the other body must satisfy

$$\varphi_2 q^2 \ll 1 . \tag{22}$$

In quasi-stationary conditions q is nearly one, and the smallness of φ_1 and φ_2 is enough; but (22) shows that q *is* allowed to grow bigger and bigger—the bodies to move faster and faster—provided they go far enough apart.

The small deviations from its uniform motion that the first body suffers because of gravitation is described by the variational principle (17). Introducing in (19) an arbitrary parameter τ_1 in the place of s_1, we write

$$h_{\mu\nu} = -2\varphi_1(2\dot{y}_1^\mu \dot{y}_1^\nu - \eta_{\mu\nu} I) - 2\varphi_2(2\dot{y}_2^\mu \dot{y}_2^\nu - \eta_{\mu\nu}) , \tag{19'}$$

where

$$I \equiv \dot{y}_1^\mu \dot{y}_1^\mu \tag{23}$$

shall be taken equal to one after the variation (this being a first integral of (17)!). The Lagrangian in (17) then becomes

$$L = I - 2\varphi_1 I - 2\varphi_2(2q^2 - I) , \tag{24}$$

understanding now φ_1 and φ_2 as the potentials computed *at* l_1.

It is immediately seen that the self part φ_1 does not contribute: on one hand, being a function of the distance from l_1 alone, it has there vanishing derivatives; on the other hand, being of the first order, it allows as a factor only a zero-order quantity, hence a constant $\dot{y}_1^\mu$. We are then left with

$$\boxed{L = I - 2\varphi_2(2q^2 - I)} ; \tag{25}$$

the corresponding Euler equations read:

$$\boxed{\ddot{y}_1^\mu + \varphi_{2,\underline{\mu}}(2q^2 - 1) - 2\dot{\varphi}_2(2q\dot{y}_2^\mu - \dot{y}_1^\mu) = 0} \quad , \tag{26}$$

I having been taken equal to one.

Do our equations of motion (26) contain anything new? The answer is *no*. EI's equations of motion, among their *13* terms, contain two which are quadratic in the masses and can not be expected te be included in (26); but as far as all the other ones are concerned, (26) is nothing but *their Lorentz invariant expression*. But at the same time we conclude that EI's equations in this reduced form have a *wider* validity than was generally assumed, holding good under the weak field condition (22); in other words, although EI's method could have possibly missed terms linear in the masses but of degree higher than the second in the velocities, we see that such terms do not exist at all. We would like also to point out the clear improvement of the present derivation with respect to EI as far as simplicity and technique are concerned.

To prove our assertion, we must replace the proper time s_1 in (26) with x^0 as independent parameter, and introduce the ordinary velocities

$$u_1^i(x^0) = \frac{\mathrm{d}y_1^i}{\mathrm{d}x^0} = \frac{\dot{y}_1^i}{\dot{y}_1^0} \tag{27}$$

(latin indices running from 1 to 3); it is also convenient to take a Lorentz frame in which at $x^0 = 0$—say—the second body is momentarily at rest (although accelerated):

$$u_2^i(0) = 0 \, . \tag{28}$$

Then, at $x^0 = 0$,

$$q = \dot{y}_1^0 = \frac{\mathrm{d}x^0}{\mathrm{d}s_1} = (1 - u_1^s u_1^s)^{-\frac{1}{2}} \, , \tag{29}$$

and from (26), for $\mu = 0$, we get

$$\frac{\mathrm{d}q}{\mathrm{d}x^0} = 2q\varphi_{2,s}u_1^s \, .$$

Using this and (29) in (26) for $\mu = i$, and dividing by q^2, we get

$$\frac{\mathrm{d}u_1^i}{\mathrm{d}x^0} - \varphi_{2,i}(1 + u_1^s u_1^s) + 4\varphi_{2,s}u_1^s u_1^i = 0 \, ; \tag{30}$$

in which one can easily recognize the EI formula (12.11) (with $\dot{\zeta}^s = 0$) as far as the terms linear in the masses are concerned (5).

The advance of the perihelion, being essentially a second order effect, can not be correctly described by (26); but the deflection of a light ray near a star (the double of the Newtonian one) can be read at glance from (30) taking

$$u_1^s u_1^s = 1 ,$$

which we know now to be allowed.

* * *

The necessary preparations being made, one can now pass over to the second step of our approximation: the equations of motion one will get will certainly be *more accurate* than EI's, in the same way as our equations (26) are more accurate than Newton's.

(5) The full EI equation can be got from (3) (except for two terms) with a Lorentz-transformation. See B. BERTOTTI: *Nuovo Cimento*, **12**, 226 (1954), Sect. 3.

RIASSUNTO

Il problema del moto gravitazionale può venire utilmente attaccato usando un procedimento perturbativo in cui l'ipotesi di « quasi-stazionarietà » è sostituita da un'altra più generale: benchè il campo sia ancora debole, nessuna restrizione è posta sulla velocità dei corpi. Ciascuno di essi è descritto da una conveniente distribuzione di energia e momento, e si suppone dotato di una proprietà semplice e rigorosa di simmetria sferica. Le equazioni di moto che si ottengono per il caso di due corpi al *primo* stadio di approssimazione coincidono con le equazioni di Einstein [vedi (1)], eccezion fatta per i due termini che non sono lineari nelle masse.

IL NUOVO CIMENTO Vol. IV, N. 4 1° Ottobre 1956

Basic Principles of Unified Field Theory.

R. S. Mishra

Department of Mathematics, University of Delhi - Delhi

(ricevuto il 30 Luglio 1956)

Summary. — In this paper the basic principles of Einstein's, Schrödinger's and Bonnor's unified field theory have been studied. Originally the field equations were given in terms of contracted curvature tensor $R_{\mu\lambda}$ Here the relations are obtained between $R_{\mu\lambda}$ and some other tensors like Einstein's tensor, transposed tensor and the tensor $T^{\alpha}_{\beta[\gamma\alpha]}$ and the field equations are modified in terms of these tensors. Incidentally it has been shown how these tensors are obtained in a number of ways in Ricci identities when the covariant differentiations are performed taking into consideration the nature of the indices.

1. – Introduction.

Einstein's [1,2] Unified Field Theory is based on three principles (Hlavaty [3]):

(i) The basic tensor $g_{\mu\lambda}$ is non-symmetric.

(ii) The connections $\Gamma^{\nu}_{\mu\lambda}$ are defined by

$$g_{\underset{+\ -}{\lambda\ \mu;\nu}} \equiv \frac{\partial g_{\lambda\mu}}{\partial x_\nu} - g_{\alpha\mu}\Gamma^{\alpha}_{\lambda\nu} - g_{\lambda\alpha}\Gamma^{\alpha}_{\nu\mu} = 0\,, \tag{1.1}$$

$$S_\lambda \equiv S^{\alpha}_{\lambda\alpha} = \frac{1}{2}(\Gamma^{\alpha}_{\lambda\alpha} - \Gamma^{\alpha}_{\alpha\lambda}) = 0\,. \tag{1.2}$$

(1) A. Einstein: *The Meaning of Relativity*, 3rd ed. (Princeton).
(2) A. Einstein: *The Meaning of Relativity*, 4th ed. (Princeton).
(3) V. Hlavaty: *Journ. Rational Mech. Analy.*, **3**(1), 103 (1954).

(iii) In order to get $g_{\mu\nu}$ a set of intrinsic conditions are imposed which can be condensed into

$$P_{\mu\lambda} = \frac{\partial}{\partial x^{[\mu}} X_{\lambda]} , \tag{1.3}$$

where $P_{\mu\lambda}$ is the Einstein's tensor ([1,2]) given by

$$P_{\lambda\mu} = \frac{\partial}{\partial x^{\alpha}} \Gamma^{\alpha}_{\lambda\mu} - \Gamma^{\alpha}_{\lambda\beta}\Gamma^{\beta}_{\alpha\mu} - \frac{1}{2}\left(\frac{\partial}{\partial x^{\mu}} \Gamma^{\alpha}_{(\lambda\alpha)} + \frac{\partial}{\partial x^{\lambda}} \Gamma^{\alpha}_{(\mu\alpha)} \right) + \Gamma^{\alpha}_{\lambda\mu}\Gamma^{\beta}_{(\alpha\beta)} \tag{1.4}$$

and $A_{(\alpha\beta)}$, $A_{[\alpha\beta]}$ are the symmetric and skew-symmetric parts of $A_{\alpha\beta}$ and X_{λ} is a gradient or a vector.

The object of this note is to express the conditions (1.2) and (1.3) in different ways.

2. – Transposed Einstein's Tensor.

The tensor $\tilde{P}_{\lambda\mu}$ transposed to $P_{\lambda\mu}$ is given by

$$\tilde{P}_{\lambda\mu} = \frac{\partial}{\partial x^{\alpha}} \Gamma^{\alpha}_{\mu\lambda} - \Gamma^{\alpha}_{\beta\lambda}\Gamma^{\beta}_{\mu\alpha} - \frac{1}{2}\left(\frac{\partial}{\partial x^{\mu}} \Gamma^{\alpha}_{(\alpha\lambda)} + \frac{\partial}{\partial x^{\lambda}} \Gamma^{\alpha}_{(\alpha\mu)} \right) + \Gamma^{\alpha}_{\mu\lambda}\Gamma^{\beta}_{(\alpha\beta)} = P_{\mu\lambda} , \tag{2.1}$$

by virtue of (1.4).

Hence the condition (1.3) may be replaced by

$$\tilde{P}_{\lambda\mu} = \frac{\partial}{\partial x^{[\mu}} X_{\lambda]} . \tag{2.2}$$

From (2.1), we get the results,

$$P_{(\mu\lambda)} = \tilde{P}_{(\lambda\mu)} ,$$

and

$$P_{[\mu\lambda]} + \tilde{P}_{[\mu\lambda]} = 0 .$$

Hence:

The symmetric parts of the Einstein's tensor and its transposed tensor are equal and the sum of their skew-symmetric parts vanishes.

3. – Curvature Tensor and Transposed Curvature Tensor.

The coefficients $\Gamma^{\lambda}_{\beta\gamma}$ and $\bar{\Gamma}^{i}_{jk}$ in the coordinate systems x^{λ} and y^{i} are related by the equations

$$\frac{\partial^2 x^{\alpha}}{\partial y^{h}\,\partial y^{i}} + \Gamma^{\alpha}_{\beta\gamma}\frac{\partial x^{\beta}}{\partial y^{h}}\frac{\partial x^{\gamma}}{\partial y^{i}} = \bar{\Gamma}^{j}_{hi}\frac{\partial x^{\alpha}}{\partial y^{j}}\,. \tag{3.1}$$

Substituting for $\partial^2 x^{\lambda}/\partial y^{h}\,\partial y^{i}$ from (3.1) in the condition of integrability

$$\frac{\partial}{\partial y^{j}}\left(\frac{\partial^2 x^{\alpha}}{\partial y^{h}\,\partial y^{i}}\right) = \frac{\partial}{\partial y^{i}}\left(\frac{\partial^2 x^{\alpha}}{\partial y^{j}\,\partial x^{h}}\right), \tag{3.2}$$

of the equation (3.1), one finds that $R^{\alpha}_{\beta\gamma\delta}$ given by

$$R^{\alpha}_{\beta\gamma\delta} = \frac{\partial}{\partial x^{\delta}}\Gamma^{\alpha}_{\beta\gamma} - \frac{\partial}{\partial x^{\gamma}}\Gamma^{\alpha}_{\beta\delta} + \Gamma^{\alpha}_{\omega\delta}\,\Gamma^{\omega}_{\beta\gamma} - \Gamma^{\alpha}_{\omega\gamma}\Gamma^{\omega}_{\beta\delta}\,, \tag{3.3}$$

are components of a tensor. The tensor $R^{\alpha}_{\beta\gamma\delta}$ is called the curvature tensor of the connections $\Gamma^{\alpha}_{\beta\gamma}$.

If (Todeschini [1])

$$v^{\lambda}_{-;\alpha} = \frac{\partial v^{\lambda}}{\partial x^{\alpha}} - v^{\mu}\Gamma^{\lambda}_{\mu\alpha}$$

and

$$v^{\lambda}_{+;\alpha} = \frac{\partial v^{\lambda}}{\partial x^{\alpha}} - v^{\mu}\Gamma^{\lambda}_{\alpha\mu}\,,$$

it is easy to prove that the tensor $R^{\alpha}_{\beta\gamma\delta}$ occurs in the following identities

$$v^{\lambda}_{+;\nu\sigma} - v^{\lambda}_{+;\sigma\nu} = 2v^{\lambda}_{+;\varrho}S^{\varrho}_{\nu\sigma} + v^{\mu}R^{\lambda}_{\mu\nu\sigma} \tag{3.4}$$

$$v^{\lambda}_{+;\nu\sigma} - v^{\lambda}_{+;\sigma\nu} = 2v^{\lambda}_{+;\varrho}S^{\varrho}_{\sigma\nu} + v^{\mu}R^{\lambda}_{\mu\nu\sigma} \tag{3.5}$$

$$v^{\lambda}_{+;\nu\sigma} - v^{\lambda}_{-;\sigma\nu} = v^{\mu}R^{\lambda}_{\mu\nu\sigma}\,. \tag{3.6}$$

[1] B. Todeschini: *Atti Accad. Naz. Lincei, Rend. cl. Sci. Fis. Mat. Nat.*, ser. 8ª, **14**, 495 (1953).

Hlavaty [3] has shown that if $R_{\mu\lambda}(=R^{\alpha}_{\mu\lambda\alpha})$ and $V_{\mu\lambda}(=R^{\alpha}_{\alpha\mu\lambda})$ be the contracted curvature tensors of the connections $\Gamma^{\alpha}_{\beta\gamma}$, then

$$P_{\lambda\mu} - R_{\lambda\mu} = S_{\underset{+}{\lambda};\,\mu} \tag{3.7}$$

and

$$V_{\mu\lambda} = 2\,\frac{\partial}{\partial x^{[\mu}} S_{\lambda]}\,. \tag{3.8}$$

By virtue of (3.7) and (3.8), the conditions (1.2) and (1.3) taken together may be replaced by

$$V_{\mu\lambda} = 0 \tag{3.9}$$

$$R_{\mu\lambda} = \frac{\partial}{\partial x^{[\mu}} X_{\lambda]}\,, \tag{3.10}$$

taken together; though (1.2) is not equivalent to (3.9), whereas (1.3) is equivalent to (3.10). From the equations (3.1) and their conditions of integrability

$$\frac{\partial}{\partial y^{j}}\left(\frac{\partial^{2} x^{\alpha}}{\partial y^{h}\,\partial y^{i}}\right) = \frac{\partial}{\partial y^{h}}\left(\frac{\partial^{2} x^{\alpha}}{\partial y^{i}\,\partial y^{j}}\right),$$

one finds that the quantities given by

$$\widetilde{R}^{\alpha}_{\beta\gamma\delta} = \frac{\partial}{\partial x^{\delta}}\Gamma^{\alpha}_{\gamma\beta} - \frac{\partial}{\partial x^{\gamma}}\Gamma^{\alpha}_{\delta\beta} + \Gamma^{\alpha}_{\delta\omega}\Gamma^{\omega}_{\gamma\beta} - \Gamma^{\alpha}_{\gamma\omega}\Gamma^{\omega}_{\delta\beta}\,, \tag{3.11}$$

are also components of a tensor.

Comparing (3.3) with (3.11), it is easy to see that

The tensors $R^{\alpha}_{\beta\gamma\delta}$ and $\widetilde{R}^{\alpha}_{\beta\gamma\delta}$ are mutually transposed tensors.

The transposed curvature tensor $\widetilde{R}^{\alpha}_{\beta\gamma\delta}$ may also be found to occur in the following identities

$$v^{\underset{-}{\lambda}}_{\underset{-}{;}\nu\sigma} - v^{\lambda}_{\underset{-}{;}\sigma\nu} = 2v^{\underset{-}{\lambda}}_{\underset{-}{;}\alpha} S^{\alpha}_{\nu\sigma} + v^{\alpha}\widetilde{R}^{\lambda}_{\alpha\nu\sigma} \tag{3.12}$$

$$v^{\underset{-}{\lambda}}_{\underset{+}{;}\nu\sigma} - v^{\underset{-}{\lambda}}_{\underset{+}{;}\sigma\nu} = 2v^{\lambda}_{\underset{-}{;}\alpha} S^{\alpha}_{\sigma\nu} + v^{\alpha}\widetilde{R}^{\lambda}_{\alpha\nu\sigma} \tag{3.13}$$

$$v^{\underset{-}{\lambda}}_{\underset{-}{;}\nu\sigma} - v^{\underset{-}{\lambda}}_{\underset{-}{;}\sigma\nu} = v^{\alpha}\widetilde{R}^{\lambda}_{\alpha\nu\sigma}\,. \tag{3.14}$$

From (3.11), the transposed tensor of $R_{\lambda\mu}$ is given by

$$\widetilde{R}_{\lambda\mu} = \widetilde{R}^{\alpha}_{\lambda\mu\alpha} = \frac{\partial}{\partial x^{\alpha}} \Gamma^{\alpha}_{\mu\lambda} - \frac{\partial}{\partial x^{\mu}} \Gamma^{\alpha}_{\alpha\lambda} - \Gamma^{\alpha}_{\mu\omega}\Gamma^{\omega}_{\alpha\lambda} + \Gamma^{\alpha}_{\mu\omega}\Gamma^{\omega}_{\alpha\lambda} . \tag{3.15}$$

From (1.4) and (3.15), it is easy to prove that

$$P_{\lambda\mu} - \widetilde{R}_{\mu\lambda} = \frac{1}{2}\left[\frac{\partial}{\partial x^{\lambda}} \Gamma^{\alpha}_{(\alpha\mu)} - \frac{\partial}{\partial x^{\mu}} \Gamma^{\alpha}_{(\lambda\alpha)}\right] - \frac{\partial}{\partial x^{\lambda}} S_{\mu} + S_{\omega}\Gamma^{\omega}_{\lambda\mu} . \tag{3.16}$$

But, since (HLAVATY [3], p. 119)

$$\frac{\partial}{\partial x^{\lambda}} \Gamma^{\alpha}_{(\alpha\mu)} - \frac{\partial}{\partial x^{\mu}} \Gamma^{\alpha}_{(\lambda\alpha)} = 0 . \tag{3.17}$$

the equation (3.16) assumes the form

$$P_{\lambda\mu} - \widetilde{R}_{\mu\lambda} = - S_{\mu\,;\lambda} . \tag{3.18}$$

The transposed tensor of $V_{\mu\lambda}$, is given by

$$\widetilde{V}_{\mu\lambda} = \frac{\partial}{\partial x^{\mu}} \Gamma^{\alpha}_{\alpha\lambda} - \frac{\partial}{\partial x^{\lambda}} \Gamma^{\alpha}_{\alpha\mu} ,$$

which by virtue of (3.17), assumes the form

$$\widetilde{V}_{\mu\lambda} = - \frac{\partial}{\partial x^{\mu}} S_{\lambda} + \frac{\partial}{\partial x^{\lambda}} S_{\mu} = 2 \frac{\partial}{\partial x^{[\lambda}} S_{\mu]} = - V_{\mu\lambda} , \tag{3.19}$$

by virtue of (3.8).

Using (1.2) in (3.18) and (3.19), we get

$$P_{\lambda\mu} = \widetilde{R}_{\mu\lambda}$$

and

$$\widetilde{V}_{\mu\lambda} = 0 .$$

Hence the condition (1.2) and (1.3) taken together may be replaced by

$$\widetilde{V}_{\mu\lambda} = 0 \tag{3.20}$$

and

$$R_{\lambda\mu} = \frac{\partial}{\partial x^{[\mu}} X_{\lambda]} , \tag{3.21}$$

taken together. Here again (1.3) is equivalent to (3.21) but (1.2) is not equivalent to (3.20).

4. – The Quantities $T^{\lambda}_{\beta\gamma\delta}$ and Their Transposed Quantities.

It is easy to calculate that

$$(4.1)\qquad v^{\lambda}_{\underset{+}{+};\nu\sigma} - v^{\lambda}_{\underset{-}{+};\sigma\nu} = 2S^{\lambda}_{\delta\nu}\frac{\partial}{\partial x^{\sigma}}v^{\delta} + 2S^{\lambda}_{\delta\sigma}\frac{\partial}{\partial x^{\nu}}v^{\delta} + 2v^{\delta}S^{\lambda}_{\mu\delta}\Gamma^{\mu}_{\nu\sigma} + v^{\mu}T^{\lambda}_{\mu\nu\sigma}\,,$$

where

$$(4.2)\qquad T^{\alpha}_{\beta\gamma\delta} = \frac{\partial}{\partial x^{\delta}}\Gamma^{\alpha}_{\beta\gamma} - \frac{\partial}{\partial x^{\gamma}}\Gamma^{\alpha}_{\delta\beta} + \Gamma^{\varepsilon}_{\beta\gamma}\Gamma^{\alpha}_{\varepsilon\delta} - \Gamma^{\varepsilon}_{\delta\beta}\Gamma^{\alpha}_{\gamma\varepsilon}\,.$$

The transposed quantities of $T^{\alpha}_{\beta\gamma\delta}$ are given by

$$(4.3)\qquad \widetilde{T}^{\alpha}_{\beta\gamma\delta} = \frac{\partial}{\partial x^{\delta}}\Gamma^{\alpha}_{\gamma\beta} - \frac{\partial}{\partial x^{\gamma}}\Gamma^{\alpha}_{\beta\delta} + \Gamma^{\varepsilon}_{\gamma\beta}\Gamma^{\alpha}_{\delta\varepsilon} - \Gamma^{\varepsilon}_{\beta\delta}\Gamma^{\alpha}_{\varepsilon\gamma}\,,$$

which may be found to occur in the following identity

$$(4.4)\qquad v^{\lambda}_{\underset{+}{;}\nu\sigma} - v^{\lambda}_{\underset{+}{+};\sigma\nu} = 2S^{\lambda}_{\nu\delta}\frac{\partial}{\partial x^{\sigma}}v^{\delta} + 2S^{\lambda}_{\delta\sigma}\frac{\partial}{\partial x^{\nu}}v^{\delta} + 2v^{\delta}S^{\lambda}_{\delta\mu}\Gamma^{\mu}_{\nu\sigma} + v^{\mu}\widetilde{T}^{\lambda}_{\mu\nu\sigma}\,.$$

Comparing (4.2) with (3.3) and (4.3) with (3.11), we find that:

The quantities $T^{\alpha}_{\beta\gamma\delta}$ are obtained by replacing the negative terms in $R^{\alpha}_{\beta\gamma\delta}$ by their transposed quantities and similarly $\widetilde{T}^{\alpha}_{\beta\gamma\delta}$ are obtained by replacing the negative terms in $\widetilde{R}^{\alpha}_{\beta\gamma\delta}$ by their transposed quantities and vice-versa.

From (4.2) and (4.3), it is easy to see that:

The skew-symmetric parts of $T^{\alpha}_{\beta\gamma\delta}$ and $\widetilde{T}^{\alpha}_{\beta\gamma\delta}$ in the last two indices are equal.

Summing (4.2) with (4.3) and (3.3) with (3.11), we find

$$(4.5)\qquad T^{\alpha}_{\beta\gamma\delta} + \widetilde{T}^{\alpha}_{\beta\gamma\delta} = R^{\alpha}_{\beta\gamma\delta} + \widetilde{R}^{\alpha}_{\beta\gamma\delta} = 2T^{\alpha}_{\beta[\gamma\delta]} = 2\widetilde{T}^{\alpha}_{\beta[\gamma\delta]}\,.$$

From the equations (4.5) we deduce the following properties:

(i) *Though the quantities $T^{\alpha}_{\beta\gamma\delta}$ and $\widetilde{T}^{\alpha}_{\beta\gamma\delta}$ are not components of tensors their sum and their skew-symmetric parts in the last two indices are components of tensors.*

(ii) *The sum of* $T^{\alpha}_{\beta\gamma\delta}$ *and* $\widetilde{T}^{\alpha}_{\beta\gamma\delta}$ *is the same as the sum of the curvature tensor with respect to* $\Gamma^{\alpha}_{\beta;\gamma}$ *and its transposed tensor. Both these sums are separately equal to twice the skew-symmetric part of* $T^{\alpha}_{\beta\gamma\delta}$ *or* $\widetilde{T}^{\alpha}_{\beta\gamma\delta}$ *in the last two indices.*

Interchanging γ and δ in $\widetilde{T}^{\alpha}_{\beta\gamma\delta}$ and adding to (4.2), we find that

$$T^{\alpha}_{\beta\gamma\delta} + \widetilde{T}^{\alpha}_{\beta\delta\gamma} = 0, \tag{4.6}$$

whence

$$T^{\alpha}_{\beta[\gamma\delta]} = \widetilde{T}^{\alpha}_{\beta[\gamma\delta]},$$

a result already established, and

$$T^{\alpha}_{\beta(\gamma\delta)} + \widetilde{T}^{\alpha}_{\beta(\gamma\delta)} = 0. \tag{4.7}$$

Hence:

The sum of the symmetric parts of $T^{\alpha}_{\beta;\gamma\delta}$ *and* $\widetilde{T}^{\alpha}_{\beta;\gamma\delta}$ *in the last two indices vanishes.*

The last result could also be established from (4.5), since $R^{\lambda}_{\beta\gamma\delta}$ and $\widetilde{R}^{\lambda}_{\beta;\gamma\delta}$ are both skew-symmetric in the last two indices. Putting $W_{\gamma\delta} = T^{\lambda}_{\alpha\gamma\delta}$ and $\widetilde{W}_{\gamma\delta} = \widetilde{T}^{\alpha}_{\alpha\gamma\delta}$, we have from (4.5)

$$W_{\gamma\delta} + \widetilde{W}_{\gamma\delta} = V_{\gamma\delta} + \widetilde{V}_{\gamma\delta} = 2W_{[\gamma\delta]} = 2\widetilde{W}_{[\gamma\delta]} = 0, \tag{4.8}$$

by virtue of (3.19).

Also contracting (4.5) with respect to the indices, we have

$$T_{\beta\gamma} + \widetilde{T}_{\beta\gamma} = R_{\beta\gamma} + \widetilde{R}_{\beta\gamma} = 2T^{\alpha}_{\beta[\gamma\alpha]} = 2\widetilde{T}^{\alpha}_{\beta[\gamma\alpha]}.$$

Putting the values of $R_{\beta;\gamma}$ and $\widetilde{R}_{\beta;\gamma}$ from (3.10) and (3.21) in this equation, we have

$$\frac{\partial}{\partial x^{[\beta}} X_{\gamma]} + \frac{\partial}{\partial x^{[\gamma}} X_{\beta]} = 2T^{\alpha}_{\beta[\gamma\alpha]} = 2\widetilde{T}^{\alpha}_{\beta[\gamma\alpha]},$$

or

$$T^{\alpha}_{\beta[\gamma\alpha]} = \widetilde{T}^{\alpha}_{\beta[\gamma\alpha]} = 0.$$

Hence, the equations (1.2) and (1.3) taken together may be replaced by

$$W_{[\gamma\delta]} = \widetilde{W}_{[\gamma\delta]} = 0, \tag{4.9}$$

and

$$T^{\alpha}_{\beta[\gamma\alpha]} = \widetilde{T}^{\alpha}_{\beta[\gamma\alpha]} = 0, \tag{4.10}$$

taken together.

Thus we see that:

In Einstein's Unified Field Theory the transposed tensor $\widetilde{P}_{\mu\lambda}$ of Einstein's tensor $P_{\mu\lambda}$, the contracted curvature tensor $R_{\mu\lambda}$ and its transposed tensor $\widetilde{R}_{\mu\lambda}$ play roles analogous to Einstein's tensor $P_{\mu\lambda}$, whereas the tensor $T^{\alpha}_{\mu[\nu\alpha]}$ plays similar role in Unified Field Theory as $G_{\mu\nu}$ (Ricci tensor) plays in General Theory of Relativity for empty space.

To summarise, the field equations (1.2) and (1.3) may be replaced by

$$S_{\lambda} = 0 \tag{4.11}$$

$$\widetilde{P}_{\lambda\mu} = \frac{\partial}{\partial x^{[\mu}} X_{\lambda]} . \tag{4.12}$$

The equations (1.2) and (1.3) taken together may be replaced by

$$V_{\mu\lambda} = 0 \tag{4.13}$$

$$R_{\mu\lambda} = \frac{\partial}{\partial x^{[\mu}} X_{\lambda]} \tag{4.14}$$

or

$$\widetilde{V}_{\mu\lambda} = 0 \tag{4.15}$$

$$\widetilde{R}_{\lambda\mu} = \frac{\partial}{\partial x^{[\mu}} X_{\lambda]} \tag{4.16}$$

or

$$W_{[\gamma\delta]} = \widetilde{W}_{[\gamma\delta]} = 0 \tag{4.17}$$

$$T^{\alpha}_{\beta[\gamma\alpha]} = \widetilde{T}^{\alpha}_{\beta[\gamma\alpha]} = 0 . \tag{4.18}$$

taken together.

From the above equations it is clear that the condition (1.3) may also be replaced by one of the following equations

$$P_{\mu\lambda} \text{ or } R_{\mu\lambda} \text{ or } \widetilde{P}_{\lambda\mu} \text{ or } \widetilde{R}_{\lambda\mu} = \frac{\partial}{\partial x^{[\mu}} X_{\lambda]} . \tag{4.19}$$

$$T^{\alpha}_{\beta[\gamma\alpha]} = \widetilde{T}^{\alpha}_{\beta[\gamma\alpha]} = 0 .$$

5. – Schrödinger's Field Equations.

In Schrödinger's theory, the field equations (1.1) and (1.2) are the same, but the equations (1.3) are replaced by

$$P_{(\mu\lambda)} = \alpha g_{(\mu\lambda)}$$

$$P_{[\mu\lambda],\alpha} + P_{[\lambda\alpha],\mu} + P_{[\alpha\mu],\lambda} = \alpha[g_{[\mu\lambda],\alpha} + g_{[\lambda\alpha],\mu} + g_{[\alpha\mu],\lambda}] .$$

These two equations may be condensed into

$$P_{\mu\lambda} - \alpha g_{\mu\lambda} = \frac{\hat{c}}{\hat{c}x^{[\mu}} Y_{\lambda]} , \tag{5.1}$$

where Y_λ is a vector.

From the above considerations, condition (5.1) may be replaced by one of the following equations

$$P_{\mu\lambda} \text{ or } R_{\mu\lambda} \text{ or } \widetilde{R}_{\lambda\mu} \text{ or } \widetilde{P}_{\lambda\mu} = \alpha g_{\mu\lambda} + \frac{\hat{c}}{\hat{c}x^{[\mu}} Y_{\lambda]} ,$$

$$T^{\alpha}_{\mu[\lambda\alpha]} = \widetilde{T}^{\alpha}_{\mu[\lambda\alpha]} = \alpha g_{(\mu\lambda)} .$$

6. – Bonnor's Field Equations.

Similarly in Bonnor's theory, the field equations (1.1) and (1.2) are the same, but the equations (1.3) are replaced by [5])

$$R_{(\mu\lambda)} + p^2 U_{(\mu\lambda)} = 0$$

and

$$R_{[\mu\lambda],\nu} + R_{[\lambda\nu],\mu} + R_{[\nu\mu],\lambda} + p^2[U_{[\mu\lambda],\nu} + U_{[\lambda\nu],\mu} + U_{[\nu\mu],\lambda}],$$

where

$$U_{\mu\lambda} = g_{(\lambda\mu)} - g^{[\nu k]} g_{\mu\nu} g_{k\lambda} + \frac{1}{2} g^{[\nu k]} g_{k\nu} g_{\mu\lambda} .$$

[5]) W. B. Bonnor: *Proc. Roy. Soc. Lond.*, A **226**, 336 (1954).

These two equations, as before, can be condensed into

$$R_{\mu\lambda} + p^2 U_{\mu\lambda} = \frac{\partial}{\partial x^{[\mu}} Z_{\lambda]}\,, \tag{6.1}$$

where Z_λ is a vector.

Condition (6.1) can, therefore, be replaced by one of the following equations

$$P_{\mu\lambda} \text{ or } R_{\mu\lambda} \text{ or } \widetilde{R}_{\lambda\mu} \text{ or } \widetilde{P}_{\lambda\mu} = \frac{\partial}{\partial x^{[\mu}} Z_{\lambda]} - p^2 U_{\mu\lambda}$$

$$T^{\alpha}_{\mu[\lambda\alpha]} = \widetilde{T}^{\alpha}_{\mu[\lambda\alpha]} = -\,p^2 U_{(\mu\lambda)}\,.$$

RIASSUNTO (*)

Si studiano nel presente lavoro i principi fondamentali della teoria del campo unificato di Einstein, Schrödinger e Bonnor. Originalmente le equazioni di campo erano date in termini del tensore di curvatura contratto $R_{\mu\lambda}$. Qui si ottengono relazioni tra $R_{\mu\lambda}$ e alcuni altri tensori, come il tensore di Einstein, il tensore trasporto e il tensore $T^{\alpha}_{\beta[\gamma\alpha]}$ e si modificano le equazioni di campo in termini di tali tensori. Si mostra anche come questi tensori si ottengano in vari modi nelle identità di Ricci se si eseguono le derivazioni covarianti tenendo conto della natura degli indici.

(*) *Traduzione a cura della Redazione.*

IL NUOVO CIMENTO Vol. IV, N. 4 1° Ottobre 1956

A V^0-Decay with an Electron Secondary.

C. D'Andlau, R. Armenteros, A. Astier, H. C. DeStaebler, B. P. Gregory, L. Leprince-Ringuet, F. Muller, C. Peyrou (*) and J. H. Tinlot (+)

Laboratoire de Physique de l'Ecole Polytechnique - Paris

(ricevuto il 6 Agosto 1956)

Summary. — Description and discussion of an anomalous V^0-decay of particular interest discovered in a survey of photographs taken in the Ecole Polytechnique magnet cloud chamber.

We report in this note on a V^0-event (1) which appears to be of particular interest since both secondaries can be identified: one as a low energy electron (from momentum and a visual ionization estimate), and the other as a π-meson because it decays. The event (no. 59647) was noted during the course of a survey of anomalous V^0 decays photographed in the Ecole Polytechnique magnet cloud chamber (2). As shown in Fig. 1, and in the photograph, a V^0 appears approximately in the center of the chamber (track a, b) and is accompanied by 4 penetrating shower particles emerging from the lead above the chamber. Since these 4 particles do not seem to come from a unique point in the lead, we cannot assign an origin to the V^0-event. Track a leaves the illuminated region at the back of the chamber. Track b is deflected by

(*) Now at Berne University, Switzerland.

(+) Now at Rochester University, U.S.A.

(1) A preliminary report was presented at the Sixth Annual Rochester Conference on High Energy Physics (April 1956).

(2) The experimental arrangement is described in B. Gregory, A. Lagarrigue, L. Leprince-Ringuet, F. Muller and C. Peyrou: *Nuovo Cimento*, **11**, 292 (1954). (The magnetic field for most of the recent work has been increased to 5000 gauss).

an angle of $4.9° \pm 0.5°$ at V, and then, as track c, leaves the illuminated region at the front. As it is seen from the data in Table I, the decay dynamics do not fit any of the known two-body decay schemes except that of the Λ^0. But as it will be shown, this last interpretation is ruled out by the identification of the negative particle.

TABLE I.

Particle	Sign	Momentum (MeV/c)	Estimated relative ionization (I/I_0)
a)	—	39.5 ± 1.5	> 1 < 3
b)	+	$609\ ^{+600}_{-200}$	$\geqslant 1$
c)	+	$365\ ^{+140}_{-80}$	$\geqslant 1$
$\theta_1 = 83° \pm 1°$			$\theta_2 = 4.9° \pm 0.5°$

Let us consider first the negative particle. Its momentum is (39.5 ± 1.5) MeV/c, and its trajectory makes an angle of about 50° with the plane of the cloud chamber front glass. The relative ionization (I/I_0) of an electron of this momentum in argon gas is 1.3. Because of the inclination the apparent ionization would be 2.0 for an electron, 5.9 for a μ-meson and 9.0 for a π-meson. We consider that the apparent ionization of the track is less than 3.0, and therefore that the particle is most probably an electron. In-as-much as visual estimates of ionization are notoriously subjective, we have considered an argument based on the depth at which the trajectory leaves the illuminated region. The point of disappearance may be expected to depend upon the ionization of the particle, since the limits of the illuminated region are not sharply defined. The form of this dependence was approximately determined by making use of a number of secondaries from Λ^0 decays found in the same group of photographs. In a few cases, the proton secondary (whose ionization is well known) leaves the illuminated region in the same general region as does track *a*. It was found in this way that tracks having relative ionization 3 should be visible about 2 cm deeper than the point of disappearance of track *a*. This observation means that we have not grossly understimated the ionization by visual estimation, and supports the conclusion that *a* is an electron.

The positive trajectory *b* is short, and the momentum cannot accurately be determined by curvature measurement ($p_b = 609\ ^{+600}_{-200}$ MeV/c). However, the deflection at V suggests that *b* is the track of a π-meson which decays into a μ-meson, track *c*. Although admittedly the errors in the measured

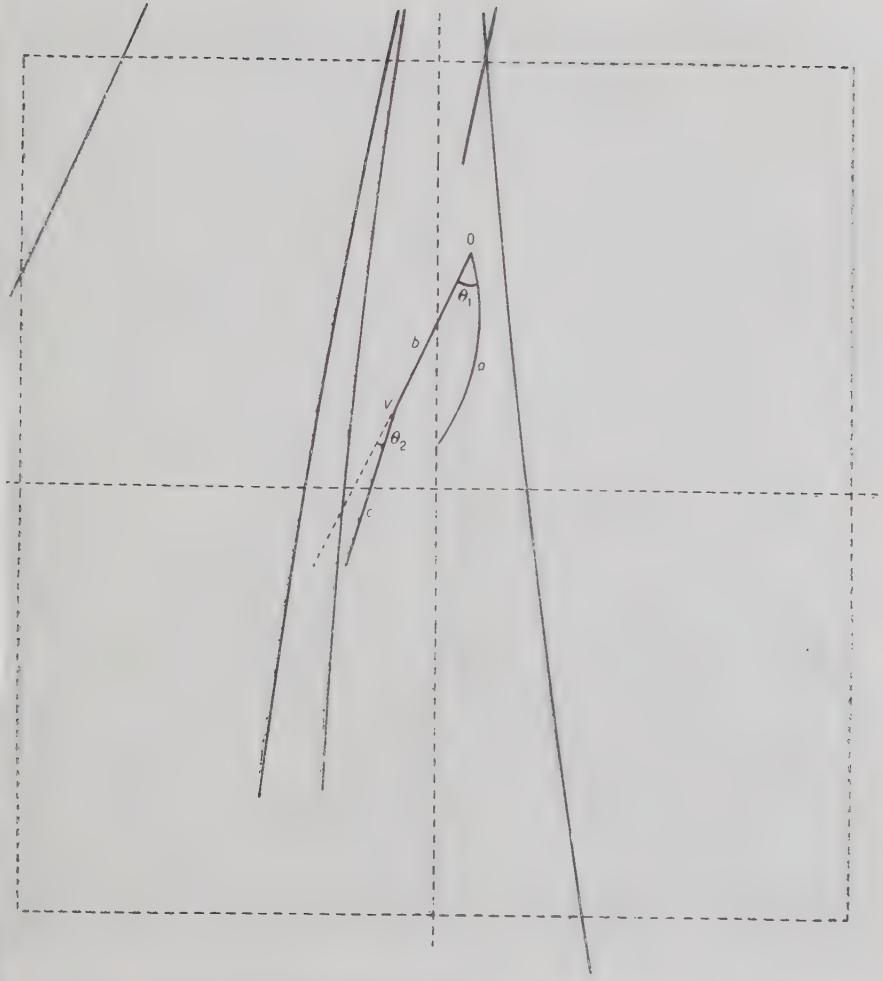

Fig. 1. – Drawing of event 59647. Track *a* is negative and track *b* is positive if the particles travelled downwards.

Fig. 1. – Drawing of event 59647. Track a is negative and track b is positive if the particles travelled downwards.

Fig. 2 – Photograph of event 59 647.

momenta are large, this interpretation is in agreement with the measurements and to proceed with the analysis we assume that it is the correct one.

Under this assumption we may compare the measured angle and momenta with the known dynamics of π-μ decay and determine a new value of the momentum of track b for use in computation. To the measured value of the angle at V, $4.9^\circ \pm 0.5^\circ$, corresponds a maximum value of π momentum (480 $\pm$ 55) MeV/c; we shall take 535 MeV/c as an upper value for the momentum of b. The π-μ dynamics do not give a very meaningful lower momentum for b, and therefore we take this to be given by the measured sagitta increased by one standard deviation and obtain $p_b = 409$ MeV/c. The measured momentum of c, interpreted as the μ-meson, is consistent with these two values of p_b.

From the measured electron momentum and the lower and upper values of the π momentum we obtain Q (π^+, e^-) values of 83 and 101 MeV. We note that the Q (π^-, π) values corresponding to these values of p_b are 121 and 161 MeV and therefore the event cannot easily be interpreted as a 0^0 or as a neutral τ decay even if we neglect the information obtained from the ionization of the negative track.

TABLE II. – *Q-values for two-body decay calculated under various assumptions.*

p_a MeV/c	p_b MeV/c	particle a	particle b	calculated Q MeV
39.5	535 (*)	π-meson	electron	101
39.5	409 (*)	π-meson	electron	83
39.5 $\pm$ 1.5	$609\ ^{+600}_{-200}$	electron	electron	205^{+105}_{-31}
39.5	535 (*)	π-meson	π-meson	161
39.5	409 (*)	π-meson	π-meson	121

(*) The upper value is set by the π-μ decay dinamics, the lower value by curvature measurements.

Let us consider the possibilities for alternative interpretations of the event. One might first assume that it does not represent the decay of a neutral particle, but rather a V-event with an identified electron secondary produced by an upward moving charged particle [3]. We then note that in approximately

[3] The possibility that b-a represent a μ-e event is ruled out since the maximum allowed momentum of track b would be 84 MeV/c given the angle at 0 and the measured electron momentum.

50000 photographs taken in the same conditions, in which about 300 charged V-events were detected, no case of electron decay, or of double deflection, has been observed, and that all of the charged V primaries and the vast majority of all shower particles enter the chamber from the upper hemisphere. It thus seems highly unlikely that the event is a charged V-decay although the validity of statistical arguments based on the observation of one event is admittedly doubtful.

As another alternative, one might suggest that tracks *a* and *b* are those of a pair of electrons, one of which is scattered at V. There are only two evident mechanisms for producing an isolated electron pair in the gas: pair production by a « real » photon, and internal production by a « virtual » photon produced locally, such as by the decay of a π^0-meson. In discussing either case, it is very helpful to consider the expected distribution of « Q-values » for two-electron decay, where the Q-value is simply the sum of the total energies of the two electrons in their center of mass system. Its value evidently can range up to the π^0-mass for « virtual » pairs, and up to the energy of the photon for « real » pairs. The distribution for « real » pairs, as given by BORSELLINO [1], has its maximum slightly above 1 MeV, and falls off approximately as Q^{-3} for values above a few MeV. The distribution for « virtual » pairs from π^0-decays can be obtained from the work of KROLL and WADA [5] One finds that this distribution also has a maximum slightly above 1 MeV but only falls somewhat faster than Q^{-1} for larger values; for example, there is an 8% chance of finding Q above 50 MeV, and 1% above 80 MeV. Since the value of Q (e^+, e^-) for the event presented here is (205^{+105}_{-31}) MeV, (see Table II), the probability of its being a « virtual » π^0 produced pair or a « real » pair is exceedingly small.

We thus reach the conclusion that the event represents the decay of a V^0-particle into a negative electron and a positive particle which is most likely a π-meson. Since we do not know the line of flight, we cannot find out whether or not one or more neutral secondaries were produced in the decay, and we can only say that Q (π^+, e^-) is most probably between 83 and 101 MeV.

The strong similarity between our event and that obtained by COWAN [6] has to be noted. Although the ionization-momentum measurements of the negative secondary of his event were consistent with either a proton or an electron, we may assume that the electron interpretation is the correct one and hence that Cowan's event and ours represent the decay of the same

[1] A. BORSELLINO: *Phys. Rev.*, **89**, 1023 (1953).

[5] N. KROLL and W. WADA: *Phys. Rev.*, **98**, 1355 (1955). See their equation (3); the Q-value is denoted by x.

[6] E. W. COWAN: *Phys. Rev.*, **94**, 161 (1954).

V^0-particle. If this is so and since the $Q(\pi^+, e^-)$ of Cowan's event was (225 ± 20) MeV, (to be compared with 92 ± 9 for our event) the presence of one or more neutral secondaries in the decay is necessary. This conclusion might be reinforced by the two events obtained by BLOCK, HARTH and BLEVINS [7] in which one branch of a V^0-event could be identified as a low energy electron, while the other was not identified. However, the $Q(e^+, e^-)$-values for these two events are about 73 and 110 MeV so that the possibility that the two events represent π^0-decays cannot be eliminated.

[7] M. M. BLOCK, E. M. HARTH and M. E. BLEVINS: *Phys. Rev.*, **100**, 959 (1955). A fuller account of the work of the Duke has group appeared in *Nuovo Cimento*, **4**, 46 (1956).

RIASSUNTO

Descrizione e discussione di un decadimento V^0 anomalo di particolare interesse, scoperto durante un esame di fotografie prese nella camera a nebbia magnetica dell'Ecole Polytechnique.

NOTE TECNICHE

Etude des déformations d'une lame de suspension élastique.

J. E. Plainevaux

Université Libre de Bruxelles

(ricevuto il 3 Agosto 1956)

Résumé. — Le présent travail développe une méthode générale de calcul des déformations planes d'une lame isolée de suspension élastique. La méthode permet, en particulier, la détermination du raccourcissement vertical d'une lame dont les tangentes aux extrémités de la fibre neutre ne sont pas parallèles. Les formules obtenues présentent de l'intérêt pour le calcul d'une lame de suspension raidie dans sa partie centrale ainsi que pour l'étude de suspensions qui ne sont plus symétriques et symétriquement chargées. L'application de ces formules à l'étude du tangage (beccheggio, pitching) d'une suspension et à la détermination de la hauteur optimum de poussée d'une platine est prévue pour un travail ultérieur.

Dans des études précédentes [1] nous avons déterminé quelques propriétés et indiqué des procédés de calcul applicables aux suspensions élastiques symétriques à compensation munies ou non d'un asservissement. De tels systèmes proviennent de la combinaison de montages en U et en U renversé. Toutes ces études étaient limitées à des suspensions symétriques et symétriquement chargées.

Une excellente bibliographie sur l'état de nos connaissances concernant les suspensions élastiques est due à P. J. Geary [2].

Nous nous proposons de montrer ultérieurement qu'il est possible d'étudier, tout au moins approximativement, l'effet de certaines dissymétries de la suspension et de la sollicitation, en nous bornant aux cas de déformations planes.

Sur cette question particulière, nous ne connaissons qu'un article récent de Jones et Young [3].

Avant d'étudier les suspensions dissymétriques, il est nécessaire de posséder

---

[1] J. E. Plainevaux: *Nuovo Cimento*, **10**, 1451 (1953); **11**, 626 (1954); **12**, 37 (1954).

[2] P. J. Geary: *Flexure Devices*, in *B.S.I.R.A.* Research Report M 18 (1954).

[3] R. V. Jones et I. R. Young: *Journ. Sci. Instr.*, **33**, 11 (1956).

une méthode de calcul des déformations planes d'une lame élastique dans le cas général. C'est ce qui fait l'objet de la présente note.

1. – Lame sollicitée à la compression. (Montage en U renversé avec possibilité d'instabilité par flambage).

Considérons Fig. 1, une lame flexible OA de longueur L, rapportée à un système d'axes rectangulaires OX, OZ tel que la tangente à la fibre neutre en O soit confondue avec l'axe OZ. La lame est encastrée à l'origine O, où elle est soumise aux forces P et F ainsi qu'à un moment d'encastrement M_0.

En son extrémité supérieure A, la lame est soumise aux forces P et F comme indiqué à la figure, ainsi qu'au moment M_A. La force P tend à faire flamber la lame dans le cas qui nous occupe.

Désignons par f l'abscisse du point A, ce sera la flèche horizontale de la lame. La tangente à la ligne élastique en A fait avec l'axe des ordonnées OZ un angle θ. L'ordonnée du point A est $L - \lambda$, λ étant une quantité petite.

Si on se borne aux petites déformations, ou plus exactement, si on peut confondre la courbure avec la dérivée seconde de X par rapport à Z, l'équation différentielle de la lame élastique est donnée par:

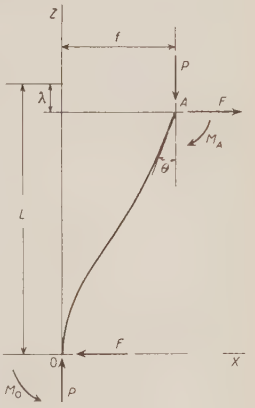

Fig. 1.

$$EI\frac{\mathrm{d}^2X}{\mathrm{d}Z^2} + PX = M_0 - FZ\,,$$

I étant le moment d'inertie de la lame (d'épaisseur constante) par rapport à la fibre neutre et E le module d'élasticité du matériau constituant la lame. Si besoin est, on remplacera dans cette formule ainsi que dans toutes les suivantes, E par le module réduit $E' = E(1 \quad \nu^2)$, ν étant le coefficient de Poisson.

Introduisons les variables réduites:

$$z = \frac{Z}{L}\,;\quad 4\beta^2 = \frac{PL^2}{EI}\,;\quad \varphi = \frac{FL^2}{EI}\,;\quad m_0 = \frac{M_0 L}{EI}\,.$$

Avec ces notations, l'écriture de l'équation différentielle s'allège:

$$\frac{\mathrm{d}^2X}{\mathrm{d}z^2} + 4\beta^2 X = L(m_0 - \varphi z),$$

dont la solution générale est

$$X = C_1 \sin 2\beta z + C_2 \cos 2\beta z + \frac{L}{4\beta^2}(m_0 - \varphi z),$$

avec pour la pente de la ligne élastique:

$$\frac{\mathrm{d}X}{\mathrm{d}Z} = \frac{1}{L}\frac{\mathrm{d}X}{\mathrm{d}z} = \frac{2\beta C_1}{L}\cos 2\beta z - \frac{2\beta C_2}{L}\sin 2\beta z - \frac{\varphi}{4\beta^2}\,.$$

Dans ces deux équations C_1 et C_2 désignent deux constantes arbitraires qu'on détermine par les conditions à l'origine:

$$\text{en } z = 0 \qquad X \quad \frac{dX}{dZ} = 0 .$$

Tous calculs effectués, la solution s'écrit sous la forme:

$$X = \frac{\varphi L}{4\beta^3}(\sin 2\beta z - 2\beta z) + \frac{m_0 L}{4\beta^2}(1 - \cos 2\beta z) .$$

Introduisons dans la solution précédente la flèche horizontale f au point A ainsi que l'inclinaison θ de la tangente à la ligne neutre au même point. En $Z = L$, c'est-à-dire en $z = 1$ on a:

$$\begin{cases} X = f , \\ \dfrac{dX}{dZ} = \dfrac{dX}{L\,dz} = \operatorname{tg}\theta , \end{cases}$$

cela nous permet d'écrire les deux relations suivantes:

$$\begin{cases} \dfrac{f}{L} = \dfrac{\varphi}{8\beta^3}(\sin 2\beta - 2\beta) + \dfrac{m_0}{4\beta^2}(1 \quad \cos 2\beta) , \\ \operatorname{tg}\theta = \dfrac{\varphi}{4\beta^2}(\cos 2\beta - 1) + \dfrac{m_0}{2\beta}\sin 2\beta . \end{cases}$$

Au moyen de ces deux équations, calculons la force horizontale réduite φ et le moment d'encastrement réduit m_0. Tous calculs effectués, on trouve:

$$\varphi = \frac{FL^2}{EI} = \frac{f}{L}\frac{4\beta^3}{\operatorname{tg}\beta \quad \beta} - \operatorname{tg}\theta\frac{2\beta^2 \operatorname{tg}\beta}{\operatorname{tg}\beta \quad \beta} ,$$

$$m_0 = \frac{M_0 L}{EI} = \frac{f}{L}\frac{2\beta^2 \operatorname{tg}\beta}{\operatorname{tg}\beta - \beta} + \operatorname{tg}\theta\left[\beta \operatorname{cotg}\beta \quad \frac{\beta^2 \operatorname{tg}\beta}{\operatorname{tg}\beta - \beta}\right]$$

ce qui montre bien que la force horizontale F et le moment d'encastrement à l'origine sont des fonctions linéaires et homogènes de la flèche horizontale et de la pente à l'extrémité de la lame.

Du fait de la déformation de la lame, il y a raccourcissement de celle-ci suivant la verticale. Le point A descend d'une certaine longueur λ considérée généralement comme négligeable en résistance des matériaux car cette longueur est du second ordre par rapport aux quantités f et $\operatorname{tg}\theta$.

Cette descente de l'extrémité supérieure de la lame est sensiblement donnée

par:

$$\lambda = \frac{1}{2}\int_0^L \left(\frac{dX}{dZ}\right)^2 dZ .$$

En effet, on a

$$\lambda = \int_0^L ds - dZ$$

avec $ds = \sqrt{1 + (dX/dZ)^2}\,dZ$, ce qui conduit à:

$$\lambda = \int_0^{L-\lambda} \left(\sqrt{1 + \left(\frac{dX}{dZ}\right)^2} - 1\right) dZ .$$

Supposant dX/dZ petit, développant en série et négligeant les termes d'ordres supérieurs on a bien la formule approchée annoncée qui s'écrit encore:

$$\lambda = \frac{1}{2L}\int_0^1 \left(\frac{dX}{dz}\right)^2 dz$$

en introduisant la variable réduite z.

Dérivant la valeur trouvée précédemment pour X, on trouve:

$$\frac{dX}{dz} = -\frac{1}{2}\sin 2\beta z \begin{vmatrix} m_0 L & \varphi L \\ \beta & 2\beta^2 \end{vmatrix} \operatorname{tg} \beta z .$$

Introduisant cette dérivée dans l'intégrale donnant la valeur de la descente λ de l'extrémité de la lame A, on trouve après de longs calculs:

$$\frac{\lambda}{L} = \left(\frac{f}{L}\right)^2 \frac{\beta[\beta(3 + \operatorname{tg}^2\beta) - 3\operatorname{tg}\beta]}{4(\operatorname{tg}\beta - \beta)^2} + \frac{f}{L}\operatorname{tg}\theta\left[\frac{1}{2} - \frac{\beta[\beta(3 + \operatorname{tg}^2\beta) - 3\operatorname{tg}\beta]}{4(\operatorname{tg}\beta - \beta)^2}\right] +$$
$$+ \operatorname{tg}^2\theta\left[\frac{\beta(-1 + \operatorname{cotg}^2\beta) - \operatorname{cotg}\beta}{16\beta} + \frac{\beta[\beta(3 + \operatorname{tg}^2\beta) - 3\operatorname{tg}\beta]}{16(\operatorname{tg}\beta - \beta)^2}\right].$$

La descente λ de l'extrémité supérieure A de la lame est donc bien, comme annoncé, du second ordre par rapport à la flèche horizontale f et à l'inclinaison $\operatorname{tg}\theta$ de la fibre élastique au point considéré; la descente λ est en effet donnée par une forme quadratique homogène de degré deux en ces variables.

Il reste encore à déterminer le moment M_A appliqué à l'extrémité supérieure de la lame; on a:

$$\frac{M_A}{EI} = \left(\frac{d^2X}{dZ^2}\right)_L = \frac{1}{L^2}\left(\frac{d^2X}{dz^2}\right)_1 .$$

Dérivant deux fois par rapport à z l'expression trouvée pour X, on obtient:

$$\frac{M_A L}{EI} = \operatorname{tg}\theta\left[\beta\operatorname{cotg}\beta - \frac{\beta^2\operatorname{tg}\beta}{\operatorname{tg}\beta-\beta}\right] - \frac{f}{L}\frac{2\beta^2\operatorname{tg}\beta}{\operatorname{tg}\beta-\beta}.$$

Rappelons que dans ces formules, on a:

$$\beta^2 = \frac{PL^2}{4EI}.$$

Si dans les formules précédentes, on annule $\operatorname{tg}\theta$, on retrouve les relations déjà trouvées (1) par une autre voie. Dans ce travail on utilisait un paramètre α égal au rapport de la charge P appliquée à la charge critique d'Euler. Entre β et ce paramètre existe la relation:

$$\pi^2\alpha = 4\beta^2.$$

2. – Cas où la charge verticale P est faible.

Les suspensions élastiques de précision sont toujours construites de telle manière que la charge verticale P soit faible. D'une manière plus précise, la quantité

$$\frac{4\beta^2}{\pi^2} = \frac{PL^2}{\pi^2 EI},$$

égale au rapport de P à la charge critique d'Euler, est petite par rapport à l'unité. Dans ces conditions, il est licite de développer en série les coefficients de f/L et de $\operatorname{tg}\theta$ dans les formules trouvées précédemment et de se borner aux premiers termes des développements. Tous calculs effectués, on trouve les résultats suivants, où p est mis à la place de PL^2/EI:

$$\text{(I)}\quad \begin{cases} \dfrac{M_A L}{EI} = 4\operatorname{tg}\theta\left[1-\dfrac{p}{30}-\dfrac{11p^2}{25200}-\ldots\right]-6\dfrac{f}{L}\left[1-\dfrac{p}{60}-\dfrac{p^2}{8400}\quad\ldots\right] \\ \dfrac{FL^2}{EI} = -6\operatorname{tg}\theta\left[1-\dfrac{p}{60}-\dfrac{p^2}{8400}-\ldots\right]+12\dfrac{f}{L}\left[1-\dfrac{p}{10}-\dfrac{p^2}{8400}-\ldots\right] \\ \dfrac{M_0 L}{EI} = -2\operatorname{tg}\theta\left[1+\dfrac{p}{60}+\dfrac{13p^2}{25200}+\ldots\right]+6\dfrac{f}{L}\left[1-\dfrac{p}{60}-\dfrac{p^2}{8400}-\ldots\right] \\ \dfrac{\lambda}{L} = \dfrac{\operatorname{tg}^2\theta}{15}\left[1+\dfrac{11p}{420}+\dfrac{p^2}{1200}+\ldots\right]-\dfrac{1}{10}\dfrac{f}{L}\operatorname{tg}\theta\left[1+\dfrac{p}{70}+\dfrac{p^2}{4200}+\ldots\right]+ \\ \qquad\qquad +\dfrac{3}{5}\left(\dfrac{f}{L}\right)^2\left[1+\dfrac{p}{420}+\dfrac{p^2}{25200}+\ldots\right]. \end{cases}$$

(1) J. E. PLAINEVAUX: *Nuovo Cimento*, **12**, 37 (1954).

3. – Lame sollicitée à la traction. (Suspension en U, toujours stable).

L'étude faite est encore valable pour une lame sollicitée en traction à la condition de remplacer P par $-P$. Cela revient, dans les résultats trouvés à remplacer β^2 par $-\beta^2$. Les résultats s'expriment par les fonctions hyperboliques correspondantes aux fonctions circulaires obtenues,

$$\frac{M_A L}{EI} = \operatorname{tg}\theta\left[\beta \operatorname{Cth}\beta + \frac{\beta^2 \operatorname{tgh}\beta}{\beta - \operatorname{tgh}\beta}\right] - \frac{f}{L}\frac{2\beta^2 \operatorname{tgh}\beta}{\beta - \operatorname{tgh}\beta}$$

$$\frac{FL^2}{EI} = \frac{f}{L}\frac{4\beta^3}{\beta - \operatorname{tgh}\beta} - \operatorname{tg}\theta\,\frac{2\beta^2 \operatorname{tgh}\beta}{\beta - \operatorname{tgh}\beta}$$

$$\frac{M_0 L}{EI} = \frac{f}{L}\frac{2\beta^2 \operatorname{tgh}\beta}{\beta - \operatorname{tgh}\beta} + \operatorname{tg}\theta\left[\beta \operatorname{Cth}\beta - \frac{\beta^2 \operatorname{tgh}\beta}{\beta - \operatorname{tgh}\beta}\right]$$

$$\frac{\lambda}{L} = \left(\frac{f}{L}\right)^2 \beta\left[\frac{\beta(3 - \operatorname{tgh}^2\beta) - 3\operatorname{tgh}\beta}{4(\beta - \operatorname{tgh}\beta)^2}\right] + \frac{f}{L}\operatorname{tg}\theta\left[\frac{1}{2} - \frac{\beta[\beta(3 - \operatorname{tgh}^2\beta) - 3\operatorname{tgh}\beta]}{4(\beta - \operatorname{tgh}\beta)^2}\right] +$$

$$+ \operatorname{tg}^2\theta\left[\frac{\operatorname{Cth}\beta - \beta(1 + \operatorname{Cth}^2\beta)}{16\beta} + \frac{\beta[\beta(3 - \operatorname{tgh}^2\beta) - 3\operatorname{tgh}\beta]}{16(\beta - \operatorname{tgh}\beta)^2}\right].$$

4. – Cas où la charge verticale stabilisante P est faible.

Dans ce cas on développe en série les coefficients de f/L et de $\operatorname{tg}\theta$ dans les formules précédentes et on se borne aux premiers termes des développements. Tous calculs effectués, on trouve les résultats suivants où p est mis à la place de PL^2/EI pour simplifier l'écriture:

$$\text{(II)}\quad \begin{cases} \dfrac{M_A L}{EI} = -4\operatorname{tg}\theta\left[1 + \dfrac{p}{30} - \dfrac{11p^2}{25200} + \ldots\right] - 6\dfrac{f}{L}\left[1 + \dfrac{p}{60} - \dfrac{p^2}{8400} - \ldots\right] \\ \dfrac{FL^2}{EI} = -6\operatorname{tg}\theta\left[1 + \dfrac{p}{60} - \dfrac{p^2}{8400} + \ldots\right] + 12\dfrac{f}{L}\left[1 + \dfrac{p}{10} - \dfrac{p^2}{8400} + \ldots\right] \\ \dfrac{M_0 L}{EI} = -2\operatorname{tg}\theta\left[1 - \dfrac{p}{60} + \dfrac{13p^2}{25200} - \ldots\right] + 6\dfrac{f}{L}\left[1 + \dfrac{p}{60} - \dfrac{p^2}{8400} - \ldots\right] \\ \dfrac{\lambda}{L} = \dfrac{\operatorname{tg}^2\theta}{15}\left[1 - \dfrac{11p}{420} + \dfrac{p^2}{1200} - \ldots\right] - \dfrac{1}{10}\dfrac{f}{L}\operatorname{tg}\theta\left[1 - \dfrac{p}{70} + \dfrac{p^2}{4200} - \ldots\right] + \\ \qquad + \dfrac{3}{5}\left(\dfrac{f}{L}\right)^2\left[1 - \dfrac{p}{420} + \dfrac{p^2}{25200} - \ldots\right]. \end{cases}$$

Les groupes de formules (I) et (II) sont d'usage continuel pour l'étude des suspensions à lames.

5. – Conclusions.

Les formules développées sont d'utilisation très générale pour le calcul des lames de suspensions élastiques dans les deux cas suivants:

a) Lames de suspension raidies dans leur partie centrale. Les points *O* et *A* de la Fig. 1 sont alors les extrémités de la partie flexible de la lame comprise entre un encastrement et le « sandwich » raidisseur de la lame. Pour les lames raidies dans leur partie centrale, seules des formules utilisables pour des suspensions identiques à compensation étaient disponibles [5].

b) Cas d'une suspension élémentaire en U ou en U renversé dissymétrique ou chargée dissymétriquement dans son plan.

Dans un prochain travail, nous montrerons comment les formules développées ici permettent d'étudier le mouvement de tangage (beccheggio, pitching) d'une suspension. La même méthode nous permettra de préciser la question de la hauteur optimum à laquelle il faut placer la bielle de poussée pour rendre minimum l'effet de tangage de la platine. Cette question a déjà été amorcée par Jones et Young dans [3].

---

[5] J. E. Plainevaux: *Nuovo Cimento*, **11**, 626 (1954).

RIASSUNTO (*)

Il presente lavoro sviluppa un metodo generale di calcolo delle deformazioni piane di una lama di sospensione elastica isolata. Il metodo permette, in particolare, la determinazione del raccorciamento verticale d'una lama le cui tangenti alle estremità della fibra neutra non sono parallele. Le formule ottenute interessano per il calcolo di una lama di sospensione irrigidita nel suo tratto centrale, come pure per lo studio di sospensioni dissimmetriche e dissimetricamente caricate. L'applicazione di tali formole allo studio del beccheggio (tangage, pitching) di una sospensione e alla determinazione dell'altezza optimum di spinta di una platina sarà data in un prossimo lavoro.

(*) *Traduzione a cura della Redazione.*

LETTERE ALLA REDAZIONE

(La responsabilità scientifica degli scritti inseriti in questa rubrica è completamente lasciata dalla Direzione del periodico ai singoli autori)

Graphical Determination of the Path of a Scattered Particle.

N. C. Barford and G. T. Reynolds (*)

The Physics Department, Imperial College - London

(ricevuto il 10 Giugno 1956)

In multiplate cloud chamber observations a charged particle is seen to enter a plate at a particular point A and direction φ_1, and to emerge at another point B and direction φ_2, as indicated in Fig. 1. The quantity to be determined in such cases is the length of the path of the particle in the plate. In the case indicated in Fig. 1*a*, the procedure often adopted is to extend the entering and emerging tracks and consider the path AOB as the length of traversal. Such a procedure is obviously not possible in a situation indicated in Fig. 1*b*, for which some arbitrary length must be adopted. In practice the scatterings are not as extreme as indicated in the figure, and are confused by the track distortions normally observed near the plates. However, in some important cases it is possible to take these distortions into account and it becomes desirable to have a basis for determining path length for those situations in which there is evidence for scattering in the plate during traversal. These considerations become quantitatively important in observations involving S particles and their decay secondaries, and an analytical procedure has been suggested by the Ecole Polytechnique cloud chamber group [1]. The purpose of the present note is to suggest a simple method for determining the path length by graphical methods, analogous to that indicated in Fig. 1, but with an analytical basis.

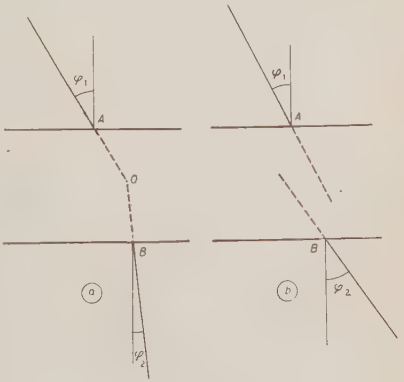

Fig. 1.

(*) On leave of absence from Princeton University, Princeton, New Jersey.

(1) R. Armenteros, B. Gregory, A. Hendel, A. Lagarrigue, L. Leprince-Ringuet, F. Muller and C. Peyrou: *Nuovo Cimento*, **1**, 915 (1955).

In considering the problem of Coulomb scattering, ROSSI and GREISEN (2) show that if $F(t, l, \theta)\,\mathrm{d}l\,\mathrm{d}\theta$ is the probability that a particle has suffered a projected displacement between l and $l + \mathrm{d}l$, and is travelling at an angle between θ and $\theta + \mathrm{d}\theta$ relative to the initial path, after traversing a thickness t, then

$$F(t, l, \theta) = \frac{\sqrt{3}\omega^2}{2\pi t^2} \exp\left[-\omega^2\left(\frac{\theta^2}{t} - \frac{3l\theta}{t^2} + \frac{3l^2}{t^3}\right)\right],$$

where l and t are measured in radiation lengths, θ is the projected angle in the (t, l) plane and ω is given by

$$\omega = 2p\beta c/E_s; \qquad E_s = (4\pi/\alpha)^{\frac{1}{2}}mc^2 = 21 \cdot 10^6 \text{ eV}.$$

Thus, referring to Fig. 2, the probability that a particle entering the plate at position A in direction to the normal φ_1 (corresponding to direction θ_i with respect to AB) has a displacement l_0 at t_0 (half the distance from A to B) and a direction θ_0 with respect to AB is given by

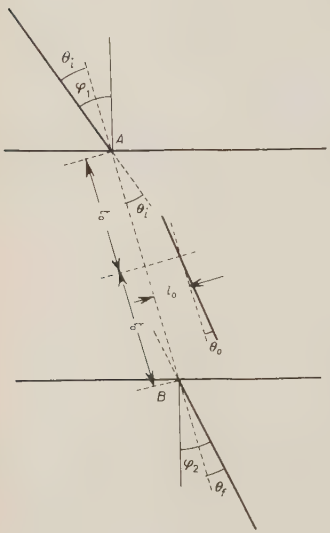

Fig. 2.

$$F(t_0, l_1, \theta_1),$$

where $l_1 = l_0 - t_0\theta_i$ and $\theta_1 = \theta_0 - \theta_i$.

Similarly, the probability that the particle will then emerge at B and make the angle φ_2 with the normal (corresponding to the angle θ_f with AB) is given by

$$F(t_0, l_2, \theta_2),$$

where $l_2 = -(l_0 + t_0\theta_0)$ and $\theta_2 = \theta_f - \theta_0$.

(A sign convention has been adopted for the angles such that they are positive when measured counter clockwise from the respective extensions of the line AB).

Thus, the probability that a particle enter at A, φ_1 and leave at B, φ_2, having passed through the mid-distance with displacement l_0, θ_0 is given by

$$(1) \qquad F(t_0, l_1, \theta_1)F(t_0, l_2, \theta_2) = \frac{3\omega^4}{4\pi^2 t_0^4} \exp\left[\omega^2(\gamma_1^2 + \gamma_2^2 - (\gamma_1 + \alpha l_0)^2 - (\gamma_2 + \alpha_2\theta_0)^2)\right]$$

where $\gamma_1^2 = 3(\theta_f - \theta_i)^2/(8t_0)$; $\gamma_2^2 = (\theta_i + \theta_f)^2/(8t_0)$; $\alpha_1^2 = 6/t_0^3$; $\alpha_2^2 = 2/t_0$.

Therefore, the most probable displacement at t_0 is given by

$$(2) \qquad \bar{l}_0 = -\gamma_1/\alpha_1 = t_0(\theta_i - \theta_f)/4,$$

(2) B. ROSSI and K. GREISEN: *Rev. Mod. Phys.*, **13**, 240 (1941).

and the most probable angle is

$$\bar{\theta}_0 = -\gamma_2/\alpha_2 = -(\theta_i + \theta_f)/4 . \tag{3}$$

Several examples of the application of these results are shown in Fig. 3.

The expression (1) may also be used to give an estimate of the errors involved. If r is the projected length of the three-segment path determined by (2) and (3), the r.m.s. deviation is given by

$$\sigma_r = \frac{T\Phi}{8\sqrt{6}} [\theta_i^2 + \theta_i\theta_f + \theta_f^2]^{\frac{1}{2}} ,$$

where

$$\Phi = \sqrt{T} E_s/(p\beta c)$$

is the r.m.s. angle of scattering in the plate for the distance

$$T = 2t_0 .$$

If we consider the projected angle of scatter, $\mathrm{d}\psi$, suffered by a particle in traversing a projected element of path $\mathrm{d}s$ we know that its mean value is zero and its mean square value is proportional to $\mathrm{d}s$. Hence, if we apply the principle of least squares, the most probable projected path will be that which minimizes the integral

$$P = \int \frac{(\mathrm{d}\psi)^2}{\mathrm{d}s} \mathrm{d}x ,$$

where x is an axis in the plane of projection. Taking y as a perpendicular axis in the same plane, we have

$$\operatorname{tg} \psi = p = \mathrm{d}y/\mathrm{d}x ,$$

$$q = \mathrm{d}^2y/\mathrm{d}x^2 ,$$

$$\mathrm{d}s = (\mathrm{d}x^2 + \mathrm{d}y^2)^{\frac{1}{2}} .$$

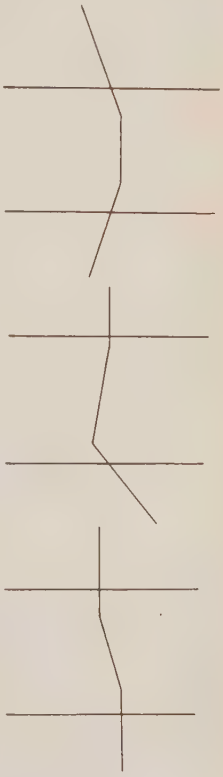

Fig. 3.

The boundary values will be $y = y_0$, $p = p_0$ at $x = x_0$ and $y = y_1$, $p = p_1$ at $x = x_1$, say. Then

$$P = \int_{x_0}^{x_1} \frac{q^2\,\mathrm{d}x}{(1 + p^2)^{\frac{5}{2}}} \equiv \int_{x_0}^{x_1} I(x, y, p, q)\,\mathrm{d}x .$$

For this problem in the calculus of variations the Euler equation is

$$\frac{\partial I}{\partial y} - \frac{\mathrm{d}}{\mathrm{d}x}\left(\frac{\partial I}{\partial p}\right) + \frac{\mathrm{d}^2}{\mathrm{d}x^2}\left(\frac{\partial I}{\partial q}\right) = 0 .$$

Since I does not contain x or y explicitly this may be integrated at once to give

$$I = Kp + C = q^2/(1 + p^2)^{\frac{1}{2}}, \tag{4}$$

where K and C are constants.

This equation can be solved numerically in special cases. In Fig. 4 the results are shown for a particle entering at A in the direction OA and leaving at E in a parallel direction. In this figure the paths obtained by the application of equations

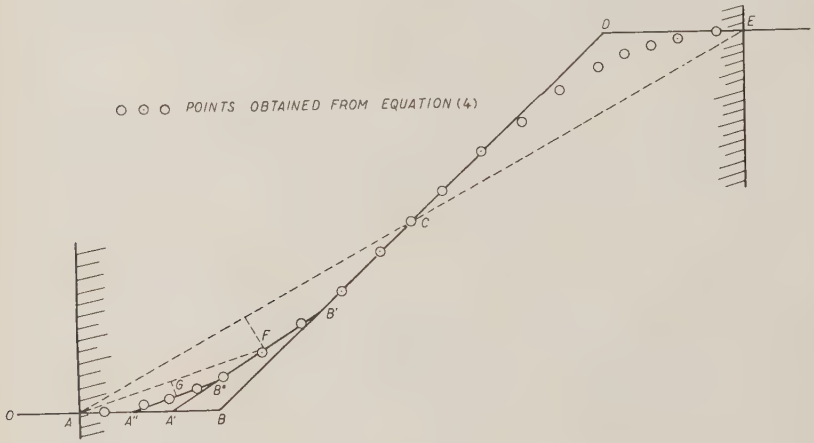

Fig. 1.

(2) and (3) are also shown. The path $ABCDE$ results from the first application. If the first half of this (ABC) is chosen for a second application, the path $AA'FB'C$ results. A further application to the section $AA'F$ leads to $AA''CB''F$. It is interesting to note how closely the graphically determined path coincides with that determined by equation (4). When one considers that the example chosen is an extreme one in terms of multiplate cloud chamber experience, it is evident that even one or two applications of the graphical method suffice to determine a path that has statstical significance.

To deal with the usual three-dimensional problem, it is necessary to consider the projections in two perpendicular planes. One application of the method in each plane will then determine a first five-segment approximation to the most probable path in space.

In some multiple cloud chambers the distortions are such that the lateral displacement of a track observed to pass through a plate cannot be determined accurately; and the angles of entry and exit are considered as the only reliable data. In such cases the principles of reference [2] can be applied to determine the most probable displacement for a particle entering and leaving at the observed angles, and the graphical method then used as before. The corresponding problem in the calculus of variations is one in which only the boundary conditions $p = p_0$ at $x = x_0$ and $p = p_1$ at $x = x_1$ are given.

IL NUOVO CIMENTO Vol. IV, N. 4 1° Ottobre 1956

Laboratory Energy Distribution of Λ^0 Particles.

G. T. Reynolds (*)

The Physics Department, Imperial College - London

(ricevuto il 10 Giugno 1956)

In has been pointed out [1-3] that cosmic ray experiments indicate that the number of low energy Λ^0 hyperons (kinetic energy $\lesssim 100$ MeV) produced in penetrating showers appears unusually large compared to the number of higher energy Λ^0's. One explanation suggested [2] was that the emission in the center of mass system might be anisotropic. This possibility seems indicated also by observations of Λ^0's produced by π^--mesons of 1.4 GeV incident on protons [4]. The purpose of this note is to point out several interactions that should be considered in evaluating the possible anisotropy of Λ^0 production in complex nuclei on the basis of the laboratory energy distribution. These interactions of Λ^0's in nuclei before emerging from the layer of producing material may distort the energy distribution at production.

The simplest such reaction is a scattering of the Λ^0 by a nucleon and has been considered by several authors [5,6]. This would generally decrease the energy of the Λ^0 and, if the cross section is assumed to be similar to the n-p cross section as a function of energy in the energy range of interest, would affect most the lower energy Λ^0's.

A further interesting possibility is a reaction suggested by the Gell-Mann scheme [7]:

$$\Lambda^0 + n \rightarrow \Sigma^- + p \,, \qquad (1)$$

or

$$\Lambda^0 + p \rightarrow \Sigma^+ + n \,. \qquad (2)$$

These reactions have a laboratory threshold of approximately 170 MeV if the nucleon is at rest. The effect of 25 MeV Fermi energy of the nucleon is to reduce the threshold, but in no case of disruption of the nucleus could it fall below 55 MeV. Since the cross sections for these reactions should presumably increase in the region above threshold, they might be

(*) On leave of absence from Princeton University, Princeton, New Jersey.

(1) J. Ballam, D. R. Harris, A. L. Hodson, R. R. Rau, G. T. Reynolds, S. B. Treiman and M. Vidale: *Phys. Rev.*, **91**, 1019 (1953).

(2) G. T. Reynolds and S. B. Treiman: *Phys. Rev.*, **94**, 207 (1954).

(3) D. B. Gaythier and C. C. Butler: *Phil. Mag.*, **46**, 467 (1955).

(4) W. B. Fowler, R. P. Shutt, A. M. Thorndike and W. L. Whittemore: *Phys. Rev.*, **91**, 1287 (1953); **93**, 861 (1954).

(5) R. Jastrow: *Phys. Rev.*, **97**, 181 (1955).

(6) G. D. James and R. A. Salmeron: *Phil. Mag.*, **46**, 571 (1955).

(7) M. Gell-Mann: *Pisa Conference* (June 1955).

significant in removing Λ^0's preferentially from the laboratory energy intervals above, say, 100 MeV, and thus distort the original energy spectrum to favour a relatively large number of low energy Λ^0's.

Further reactions with essentially the same thresholds are:

$$\Lambda^0 + n \rightarrow \Sigma^0 + n , \tag{3}$$

$$\Lambda^0 + p \rightarrow \Sigma^0 + p . \tag{4}$$

Since the Σ^0 presumably decays with very short lifetime to Λ^0 and photon, these reactions would result in decreasing the energy of the Λ^0 as observed in the laboratory frame of reference, thus distorting the original spectrum in favour of low energies.

It should also be pointed out that the following reactions may supply Λ^0's to the laboratory sample:

$$\Sigma^- + p \rightarrow \Lambda^0 + n ,$$

$$\Sigma^+ + n \rightarrow \Lambda^0 + p .$$

However, although these reactions require consideration in interpreting observed θ^0/Λ^0 ratios, they will distort the energy spectrum of the Λ^0's statistically mainly only in the sense of the shape of the Σ energy spectrum itself.

Discussions with K. H. Barker have been helpful.

* * *

It is a pleasure to acknowledge a grant from the John Simon Guggenheim Foundation, which helped make this work possible.

IL NUOVO CIMENTO Vol. IV, N. 4 1° Ottobre 1956

On a New Nucleon-Nucleon Potential.

E. Clementel and C. Villi (*)

Istituto di Fisica dell'Università - Padova
Istituto di Fisica dell'Università - Trieste (*)
Istituto Nazionale di Fisica Nucleare - Sezione di Padova

(ricevuto il 26 Luglio 1956)

The relationship to a more fundamental underlying theory of recent semifield, semiphenomenological investigations on meson-nucleon and nucleon-nucleon scattering, the ultimate success of which in fitting the experimental data largely depends on the numerical value given to two parameters, the cut-off length k_m^{-1} respectively the core radius r_c, is not clear (1). There are, however, some warning signals which might suggest the meaning of these parameters, the values of which are always found to be between about $0.2/\mu$ and $0.5/\mu$. One of these is the well known possibility to improve the fit of nucleon-nucleon scattering at intermediate energies (2) by letting the mass of the meson be larger than that of the pion. Furthermore, the increase of the meson mass gives acceptable binding energy for a heavy nucleus either in terms of a phenomenological potential (3) or starting from a non-linear description of the meson field (4). It is a remarkable fact that the « effective » meson mass (5) is close to the average between the mass of the pion and that of known heavy mesons (~ 493 MeV). It is also a remarkable fact that the core radius, chosen by Lévy (6) in order to fit the deuteron ground state, and

(1) A system of units where $\hbar = c = 1$ is used; $\mu^{-1} = 1.4.10^{-13}$ cm is the Compton wave length of the π-meson.

(2) G. Breit: *Phys. Rev.*, **84**, 1053 (1951).

(3) R. Huby: *Proc. Phys. Soc.*, A **62**, 62 (1949).

(4) E. Clementel and C. Villi: *Nuovo Cimento*, **1**, 1273 (1955). Apart from the different kind of coupling, the remarkable difference between the « effective » meson mass defined in Eq. (12) and the equivalent definition of S. D. Drell and E. M. Henley (*Phys. Rev.*, **88**, 1053 (1952); Eq. (11)) lies in the product λg having the dimension of a length. If one neglects damping effects due to the non-linearities, the effective meson mass appears to be larger [M. H. Johnson and E. Teller: *Phys. Rev.*, **98**, 781 (1955)]. The choice $\alpha_n = \beta^n/n!$ in the non-linearity power series considered in this note would have led to an exponential coupling, giving a highly singular two-nucleon potential [R. Glauber: *Phys. Rev.*, **84**, 398 (1952)].

(5) A value of the « effective » meson mass very close to that evaluated in ref. (4) (~ 326 MeV) is also obtained using into the Fornaguerra relation $\mu^* = \mu[1 + 3\lambda^2 V_n^2]^{\frac{1}{2}}$ (*Nuovo Cimento*, **1**, 132 (1955)) the value $\lambda = 11.86$ (L. S. Schiff: *Phys. Rev.*, **84**, 1 (1951)) and calculating V_n from the normal nuclear density.

(6) M. M. Lévy: *Phys. Rev.*, **88**, 725 (1952).

the cut-off distance assumed in previous calculations ([7]) of the deuteron quadrupole moment, is rather close to the Compton wave length of such an « effective » meson. Finally, the core radius, given by the Bruckner and Watson theory ([8]) for singlet states in the case of complete pair suppression, is approximately equal to the Compton wave length of known heavy mesons.

All these circumstances, of course, might be fortuitous. However, it is difficult to accept and justify the idea that the values of the parameters introduced into a theory, and essential to fit the data, have not some physical meaning and no link with a real state of affairs. For this reason, it is probably not unrealistic to think that from all the previous circumstances emerges in a rather systematic way that the description of nuclear interactions through the pion field only is an oversimplified picture, which breaks down at short distances, where the effects of another field, besides the one included, come into play. It is therefore understandable that a theory which systematically ignores the eventual role of a heavy meson field is necessarily bound to involve some characteristic parameters related to it and giving rise, in an obscure way, to a sort of field theoretical compromise between the explicitly considered pion field and the neglected and largely unknown heavy meson field. In the more optimistic case one might hope that current theories are able to describe nuclear interactions at high energies by means of a pion field which is « equivalent » to the true field, this « equivalence » being brought about in a crude way just by the ad hoc introduction and adjustement of certain empirical constants.

Let us suppose that the current descriptions of nuclear interactions break down at about the Compton wave length—say—of the K-meson ([9]). This certainly does not mean that the influence of the heavy meson field is expected to be appreciable only when the nucleon relative wave length is equal or smaller than the Compton wave length of the K-meson ([10]). Assuming this point of view, one can easily understand, for instance, the remarkable success at low energies of the repulsive core idea ([11]) and its failure to yield appropriate polarization as well as sufficient isotropy for p-p scattering at higher energies ([12]), where the structure of the meson field, other than the pion field, cannot probably be accounted for simply by a core repulsion.

Since the local two-nucleon potential ([13]), valid when the interacting nucleons are far apart from each other, must assume a non-local feature at short distances, it is tempting to derive it from a fundamental modification of the Lagrangian density $\boldsymbol{L}$ of the field system (free field Lagrangian plus the interaction Lagrangian), such that (*a*) it preserves the linearity of the field, (*b*) it implies a suppression of high momentum components and (*c*) it gives the current description of the field system at the limit $k_m = \infty$. The simplest, but not unique, way to proceed along these lines is to introduce a Lagrangian density function $\boldsymbol{\mathcal{L}}$ dependent at least also

---

([7]) H. A. BETHE: *Phys. Rev.*, **54**, 260, 290 (1940).

([8]) K. A. BRUCKNER and K. M. WATSON: *Phys. Rev.*, **92**, 1023 (1953).

([9]) D. I. BLOKHINTSEV: *Journ. of Exp. and Theor. Phys.* (*USSR*), **1**, 23 (1956).

([10]) The nuclear interactions between two nucleons are not negligible at an energy smaller than ~ 40 MeV, although only at this energy the nucleon relative wave length is of the order of the Compton wave length of the pion!

([11]) R. JASTROW: *Phys. Rev.*, **79**, 389 (1950); **81**, 165 (1951).

([12]) L. G. B. GOLDFARB and D. FELDMAN: *Phys. Rev.*, **88**, 1199 (1952); D. SWANSON: *Phys. Rev.*, **89**, 740 (1953); **89**, 85 (1950).

([13]) R. S. CHRISTIAN and E. W. HART: *Phys. Rev.*, **77**, 443 (1950); R. S. CHRISTIAN and H. P. NOYES: *Phys. Rev.*, **79**, 85 (1950).

on the second order derivatives of the field variables $\varphi_\alpha(\boldsymbol{x})$, and require that

$$\delta \int \mathcal{L}(\varphi_\alpha; \varphi_{\alpha,\mu}; \varphi_{\alpha,\mu\nu})\, \mathrm{d}^4x = 0 \qquad (\varphi_{\alpha,\mu} = \partial\varphi_\alpha/\partial x_\mu). \tag{1}$$

Performing variations with respect to φ_α and $\varphi_{\alpha,\mu}$, vanishing at the surface of the integration volume, one readily obtaines a generalized field equation. For the particular choise

$$\mathcal{L} = L - \tfrac{1}{2} k_m^{-2} \sum_{\mu\nu} (\varphi_{\alpha,\mu\nu})^2 , \tag{2}$$

satisfying the requirements (a), (b) and (c), in the static approximation of the charge-symmetric theory for a pseudoscalar field with pseudovector coupling, the field equation reads [14]

$$(\nabla^2 - \mathcal{M}^2)\varphi_\alpha = -\left(\frac{f}{\mu}\right)\tau_\alpha \boldsymbol{\sigma}\cdot\boldsymbol{\nabla}\,\delta(\boldsymbol{r}) \tag{3}$$

where the operator

$$\mathcal{M} = \mu\left\{1 + \frac{\nabla^2\nabla^2}{k_m^2\mu^2}\right\}^{\frac{1}{2}}, \tag{4}$$

acting formally as an «effective mass» operator, reduces to the constant μ at the limit $k_m = \infty$. Eq. (3), which can be considered as the extension of the Bopp equation [15] to the ps(pv) meson field, will be regarded as the equation obeyed by the «equivalent» pion field and not as a particular case of a multi-meson field equation, i.e. we tentatively assume that a theoretical scheme based on the Lagrangian (2) contains only that part of the theory in which, at the present stage, we have reason to believe. This reinterpretation of Eq. (3) allows to circumvent some difficulties arising when a fourth order equation is split into a system of two Klein-Gordon equations, associated to different kinds of bosons [16].

The solution of Eq. (3) which behaves at large distances as the solution corresponding to $k_m = \infty$ and gives rise to a δ-function at the origin, is

$$\varphi_\alpha(r) = (f/\mu\alpha)\tau_\alpha^{(1)}\boldsymbol{\sigma}\cdot\boldsymbol{\nabla}\left\{\sum_{\nu=0}^{1}(-1)^\nu\beta_\nu h_0(i\beta_\nu r)\right\}, \tag{5}$$

where $h_n(z_\nu)$ is the Hankel spherical function of the first kind [17] and

$$\alpha(k_m) = [1 - (2\mu/k_m)^2]^{\frac{1}{2}}, \qquad \beta_\nu(k_m) = (2)^{-\frac{1}{2}}k_m[1 - (-1)^\nu\alpha(k_m)]^{\frac{1}{2}}. \tag{6}$$

The parameters β_ν $(\nu = 0, 1)$ are real provided $k_m^{-1} \leqslant 0.5/\mu$. For k_m^{-1} varying between 0 - $0.5/\mu$, β_0 varies very slowly, being very close to μ for $0 \leqslant k_m^{-1} \lesssim 0.1/\mu$. For k_m^{-1}

---

[14] Apart from a slightly different definition of the constants k_m and μ, the π-field considered by BUDINI in his theory of the pion-nucleon interactions (*Nuovo Cimento*, **3**, 1104 (1956)), obeys a fourth order equation following from the Lagrangian (2). We thank Prof. P. BUDINI for a discussion on this point.

[15] V. F. BOPP: *Ann. d. Phys.*, **38**, 345 (1940).

[16] A. PAIS and G. E. UHLENBECK: *Phys. Rev.*, **79**, 145 (1950); Y. KATAYAMA: *Progr. of Theor. Phys.*, **3**, 561 (1953).

[17] P. M. MORSE and H. FESHBACH: *Methods of Theoretical Physics* (New York, 1953), p. 1573.

equal to about twice the Compton wave length of the nucleon, β_1^{-1} corresponds to the Compton wave length of the K-meson and for k_m^{-1} equal to the Lévy core radius ($r_c = 0.38/\mu$). β_1^{-1} corresponds to the Compton wave length of the « effective » meson. It is rather surprising that the second order derivatives included into the field Lagrangian (2) produce at short distances the general trend of the modifications of the static potential which already have been found necessary to fit the data. It is easy to prove that a point source field obeying the generalized Eq. (3) is exactly equivalent to an extended source field described by the Klein-Gordon equation ($\mathcal{M} \equiv \mu$). The choice between these two alternatives is an open problem [18].

The potential energy between two nucleons, following from Eq. (5), is

$$V(r) = -(f^2/\mu^2\alpha)(\boldsymbol{\tau}^{(1)}\cdot\boldsymbol{\tau}^{(2)})(\boldsymbol{\sigma}^{(1)}\cdot\boldsymbol{\nabla})(\boldsymbol{\sigma}^{(2)}\cdot\boldsymbol{\nabla})\sum_{\nu=0}^{1}(-1)^{\nu}\beta_\nu h_0(i\beta_\nu r)\,. \tag{7}$$

A straightforward calculation gives

$$V(r) = V_c(r) + S_{12}V_t(r)\,, \tag{8}$$

where S_{12} is the well known tensor operator and

$$V_c(r) = -(f^2/3\alpha)(\boldsymbol{\tau}^{(1)}\cdot\boldsymbol{\tau}^{(2)})(\boldsymbol{\sigma}^{(1)}\cdot\boldsymbol{\sigma}^{(2)})\sum_{\nu=0}^{1}(-1)^{\nu}(\beta_\nu^3/\mu^2)h_0(i\beta_\nu r)\,, \tag{9}$$

$$V_t(r) = (f^2/3\alpha)(\boldsymbol{\tau}^{(1)}\cdot\boldsymbol{\tau}^{(2)})\sum_{\nu=0}^{1}(-1)^{\nu}(\beta_\nu^3/\mu^2)h_2(i\beta_\nu r)\,. \tag{10}$$

The two-nucleon potential (8) can be reduced to the phenomenological potential obtained by NOYES and PANDYA [19] multiplying the ladder approximation Bethe-Salpeter kernel by a covariant cut-off factor ($a=0$; $b=1$; $\mu\equiv\beta_0$; $K\mu\equiv\beta_1$; $V_0/\mu = f^2/3\alpha$). The fundamental difference between the potential suggested by NOYES and PANDYA and the potential (8) lies in the fact that in the former the parameters corresponding to β_0 and β_1 are left arbitrary, while in the latter they are entirely fixed, through Eqs. (6), by the value of the cut-off k_m. It follows that this model provides an entirely different fitting mechanism of the low energy data than that used, with negative result, by these Authors.

The potential (8) shows several interesting features. For even singlet and triplet states and at large distances the central part $V_c(r)$ is attractive. The maximum attraction, dependent of course on k_m, lies somewhere in the interval $0.7/\mu \leqslant r \leqslant 0.9/\mu$. At internucleon separation $r^* = 2(\beta_1^2 - \beta_0^2)^{-1}\ln(\beta_1/\beta_0)$ the central part becomes zero and then ($r < r^*$) strongly repulsive. At $r = 0$ the potential exhibits infinite repulsion. This situation is reversed for odd singlet and triplet states. It is seen that in this model the strong core effect, required to fit the flat cross-section of the unpolarized p-p experiments, comes out from the Lagrangian (2) and

---

(18) For scalar and neutral fields the potential is given by

$$\varphi(r) = -(G/4\pi\alpha)[\beta_0 h_0(i\beta_0 r) - \beta_1 h_0(i\beta_1 r)]\,,$$

which reduces to the potential suggested by L. ROSENFELD [*Nuclear Forces* (Amsterdam, 1948), p. 67], assuming $a_1 = -a_2 = \alpha^{-1}(k_m)$ and $a_n = 0$ for $n > 2$.

(19) H. P. NOYES and S. P. PANDYA: *Phys. Rev.*, **102**, 269 (1956).

from the pv coupling, without resorting to the Lévi reinterpretation of the δ-function repulsion. Since the repulsive interaction depends strongly on k_m, it follows that if the cut-off has something to do with the structure of the field at short distances, the existence of the core, following in the present scheme necessarily from the postulated cut-off, does not suppress forces from heavy mesons, but rather accounts in an unknown way for these forces, which are not included in current theories, but nevertheless exist in nature. The tensor potential $V_t(r)$ has the correct sign. The inadmissible singularity r^{-3} is entirely removed as a consequence of the introduction of the second order derivatives into the Lagrangian (2), which force the tensor interaction to behave as r^{-1} at short distances.

It is interesting to note that the central part of the two-nucleon potential (8) reproduces fairly well the qualitative features of the second plus fourth order contributions to the central part of the Gartenhaus potential ([20]), except at the origin where the latter exhibits a strong but finite repulsion in even states. Finally, apart from the different meaning of the parameters and the different philosophy underlying Eq. (3), the tensor potential (10) has the same mathematical structure of the tensor potential obtained by SCHWINGER ([21]), modifying the Møller-Rosenfeld mixed theory ([22]).

The capability of the field Lagrangian (2) to reproduce in the static approximation a physical description of nuclear interactions, which for the central part is similar and for the tensor part is identical to that obtained from basically different approaches, deserves a further investigation.

* * *

We are pleased to acknowledge an illuminating discussion with Prof. L. ROSENFELD.

([20]) S. GARTENHAUS: *Phys. Rev.*, **100**, 900 (1956).

([21]) J. SCHWINGER: *Phys. Rev.*, **61**, 387 (1942); J. M. JAUCH and N. NU: *Phys. Rev.*, **65**, 289 (1944).

([22]) C. MOLLER and L. ROSENFELD: *Kgl. Danske Vid.*, **17**, 8 (1940); L. ROSENFELD: *Helv. Phys. Acta*, **23**, 211 (1950).

Interaction and Decay of K^+ Mesons in Flight.

C. Marchi, E. Pedretti and S. Stanic (*)

Istituto di Fisica dell'Università - Bologna

Istituto Nazionale di Fisica Nucleare - Sezione di Padova, Sottosezione di Bologna

(ricevuto il 2 Agosto 1956)

One stack of 24 « stripped emulsions » G-5, having an area of (7.5×15) cm^2 and a thickness of 600 μm, was exposed at the beam of positive particles of Berkeley's bevatron. The positive particles of the beam had momenta between 400 and 420 MeV/c.

The tracks due to K-mesons were taken after 3 cm from the entrance edge of the beam, i.e. after the range of the protons having the same momentum. The tracks have been taken which have the direction of the beam and a grain density between 1.5 and 3 times minimum. The measurements of the grain density were made along ~ 300 μm in each track.

The tracks were followed from plate to plate until they either stopped or got out of the stack. The results obtained are in Table I. Of the 278 K-particles which stopped at the end of their range inside the emulsions, 10 were identified as τ-mesons and 10 were interpreted as τ' or $K_{\mu 3}$. The remaining 258 were considered K_L. In 49 cases of the K_L group no secondary tracks were observed but measurements of ionization and range indicated that they were K_L. The reason why the secondary tracks were

Table I.

	Total No.	K-mesons	Other particles
No. of particles which come to rest without having suffered any inelastic collisions	351	278	73
No. of particles which leave the stack	186	67%	33%
No. of particles which suffer inelastic collisions	47	19	28
No. of particles which stop in flight	4	4	0
No. of particles which decay in flight	13	13	0

(*) On leave from the University of Santiago (Chile).

not observed is that the minimum density of grains in the emulsion analysed had a very low value. One K_{L^-} decay having three tracks at minimum ionization has been found. One of the tracks is a light meson and the other two, that go in a direction opposite to the first, are an electron pair. This fact indicates the presence of a π^0 in the decay.

In order to obtain the interaction mean free paths and the mean life of the K-particles we subtracted from the total length observed the infection due to other particles and eliminated all the events which were not produced by K. In this way we obtained the length of track due to K-mesons.

The infection of particles which leave the stack was obtained from the number of spurious tracks which were followed to the end of their range, from the number of interactions due to non K-particles at random among those which leave the stack.

The total length of track is:

$$L = (23.00 \pm 0.43) \text{ m}$$

the interactions were divided in three groups: elastic, anelastic and charge-exchange scattering, according to the well known hypothesis that absorption processes are not possible for the K^+. No evidence against this hipothesis was found.

Six anelastic scatterings with visible excitation of the hit nucleus and 54 without visible excitation were found.

The distinction of the elastic from the anelastic scatterings was made by statistical means, using grain density measurements. The distribution of the relative variation of grain density $\Delta\nu/\bar{\nu}$ was also made.

From Fig. 1 one sees that the distribution for the smaller angles is better centered on the zero. We consider the dispersion of the distribution of the $\Delta\nu/\bar{\nu}$ as due mainly to the errors of the measurements. In this way were recognized 9 (with geometrical correction factor 12.8) inelastic events (with $\Delta E/E_0 > 20\%$) without visible excitation and 45 elastic scatterings ($\Delta E/E_0 < 20\%$).

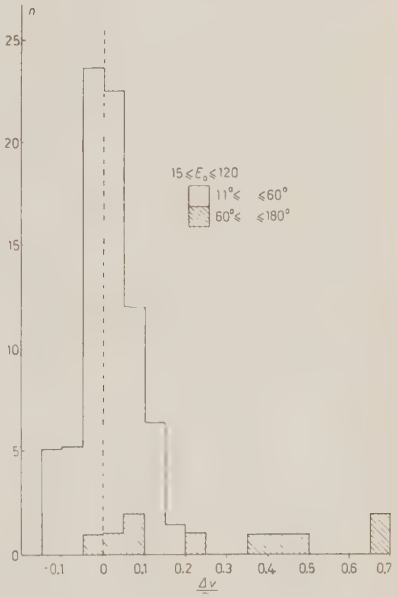

Fig. 1.

For the mean free path for the anelastic scattering ($\Delta E/E_0 > 20\%$) one gets

$$\lambda = (1.22 \pm 0.28) \text{ m} .$$

In Table II are given the scattering angles in the L-system, the geometrical correction factor for the cut-off at 11°, the primary energy, and the relative energy loss of 45 elastic events with energies between 15 and 130 MeV.

In Table III are given the scattering angles in the Laboratory system, the geometrical correction factor for the cut-off at 11°, the primary energy, the relative energy loss and the number of prongs of 21 anelastic events with energies between 20 and 130 MeV.

TABLE II.

No.	ϑ degrees	j	Elastic events E_0 (Mev)	$\Delta E/E_0$ %
1	11.9	2.7	37.4	— 3.2
2	11.9	2.7	37.4	— 3.2
3	12.1	2.64	50.6	— 7.9
4	12.5	2.44	69.7	— 2.1
5	12.65	2.34	94.6	2.5
6	12.95	2.26	79.7	— 21.6
7	13.0	2.16	75.6	4.8
8	13.3	2.08	22.2	— 5.8
9	13.7	1.96	23.6	— 16.1
10	14.2	1.90	28.6	3.2
11	14.58	1.89	72.8	4.0
12	14.6	1.89	55.5	9.9
13	15.0	1.84	36.5	8.2
14	15.35	1.76	69.9	— 17.7
15	16.2	1.70	99.2	— 0.3
16	16.4	1.68	98.0	— 17.3
17	17.8	1.56	49.0	0
18	17.8	1.56	28.6	— 3.8
19	18.9	1.49	79.7	— 4.9
20	20.05	1.35	29.7	0.2
21	20.2	1.35	79.7	1.8
22	20.3	1.35	32.4	8.3
23	21.2	1.35	18.5	13.5
24	23.05	1.35	122.0	0
25	23.6	1.35	94.6	6.3
26	25.6	1.35	94.6	— 14.1
27	29.5	1.35	250.0	2.0
28	30.8	1.205	90	— 15.5
29	30.95	1.205	99.2	— 1.0
30	31.45	1.205	53.7	0.3
31	32.8	1.205	118.0	— 3.4
32	33.65	1.205	58.9	4.9
33	36.3	1.205	84.9	0.2
34	38.2	1.205	79.7	12.3
35	38.6	1.205	58.2	— 0.3
36	38.7	1.205	71.0	14.7
37	40.9	1.13	77.8	1.0
38	44.8	1.13	83.6	7.9
39	45.0	1.13	68.4	— 0.9
40	45.5	1.13	72.8	— 4.3
41	49.7	1.13	79.0	2.5
42	60.7	1.055	25.9	8.9
43	81.4	1.0	38.0	5.3
44	91	1.0	27.4	13.9
45	106.8	1.0	45	10.6

In order to obtain the mean free path for all incoherent events we added to the before mentioned events the charge-exchange cases which are represented by the stars in which there is no K scattered and by the stops.

Because of the inefficiency in the observation of the tracks which are at minimum ionization, it is to be expected that some of the stops should be decays in flight instead of charge-exchange interactions. We evaluate this inefficiency from the loss of secondaries of K^+ at the end of their range, and attribute 2 of the 4 stops to decays in flight. The other 2 are considered as charge-exchange events without visible excitation of the nucleus hit, and are added to the 4 events with visible excitation obtained from the analysis of the stars.

Our experiment gives for the ratio between the charge-exchange and the anelastic events the value $R = 0.32^{+0.17}_{-0.13}$.

The mean free path for all incoherent events is:

$$\lambda = (0.93 \pm 0.19)\ \mathrm{m}\ .$$

This value is in agreement with the values found by other Authors [1-3]. This gives for the scattering cross-section of the nucleon (averaging for protons and neutrons) about 6 m barn. From the total time of flight and from the number of decays in flight we found the mean life of the K-mesons to be

$$T = (1.13 \pm 0.31)\cdot 10^{-8}\ \mathrm{s}\ .$$

Conclusions. – No contradiction with Gell-Mann's theory was found. We

(1) Privately circulated preprint by the Göttingen Group.

(2) Privately circulated preprint by the Padua Group.

(3) J. E. LANNUTTI, W. W. CHUPP, G. GOLDHABER, S. GOLDHABER, E. HELMY, E. HOFF, A. PEVSNER and D. M. RITSON: *Phys. Rev.*, **101**, 1617 (1956).

TABLE III.

No.	ϑ (degrees)	f	E_0 (MeV)	$\Delta E/E_0$ (%)	(No. of prongs)
1	14.4	1.9	80	23.9	0
2	11.2	3.34	23.9	20.9	0
3	98.7	1.0	44.5	45.4	0
4	65.7	1.055	62.2	26.7	0
5	19.2	1.48	52.8	22.0	0
6	106.8	1.0	94.6	64.6	recoil nucleus
7	117.6	1.0	97.0	42.5	» »
8	70.8	1.0	65.0	48.9	» »
9	76.2	1.0	87.4	66.8	» »
10	(32.6)	—	72.8	(43.7)	1 prong, K′ uncertain
11	(76.5)	—	116.0	(80.8)	2 prongs K′ »
12	(82.5)	—	64.0	—	2 » K′ » recoil nucleus
13	21.9	—	104.0	41.3	1 prong
14	168.6	—	105.8	55.8	1 » » »
15	121.4	—	74.2	66.8	2 prongs » »
16	—	—	102.0	—	0 stop
17	—	—	112.0	—	0 stop
18	—	—	110.0	—	1 prong
19	—	—	119.0	—	1 »
20	—	—	127.0	—	2 prongs » »
21	—	—	99.0	—	4 » » »

found:

$$\lambda \text{ Anel. scatt.} = (1.22 \pm 0.28) \text{ m}$$

$$\lambda \text{ Incoher. events} = (0.93 \pm 0.19) \text{ m}.$$

$$\bar{\sigma} = 6 \text{ m barn}$$

$$\frac{\text{Charge exchange}}{\text{anelastic events}} = 0.32^{+0.17}_{-0.13}$$

We noticed also that the mean free path for the anelastic events is energy-indipendent, while the charge-exchanges found are in the high energy region.

This experiment was possible due to the kind co-operation of the Berkeley Group, who exposed our emulsions to the Bevatron.

* * *

We are particularly indebted for this, to Dr. E. J. LOGFREN and Dr. S. GOLDHABER.

One of us (S. S.) wishes to thank the Istituto di Fisica dell'Università di Bologna for a fellowship.

We are grateful to Prof. G. PUPPI and Dr. G. QUARENI for useful suggestions and discussion and to Dr. R. GESSAROLI for help in the measurements.

A Carbon Dioxide-Hexane Gas Bubble Chamber.

B. Hahn

Department of Physics, University of Fribourg - Fribourg, Switzerland

(ricevuto il 3 Agosto 1956)

A gas bubble chamber is a new kind of detector for ionizing particles, and makes use of the metastability of a gas-liquid system, in which a gas is dissolved supersaturated in a liquid. A supersaturated state can be produced by solving a gas under pressure in a liquid, and by subsequent pressure release. Such a system becomes metastable with respect to gas bubble formation.

The mechanism for formation of macroscopic bubbles by ionizing particles in a gas bubble chamber must be essentially the same as that proposed by Glaser [1] for his vapour bubble chamber. The surface tension of microscopic bubbles has to become overcompensated by the vapour (gas) pressure in the bubble, and by the repulsive force of charge produced by the ionizing particles. The vapour (gas) pressure which will be required for bubble growth will be small for small surface tension and small dielectric constant of the liquid (gas-liquid system) for a given amount of charge located near the bubble surface.

The gas bubble chamber might be considered as a system of two liquids, in which the dissolved gas represents the second liquid. In this sense the gas bubble chamber is a modified Glaser bubble chamber, the first liquid controlling the vapour pressure and the growth of the vapour bubbles of the second liquid. The vapour pressure of the second liquid is strongly correlated to the mixing ratio of the two liquids and only slightly to temperature. Thus, the required vapour pressure for bubble formation has not to be « realized » by temperature, like in the Glaser bubble chamber, and for certain gas-liquid systems operation at room temperature becomes possible. The velocity of bubble growth in the gas bubble chamber generally will be slowed down by the presence of the first liquid, allowing slow expansion and photographing. Moreover the sensitive time of the chamber will become relatively long.

Recently Argan and Gigli [2] announced the successfull construction of a carbon dioxide-ethyl ether gas bubble chamber in which beautiful bubble tracks caused by γ radiation became visible.

Independently of the work mentioned above, a carbon dioxide–n-hexane gas

[1] D. A. Glaser: *Suppl. Nuovo Cimento*, **11**, 361 (1954).

[2] P. E. Argan and A. Gigli: *Nuovo Cimento*, **3**, 1171 (1956).

Fig. 1.

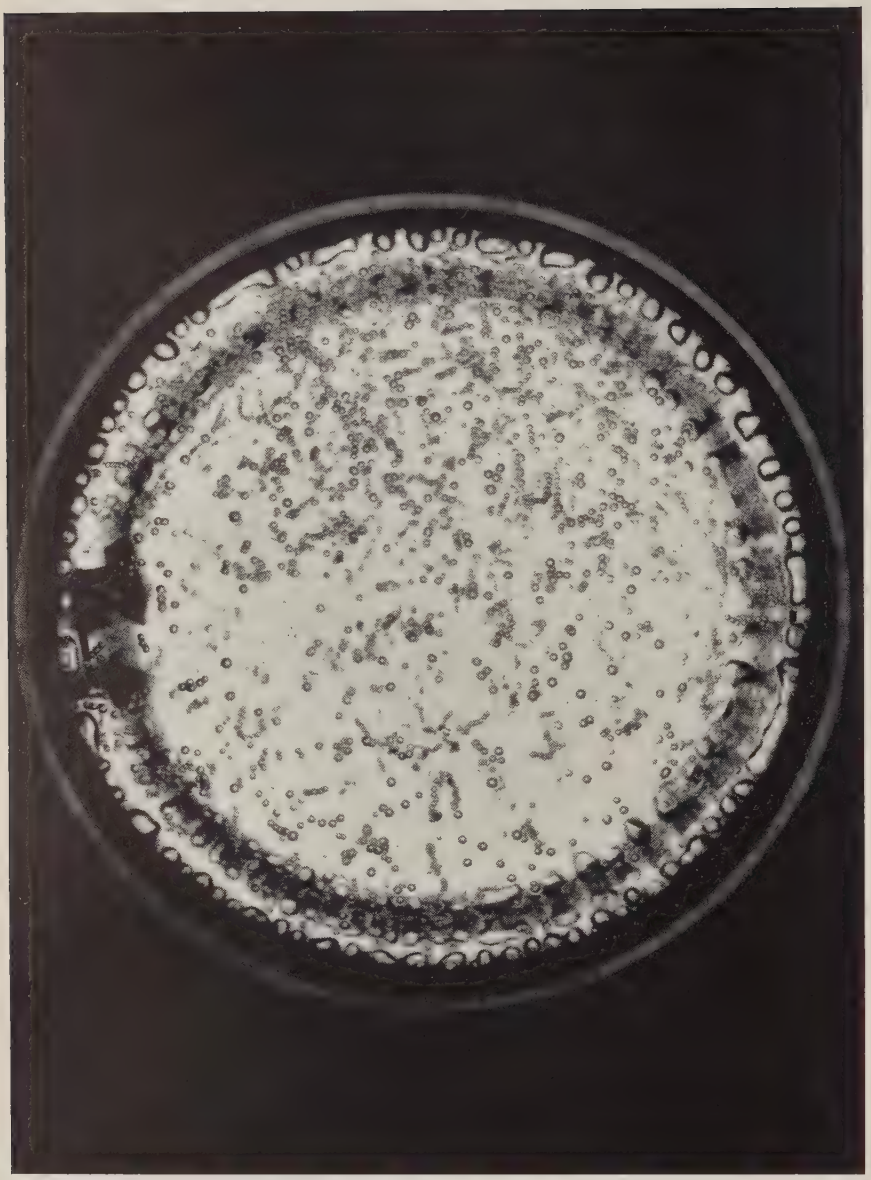

Fig. 2.

bubble chamber has been put into operation at our laboratory (*). Our chamber is a cylindrical brass tube, four cm in diameter and five cm long, with two end windows made from a resin (Araldite from CIBA, Basel, Switzerland). These windows are sealed with O-rings to the brass chamber. The bubble chamber is connected through a high pressure valve to a mixing vessel. The pressure release of the bubble chamber is provided by a moving expansion piston, which is located in a separate expansion chamber. The piston, which is sealed with a O-ring, moves under the action of the liquid on one side and compressed air on the opposite side of the piston. In order to expand the chamber, the compressed air is released by opening a high pressure valve. The expansion time is of the order of 100 ms and photographs are taken with a 1 ms flash light and open camera. The flash is triggered at a moment, when the pointer of a manometer, which measures the pressure of the compressed air, touches a mouvable contact, mounted on the manometer. Pre-expansion pressures up to 50 atm have been applied to the system.

Several organic liquids in combination with carbon dioxide and argon have been tried. Two gas-liquid systems, which yielded bubble tracks under the conditions mentioned above, were carbon dioxide-n-hexane and carbon dioxide-triethylamine. Carbon dioxide dissolves in the mentioned liquids in large quantities. At a pressure of 50 atm carbon dioxide dissolves in hexane approximately by 180 percent by weight at room temperature. The surface tension of n-hexane is 18.4 dyn/cm at 20 °C, and the surface tension of the carbon dioxide-hexane system has been roughly estimated to $8 \div 10$ dyn/cm. The dielectric constant for hexane is 1.87 at 20 °C and for liquid carbon dioxide approximately 1.6.

In Fig. 1 and Fig. 2 photographs of bubble formation in a carbon dioxide-hexane gas bubble chamber are shown. The pre-expansion pressure was approximately 50 atm. The pictures were taken during the expansion, at a moment when the pressure in the chamber was around $10 \div 20$ atm. In the first picture, the chamber was exposed to a beam of ^{60}Co γ-rays, emerging from a lead collimator. As expected, the bubbles appear predominantely in a central region across the chamber. The visible bubbles are $0.1 \div 0.3$ mm in diameter. No bubble formation occured at the chamber walls, except at the corners. The second picture was taken at a later moment than the first picture during the expansion process. It shows bubble tracks of different age, which were caused by a Ra source, located near the chamber. The attenuation of the bubble track density due to the $1/r^2$ law is evident. Bubbles up to 0.5 mm in diameter appear in this picture (corner bubbles excepted).

For comparison a pure carbon dioxide chamber has been investigated under the same conditions as those for the gas bubble chamber (pre-expansion pressure ~ 58 atm). No bubbles due to radiation could be observed, however violent bubbie formation occured all over the chamber walls, and at a later moment at the chamber windows.

(*) The mentioned paper of the italian group came to the attention of the author only at a moment, when preliminary experiments assured bubble formation in our gas bubble chamber.

On the Ratio Between γ- and α-Activities in ^{210}Po.

A. Ascoli, M. Asdente and E. Germagnoli
Laboratori CISE - Milano

(ricevuto l'8 Agosto 1956)

^{210}Po is known to be a practically pure α emitter. Its decay scheme is given in Fig. 1 and its half-life is

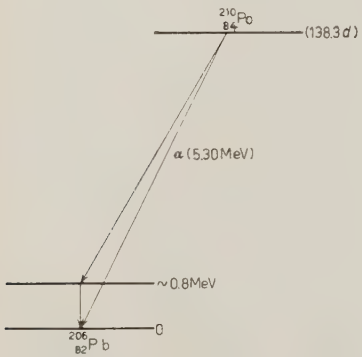

Fig. 1. – Decay scheme of ^{210}Po.

138.3 d [1]. ^{210}Po sources are extensively used, and for several investigations an absolute calibration of the source is required.

A direct measurement of the intensity of emitted α particles can be carried out with satisfactory accuracy if the source is very thin and weak enough to be introduced into an ionization chamber of well defined geometry. If the intensity of the source is remarkable its absolute calibration by means of α counting becomes more troublesome and a current chamber, intrinsically capable of less accuracy, is generally used.

The fact that γ-rays are emitted in a weak branching, as is shown in Fig. 1, makes possible an easy and quick calibration of intense ^{210}Po sources, provided the γ/α ratio is well known. Values of such ratio are found in the literature [1], but a considerable spread can be noticed in the results of different authors. It seemed consequently worthwhile to determine the ratio γ/α again.

For the present measurement a thin source, whose activity is approximately 4 mC, has been used. It has been supplied by the Radiochemical Centre of Amersham (England).

^{210}Po is electroplated onto Pt and covered with a thin mica sheet (1 mg cm^{-2}): the diameter of the source is 5.5 mm.

The γ activity has been measured by means of a single crystal scintillation spectrometer, the cylindrical NaI(Tl) crystal being 2.50 cm high and 3.75 cm in diameter.

The energy distribution of pulses has been analyzed with a fast 10 channel pulse analyzer. A typical γ spectrum from ^{210}Po is shown in Fig. 2.

[1] J. M. Hollander, I. Perlmann and G. T. Seaborg: *Rev. Mod. Phys.*, **23**, 469 (1953).

The energy of γ-rays was found to be 755 keV and the γ intensity of the source was evaluated from the area under the

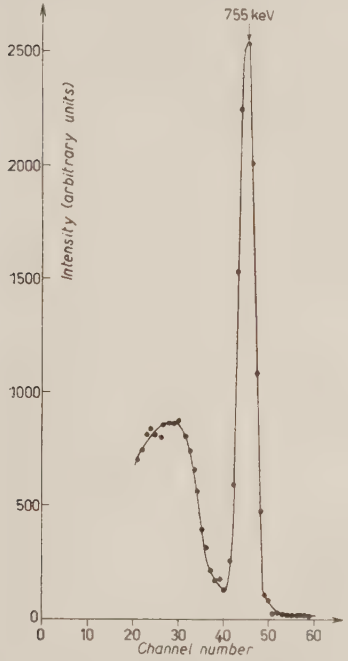

Fig. 2. – Energy spectrum of γ-rays emitted from ^{210}Po.

photopeak in some spectra which were obtained in a 2π geometry; if the photoelectric efficiency of the crystal is taken into account according to the curves given by BELL [2] we obtain:

$$I_\gamma = (1.61 \pm 0.07) \cdot 10^3 \text{ s}^{-1}$$

as an average of several measurements.

The α activity has been measured in the same day with the help of a scintillation detector employing a thin CsI crystal optically coupled to a RCA 5819 photomultiplier. In order to avoid too large a counting rate the source was located, in vacuo, at the distance of 12.30 cm from the detector, which was almost completely shielded with a diaphragm allowing α-particles to pass only through a small hole whose diameter resulted to be $13.94 \cdot 10^{-2}$ cm.

A few collimators were located between the source and the detector in order to minimize the contribution to the counting rate due to scattered α-particles.

In the above described geometry the effective solid angle was calculated to be $8.03 \cdot 10^{-6}$ and the α intensity was

$$I_\alpha = (1.33 \pm 0.07) \cdot 10^8 \text{ s}^{-1}$$

as an average of a few determinations which were obtained with different angular positions of the source to take into account the possible disuniformity of the emitting layer and deviations from the ideal geometry. The efficiency of the α detector was taken to be equal to 1.

The γ/α ratio results consequently

$$\frac{I_\gamma}{I_\alpha} = (1.21 \pm 0.08) \cdot 10^{-5}$$

which is considerably smaller than the previously quoted values but in very close agreement with a recent result published by ROJO, HAKEEM and GOODRICH [3].

The branching ratio can be obtained if I_γ is corrected to take into account the internal conversion probability in the considered γ transition.

The total conversion coefficient has been assumed to be $3 \cdot 10^{-2}$ [4]. Consequently we obtain for the branching ratio

$$(1.25 \pm 0.08) \cdot 10^{-5} .$$

* * *

Thanks are due to Dr. A. MALVICINI for his help in preparing the α counting device.

(2) P. R. BELL: in *Beta- and Gamma-Ray Spectroscopy*, K. SIEGBAHN Editor, p. 132 (Amsterdam, 1955).

(3) O. ROJO, M. A. HAKEEM and M. GOODRICH: *Phys. Rev.*, **99**, 1629 (1955).

(4) D. E. ALBURGER and G. FRIEDLANDER: *Phys. Rev.*, **81**, 523 (1951).

Mesonic Decay in Flight of a Triton Hyperfragment.

F. Brisbout, M. W. Friedlander and P. Iredale (*)
H. H. Wills Physical Laboratory - University of Bristol

(ricevuto il 25 Agosto 1956)

In the course of an investigation in which stopped π-mesons were traced back to their origins within a stack of stripped emulsions, one hyperfragment was found (+). This event may be identified with the hyper-triton, first reported by Bonetti *et al.* [1]; the point of interest in this particular case is that the fragment has undergone decay in flight. A closely similar event has recently been reported by Skjeggestad and Sørenson [2].

Emitted from a star of type 17+6p, the fragment travels for 8.34 mm in emulsion, before decaying in flight. Three charged secondary particles are emitted, all of which come to rest within the emulsion stack. Two are well identified as proton and π^--meson respectively, but the track of the remaining particle is so steep that unambiguous identification is not possible; it appears to have been produced by a proton or deuteron, but it is not possible to distinguish between these possibilities. The information regarding these tracks is summarized in Table I.

The track of the primary particle is contained in eight emulsion sheets, and has an average length of 1.08 mm per sheet. Ionization and scattering measurements were made in each of the six intermediate sheets. The mean value of the normalized grain-density, g^*, as determined from the mean gap length, was ~ 11; the mean value of $p\beta$ was (84 ± 13) MeV/c (using second differences) and 105 ± 17 (using third differences, to correct for distortion). For the observed ionization, the corresponding value of $p\beta$ would be ~ 33 MeV/c for a proton, ~ 65 MeV/c for a deuteron and ~ 98 MeV/c for a triton. An α-particle having a velocity corresponding to this ionization would not have sufficient energy to create a π-meson in a collision. The possibility of the primary particle having been a helium hyperfragment, whose decay is observed, may also be excluded, on the basis of charge conservation. A proton or deuteron having the observed ionization, would not have travelled the observed distance. We therefore identify the primary particle as a triton.

On this assumption, the residual range at the point of decay has been calculated

(*) Now at A.E.R.E., Harwell.

(+) A preliminary report of this event was given at the Pisa Conference (1955).

[1] A. Bonetti, R. Levi Setti, M. Panetti and G. Tomasini: *Nuovo Cimento*, **11**, 210 (1954).

[2] O. Skjeggestad and S. O. Sørenson: *Nuovo Cimento*, **3**, 652 (1956)

from the ionization measurements, and the energy and velocity thereby deduced. These results are considered to be more reliable than those obtained from the scattering measurements, which, on such a steep track, most probably yield an understimate of the true energy.

The mean velocity of the triton was $\beta = 0.21 \pm 0.01$ and its proper time of flight $1.3 \cdot 10^{-10}$ s. Had the fragment not decayed in flight, it would have come to rest within the stack.

The space angle between tracks (1) and (2) is 124°; assuming that these arise from the decay of the Λ^0-particle in the fragment, the apparent Q-value for this decay is calculated to be (34.4 ± 1.4) MeV.

For each of the two possible identities of particle (3), the total momentum and energy at the decay were calculated, and the results are displayed in Table II.

From this, it would appear that the decay scheme

$$^3H_\Lambda \rightarrow p + p + \pi^- + n$$

permits the better balance of energy and momentum (with the neutron having about 3 MeV), but it must be emphasized that the alternative.

$$^3H_\Lambda \rightarrow p + d + \pi^-$$

cannot be excluded, since the energy and particularly the angular measurements are not of sufficient accuracy because of

TABLE I.

	Residual range (mm)	Energy (MeV)	Azimuthal angle	Dip angle in emulsion
Fragment (*) . . .	2.9 ± 1.1	43 ± 10	0	− 33°
Secondaries:				
(1) Proton	3.47	28.5	− 1.9°	− 6°
(2) π-meson . . .	10.04	23.3	+ 168.5°	+ (61° ± 5°)
(3) assumed:				
proton	4.40	32.8	− 1.1°	+ (38° ± 2°)
deuteron . . .		44.1		

(*) Assumed hypertriton.

TABLE II.

	Momentum perpendicular to emulsion sheet (MeV/c)	Momentum in emulsion plane (MeV/c)	Total Energy (MeV)
Triton	278 ± 27	426 ± 41	81 ± 10 (*)
Secondaries, assuming:			
(*a*) 3 = deuteron . .	301 ± 13	515 ± 12	96
(*b*) 3 = proton . . .	203 ± 6	389 ± 8	85

(*: energy includes Λ^0 Q-value of 37 MeV)

(*Note*: the errors quoted in the table, arise from the following causes: for the triton, from the ionization measurements; for the outgoing prongs, from uncertainties in the dip angles for the two steep tracks. This latter error does not, however, affect the energy estimates, which rely upon their ranges.)

the steepness of the tracks. It is therefore not considered justified to calculate a value of the binding energy of the Λ^0-particle in the fragment.

Other assumptions as to the nature of the primary of secondary particles. lead to greater momentum and energy disparities. All other tracks from the original star were followed and identified where possible but no associated unstable particle was found.

* * *

We are grateful to Professor C. F. POWELL, for the hospitality and facilities of his laboratory. One of us (P.I.) wishes to thank the D.S.I.R. for a maintenance grant.

IL NUOVO CIMENTO Vol. IV, N. 4 1° Ottobre 1956

On the Conservation of the Nucleons.

B. Ferretti

Istituto di Fisica e Scuola di Perfezionamento in Fisica Nucleare dell'Università - Roma
Istituto Nazionale di Fisica Nucleare - Sezione di Roma

(ricevuto il 25 Agosto 1956)

The discovery of the « strange particles » has focused the attention on the foundamental problem of the conservation of the nucleons. From one side indeed this strong law of conservation, which is necessary to postulate owing to the stability of matter, provides the main distinction in the classification of the new particles (heavy mesons and hyperons) [1].

On the other side, considering the relatively great number of types of fundamental particles and of apparently different interactions between these particles, the want of a satisfactory reason for the conservation of the nucleons was more clear than before.

Effectively, this problem was discussed already in the first attempt of theoretical treatment of the new particles [2].

I have already remarked [3] that we probably do not know even a really good formulation of the conservation law of the nucleons from the point of view of relativistic physics. It seems indeed necessary, in order to give a satisfactory formulation of this law, to define some ideal procedure of measurement of the quantity that is conserved.

It has been therefore investigated, first whether such a procedure could be proposed using fields of which the nucleons could be sources, and in second place, following the analogy with the conservation of the electric charge, whether the structure of the field equations could provide a reason for the conservation law in discussion.

It has to be emphasized that this investigation concerns the general conditions which must be satisfied by the structure of a certain field Φ in order that from this structure alone a local conservation law for the particles which are sources of Φ, may be deduced. The conclusions of the present investigation, therefore, are not relevant for the possibility of a general principle from which both the structure of the field and the conservation law may be derived.

The main result of the investigation will be resumed as follows: it is possible

(1) B. Ferretti: *Bristol Conference on* V *Particles and Heavy Mesons, Phil. Mag.*, **37**, 104 (1951).
(2) A. Pais: *Proc. Nat. Ac. Sci.*, 484 (1954).
(3) B. Ferretti: *Suppl. Nuovo Cimento*, **2**, 872 (1955).

to define a procedure of measurement of the nucleonic four current (4) independent from the equations of motion of the matter field Ψ (to be distinguished from the created field Φ) if and only if the source of the field Φ is the four-current itself. This conclusion follows essentially from the fact that the commutation relations of the four-current components with any other different expression (scalar, pseudoscalar, and so on) formed with the matter field Ψ do depend from the equation of motion of this field.

On the other hand the possibility of defining a procedure of measuring the four-current by means of the measure on Φ independently from the equation of motion of Ψ seems to be a necessary condition for deriving a justification of the conservation law from the structure of the field Φ alone. The same conclusion, therefore, holds even for allowing the possibility of such a justification.

The result of this research seems consequently to enforce the point of view which has been taken by YANG and LEE (5) in their discussion of the nucleonic conservation.

It may be shown indeed that the verification of their hypothesis that the nucleonic field Ψ admits the gauge transformation group $\Psi \to \exp[i\alpha(xyzt)]\Psi$ is not only sufficient, but a necessary condition for the validity of a local conservation law of the nucleons.

It may be doubted however that from this hypothesis alone we may derive the conclusion that the only field which is capable of giving the justification of the conservation law of the nucleons has to be a neutral vectorial zero mass field.

(4) It is almost a trivial remark that the assumption of a local conservation law and the fact that the quantity which is conserved is invariant for Lorentz transformation, is sufficient to exclude any other formulation of the conservation law, than by means of the usual four-current (or an immediate generalization of the four current, cf. (3)).

(5) T. D. LEE and C. N. YANG: *Phys. Rev.*, **98**, 1501 (1955).

IL NUOVO CIMENTO Vol. IV, N. 4 1° Ottobre 1956

On the Bubbles Formation in Supersaturated Gas-Liquid Solutions.

P. E. Argan and A. Gigli

Istituto di Fisica dell'Università - Genova
Istituto Nazionale di Fisica Nucleare - Sezione Aggregata di Genova

(ricevuto il 19 Settembre 1956)

In a letter recently appeared in this journal [1] we reported some preliminary results concerning the effect of ionizing particles on a supersaturated gas-liquid solution (carbon dioxide-ethyl ether).

We have shown that at high supersaturations the result is the formation of small gas bubbles and therefore the release of the gas from the liquid. The effect may be used for visualizing the path of ionizing particles in form of tracks of small bubbles in the interior of the gas-liquid system.

In this letter the conditions for the observation of the effect are specified and further results obtained with systems other than carbon dioxide-ether are reported (in particular, with hydrogen-rich systems).

The mechanical equilibrium of a spherical gas bubble enclosing n ion charges in a gas-liquid solution, may be discussed, at least in a rough approximation, by means of the equations obtained for the similar case of a vapor bubble in the interior of its own liquid. Such equations can be derived from the known relations among the gas pressure inside the bubble, the hydrostatic pressure, the bubble radius, the surface tension and the dielectric constant of the system, where the two last quantities are dependent on the concentration of the solution.

On the contrary, a remarkable difference may be expected between a superheated liquid and a supersaturated solution as far as the formation and the rate of growth of bubbles are concerned. The mechanism of bubble formation is scarcely known both in the case of superheated liquids and of supersaturated solutions. In a superheated liquid the rate of growth of the bubbles is extremely high (~ 1 mm/μs) owing to the nature of process from which bubbles arise, that is only the evaporation of the liquid at the vapor-liquid surface. In a supersaturated solution the growth of a bubble takes place, at least in part, at the expenses of the dissolved gas and the rate of growth will be remarkably influenced by the rate of diffusion of the gas through the liquid.

For supersaturated gas-liquid solutions we assume the necessary condition for a bubble to grow visible to be ex-

[1] P. E. Argan and A. Gigli: *Nuovo Cimento*, **3**, 1171 (1956).

pressed by the following relation:

$$(1) \qquad p - P > \left| \frac{3}{2} \left(\frac{1\pi}{n^2 e^2} \right)^{\frac{1}{3}} \cdot \gamma(c)^{\frac{4}{3}} \cdot \varepsilon(c)^{\frac{1}{3}} \right| T = \text{room temperature}$$

where p is the sum of partial pressures of gas and saturated vapor inside the bubble, P the hydrostatic pressure, n the number of ion charges of the same sign enclosed in the bubble, e the elementary charge, $\gamma(c)$ the surface tension, $\varepsilon(c)$ the dielectric constant and c the concentration.

The relation (1) is based on an electrical model in which it is assumed that n ions of the same sign enclosed in the bubble, owing to electrostatic repulsion, give a positive contribution to the pressure p. Such a representation, whose approximation is better the larger the number n, was proposed by GLASER [2] to evaluate the operating conditions (temperature and pressure) of the superheated liquid bubble chamber [3]; in the present relation, the concentration c of the solution at room temperature appears instead of the temperature T.

In the lack of a better theory, we assume that relation (1) can be reasonably used to determine what the concentration of the solution must be in order that its supersaturated state, expressed in terms of $p - P$, be sensitive to clusters of n charges. Therefore, it is to be expected that the formation of bubbles on charged centers with $n' > n$ will happen at lower and lower pressure drops $p - P$, the more soluble is the gas in the liquid and the steeper is the lowering of the surface tension and of the dielectric constant with the concentration.

A conveniently low value of $p - P$ is shown by the system carbon dioxide-ether; on the basis of relation (1), this system should be sensitive to the effect of charged clusters with n between 2 and 10 if the pressure drops from the equilibrium values between 50 and 35 atm to atmospheric pressure. Experiments carried out with equilibrium pre-expansion pressures ranging in this interval have given a positive result [1]. Unfortunately the few data available in the literature permit only a rough estimate of the interesting parameters. Precise determinations of the properties of this system are at present in progress in our laboratory.

In order to obtain more favorable experimental conditions, namely a lower pre-expansion pressure, we have undertaken in the last months a systematic search on several gas-liquid systems. In particular a detailed study was made with liquid propane ($\gamma = 7.22$, $\varepsilon = 1.66$ at $t = 25\,^{\circ}\mathrm{C}$) and gaseous methane and carbon-dioxide.

In Table I some numerical data concerning the methane-propane system are shown. These values were obtained by interpolation of the data of WEINAUG and KATZ [4] and by measurements and calculations [5] made by us.

In the first three columns are shown the values of the mole fractions of the methane in the liquid and gaseous phases at the corresponding equilibrium pressures. These pressures represent also the lowest pre-expansion pressures necessary to the formation of bubbles from n-fold (column 8) charge clusters. The pairs

[2] D. A. GLASER: *Suppl. Nuovo Cimento*, **11**, 361 (1954).

[3] There are good reasons for doubting that such a model offer a consistent representation of the physical phenomena which determine the formation and the growth of bubbles in superheated liquids (see for instance: P. BASSI, A. LORIA, J. A. MEYER, P. MITTNER and I. SCOTONI: *Nuovo Cimento*, **4**, 491 (1956)). The same reasons are very likely valid also in the case of supersaturated solutions.

[4] C. F. WEINAUG and D. L. KATZ: *Ind. Eng. Chem.*, **35**, 239 (1943).

[5] The dielectric constants were calculated from the molecular polarizabilities of the constituents of the systems; see: LANDOLT and BÖRNSTEIN: I. 3 Teil, Molekeln II, pp. 514 and 515.

TABLE I. – *Properties of the Methane-Propane System.*

Mole Fraction Methane		p (atm)	Density (g/cm³)		Surface tension $\gamma(c)$ (dine/cm)	Dielectric constant $\varepsilon(c)$	n
Liquid	Vapor		Liquid	Vapor			
1	2	3	4	5	6	7	8
0.117	0.600	31.0	0.460	0.046	4.65	1.59	2
0.095	0.563	27.2	0.465	0.040	5.05	1.60	3
0.080	0.525	24.3	0.468	0.037	5.35	1.61	4
0.069	0.495	22.4	0.471	0.034	5.55	1.62	5
0.058	0.463	20.6	0.474	0.032	5.75	1.62	6
0.052	0.435	19.3	0.477	0.031	5.90	1.63	7
0.047	0.412	18.4	0.478	0.030	6.00	1.63	8
0.040	0.385	17.4	0.480	0.029	6.10	1.63	9
0.038	0.365	16.8	0.480	0.028	6.15	1.64	10

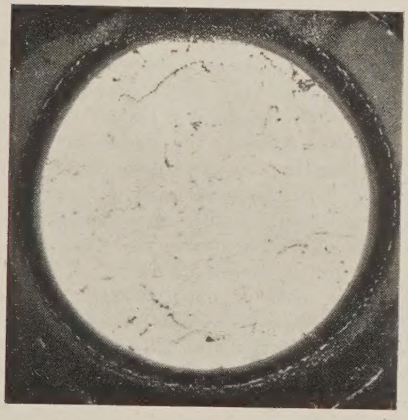

Fig. 1. – Photograph of the chamber taken 1.8 ms after the expansion of the methane-propane system from 29 to 1 atm. The effect of a 10 mC radium source placed at the side of the chamber at a distance of ~ 35 cm is clearly visible in the form of bubble tracks formed on the electron paths. Flash duration of about 100 μs. Volume expansion ratio of 1.05.

Fig. 2. – Photograph of the chamber taken 1.8 ms after the expansion of the carbon dioxide propane system from 27 to 1 atm. Other experimental conditions are the same as in Fig. 1.

of n and ρ values were evaluated from relation (1) using, for the surface tension and the dielectric constant of the solution, the values given in columns 6 and 7 of the same table. To check these calculations, experiments were carried out with the chamber briefly described in our previous letter [1], by reducing the pressure of the gas-liquid mixture

TABLE II. – *Properties of the Carbon Dioxide-Propane System.*

Mole fraction Carbon dioxide		p (atm)	Density (g/cm³)		Surface tension $\gamma(c)$ (dine/cm)	Dielectric constant $\varepsilon(c)$	n
Liquid	Vapor		Liquid	Vapor			
1	2	3	4	5	6	7	8
0.320	0.665	30.0	0.540	0.077	4.65	1.30	2
0.250	0.613	26.2	0.530	0.067	5.10	1.38	3
0.200	0.561	23.4	0.524	0.061	5.40	1.44	4
0.175	0.526	21.7	0.520	0.055	5.60	1.47	5
0.145	0.490	20.2	0.517	0.050	5.75	1.50	6
0.125	0.460	19.0	0.515	0.047	5.90	1.52	7
0.110	0.430	17.8	0.513	0.045	6.00	1.54	8
0.090	0.400	16.8	0.511	0.043	6.13	1.56	9
0.083	0.380	16.2	0.510	0.041	6.20	1.58	10

from the initial equilibrium value of $20 \div 30$ atmospheres to atmospheric pressure.

Tank propane (96% propane, 2.5% octane, 1% isobutane and 0.5% n-butane) and methane were used. A 10 mC radium source placed at the side of the chamber was the ionizing agent.

For concentrations of the system corresponding to low equilibrium pressures no bubbles are observed. If the equilibrium pressure is just of the order of 20 atm, bubbles appear randomly distributed in the solution. As the equilibrium pressure is raised ($\sim 24 \div 30$ atm) it becomes possible to correlate the bubbles in ever clearer tracks. Fig. 1 shows a typical photograph obtained after the expansion from 29 to 1 atm. These results are well explained by the adopted model: in fact at higher concentrations the system is to be expected to become more sensitive to smaller charge clusters.

Table II refers to the carbon dioxide-propane system. Some of the numerical values (columns 1, 2, 3, 4 and 5) were computed by interpolation from the data of REAMER, SAGE and LACEY [6], while the surface tensions γ (column 6) were measured by us by the method of capillary rise [3]. The effect under study was effectively observed reducing the pressure of this system from the equilibrium value of $20 \div 30$ atm to the atmospheric pressure, as shown in Fig. 2.

The positive experiments we have carried out with systems remarkably different with regard to the concentrations (column 1 of Tables I and II), the equilibrium pressures (~ 50 atm for CO_2-ether), the density of the sensitive medium and the molecular structure of the components, have convinced us that the possibility of observation of bubbles in strongly supersaturated gas-liquid solutions around charged centers must be quite general. Therefore we think that very many other systems will be success-

[6] H. H. REAMER, B. H. SAGE and W. N. LACEY: *Ind. Eng. Chem.*, **43**, 2515 (1951).

fully experimented and probably solutions will be found suitable for work with lower pre-expansion pressures. The methane-propane system is certainly of particular interest as a hydrogen-rich medium; the working pressure is not too high and probably this system should be very useful for the operation of large gas bubble chambers.

We wish to point out that, in the case of supersaturated solutions the model, on which relation (1) is based, appears to be accurate enough for the evaluation of the conditions (concentration and equilibrium pressure) under which the effect is observable and therefore for a convenient choice of the components of the solutions.

Finally it should be remarked that all the solutions experimented by us had low values of the density (column 4 of Tables I and II). It is very likely that solutions of larger densities (and possibly containing a variety of target nuclei) can be found with properties suitable for the performance of special gas bubble chambers.

Details concerning the apparatus and the experimental methods will be given at later time.

ERRATA-CORRIGE

B. LÜTHI and J. L. OLSEN — **A New Effect in the Magnetoresistance of Aluminium,** *Nuovo Cimento*, **3**, 840 (1956).

The authors regret an unfortunate error in the above letter. In Fig. 1 the equation next to the vertical arrow reading

$$\frac{H}{\varrho} = \frac{2}{10} nec$$

should be changed to

$$\frac{H}{\varrho} = 4\ nec$$

In the first line of the text below Fig. 1

$$H/\varrho > 2\ nec/10$$

should be corrected to read

$$H/\varrho > 4\ nec\ .$$

Direttore responsabile: G. POLVANI

Tipografia Compositori - Bologna

Questo fascicolo è stato licenziato dai torchi il 27-IX-1956